Computers & Structures Vol. 25, No. 4, pp. 469–605, 1987
Printed in Great Britain.

0045-7949/87 $3.00 + 0.00

PANDA2—PROGRAM FOR MINIMUM WEIGHT DESIGN OF STIFFENED, COMPOSITE, LOCALLY BUCKLED PANELS

DAVID BUSHNELL
Lockheed Palo Alto Research Laboratory, 3251 Hanover St, Palo Alto, CA 94304, U.S.A.

(*Received* 20 *May* 1986)

Abstract—PANDA2 finds minimum weight designs of laminated composite flat or curved cylindrical panels or cylindrical shells with stiffeners in one or two orthogonal directions. The panels or shells can be loaded by as many as five combinations of in-plane loads and normal pressure. The axial load can vary across the panel. Constraints on the design include crippling, local and general buckling, maximum tensile or compressive stress along the fibers and normal to the fibers in each lamina, and maximum in-plane shear stress in each lamina. Local and general buckling loads are calculated with the use of either closed-form expressions or discretized models of panel cross sections. An analysis branch exists in which local post buckling of the panel skin is accounted for. In this branch a constraint condition that prevents stiffener popoff is introduced into the optimization calculations. Much of this paper represents a tutorial run through the PANDA2 processors for a hat-stiffened panel under combined axial compression, in-plane shear and normal pressure. Examples follow in which results from PANDA2 are compared with those in the literature and those obtained with the STAGS and EAL computer programs. Results of an extensive study are given for an optimized, blade-stiffened panel design so that it buckles locally at about 10% of the design load. The axially stiffened panel is subjected to pure axial compression, pure normal pressure, combined axial compression and normal pressure, and combined axial compression and residual stresses and deformations that arise from a simulated curing process. An example is provided of a design process applied to a ring and stringer stiffened cylindrical shell similar in geometry and loading to the 2/3 interstage of the ARIANE 4 booster.

1. PURPOSE OF PANDA2

The purpose of PANDA2 is to find the minimum weight design of a stiffened flat or curved panel or complete cylindrical shell made of laminated composite material. Of course, simple isotropic panels and cylindrical shells can also be designed.

1.1 *Definition of 'panel'*

A panel is defined here as a structure that is either flat or is part of a cylinder. In most cases the user will probably want to analyze a flat panel or a panel that spans less than about 45° of circumference. However, in PANDA2 complete cylindrical shells can be treated by the user's setting up a model of a panel that spans 180°. The buckling loads given by PANDA2 for half of a cylindrical shell are the same as those given in the literature for a complete cylindrical shell because:

1. the panel is assumed by PANDA2 to be simply supported along its straight edges;
2. a deep cylindrical panel spanning 180° of circumference with simple supports along the generators at 0° and at 180° behaves in the same way as a complete cylindrical shell: the number of circumferential half-waves in the 180° panel in the critical general instability buckling pattern is the same as the number of full circumferential waves in the 360° cylindrical shell.

Later an example is given in which a complete cylindrical shell with a single set of axial and shear loads that vary around the circumference is analyzed as a curved panel spanning 45° and subjected to multiple sets of uniform loads. The panel is optimized for two combinations of in-plane loads: that corresponding to maximum axial compression and that corresponding to maximum in-plane shear. It is usually best to treat complete cylindrical shells in this way rather than try to set up a model for the entire cylinder, because buckling is usually local and concentrated in the areas of maximum load and because PANDA2 was really intended to treat panels, not complete cylindrical shells. Therefore, it is best applied to panels.

In PANDA2 the curved edges of a cylindrical panel lie in the plane of the screen (axial coordinate $x = 0$) and parallel to the plane of the screen (axial coordinate $x = L$, where L is the length of the panel). The axial coordinate direction x is normal to the plane of the screen and pointing out of the screen. Thus, an axial load on the panel is normal to the screen, with axial tension pointing out of the screen.

The width of the panel is the arc length along the curved edge. For example, the width of a deep cylindrical panel spanning 180° is πR, where R is the radius of curvature. The coordinate in the width direction is called y. In the following, this direction is referred to with use of the words 'circumferential' or 'hoop' or 'transverse'.

The properties of the panel are assumed to be uniform in the axial (x) direction and periodic in the circumferential (y) direction. The panel may be unstiffened, stiffened by stringers alone, stiffened by rings alone, or stiffened by both rings and stringers. Stiffeners referred to as 'stringers' are always normal to the screen; stiffeners referred to as 'rings' always lie in the plane of the screen or parallel to the plane of the screen. Both stringers and rings must be uniformly spaced. All stringers must be the same. All rings must be the same. The rings can be different from the stringers.

1.2 *Types of stiffeners*

PANDA2 can handle panels with stringers and/or rings with the following cross sections:

1. T-shaped
2. J-shaped (angle with flange away from skin)
3. Rectangular (blade stiffeners)
4. Hat-shaped or corrugated stiffeners.

The portion of the panel skin near the stiffeners can have different properties than those of the panel skin away from the stiffeners. For example, optimum designs of panels with T-shaped stringers have thickened bases under the stringers that help to prevent fracture or delamination along the attachment line of the stringer to the skin. Figures 1 and 2 show an example of a flat panel with T-shaped stringers.

1.3 *Boundary conditions*

In the PANDA2 system the panel is assumed to be simply supported along the two edges normal to the plane of the screen (at $y = 0$ and at y = panel width). The panel can be either simply supported or clamped along the other two boundaries (at $x = 0$ and $x = L$), but the conditions must be the same at both of these two boundaries. The PANDA2 analysis is always performed for simple support on all four edges. However, experience has shown that clamping at $x = 0$ and at $x = L$ can be simulated by the analysis of a shorter simply supported panel: A panel clamped at $x = 0$ and $x = L$ has general instability loads approximately equal to those of a panel simply supported at $x = 0$ and $x = L/3.85^{1/2}$. Therefore, in PANDA2, clamping at $x = 0$ and $x = L$ is simulated by calculation of general instability or wide column instability of a simply supported panel with length equal to $L/3.85^{1/2}$.

In PANDA2 local buckling behavior and local stress concentrations near stiffeners are assumed to be independent of the boundary conditions along the four panel edges. This is a good assumption if there are more than two or three halfwaves in the local buckling pattern over the length and width of the entire panel.

1.4 *Loading*

The panel can be loaded by up to five independent sets of in-plane loads, N_x, N_y and N_{xy}, and normal pressure p. Buckling loads, postbuckling behavior, and maximum stresses are calculated for each of the five

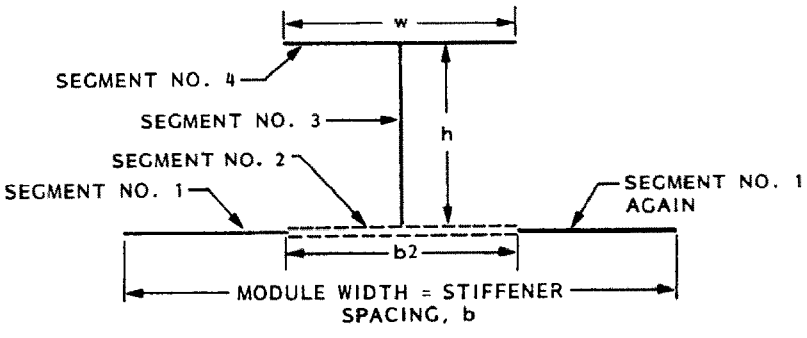

Fig. 1. Single module of a panel with T-shaped stringer. (Axial load N_x acts normal to the screen.)

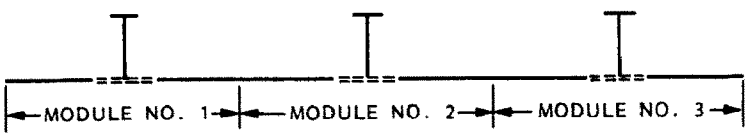

Fig. 2. Panel with T-shaped stringers. There are three modules in this example.

load sets applied by itself. Optimization is global, that is, PANDA2 determines the best design that is capable of surviving all of the five load sets when each set is applied separately, as it would be during different phases of a panel's lifetime or over different areas of a large, uniform structure such as a complete cylindrical shell. Associated with each of the five independent load sets, there can be two load subsets, Load Set A and Load Set B. Load Set A consists of what are termed in the PANDA2 output as 'eigenvalue loads'; these are loads that are to be multiplied by the critical buckling load factor (eigenvalue). Load Set B consists of loads that are not multiplied by the critical buckling load factor. Stated mathematically, the critical load is given by

$$N_{cr} = N(\text{load set B}) + (\text{buckling load factor})\, N(\text{load set A}). \tag{1.1}$$

The following table lists the components and properties of the loading in PANDA2:

Loads on a panel permitted by PANDA2

Name of load	Load set A or B	Definition and [example of units]	Properties
N1	A	Axial in-plane load [lb/(in. of circ. arc)] negative for compression	Uniform or linearly varying across panel width; uniform along panel length
N2	A	Hoop in-plane load [lb/(in. axial length)]	Uniform along panel length and width
N12	A	In-plane shear load [lb/(in. axial or circ.)]	Uniform along panel length and width
N10	B	Axial in-plane load [lb/(in. of circ. arc)]	Uniform along panel length and width
N20	B	Hoop in-plane load [lb/(in. of axial length)]	Uniform along panel length and width
N120	B	In-plane shear load [lb/(in. axial or circ.)]	Must be zero
p	B	Normal pressure [psi]	Uniform over panel
Thermal	B	Temperature that simulates curing of composite panel	Uniform in each panel module segment (see Fig. 1)

1.5 *Types of analysis*

PANDA2 performs the following analyses:

1. *Constitutive law.* (a) PANDA2 obtains the integrated constitutive law (the 6×6 matrix $C(i, j)$) for each segment of a panel module (Figs 1 and 2).

(b) It obtains thermal resultants and strains from curing for each segment of a panel module.

(c) It obtains the integrated constitutive law (the 6×6 matrix $C_s(i, j)$) for the panel with either and both sets of stiffeners 'smeared out'. ('Smearing out' the stiffeners means averaging their properties over the entire area of the panel. See eqns (40) of [8], for example.)

(d) It obtains the thermal forces and moments and residual deformations of a panel in which skin and stiffeners have been cocured.

(e) It obtains the tangent stiffness $C_{TAN}(i, j)$ of the panel skin in its locally post-buckled state, if applicable.

(f) It obtains the tangent stiffness $C_{STAN}(i, j)$ of the panel with smeared stiffeners, using $C_{TAN}(i, j)$ for the stiffness of the panel skin.

2. *Equilibrium.* (a) PANDA2 obtains bowing of the panel due to curing.

(b) It obtains static response of the panel to uniform normal pressure, using nonlinear theory. Two problems are solved:

(i) overall static response of entire panel with smeared stiffeners, and
(ii) local static response of a single panel module with a discretized cross section (Fig. 1).

(c) Average strain and resultant distribution in all of the panel parts (Fig. 1) are determined for:

(i) the panel loaded by all loads except normal pressure. The effect of bowing of the panel due to both curing and normal pressure is included;
(ii) the panel loaded by normal pressure.

(d) Stresses in material coordinates in each layer in each laminate of the panel module (Fig. 1) are calculated either for the post-locally buckled panel, or for the unbuckled panel, whichever is applicable.

(e) Tensile forces in parts of the stiffener web(s) that tend to pull the web from the panel skin are calculated, and these forces are compared to a maximum allowable 'peel force' that the user has previously obtained from peel tests on sample coupons that bear some similarity to the concept for which he or she is seeking an optimum design.

3. *Buckling.* (a) PANDA2 obtains buckling load factors from a PANDA-type of analysis (closed form; see [1] and [8]) for general instability, local buckling, crippling, rolling of stiffeners.

(b) It obtains the load factor for local skin buckling from a BOSOR4-type [2] of analysis in which the cross section of a single panel module is discretized (Figs 1, 2, 20(a, b), 22(a, b)).

(c) It obtains a load factor for wide column buckling from a BOSOR4-type of analysis of a discretized single panel module (Figs. 2, 20(c), 22(c)).

(d) It obtains a load factor for general instability from a BOSOR4-type of analysis of the entire panel with smeared stiffeners. The width of the panel is discretized.

(e) It generates an elaborate discretized model of the entire panel width with stringer parts treated as flexible shell branches. This model can be used directly as input to BOSOR4. (See Fig. 21).

1.6 *Philosophy of PANDA2*

PANDA2 represents a more detailed treatment of certain behavior not handled by PANDA [1]. In particular, optimum designs can be obtained for panels with locally post-buckled skin and for panels with hat stiffeners. In addition, PANDA2 will handle nonlinear static response to normal pressure and panels with nonuniform axial loading. Also, PANDA2 optimizes panels for multiple sets of loads.

Optimization is carried out based on several independently treated structural models of the panel. These might be classified into three model types as follows.

1.6.1 *Model type* 1. Included are PANDA-type models [1] for general, local and panel buckling, crippling of stiffener parts, and rolling of stiffeners with and without participation of the panel skin. Buckling load factors are calculated from closed-form equations rather than from discretized models. The formulas are given in [1]. (See [1, Table 1 and Figs 1–4].) (Numbers [i] refer to references given below.)

1.6.2 *Model type* 2. Buckling load factors and post-local buckling behavior are calculated for what is termed in PANDA2 a 'panel module'. Such a module is depicted in Figs 1 and 2. A module includes the cross section of a stiffener plus the panel skin of width equal to the spacing between stiffeners. In this model the panel module cross section is divided into segments, each of which is discretized and analyzed via the finite difference energy method [2]. Variation of deflection in the axial direction is assumed to be harmonic ($\sin(nx)$ or $\cos(nx)$). This one-dimensional discretization is similar to that used in the BOSOR programs for the analysis of shells of revolution [2]. In fact, many of the subroutines for buckling and vibration analysis are taken from BOSOR4 and modified slightly. The modification is necessary to handle prismatic structures instead of shells of revolution.

Both local and wide-column instability can be handled with the same discretized structural model. Symmetry conditions are applied at the left and right edges of the single module model; that is, symmetry conditions are applied midway between stringers.

The single module model gives a good approximation to the local skin buckling mode if there are more than three or four equally spaced stringers in the panel. What goes on locally between interior stringers in a panel, stringers which are rotating about their axes only, not bending, is only weakly affected by the boundary conditions at panel edges that may be several bays away.

The wide column buckling model in PANDA2 is applied to an axial length of panel between adjacent rings, or if there are no rings, to the entire axial length of the panel, L. The wide-column buckling load predicted from the single panel module is always lower and usually reasonably close to the general instability load of the entire width of the panel between rings because the axial bending stiffness of a stringer-stiffened panel is usually much, much greater than the transverse bending stiffness of the portion of the panel between adjacent rings. Hence, the strain energy in the buckled panel, and therefore the buckling behavior, is only weakly dependent on bending of the panel transverse to the stringers. Therefore, the boundary conditions along the edges of the panel parallel to the stringers are not important. On the other hand, local bending of the skin and local deformation of the stringer parts in the wide column buckling mode may significantly affect the wide column buckling load. These effects are not included in the closed-form PANDA-type model of general instability, but they are included in the single panel module model of wide column buckling.

Buckling modal interaction between local and general buckling that is due to initial local imperfections in the panel skin is included in PANDA2 [34].

1.6.3 *Model type* 3. Also included in the PANDA2 collection of models is a discretized model of the entire width of the panel, treated in this case with stiffeners smeared out. This model is introduced only if the axial load varies across the width of the panel or if there exists normal pressure.

1.6.4 *Overall philosophy of PANDA2.* The overall philosophy of PANDA2 is to use several separate relatively simple models to capture different phenomena, rather than use a single multi-dimensionally

discretized finite element model with a large number of degrees of freedom. The aim is to produce a program that can yield optimum designs of rather sophisticated panels that experience very complex and very nonlinear behavior, and to do this without the use of large, general-purpose programs and their elaborate data base management systems.

For example, PANDA-type models (Model type 1) are used in PANDA2 to obtain quick, preliminary designs which one can then use as starting designs in optimization analyses based on the more elaborate discretized panel module model. Also, PANDA-type models are used to obtain buckling load factors in cases for which the discretized panel module model is not applicable, to obtain knockdown factors for the effect of in-plane shear loading, to obtain preliminary estimates of how much growth in any initial panel bowing to expect under compressive in-plane loads, and to check if it is likely that a curved panel with uniform external pressure will collapse under the pressure acting by itself.

Models of type 2 (single discretized module) and type 3 (discretization of entire width with smeared stiffeners) are used in tandem to obtain from nonlinear theory the complex behavior of a stiffened plate or shell loaded by normal pressure. Model type 3 is the only one that is valid if the axial load varies across the width of the panel.

In the panels designed by PANDA2 the skin between stringers may buckle well before failure of the panel. The maximum stress components and therefore stress constraints in the optimization analysis are computed including local post buckling growth and modification of the local skin buckling mode as predicted by a modified form of a theory formulated by Koiter in 1946 [4]. Model type 2 (single discretized module) is the only model in PANDA2 valid for this analysis.

After the optimum design is obtained, the user can, if no in-plane shear load is applied, check the accuracy of the general instability load predicted from the single-module model by running a multi-module model with BOSOR4 [2]. The input data file for this multi-module model is generated automatically by the PANDA2 system.

1.7 *Architecture of the PANDA2 system*

As with PANDA, the program PANDA2 consists of several independently executable processors which share a common data base. In the processor BEGIN the user supplies a starting design (perhaps a design produced by PANDA). In DECIDE he or she chooses decision variables for the optimization analysis and their upper and lower bounds, linking variables and their factors of proportionality, and 'escape' variables (explained in DECIDE). In MAINSETUP the user chooses up to five sets of combined in-plane loads and normal pressure; factors of safety for general instabililty, local instability and material failure; strategy parameters such as number and range of axial half-waves in the local buckling mode; and number of design iterations in the optimization problem. The command PANDAOPT initiates a batch run of the PANDA2 mainprocessor, which consists of two main branches: in one branch the structural analyses (stress, buckling and post-buckling) are performed and in the other new designs are produced by the optimizer CONMIN, written by Vanderplaats [3].

2. HOW TO OPERATE THE PANDA2 SYSTEM OF PROGRAMS

To operate PANDA2 you must have the BOSOR4 program system on a subdirectory with the name BOSOR4. The PANDA2 system uses many of the libraries from the BOSOR4 system, and certain commands (for example PANEL followed by BOSORALL) use BOSOR4 processors directly.

You first activate PANDA2 commands via the command PANDA2LOG. This command must be given before you do any PANDA2 work.

You then prepare input data interactively via the BEGIN command. These data establish a starting design, material properties and temperature rise pertaining to residual stresses from curing. The data that you provide interactively are stored on a file NAME.BEG, which you will find very useful in future analyses of the same design concept. (NAME is a name that you choose and retain for the entire case.)

You next type the command SETUP. As a result of SETUP, a BOSOR4-type of input data file is created. Following SETUP, you type the command BOSMODEL. This launches a batch run of a BOSOR4-type preprocessor which is almost identical to BOSORREAD (see HELP4 PROGRAMS in the BOSOR4 subdirectory and [2], last citation).

The BOSMODEL processor creates a discretized model of a single module of the panel (see Fig. 1) and a discretized model of the entire panel with smeared stiffeners. When the BOSMODEL batch run is finished, you can either type the command DECIDE or the command MAINSETUP. If you choose DECIDE, you will be asked to pick decision variables and their upper and lower bounds, linked variables and linking constants, and escape variables. If you choose MAINSETUP, you will be asked to provide loads, factors of safety, and strategy parameters for a simple buckling analysis of a fixed design.

Suppose you choose DECIDE. This choice means that you intend to do an optimization analysis. After picking decision variables and other optimization parameters in DECIDE, you type the command MAINSETUP. Now you provide up to five sets of combined in-plane loads, normal pressure, and factors of safety for general instability, local instability, and material failure, and you establish certain strategy parameters for the buckling and optimization analyses.

You then type the command PANDAOPT, which launches a batch run of the PANDA2 mainprocessor. Simple buckling analyses require up to several minutes on the VAX 11/780, and 6–10 design iterations in an optimization analysis require about 3–60 min of CPU time. The results of the PANDAOPT run are stored in a file called NAME.OPM.

After inspecting the NAME.OPM file, you may wish to do more design iterations. If you feel that the loads, factors of safety and strategy parameters established in MAINSETUP are still good, simply type the command PANDAOPT again. Look at the new NAME.OPM file. Keep repeating this cycle until you think you have an optimum design. If along the way you want to change the strategy parameters, type MAINSETUP again. If you want to change which parameters are decision variables or upper or lower bounds, or if you want to change the linking variables or linking constants of proportionality, type DECIDE again.

When you are satisfied that you have a good design, you will probably want plots of the cross section and buckling modes. You must first give the command MAINSETUP again and set up a case in which you are analyzing a given design (no optimization). When the system asks if you want plots, answer Y. After you finish with MAINSETUP, give the command PLOTTER.

All the analysis up to this point is for a single panel module or the complete panel in which the stiffeners are smeared out. You may want to check the accuracy of the simplified models for general instability. (By 'simplified models for general instability' is meant PANDA-type or discretized models in which the stiffeners are smeared out and a wide-column discrete model which covers only a single panel module.) You can check the PANDA2 results by obtaining the general instability load factor for a multi-module discretized model that represents the entire panel, not just a single module of the panel. You type the commands PANEL, BOSOR4LOG, BOSORALL and BOSORPLOT, in that order. PANEL is analogous to SETUP: It sets up an input data file, NAME.ALL, for a multi-module discretized panel. This file is a regular BOSOR4 input data file. The command BOSOR4LOG activates the BOSOR4 command set, and the command BOSORALL initiates a batch run of the BOSOR4 pre-, main- and postprocessors. BOSORPLOT gets plots of the discretized multi-module panel and of the buckling modes. The PANEL processor should not be used if there exist multiple load sets. If there exists significant in-plane applied shear load, N_{xy}, you will have to multiply the load factor obtained as just described by a knockdown factor generated by PANDA2 because the BOSOR4 buckling analysis does not include in-plane shear. BOSOR4 works for prismatic structures, such as an axially stiffened flat panel, through a 'trick' described in Chapter 7 of [30]. Figure 21 gives an example.

2.1 *Sample runstream with PANDA2*

PANDA2LOG (you activate PANDA2 commands. Please note that you must insert the following four statements in your LOGIN.COM:
$ASSIGN DISK:[USERNAME.PANDA2]PANDA2
$PANDA2LOG:= = @DISK:[USERNAME.PANDA2]PANDA2
$ASSIGN DISK:[USERNAME.BOSOR4]BOSOR4
$BOSOR4LOG:= = @DISK:[USERNAME.BOSOR4]BOSOR4)
BEGIN (you establish a starting design)
SETUP (system sets up a BOSOR4-type of input file)
BOSMODEL (system generates BOSOR4-type discrete models)
DECIDE (you establish optimization parameters)
MAINSETUP (you provide loads and set up PANDA2 analysis strategy)
PANDAOPT (system performs PANDA2 analysis)
MAINSETUP (you provide new strategy: no optimization, yes plots)
PLOTTER (you launch a batch run to generate plots)
PANEL (system sets up a BOSOR4 input file for multi-module panel)
BOSOR4LOG (you activate BOSOR4 command set)
BOSORALL (you run BOSOR4 to get general bifurcation buckling)
BOSORPLOT (BOSOR4 system generates a multi-module panel plot file)

3. PURPOSE OF BEGIN AND AN EXAMPLE

3.1 *Purpose of BEGIN*

The purpose of BEGIN is to permit you to provide a starting design in an interactive mode. You give starting dimensions, material properties, allowables. The interactive session is stored on a file called

NAME.BEG, in which NAME is a name that you have chosen for the case. (NAME must remain the same for all the PANDA2 processors.) In future runs of the same or of a slightly modified case, you will find it convenient to use the file NAME.BEG as input. Rather than answer all the questions interactively, you can use NAME.BEG or an edited version of NAME.BEG as input to BEGIN. BEGIN also generates an output file called NAME.OPB. OPB lists a summary of the case, and if you choose the tutorial option, the questions, helps, and your answers for each input datum.

3.2 *Example: a hat-stiffened panel*

Now you start to provide input data. You will be prompted by short questions. If you need help, just type H as an answer to the prompt instead of the datum called for. In most instances you will then be given more information on the datum you must provide. It may be a good idea to run the tutorial option if you are a new user of PANDA2.

Overall panel dimensions:

1. length normal to the plane of the screen, L1,
2. length in the plane of the screen, L2.

$Panel length normal to the plane of the screen, L1 = H

This is the axial length of the panel. For a cylindrical panel, this is the length of the generator of the panel.

$Panel length normal to the plane of the screen, L1 = 30

$Panel length in the plane of the screen, L2 = H

For a cylindrical panel, this is the arc length along the circumference of the entire panel. A complete cylindrical shell can be modelled by using L2 = π × radius. Then the number of half-waves over this circumferential length is the same as the number of full waves around the complete 360° circumference. When analyzing a complete cylindrical shell with loads that vary around the circumference, it is often best to divide the cylindrical shell into panels, each with uniform loading. Then the optimum design of the complete cylindrical shell can be obtained by optimizing one of the panels as if it were subjected to multiple load sets, each set consisting of uniform loads.

$Panel length in the plane of the screen, L2 = 24

$Identify type of stiffener along L1 (N, T, J, R, A) = H

N = No stiffeners along L1 at all
T = T-shaped cross section
J = J-shaped cross section (angle section with flange away from skin)
R = Rectangular cross section (blade stiffener)
A = A hat-shaped or trapezoidal cross section (enclosing area)

$Identify type of stiffener along L1 (N, T, J, R, A) = A

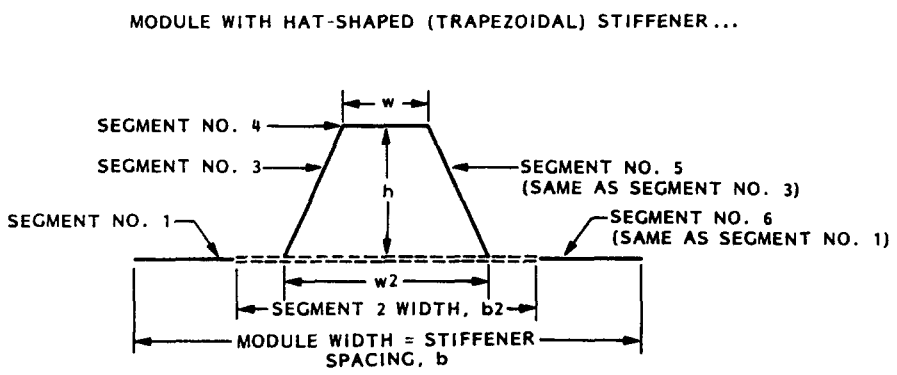

Fig. 3. Panel module with hat-shaped stiffener.

$stiffener spacing, b = 8

$width of stiffener base, b2 (must be >0, see Help) = H

Width b2 must be greater than zero. In fact, it should always be greater than a tenth of the module width, b. This segment of the module is considered by PANDA2 to consist of the skin plus the faying flange, if any, of the stiffener. In the PANDA2 model b2 must be greater than about a tenth of the total module width, b, because the section of width b2 is considered to be a separate segment which is discretized. If you make b2 too small, numerical difficulties might occur.

$width of stiffener base, b2 (must be >0, see Help) = 2.5
$height of stiffener (type H to see sketch), h = H

The height of the stiffener is measured from the surface of the stiffener base to the middle surface of the stiffener flange, as shown in Fig. 4.

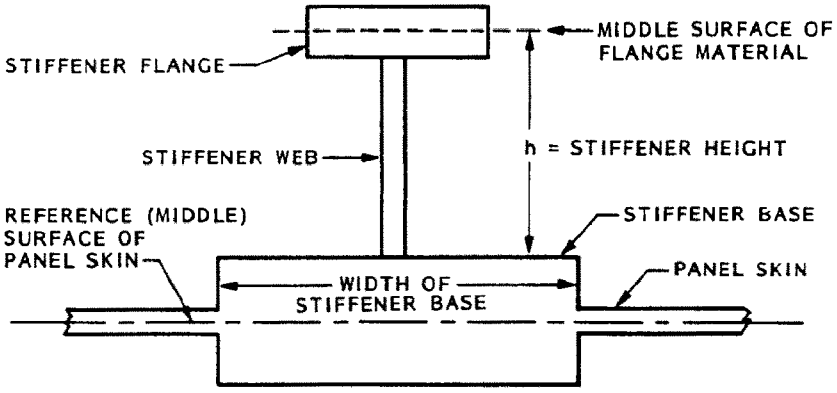

Fig. 4. Height of the stiffener is measured from the top of the stiffener base to the middle surface of the flange.

$width of outer flange of stiffener, w = 0.8
$width of hat base, w2 = 1.0
$Are the stringers cocured with the skin? = H

Stringers and skin may be cured separately, then glued together at room temperature, or they may be cocured. Which method is used very much affects the residual stresses and residual deformations of the panel. The residual stresses and deformations in cocured panels are caused by the different thermal expansion properties of the stringers and skin as the panel cools down from the curing temperature to room temperature. If this is not a composite panel, the answer here should probably be N, unless you are simulating the effect of a thermal gradient through the thickness of a stiffened panel.

$Are the stringers cocured with the skin? = Y
$What force/(axial length) will cause web peel-off? = H

Wanted here is the force-per-axial-length of stringer required to peel half of each stringer web and faying flange away from the panel skin. 'Half the stringer web' means half of the thickness. It is assumed that each half of the stringer web consists of layers that start as part or all of the faying flange on either side of the stiffener. These layers 'turn a corner' to become the stringer web. Tensile forces in the plane of the web, normal to the stringer axis, will therefore tend to peel the web halves from the faying flanges from which they derive. In the post-local buckling regime, such forces develop in each stringer web. These are calculated by PANDA2, and a constraint condition is formulated that indicates whether or not stringer popoff will occur because of web-peel-off caused by post-local buckling deformations. The force required here depends on what sort of adhesive is used between stringers and skin and its thickness. You will probably have to consult peel test data for this input datum. Units required are force/length. A typical value for graphite epoxy is in the range 40–100 lb/in. Figures 5, 6 and 7 show an example.

Figure 5(a) shows a T-stiffened panel module in its locally postbuckled state. The stiffener web bends because the flange, being deep, resists bending in its plane. Tensile forces develop in layers 1 and 2 of the web. These are maximum near the root of the web, and they tend to peel the web away from the panel skin. Figure 6(c) shows a schematic of a peel-test specimen, and Fig. 7 shows a graphite-epoxy peel-test specimen after failure. The force, F_p, per length of specimen normal to the plane of the paper is what is called for here.

$What force/(axial length) will cause web peel-off? = 50

Now you will be asked to provide properties for the panel module on a segment-by-segment basis, starting with the skin, which is segment 1, as shown in Fig. 3. In each segment of the module, the wall is considered to be divided into groups of layers. There are two types of groups:

(1) Default groups (12 layers, [90, 45, 0 −45, 0, 90]s, all of the same material and initially all of the same thickness. Winding angles cannot be chosen as decision variables in this option. Thicknesses can be decision variables. The notation [90, 45, 0, −45, 0, 90]s means [90, 45, 0, −45, 0, 90, 90, 0, −45, 0, 45, 90].)
(2) Just plain groups (any number of layers, any winding angles, any variety of material types and any variety of thickness. Winding angles can be chosen as decision variables.)

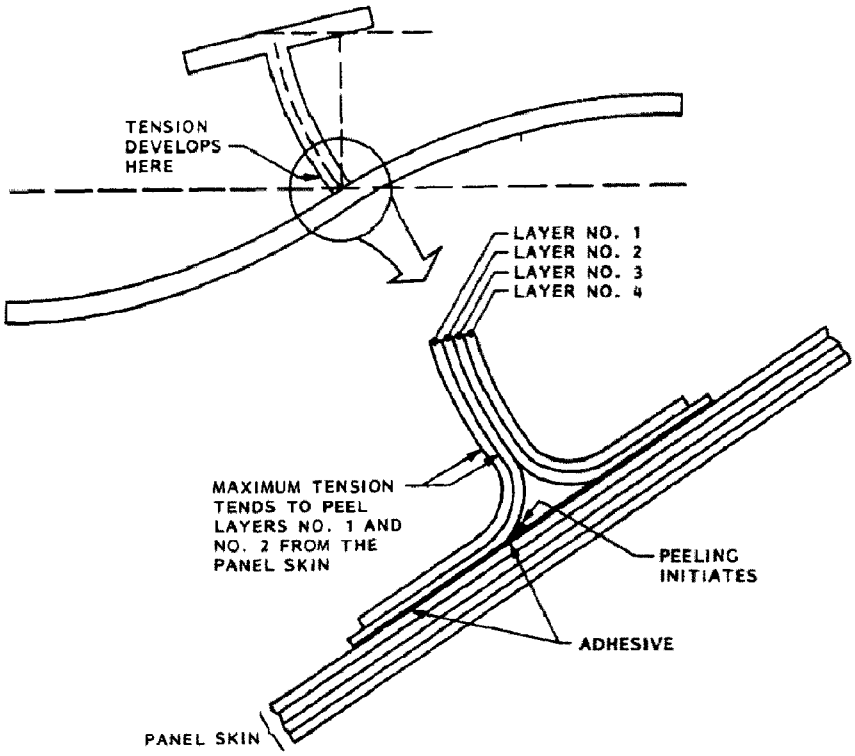

Fig. 5. Schematic of locally buckled panel, showing how bending of the stringer web gives rise to local tension in the plane of the web normal to the panel skin at the stringer line of attachment. This tension tends to peel the web from the panel skin, causing stiffener pop-off.

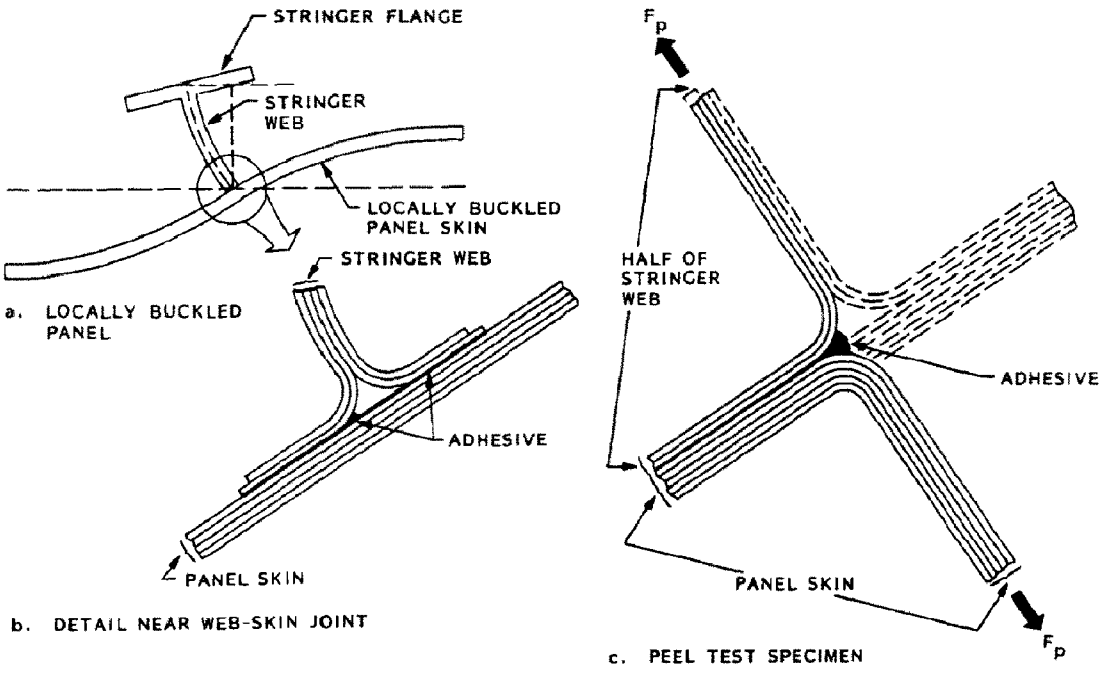

Fig. 6. Proper design of a T-peel test specimen that reproduces the local behavior near the root of the web of a stringer of a locally buckled panel that leads to stringer pop-off.

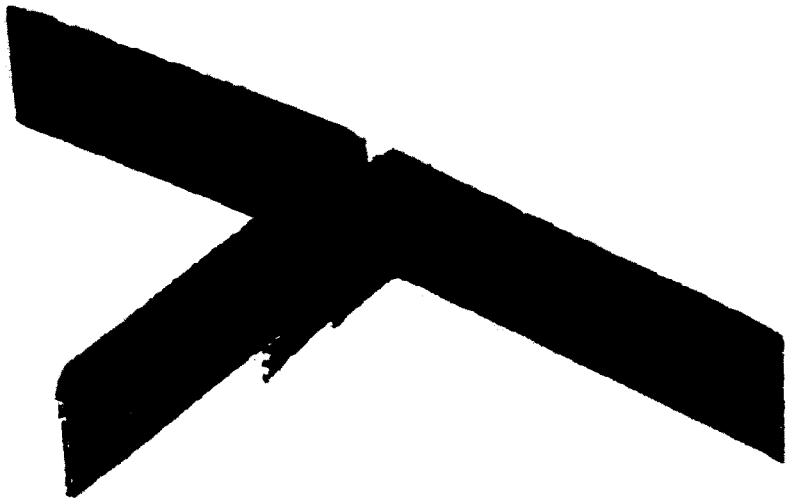

Fig. 7. Failed T-peel test specimen. In this case graphite-epoxy cloth is bonded to graphite-epoxy tape. The peel test simulates the behavior near the root of one of the webs of a hat-stiffened panel buckling locally as shown in Fig. 20(a).

For each default group (group type 1) you will be asked to give:

1. the thickness of one of the layers;
2. the material type.

For each 'just plain group' (group type 2) you must provide:

1. the number of layers through the thickness of the group;
2. whether the winding angles can ever be decision variables;
3. layer indices for each layer;
4. whether the layer is a new type of layer;
5. if it is a new type of layer: thickness, winding angle, and material type corresponding to that layer index.

$Is the next group of layers to be a 'default group'? = H

N means that you will provide a group of layers one-by-one. (This is the answer you will probably most often give.)

Y means that a group of layers will be generated each of which initially has the same thickness and material type. You will be asked to provide this single layer thickness and this material type indicator. A 'default group' has 12 layers of initially equal thickness with winding angles in the sequence: [90, 45, 0, −45, 0, 90]s.

Note that the thicknesses of the individual layers, which are initially the same in a default group, can become different during optimization iterations. However, the winding angles cannot be decision variables.

$Is the next group of layers to be a 'default group'? = N

$number of layers in the next group in Segment no. (1) = 2

$Can winding (layup) angles ever be decision variables? = H

Use with caution. Please note that weight does not change with layup angle, so that if you plan to optimize something and allow layup angles to be decision variables, you must also allow the thickness of at least one layer also to be a decision variable. Also, any decision variable that is zero or that becomes zero during design iterations is dropped by PANDA2 from the list of decision variables: it ceases being a decision variable from that moment on. Hence, if you specify that the layup angle of a layer is a decision variable, and if you also

specify that the layup angle of this layer is zero, this layer layup angle will not be a decision variable during optimization cycles. If you really want the layer layup angle to be a decision variable set it initially to 5 or 10° or use CHANGE to change it from zero to 5 to 10°.

$Can winding (layup) angles ever be decision variables? = N

$layer index (1, 2, . . .), for layer no. (1) = H

A layer index implies the following 'bundle' of properties:

1. Thickness of the layer.
2. Layup angle of the layer (degrees between the normal to the screen and the direction in which the modulus E1 (fiber direction) is measured).
3. Material type of the layer.

The three properties just listed are identical in two different layers if both of these layers have the same layer index.

$layer index (1, 2, . . .), for layer no. (1) = 1

$Is this a new layer type? = Y

Thickness, layup angle, material for layer index 1:

$thickness for layer no. (1) = .006

$layup angle (deg.) for layer index no. (1) = H

The definition of layup angle is: the angle in degrees measured from the normal to the screen to the direction in which the fiber modulus E1 is measured.

$layup angle (deg.) for layer index no. (1) = 45

$material index (1, 2, . . .) for layer index no. (1) = 2

$layer index (1, 2, . . .) for layer no. (2) = 2

$Is this a new layer type? = Y

Thickness, layup angle, material for layer index 2:

---MUCH MORE INTERACTIVE INPUT NOT SHOWN HERE---

3.3 *File generated during the interactive session with BEGIN*

An annotated file of this input is stored on HAT.BEG, which for this case is as follows:

```
N       $ Do you want a tutorial session and tutorial output?
  30    $ Panel length normal to the plane of the screen, L1
  24    $ Panel length in the plane of the screen, L2
A       $ Identify type of stiffener along L1 (N, T, J, R, A)
   8    $ stiffener spacing, b
 2.5    $ width of stiffener base, b2 (must be > 0, see Help)
 1.3    $ height of stiffener, h
0.80    $ width of outer flange of stiffener, w
   1    $ width of hat base, w2
Y       $ Are the stringers cocured with the skin?
 50.    $ What force/(axial length) will cause web peel-off?
N       $ Is the next group of layers a ''default group''?
   2    $ number of layers in the next group in Seg. no.(1)
N       $ Can winding (layup) angles ever be decision variables?
   1    $ layer index (1,2,...), for layer no.(1)
Y       $ Is this a new layer type?
0.006   $ thickness for layer index no.(1)
  45    $ layup angle (deg.) for layer index no.(1)
   2    $ material index (1,2,...) for layer index no.(1)
   2    $ layer index (1,2,...), for layer no.(2)
Y       $ Is this a new layer type?
0.006   $ thickness for layer index no.(2)
 -45    $ layup angle (deg.) for layer index no.(2)
   2    $ material index (1,2,...) for layer index no.(2)
Y       $ Any more layers or groups of layers in Seg. no.(1)
Y       $ Is the next group of layers a ''default group''?
N       $ Is this default group identical to previous group?
.0052   $ thickness of each layer of the default group
   1    $ material type in the default group
Y       $ Any more layers or groups of layers in Seg. no.(1)
N       $ Is the next group of layers a ''default group''?
   2    $ number of layers in the next group in Seg. no.(1)
N       $ Can winding (layup) angles ever be decision variables?
   2    $ layer index (1,2,...), for layer no.(15)
```

```
N       $ Is this a new layer type?
   1    $ layer index (1,2,...), for layer no.(16)
N       $ Is this a new layer type?
N       $ Any more layers or groups of layers in Seg. no.(1)
N       $ Is the next group of layers a ''default group''?
   5    $ number of layers in the next group in Seg. no.(2)
N       $ Can winding (layup) angles ever be decision variables?
   1    $ layer index (1,2,...), for layer no.(1)
N       $ Is this a new layer type?
   2    $ layer index (1,2,...), for layer no.(2)
N       $ Is this a new layer type?
   9    $ layer index (1,2,...), for layer no.(3)
Y       $ Is this a new layer type?
.0208   $ thickness for layer index no.(9)
   0    $ layup angle (deg.) for layer index no.(9)
   1    $ material index (1,2,...) for layer index no.(9)
  10    $ layer index (1,2,...), for layer no.(4)
Y       $ Is this a new layer type?
.0052   $ thickness for layer index no.(10)
  90    $ layup angle (deg.) for layer index no.(10)
   1    $ material index (1,2,...) for layer index no.(10)
   9    $ layer index (1,2,...), for layer no.(5)
N       $ Is this a new layer type?
Y       $ Any more layers or groups of layers in Seg. no.(2)
Y       $ Is the next group of layers a ''default group''?
Y       $ Is this default group identical to previous group?
   1    $ Which module seg. is the previous group in?
   1    $ Which default group in that segment is the same?
Y       $ Any more layers or groups of layers in Seg. no.(2)
N       $ Is the next group of layers a ''default group''?
   5    $ number of layers in the next group in Seg. no.(2)
N       $ Can winding (layup) angles ever be decision variables?
   9    $ layer index (1,2,...), for layer no.(18)
N       $ Is this a new layer type?
  10    $ layer index (1,2,...), for layer no.(19)
N       $ Is this a new layer type?
   9    $ layer index (1,2,...), for layer no.(20)
N       $ Is this a new layer type?
   2    $ layer index (1,2,...), for layer no.(21)
N       $ Is this a new layer type?
   1    $ layer index (1,2,...), for layer no.(22)
N       $ Is this a new layer type?
N       $ Any more layers or groups of layers in Seg. no.(2)
N       $ Is the next group of layers a ''default group''?
   4    $ number of layers in the next group in Seg. no.(3)
N       $ Can winding (layup) angles ever be decision variables?
   1    $ layer index (1,2,...), for layer no.(1)
N       $ Is this a new layer type?
   2    $ layer index (1,2,...), for layer no.(2)
N       $ Is this a new layer type?
   2    $ layer index (1,2,...), for layer no.(3)
N       $ Is this a new layer type?
   1    $ layer index (1,2,...), for layer no.(4)
N       $ Is this a new layer type?
N       $ Any more layers or groups of layers in Seg. no.(3)
N       $ Is the next group of layers a ''default group''?
  15    $ number of layers in the next group in Seg. no.(4)
N       $ Can winding (layup) angles ever be decision variables?
   1    $ layer index (1,2,...), for layer no.(1)
N       $ Is this a new layer type?
   2    $ layer index (1,2,...), for layer no.(2)
N       $ Is this a new layer type?
  11    $ layer index (1,2,...), for layer no.(3)
Y       $ Is this a new layer type?
.0208   $ thickness for layer index no.(11)
   0    $ layup angle (deg.) for layer index no.(11)
   1    $ material index (1,2,...) for layer index no.(11)
  10    $ layer index (1,2,...), for layer no.(4)
N       $ Is this a new layer type?
  11    $ layer index (1,2,...), for layer no.(5)
N       $ Is this a new layer type?
```

```
  10   $ layer index (1,2,...), for layer no.(6)
N      $ Is this a new layer type?
  11   $ layer index (1,2,...), for layer no.(7)
N      $ Is this a new layer type?
  10   $ layer index (1,2,...), for layer no.(8)
N      $ Is this a new layer type?
  11   $ layer index (1,2,...), for layer no.(9)
N      $ Is this a new layer type?
  10   $ layer index (1,2,...), for layer no.(10)
N      $ Is this a new layer type?
  11   $ layer index (1,2,...), for layer no.(11)
N      $ Is this a new layer type?
  10   $ layer index (1,2,...), for layer no.(12)
N      $ Is this a new layer type?
  11   $ layer index (1,2,...), for layer no.(13)
N      $ Is this a new layer type?
   2   $ layer index (1,2,...), for layer no.(14)
N      $ Is this a new layer type?
   1   $ layer index (1,2,...), for layer no.(15)
N      $ Is this a new layer type?
N      $ Any more layers or groups of layers in Seg. no.(4)
   1   $ choose external (0) or internal (1) stiffeners
N      $ Identify type of stiffener along L2 (N, T, J, R, A)
Y      $ Is the panel curved in the plane of the screen ?
 194   $ Radius of curvature (cylinder radius), R
N      $ Is panel curved normal to plane of screen? (ans. N)
N      $ Is this material isotropic (Y or N)?
 2.E7  $ modulus in the fiber direction,      E1(1)
14.E5  $ modulus transverse to fibers,       E2(1)
 7.E5  $ in-plane shear modulus,             G(1)
.0203  $ small Poisson's ratio,              NU(1)
 7.E5  $ out-of-plane shear modulus,         G13(1)
 4.E5  $ out-of-plane shear modulus,         G23(1)
 0.500E-07  $ thermal expansion along fibers, A1(1)
 0.160E-04  $ transverse thermal expansion,   A2(1)
270.   $ residual stress temperature (positive),TEMPTUR(1)
N      $ Want to specify  maximum effective stress (N)?
190000.  $ maximum tensile stress along fibers, matl(1)
182800.  $ max compressive stress along fibers, matl(1)
 9800   $ max tensile stress normal to fibers, matl(1)
25060   $ max compress stress normal to fibers,matl(1)
10000   $ maximum  shear  stress  in  material type(1)
0.056   $ weight density (greater than 0!) of mat'l type(1)
 Y      $ Is this unidirectional composite material (tape) ?
0.0052  $ Thickness of a single lamina of matl type(1)
 Y   $ Does max. allowable stress decrease for more layers?
 0   $ Degradation(%) in max. sig1(tension) for n layers, n=(2)
 0   $ Degradation(%) in max. sig1(comp.)   for n layers, n=(2)
20   $ Degradation(%) in max. sig2(tension) for n layers, n=(2)
 0   $ Degradation(%) in max. sig2(comp.)   for n layers, n=(2)
 0   $ Degradation(%) in max. sig12         for n layers, n=(2)
 Y   $ Any further Degradation with more layers of matl type(1)
 0   $ Degradation(%) in max. sig1(tension) for n layers, n=(3)
 0   $ Degradation(%) in max. sig1(comp.)   for n layers, n=(3)
30   $ Degradation(%) in max. sig2(tension) for n layers, n=(3)
 0   $ Degradation(%) in max. sig2(comp.)   for n layers, n=(3)
 0   $ Degradation(%) in max. sig12         for n layers, n=(3)
 Y   $ Any further Degradation with more layers of matl type(1)
 0   $ Degradation(%) in max. sig1(tension) for n layers, n=(4)
 0   $ Degradation(%) in max. sig1(comp.)   for n layers, n=(4)
37   $ Degradation(%) in max. sig2(tension) for n layers, n=(4)
 0   $ Degradation(%) in max. sig2(comp.)   for n layers, n=(4)
 0   $ Degradation(%) in max. sig12         for n layers, n=(4)
 N   $ Any further Degradation with more layers of matl type(1)
 N     $ Is this material isotropic (Y or N)?
 1.05E7 $ modulus in the fiber direction,      E1(2)
 1.05E7 $ modulus transverse to fibers,       E2(2)
  7.E5  $ in-plane shear modulus,              G(2)
 0.077  $ small Poisson's ratio,              NU(2)
  7.E5  $ out-of-plane shear modulus,         G13(2)
  4.E5  $ out-of-plane shear modulus,         G23(2)
```

```
 0.150E-05  $ thermal expansion along fibers, A1(2)
 0.150E-05  $ transverse thermal expansion,   A2(2)
 270.    $ residual stress temperature (positive),TEMPTUR(2)
 N       $ Want to specify  maximum effective stress (N)?
91035    $ maximum tensile stress along fibers, matl(2)
103845   $ max compressive stress along fibers, matl(2)
89880    $ max tensile stress normal to fibers, matl(2)
105000   $ max compress stress normal to fibers,matl(2)
 7000    $ maximum  shear  stress  in  material type(2)
0.056    $ weight density (greater than 0!), mat'l type(2)
 N       $ Is this unidirectional composite material (tape) ?
    1    $ Choose 0=simple support or 1=clamping
 - - - - - - - - END OF HAT.BEG FILE - - - - - - - - -
```

4. GENERATING BOSOR4-TYPE DISCRETIZED MODELS

Next, the commands

$SETUP
$BOSMODEL

are given by the user. These cause templates of the stiffness and load-geometric matrices to be set up for the buckling problems involving:

(1) a single panel module (Fig. 3), which is used for:

a. local buckling and postbuckling analysis;
b. wide column buckling analysis;
c. the nonlinear local static response of an axially stiffened panel to uniform normal pressure;

(2) the entire panel with smeared stiffeners, which is used for:

a. general instability for a panel with an axial load that varies across the span of the panel;
b. the nonlinear overall static response of a stiffened panel to uniform normal pressure.

Much of the BOSOR4 preprocessor software is used to do this. Therefore, in order to use PANDA2 you must have available to you the most recent version of BOSOR4.

5. PURPOSE OF DECIDE AND AN EXAMPLE

5.1 *Purpose of DECIDE*

In DECIDE you provide, in a conversationally interactive mode, strategy parameters for PANDA2 optimization. You choose which of the problem parameters are to be decision variables (allowed to change) during optimization and their lower and upper bounds. You also choose linked parameters, that is parameters that are not decision variables but vary in proportion with designated decision variables, and you assign factors of proportionality. Finally, you choose 'escape' variables, that is, variables that should be increased during any design iteration in which CONMIN fails to change the design. You should choose only thicknesses as escape variables. There is a default option for 'escape' variables in which only decision variables that are thicknesses are chosen. You should use the default option.

To repeat, there are three types of variables you choose in DECIDE:

1. *Decision variables*—These variables change independently of each other during optimization.
2. *Linked variables*—Each of these variables is proportional to one of the decision variables. You choose which one and you choose the factor of proportionality.
3. *Escape variables*—These are variables that, when increased, drive the design toward the feasible region. An escape variable must be a decision variable and should be a thickness. You can choose thickness variables by choosing the default option.

Your interactive input is saved on a file, NAME.DEC, in which NAME is the same name you used for BEGIN, SETUP, etc. In future runs of this or a similar case, you can edit the file NAME.DEC, then give the command DECIDE, and tell the system that you are using an existing file. If you err part way through a case, you can do a CONTROL Y, edit the NAME.DEC file, and re-issue the command DECIDE, telling

the system that you are adding to an existing file. The system will answer all the questions up to your error in a 'batch' mode, then return control to you. You can then complete the interactive input. (All of the PANDA2 interactive processors have this feature.)

Output from the PANDA2 processor DECIDE is stored in a file with the name NAME.OPD. You should print this file and inspect it to make sure that the case is as you intend it to be.

5.2 *Example of use of DECIDE in a runstream*

BEGIN	(you establish a starting design)
SETUP	(system sets up an input file for BOSOR4)
BOSMODEL	(system sets up BOSOR4-type discrete models)
DECIDE	(you establish optimization parameters)
MAINSETUP	(you set up loads and analysis strategy to be used by PANDAOPT)
PANDAOPT	(system performs PANDA2 optimization)

5.3 *Example: A hat-stiffened panel*

$Want to use default for thickness decision variables? = H

N means you choose thickness decision variables one-by-one.

Y means that for a certain range of layer index types, to be specified by you, the following will happen:

(1) The thickness of any layer type for which the winding (layup) angle is either 0 or 90° will be a decision variable.

(2) The thickness of any layer type will be a decision variable, regardless of winding (layup) angle, if the layup angle of any previous layer type within the given range of layer types is not equal to minus the layup angle of the current layer type.

(3) If the current layup angle is minus some previous layup angle within the given range of layer types, the current thickness will be linked to that previous thickness, and the linking constant C will be 1.0.

$Want to use default for thickness decision variables? = Y

```
LAYER INDEX TYPES FROM WHICH A RANGE MUST NOW BE CHOSEN

VAR. STR/ SEG. LAYER  CURRENT
NO.  RNG  NO.  NO.    VALUE          DEFINITION
 6   STR   1    1   6.0E-03  thickness for layer index no.(1 )
 7   STR   1    2   6.0E-03  thickness for layer index no.(2 )
 8   STR   1    3   5.2E-03  thickness for layer index no.(3 )
 9   STR   1    4   5.2E-03  thickness for layer index no.(4 )
10   STR   1    5   5.2E-03  thickness for layer index no.(5 )
11   STR   1    6   5.2E-03  thickness for layer index no.(6 )
12   STR   1    7   5.2E-03  thickness for layer index no.(7 )
13   STR   1    8   5.2E-03  thickness for layer index no.(8 )
14   STR   2    3   2.08E-02 thickness for layer index no.(9 )
15   STR   2    4   5.2E-03  thickness for layer index no.(10)
16   STR   4    3   2.08E-02 thickness for layer index no.(11)
```

$Lowest layer index for default decision variable = H

Choose a number from the right-hand side of the screen.

You are now specifying a range of layer indices for which you want PANDA2 to set up the decision variables. (These decision variables will be thicknesses only, not winding angles.) What is wanted now is the lowest layer index number for which you want PANDA2 to establish decision variables.

$Lowest layer index for default decision variable = 3

$Highest layer index for default decision variable = 8

```
                DECISION VARIABLES CHOSEN SO FAR
VAR. STR/ SEG. LAYER  CURRENT
NO.  RNG  NO.  NO.    VALUE          DEFINITION
 8   STR   1    3   5.2E-03  thickness for layer index no.(3 )
 9   STR   1    4   5.2E-03  thickness for layer index no.(4 )
10   STR   1    5   5.2E-03  thickness for layer index no.(5 )
12   STR   1    7   5.2E-03  thickness for layer index no.(7 )
13   STR   1    8   5.2E-03  thickness for layer index no.(8 )
```

PARAMETERS FROM WHICH A DECISION VAR. MUST NOW BE CHOSEN

VAR. NO.	STR/ RNG	SEG. NO.	LAYER NO.	CURRENT VALUE	DEFINITION
1	STR	0	0	8.0E+00	stiffener spacing, b
2	STR	0	0	2.5E+00	width of stiffener base, b2
3	STR	0	0	1.3E+00	height of stiffener, h
4	STR	0	0	8.0E-01	width of flange of stiffener, w
5	STR	0	0	1.0E+00	width of hat base, w2
6	STR	1	1	6.0E-03	thickness for layer index no.(1)
7	STR	1	2	6.0E-03	thickness for layer index no.(2)
14	STR	2	3	2.08E-02	thickness for layer index no.(9)
15	STR	2	4	5.2E-03	thickness for layer index no.(10)
16	STR	4	3	2.08E-02	thickness for layer index no.(11)

$Any more ranges of layer types for default decision variables? = N
$Any more decision variables (Y or N)? = Y

DECISION VARIABLES CHOSEN SO FAR

VAR. NO.	STR/ RNG	SEG. NO.	LAYER NO.	CURRENT VALUE	DEFINITION
8	STR	1	3	5.2E-03	thickness for layer index no.(3)
9	STR	1	4	5.2E-03	thickness for layer index no.(4)
10	STR	1	5	5.2E-03	thickness for layer index no.(5)
12	STR	1	7	5.2E-03	thickness for layer index no.(7)
13	STR	1	8	5.2E-03	thickness for layer index no.(8)

PARAMETERS FROM WHICH A DECISION VAR. MUST NOW BE CHOSEN

VAR. NO.	STR/ RNG	SEG. NO.	LAYER NO.	CURRENT VALUE	DEFINITION
1	STR	0	0	8.0E+00	stiffener spacing, b
2	STR	0	0	2.5E+00	width of stiffener base, b2
3	STR	0	0	1.3E+00	height of stiffener, h
4	STR	0	0	8.0E-01	width of flange of stiffener, w
5	STR	0	0	1.0E+00	width of hat base, w2
6	STR	1	1	6.0E-03	thickness for layer index no.(1)
7	STR	1	2	6.0E-03	thickness for layer index no.(2)
14	STR	2	3	2.08E-02	thickness for layer index no.(9)
15	STR	2	4	5.2E-03	thickness for layer index no.(10)
16	STR	4	3	2.08E-02	thickness for layer index no.(11)

Use an index from the left-hand column of the table above.
$Choose a decision variable (1, 2, 3, ...) = 2
$Lower bound of variable no. (2) = 1.5
$Upper bound of variable no. (2) = 2.5
$Any more decision variables (Y or N)? = Y

DECISION VARIABLES CHOSEN SO FAR

VAR. NO.	STR/ RNG	SEG. NO.	LAYER NO.	CURRENT VALUE	DEFINITION
2	STR	0	0	2.5E+00	width of stiffener base, b2
8	STR	1	3	5.2E-03	thickness for layer index no.(3)
9	STR	1	4	5.2E-03	thickness for layer index no.(4)
10	STR	1	5	5.2E-03	thickness for layer index no.(5)
12	STR	1	7	5.2E-03	thickness for layer index no.(7)
13	STR	1	8	5.2E-03	thickness for layer index no.(8)

PARAMETERS FROM WHICH A DECISION VAR. MUST NOW BE CHOSEN

VAR. NO.	STR/ RNG	SEG. NO.	LAYER NO.	CURRENT VALUE	DEFINITION
1	STR	0	0	8.0E+00	stiffener spacing, b
3	STR	0	0	1.3E+00	height of stiffener, h
4	STR	0	0	8.0E-01	width of flange of stiffener, w
5	STR	0	0	1.0E+00	width of hat base, w2
6	STR	1	1	6.0E-03	thickness for layer index no.(1)
7	STR	1	2	6.0E-03	thickness for layer index no.(2)
14	STR	2	3	2.08E-02	thickness for layer index no.(9)
15	STR	2	4	5.2E-03	thickness for layer index no.(10)
16	STR	4	3	2.08E-02	thickness for layer index no.(11)

$Choose a decision variable (1, 2, 3, ...) = 3
$Lower bound of variable no. (3) = 0.8
$Upper bound of variable no. (3) = 1.5
$Any more decision variables (Y or N)? = Y

```
          DECISION VARIABLES CHOSEN SO FAR
VAR. STR/ SEG. LAYER  CURRENT
NO.  RNG  NO.   NO.    VALUE          DEFINITION
 2   STR   0     0   2.5E+00  width of stiffener base, b2
 3   STR   0     0   1.3E+00  height of stiffener, h
 8   STR   1     3   5.2E-03  thickness for layer index no.(3 )
 9   STR   1     4   5.2E-03  thickness for layer index no.(4 )
10   STR   1     5   5.2E-03  thickness for layer index no.(5 )
12   STR   1     7   5.2E-03  thickness for layer index no.(7 )
13   STR   1     8   5.2E-03  thickness for layer index no.(8 )

PARAMETERS FROM WHICH A DECISION VAR. MUST NOW BE CHOSEN
VAR. STR/ SEG. LAYER  CURRENT
NO.  RNG  NO.   NO.    VALUE          DEFINITION
 1   STR   0     0   8.0E+00  stiffener spacing, b
 5   STR   0     0   1.0E+00  width of hat base, w2
 4   STR   0     0   8.0E-01  width of flange of stiffener, w
 6   STR   1     1   6.0E-03  thickness for layer index no.(1 )
 7   STR   1     2   6.0E-03  thickness for layer index no.(2 )
14   STR   2     3   2.08E-02 thickness for layer index no.(9 )
15   STR   2     4   5.2E-03  thickness for layer index no.(10)
16   STR   4     3   2.08E-02 thickness for layer index no.(11)

 - - -MORE DECISION VARIABLES CHOSEN IN THIS SAMPLE CASE- - -
```

$Any linked variables (Y or N)? = H

A linked variable is a variable that is not a decision variable, but is proportional to one of the decision variables, thus:

$$\text{(linked variable)} = C^*\text{(decision variable)},$$

in which C is a constant. For example, material layers with $+ALPHA$ degree orientation are usually matched with layers with $-ALPHA$ degree orientation. Suppose for a certain layer with layup angle $+ALPHA$, this layup angle is chosen as a decision variable. You want another layer in the same laminate to have the layup angle $-ALPHA$. Then, for this other layer

$$\text{(layup angle)} = -1.0^*\text{(layup angle of the layer with } +ALPHA).$$

The layup angle on the left-hand-side of the above equation is called a linked variable because its value is linked to that of the first mentioned layer. The linking constant $C = -1.0$ in this example.

$Any linked variables (Y or N)? = Y

```
            LINKED VARIABLES CHOSEN SO FAR
VAR. STR/ SEG. LAYER  CURRENT
NO.  RNG  NO.   NO.    VALUE          DEFINITION
11   STR   1     6   5.2E-03  thickness for layer index no.(6 )

PARAMETERS FROM WHICH A LINKED VARIABLE MUST NOW BE CHOSEN
VAR. STR/ SEG. LAYER  CURRENT
NO.  RNG  NO.   NO.    VALUE          DEFINITION
 1   STR   0     0   8.0E+00  stiffener spacing, b
 4   STR   0     0   8.0E-01  width of flange of stiffener, w
 7   STR   1     2   6.0E-03  thickness for layer index no.(2 )
15   STR   2     4   5.2E-03  thickness for layer index no.(10)
```

$Choose a linked variable (1, 2, 3, ...) = 4

```
LINKED VARIABLE MUST BE LINKED TO ONE OF THE DEC. VAR.
VAR. STR/ SEG. LAYER  CURRENT
NO.  RNG  NO.   NO.    VALUE          DEFINITION
 2   STR   0     0   2.5E+00  width of stiffener base, b2
 3   STR   0     0   1.3E+00  height of stiffener, h
 5   STR   0     0   1.0E+00  width of hat base, w2
```

```
 6   STR   1    1   6.0E-03  thickness for layer index no.(1 )
 8   STR   1    3   5.2E-03  thickness for layer index no.(3 )
 9   STR   1    4   5.2E-03  thickness for layer index no.(4 )
10   STR   1    5   5.2E-03  thickness for layer index no.(5 )
12   STR   1    7   5.2E-03  thickness for layer index no.(7 )
13   STR   1    8   5.2E-03  thickness for layer index no.(8 )
14   STR   2    3   2.08E-02 thickness for layer index no.(9 )
16   STR   4    3   2.08E-02 thickness for layer index no.(11)
```

$To which variable is this variable linked? = 5
$Assign a value to the linking constant, C(4) = 0.8

---ANOTHER LINKED VARIABLE IS CHOSEN---

$Any more linked variables (Y or N)? = N

```
          LINKED VARIABLES FOR THE OPTIMIZATION PROBLEM
VAR. STR/ SEG. LAYER  CURRENT
NO.  RNG  NO.   NO.    VALUE          DEFINITION
 4   STR   0    0   8.0E-01  width of flange of stiffener, w
 7   STR   1    2   6.0E-03  thickness for layer index no.(2 )
11   STR   1    6   5.2E-03  thickness for layer index no.(6 )
```

$Any escape variables (Y or N)? = H

An escape variable is a variable that when increased drives the design toward the feasible region. For example, in designs which are buckling-critical, local and general instability represent two constraint conditions that bound the feasible region. Increasing the thicknesses of any parts while keeping all other dimensions the same drives the design toward the feasible region (makes buckling less critical). Hence, a thickness should always be chosen as an escape variable. Other variables, such as layup angles, should not be used as escape variables, since their increase might well result in a decrease in the buckling load, hence driving the design toward the infeasible region.

$Any escape variables (Y or N)? = Y
$Want to have escape variables chosen by default? = H

Generally answer Y. PANDA2 will then automatically choose as escape variables all of the thicknesses that are decision variables. This is usually the best strategy and use of the default option saves you the trouble of doing it interactively.

$Want to have escape variables chosen by default? = Y

```
          ESCAPE VARIABLES FOR THE OPTIMIZATION PROBLEM
VAR. STR/ SEG. LAYER  CURRENT
NO.  RNG  NO.   NO.    VALUE          DEFINITION
 6   STR   1    1   6.0E-03  thickness for layer index no.(1 )
 8   STR   1    3   5.2E-03  thickness for layer index no.(3 )
 9   STR   1    4   5.2E-03  thickness for layer index no.(4 )
10   STR   1    5   5.2E-03  thickness for layer index no.(5 )
12   STR   1    7   5.2E-03  thickness for layer index no.(7 )
13   STR   1    8   5.2E-03  thickness for layer index no.(8 )
14   STR   2    3   2.08E-02 thickness for layer index no.(9 )
16   STR   4    3   2.08E-02 thickness for layer index no.(11)
```

5.4 *File produced during interactive session in DECIDE*

The interactive session in DECIDE generates the following input file for future runs of DECIDE. This file is called HAT.DEC:

```
Y      $ Do you want a tutorial session and tutorial output?
Y      $ Want to use default for thickness decs. variables?
   3   $ Lowest layer index for default decision variable
   8   $ Highest layer index for default decision variable
N      $ Any more ranges of layer types for defalt dec.var.?
Y      $ Any more decision variables (Y or N) ?
   2   $ Choose a decision variable (1,2,3,...)
 1.5   $ Lower bound of variable no.(2)
```

```
  2.5  $ Upper bound of variable no.(2)
Y      $ Any more decision variables (Y or N) ?
  3    $ Choose a decision variable (1,2,3,...)
 0.80  $ Lower bound of variable no.(3)
  1.5  $ Upper bound of variable no.(3)
Y      $ Any more decision variables (Y or N) ?
  5    $ Choose a decision variable (1,2,3,...)
 0.80  $ Lower bound of variable no.(5)
  2    $ Upper bound of variable no.(5)
Y      $ Any more decision variables (Y or N) ?
  6    $ Choose a decision variable (1,2,3,...)
0.006  $ Lower bound of variable no.(6)
0.012  $ Upper bound of variable no.(6)
Y      $ Any more decision variables (Y or N) ?
 14    $ Choose a decision variable (1,2,3,...)
.0052  $ Lower bound of variable no.(14)
.0260  $ Upper bound of variable no.(14)
Y      $ Any more decision variables (Y or N) ?
 16    $ Choose a decision variable (1,2,3,...)
.0052  $ Lower bound of variable no.(16)
.0260  $ Upper bound of variable no.(16)
N      $ Any more decision variables (Y or N) ?
Y      $ Any linked variables (Y or N) ?
  4    $ Choose a linked variable (1,2,3,...)
  5    $ To which variable is this variable linked?
 0.80  $ Assign a value to the linking constant, C(4)
Y      $ Any more linked variables (Y or N) ?
  7    $ Choose a linked variable (1,2,3,...)
  6    $ To which variable is this variable linked?
  1    $ Assign a value to the linking constant, C(7)
N      $ Any more linked variables (Y or N) ?
Y      $ Any escape variables (Y or N) ?
Y      $ Want to have escape variables chosen by default?
- - - - - - - - END OF HAT.DEC FILE - - - - - - - - -
```

5.5 *Output file produced by DECIDE*

The following is a partial listing of the file HAT.OPD...

SUMMARY OF INFORMATION FOR OPTIMIZATION ANALYSIS

VAR. NO.	DEC. VAR.	ESCAPE VAR.	LINK. VAR.	LINKED TO	LINKING CONSTANT	LOWER BOUND	CURRENT VALUE	UPPER BOUND	DEFINITION
1	N	N	N	0	0.00E+00	0.00E+00	8.0000E+00	0.00E+00	stiffener spacing, b
2	Y	N	N	0	0.00E+00	1.50E+00	2.5000E+00	2.50E+00	width of stiffener base, b2
3	Y	N	N	0	0.00E+00	8.00E-01	1.3000E+00	1.50E+00	height of stiffener, h
4	N	N	Y	5	8.00E-01	0.00E+00	8.0000E-01	0.00E+00	width of outer flange of stiffener, w
5	Y	N	N	0	0.00E+00	8.00E-01	1.0000E+00	2.00E+00	width of hat base, w2
6	Y	Y	N	0	0.00E+00	6.00E-03	6.0000E-03	1.20E-02	thickness for layer index no.(1)
7	N	N	Y	6	1.00E+00	0.00E+00	6.0000E-03	0.00E+00	thickness for layer index no.(2)
8	Y	Y	N	0	0.00E+00	5.20E-05	5.2000E-03	5.20E-01	thickness for layer index no.(3)
9	Y	Y	N	0	0.00E+00	5.20E-05	5.2000E-03	5.20E-01	thickness for layer index no.(4)
10	Y	Y	N	0	0.00E+00	5.20E-05	5.2000E-03	5.20E-01	thickness for layer index no.(5)
11	N	N	Y	9	1.00E+00	0.00E+00	5.2000E-03	0.00E+00	thickness for layer index no.(6)
12	Y	Y	N	0	0.00E+00	5.20E-05	5.2000E-03	5.20E-01	thickness for layer index no.(7)
13	Y	Y	N	0	0.00E+00	5.20E-05	5.2000E-03	5.20E-01	thickness for layer index no.(8)
14	Y	Y	N	0	0.00E+00	5.20E-03	2.0800E-02	2.60E-02	thickness for layer index no.(9)
15	N	N	N	0	0.00E+00	0.00E+00	5.2000E-03	0.00E+00	thickness for layer index no.(10)
16	Y	Y	N	0	0.00E+00	5.20E-03	2.0800E-02	2.60E-02	thickness for layer index no.(11)

---END OF DECIDE PROCESSING---

6. ESTABLISHING LOADS AND STRATEGY IN PANDA2

6.1 *Introduction*

Following execution of DECIDE, the user gives the command MAINSETUP. The following is a list of the interactive session that the command MAINSETUP invokes. In this particular session, the user has decided to use the tutorial option for a fixed design (no optimization).

6.2 *Example: a hat-stiffened panel*

$MAINSETUP (User establishes loading, type of analysis and strategy.)
$Do you want a tutorial session and tutorial output? Y

Next, provide in-plane loads, (N_1, N_2, N_{12}) and (N_{10}, N_{20}), which are considered to be applied to the panel edges. These are stress resultants in units, for example, of lb/in.

(N_1, N_2, N_{12}) constitute Load Set A (eigenvalue loads);
(N_{10}, N_{20}) are part of Load Set B (fixed and uniform loads).

In the absence of normal pressure, the loads corresponding to general instability bifurcation buckling are given by:

$$N_x(crit) = N_{10} + \text{eigenvalue} \times \text{factor-of-safety} \times N_1$$

$$N_y(crit) = N_{20} + \text{eigenvalue} \times \text{factor-of-safety} \times N_2$$

$$N_{xy}(crit) = \text{eigenvalue} \times \text{factor-of-safety} \times N_{12}.$$

Also, provide uniform normal pressure, p. In the presence of normal pressure, the loads corresponding to general instability bifurcation buckling are given by:

$$N_x(\text{crit}) = N_{10} + N_{10}(p) + \text{eigenvalue} \times \text{factor-of-safety} \times N_1$$

$$N_y(crit) = N_{20} + N_{20}(p) + \text{eigenvalue} \times \text{factor-of-safety} \times N_2$$

$$N_{xy}(crit) = \text{eigenvalue} \times \text{factor-of-safety} \times N_{12},$$

in which $N_{10}(p)$ and $N_{20}(p)$ are stress resultants induced by the normal pressure.

You are allowed to provide up to five load sets, that is, up to five sets of $(N_1, N_2, N_{12}, N_{10}, N_{20}, p)$. PANDA2 will generate buckling and stress or strain constraints corresponding to each of the load sets that you provide. The resulting design will be the best that PANDA2 can find that is subjected during its mission to all of the load sets.

For each combination (N_1, N_2, N_{12}) you will have to provide two 'factors-of-safety', FSGEN and FSLOC, for general and local buckling. The purpose of these factors is to compensate for initial imperfections. These factors depend on the geometry and loading, and there is a huge literature on the difficult subject of 'imperfection sensitivity'. A recent survey is contained in the book by David Bushnell [30].

Now, please provide the first Load Set A $(N_1, N_2, N_{12})\ldots$

$Resultant (e.g. lb/in.) normal to the plane of screen, $N_1(1) = H$

What is wanted is the applied line load in the L1 (axial) direction in units of force/length. Negative for compression. If this axial load varies in the L2 (circumferential) direction, use the largest compressive value applied to that edge of the panel. What is wanted now is the axial load in Load Set A, that is, the eigenvalue load: the load to be multiplied by the critical load factor (the eigenvalue) in computations of the critical applied load.

$Resultant (e.g. lb/in.) normal to the plane of screen, $N_1(1) = -3000$
$Resultant (e.g. lb/in.) in the plane of the screen, $N_2(1) = H$

What is wanted is the applied resultant, N_2, in the L2 (circumferential) direction (units of force/length). Negative for compression. This circumferential load is assumed to be uniform over the entire panel. Again, what is wanted here is the Load Set A (eigenvalue parameter) circumferential stress resultant, N_2.

$Resultant (e.g. lb/in.) in the plane of the screen, $N_2(1) = 0$
$In-plane shear in load set A, $N_{12}(1) = H$

Positive sense is the same as for the PANDA program. (See [1, Fig. 2].) Units are force/length. The in-plane shear is assumed to be uniform over the entire panel. Please note that no fixed in-plane shear component is permited $(N_{120} = 0)$.

$In-plane shear in load set A, $N_{12}(1) = 1000$
$Does the axial load vary in the L2 direction? = H

The L2 direction is in the plane of the screen (circumferential). If you answer Y you will next be asked to provide values of N_x at the beginning and end of the panel edge which lies in the plane of the screen. PANDA2 assumes that N_x varies linearly across this edge and is uniform in the direction normal to the plane of the screen. If you answer N the axial load will be uniform over the entire panel.

$Does the axial load vary in the L2 direction? = N
$Factor of safety for general instability, FSGEN(1) = H

This factor should account for unknown initial imperfections and the approximate manner in which the general instability load factor is calculated in PANDA2. Panels that buckle locally at loads far below the design load are not particularly sensitive to initial imperfections. For such panels, use

$$1.0 < \text{FSGEN} < 1.4.$$

Panels designed so that local and general instability loads are nearly equal are somewhat sensitive to initial imperfections, and FSGEN should be about 1.4 even if the panel is flat. Axially stiffened cylinders under axial compression should usually have FSGEN = 2.

Axially compressed monocoque cylinders under axial compression should have FSGEN = 4 if $r/t > 300$; FSGEN = 2 if $r/t < 100$. Cylinders under uniform external pressure should have FSGEN = 1.4. Cylinders under uniform torsion (in-plane shear) should have FSGEN = 1.3.

NOTE: The above are general guidelines only. For more details, consult the extensive NASA literature, ASME Code Case N-284, and run PANDA with the option to get interaction curves for imperfect shells. Also see [30].

$Factor of safety for general instability, FSGEN(1) = 1

$Factor of safety for local instability, FSLOC(1) = H

By 'local' is meant buckling between stringers and rings. Usually, the stringers are closely spaced, so that the portion of shell between them is very flat. In such cases the structure is stable in the locally post-buckled range and FSLOC should be 1.0.

If your stringers are spaced far apart, so that the panel between them subtends a fairly large angle (greater than 20°, say), then the panel starts to become sensitive to initial imperfections, and FSLOC should be larger than unity. You should consult the literature on this, in particular [30].

$Factor of safety for local instability, FSLOC(1) = 1

Next, please provide the fixed stress resultants, N_{10} and N_{20}. These are part of the in-plane loads in Load Set B. Note that no fixed in-plane shear resultant, N_{120}, is permitted. The fixed stress resultants, N_{10} and N_{20}, are not multiplied by the eigenvalue (eigenvalue = load factor determined in bifurcation buckling analyses). The critical general instability load can be calculated from:

$$N_x(crit) = N_{10} + N_{10}(p) + \text{eigenvalue} \times \text{factor-of-safety} \times N_1$$

$$N_y(crit) = N_{20} + N_{20}(p) + \text{eigenvalue} \times \text{factor-of-safety} \times N_2$$

$$N_{xy}(crit) = \text{eigenvalue} \times \text{factor-of-safety} \times N_{12}.$$

Note that the fixed loads are added to any stress resultants that are generated by thermal curing of a composite panel. The loads that you are now asked to provide are fixed applied loads. They would arise, for example, in the case of an internally pressurized aircraft fuselage, in which the (N_{10}, N_{20}) from the internal pressure, p ($N_{10} = pr/2$; $N_{20} = pr$), are known, fixed quantities acting in addition to unknown (N_1, N_2, N_{12}) generated for example by gust loads.

$Resultant (e.g. lb/in.) normal to plane of screen, $N_{10}(1) = H$

Same sign convention as for N_1: positive for tension. This is a Load Set B quantity.

$Resultant (e.g. lb/in.) normal to plane of screen, $N_{10}(1) = 0$

$Resultant (e.g. lb/in.) in the plane of the screen, $N_{20}(1) = H$

Same sign convention as for N_2: positive for tension. This is a Load Set B quantity.

$Resultant (e.g. lb/in.) in the plane of the screen, $N_{20}(1) = 0$

$Uniform applied pressure (positive upward), $p(1) = H$

This pressure p is part of Load Set B (fixed loads). Positive pressure always pushes upward. (Please refer to the sketches of the panel module for physical picture of what 'upward' means; see Figs 1, 2 and 8.) If the panel is curved and if stringers are external, positive pressure is inside the cylinder. If the panel is curved and if stringers are internal, positive pressure is outside the cylinder. If there are no stringers, positive pressure is inside the cylinder. Figure 8 shows the sign convention for pressure and curvature.

Note that this pressure is used primarily for determination of nonlinear bending-stretching of the panel module and of the entire panel. The pressure should not be used to calculate linear, uniform, statically determinate, fixed in-plane resultants, such as $N_{x0} = pr/2$ and $N_{y0} = pr$ for a hydrostatically internally pressurized complete cylindrical shell.

$Uniform applied pressure (positive upward), $p(1) = 1.0$

$Want to provide another load set (N_1, N_2, N_{12}, N_{10}, N_{20}, p)? = H

You can provide up to five load sets, that is, five sets of (N_1, N_2, N_{12}, N_{10}, N_{20}, p).

$Want to provide another load set (N_1, N_2, N_{12}, N_{10}, N_{20}, p)? = N

$Want to include effect of transverse shear deformation? = H

If you answer Y reduction factors are computed for various kinds of general, semi-general and local instability and crippling. These factors reduce the eigenvalues computed from classical 'normals-remain-normal' shell theory. The reduction factors are based on Timoshenko beam theory [32]. That is, a typical reduction factor has the form:

$$k = 1/[1 + nN_x\lambda/(tG_{13})],$$

in which: n is a shape factor (1.2 is now used); N_x is the local stress resultant (lb/in. for example); λ is the

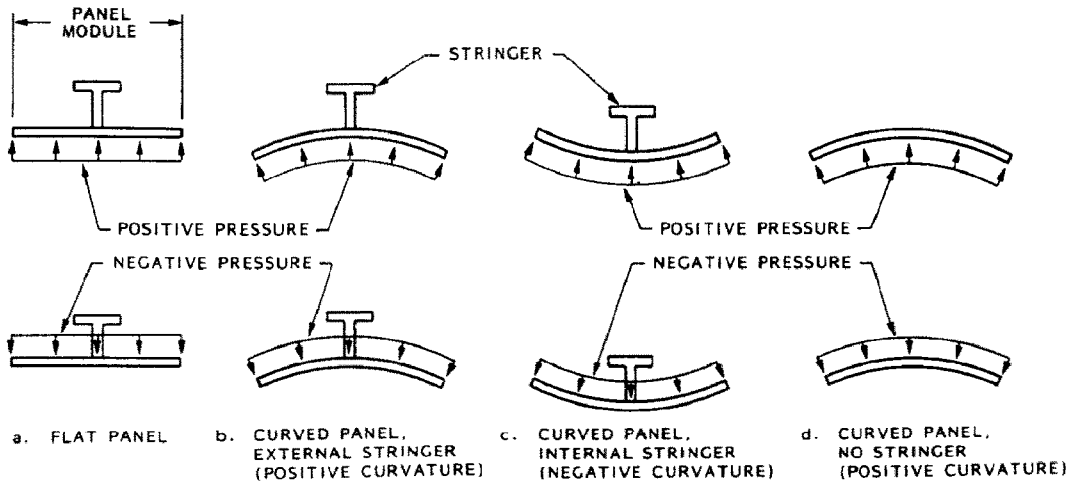

Fig. 8. Sign convention for pressure and curvature. In PANDA2 the following rules hold: (1) The stringer is always 'on top' of the panel skin; (2) If the panel is curved the user always supplies a positive number for the radius of curvature; (3) If the user specifies 'external stringer' the panel curvature will be positive, as shown in (b); (4) If the user specifies 'internal stringer' the panel curvature will be negative, as shown in (c); (5) If there are no stringers the curvature will be positive as, in (d); (6) Positive pressure always pushes upward; negative pressure always pushes downward, no matter what the curvature is or where the stiffeners are.

critical eigenvalue computed from 'normals-remain-normal' theory; t is the local effective thickness of the wall; and G_{13} is the local effective transverse shear stiffness.

$Want to include effect of transverse shear deformation? = Y

$IQUICK = quick analysis indicator (0 or 1) = H

IQUICK = 0 means discrete BOSOR4-type model will be treated.

IQUICK = 1 means only closed-form types of models will be included.

It may be best to start out with IQUICK = 1 and to refine the design later with the longer IQUICK = 0 type of analysis. In any case, before you are done with a case, you must definitely use the IQUICK = 0 option.

$IQUICK = quick analysis indicator (0 or 1) = 0

$NPRINT = output index (1 = good, 2 = debug, 3 = too much) = H

Usually use 1. NPRINT = 3 really gets a lot of output. NPRINT = 2 yields the $C(i,j)$ matrices, the evolution of eigenvalues during inverse power iterations, local buckling modal displacements, and redistributed loads due to bowing and local postbuckling behavior. Do not use 2 if you are doing an optimization analysis.

$NPRINT = output index (1 = good, 2 = debug, 3 = too much) = 1

$Choose type of analysis (1 = opt., 2 = fixed design) = H

1. Means an optimization analysis will be performed. Note that you must have previously chosen decision variables in a DECIDE run!
2. Means PANDA2 will perform a buckling analysis of a fixed design.

$Choose type of analysis (1 = opt., 2 = fixed design) = 2

$Do you want plots (Y or N)? = Y

$Do you want to vary N for minimum local buckling load? = H

N is the number of axial half-waves in the local buckling mode. Computer time can be saved if you are confident that the number of axial halfwaves N that you next choose is truly the critical value for local skin buckling. Generally answer Y.

$Do you want to vary N for minimum local buckling load? = Y

$Do you want to choose a starting N for local buckling? = H

N is the number of axial halfwaves between adjacent rings, or if no rings are present, along the entire axial length of the panel. PANDA2 starts with N calculated from the formula:

$$N = (C(5,5)/C(4,4)) \times (\text{axial length between rings})/(\text{stringer spacing} - \text{stringer base width}) + 2,$$

which is based on experimental observations that local buckles of uniformly axially compressed long, narrow, isotropic plates are almost square. However, from previous experience on this and other similar cases, you may wish to use a different starting value for N. Generally you should answer this question N for 'no'.

$Do you want to choose a starting N for local buckling? = N

$Maximum possible number of axial halfwaves, NMAX = H

Use a number that you think is less than the critical wavenumber for crippling of any stiffener parts and greater than the critical wavenumber for buckling of the skin between stiffeners. If you are unsure, use a number equal to the axial length of the panel between rings divided by the width of the stringer web. This is not a critical input. It prevents searching for minimum local buckling loads for very high axial wavenumbers that may correspond to local crippling of the stringer parts.

$Maximum possible number of axial halfwaves, NMAX = 30

$Factor of safety for stress, FSSTR = H

This factor should account for the fact that the theory used to calculate stress, especially if local buckling of the skin occurs well below the design load, is approximate. The failure criterion is also approximate. Use

$$1.0 < \text{FSSTR} < 1.5.$$

$Factor of safety for stress, FSSTR = 1

$Do you want to use Koiter post-local-buckling stiffness? = H

A panel can be designed so that the skin between stiffeners buckles locally at loads well below the design allowable. If you wish to permit local buckling in the design, answer Y. The analysis will then account for the effect of local skin buckling on the overall stiffness of the panel and will calculate stresses in the locally postbuckled skin.

$Do you want to use Koiter post-local-buckling stiffness? = Y

---END OF INTERACTIVE SESSION FOR MAINSETUP---

6.3 *File generated during the interactive session in MAINSETUP*

The interactive session just completed yields the following file, which is called HAT.OPT:

```
 Y     $ Do you want a tutorial session and tutorial output?
-3000  $ Resultant (e.g.lb/in) normal to plane of screen,N1
 0     $ Resultant (e.g. lb/in) in the plane of the screen,N2
 1000  $ In-plane shear in load set A,                  N12
 N     $ Does the axial load vary in the L2 direction?
 1     $ Factor of safety for general instability, FSGEN( 1)
 1     $ Factor of safety for local instability, FSLOC( 1)
 0     $ Resultant (e.g.lb/in) normal to plane of screen,N10
 0     $ Resultant (e.g.lb/in) in the plane of the screen,N20
 1.0   $ Uniform applied pressure (positive upward), P( 1)
 N     $ Want to provide another set (N1,N2,N12,N10,N20,p)?
 Y     $ Want to include effect of transverse shear deform.?
 0     $ IQUICK = quick analysis indicator (0 or 1)
 1     $ NPRINT= output index (1=good, 2=debug, 3=too much)
 2     $ Choose type of analysis (1=opt., 2=fixed design)
 Y     $ Do you want plots?
 Y     $ Do you want to vary N for min. local buckling load?
 N     $ Do you want to choose starting N for local buckling?
 30    $ Maximum possible number of axial halfwaves, NMAX
 1     $ Factor of safety for stress, FSSTR
 Y     $ Want to use Koiter post-local-buckling stiffness?

  - - - - END OF PROCESSING BY MAINSETUP - - - - - - -
```

7. PANDA2 MAINPROCESSOR FLOW OF CALCULATIONS

7.1 *Introduction*

Next, the user launches a batch run of the PANDA2 mainprocessor by typing the command PANDAOPT. The following is a modified list of the file HAT.OPM, which contains the results of this tutorial run. Please note that these results correspond to a hat-stiffened panel that had been optimized in previous runs. The starting design is given in the section on BEGIN and the final design is given in the following. The tutorial output has been modified to make it more suitable for presentation in a paper (introduction of section numbers, etc.).

```
BEGINNING OF TUTORIAL RUN....

********** LOAD SET NO. 1  **************
APPLIED LOADS IN LOAD SET A ("eigenvalue" loads):
    Applied     axial       stress resultant, N1= -3.0000E+03
    Applied circumferential stress resultant, N2= -3.1623E+00
    Applied    in-plane     shear  resultant,N12=  1.0000E+03
```

```
APPLIED LOADS IN LOAD SET B ( fixed uniform loads):
    Applied     axial       stress resultant,N10=  0.0000E+00
    Applied circumferential stress resultant,N20=  0.0000E+00
    Applied    in-plane    shear  resultant,N120=  0.0000E+00
    Applied pressure (positive for internal), P =  1.0000E+00
```

The following calculations are performed for each of up to five sets of user-supplied in-plane loads, N_x, N_y and N_{xy}, and pressure, p. These calculations are performed in SUBROUTINE STRUCT, which is the structural analyzer in the PANDA2 mainprocessor.

7.2 *Sign conventions for various types of panel analysis performed by PANDA2*

It is important to document the sign conventions used for stress resultants; moments; strains; changes in curvature; panel curvature; normal displacement; coordinate, z, normal to the reference surface of each segment of the panel module cross section; coordinate, x, along the panel axis (normal to the screen); coordinate y (in the plane of the screen); and coordinate, s, along the reference surface of each segment in the panel module cross section. These sign conventions are defined here. Also defined here is the convention for numbering the layers in each segment of the panel module cross section. A typical panel module is depicted in Figs 9 and 10.

The PANDA2 system consists of elements of three analyses, each of which has slightly different sign conventions:

(1) BOSOR4-type models of discretized panel modules;
(2) PANDA-type models (closed form buckling formulas);
(3) BOSOR4-type model of discretized entire panel span with smeared stiffeners.

Figures 9 and 10 show a typical panel module. For analysis type (1), BOSOR4-type models of discretized panel modules, the sign convention is described below the figures.

The (s, x, z) coordinate system is local to each panel module segment and forms a right-handed system in each module segment. The (x, y, z) coordinate system is used in the PANDA-type of analysis [1].

Positive pressure pushes up on the panel module shown in Fig. 9. The pressure acts only on the skin (segments 1, 2 and 5 in Fig. 9). Figure 8 shows the sign convention for pressure. The axial load, N_x, is normal to the plane of the screen and positive for tension. Units of this load are force/(length of s coordinate). The hoop or circumferential load, N_y, acts parallel to the plane of the screen and is positive for tension. The units of this load are force/(length of x coordinate). Positive N_{xy} is shown in [1, Fig. 2]. It is also shown in Fig. 11, along with x and y coordinates and positive winding angle. Positive reference surface strains, e_x and e_y, are tensile. Positive e_{xy} follows from positive N_{xy}. Positive axial moment, M_x, causes compression in the

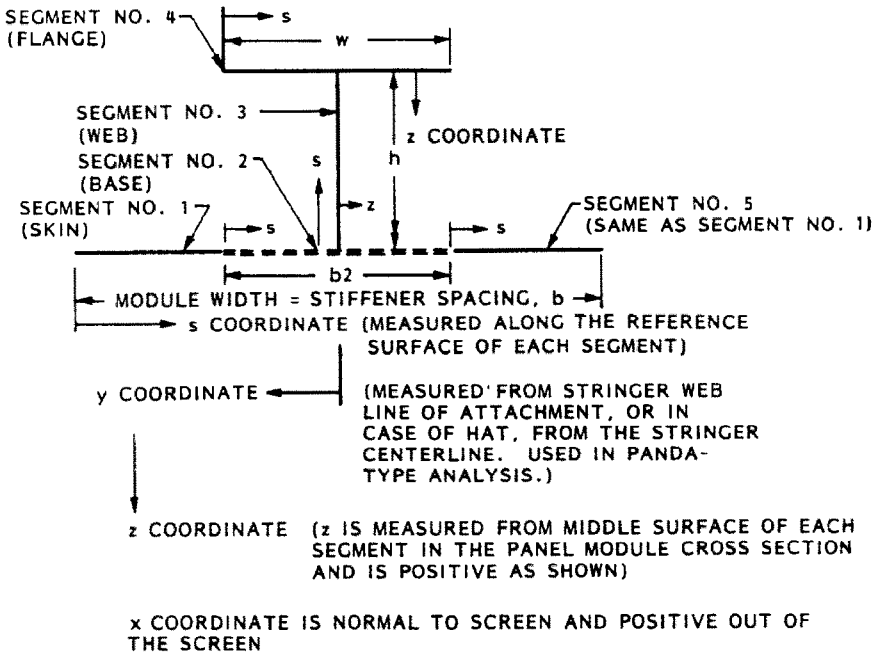

Fig. 9. Typical panel module cross section, coordinates, segments, nomenclature.

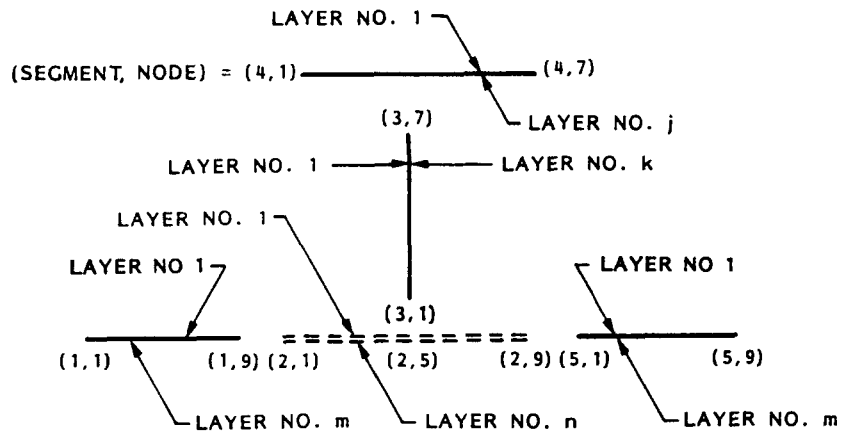

Fig. 10. Exploded view, showing layers and (segment, node) numbers.

fibers normal to the screen at the bottom of Fig. 9 and tension in the fibers at the top of Fig. 9. That is, the bottom surface of the panel module becomes concave under positive M_x.

Positive change in axial curvature, k_x, has the same effect as positive axial moment, M_x. The bottom surface becomes concave. Positive hoop (circumferential) moment, M_y, causes compression in the fibers parallel to the plane of the screen at the bottom of Fig. 9 and tension in the fibers at the top of Fig. 9. That is, the bottom surface of the panel module sketched in Fig. 9 becomes concave under positive M_y. Positive change in hoop (circumferential) curvature has the same effect as positive hoop moment, M_y.

Positive twisting moment, M_{xy}, tends to force the left side of Fig. 9 downward and the right side of Fig. 9 upward. The twisting angle increases anticlockwise as we proceed out of the screen, that is along the increasing x coordinate. Positive twist, k_{xy}, has the same effect as positive M_{xy}.

For the discretized panel module model the following kinematic expressions hold:

$$\text{axial change in curvature, } k_x = w_{,xx}$$

$$\text{hoop change in curvature, } k_y = w_{,yy}$$

$$\text{twist, } k_{xy} = -2w_{,xy}. \tag{7.1}$$

Strains anywhere in the module cross section are given by:

$$e_x(z) = e_x(\text{ref. surf.}) - zk_x(\text{ref. surf.})$$

$$e_y(z) = e_y(\text{ref. surf.}) - zk_y(\text{ref. surf.})$$

$$e_{xy}(z) = e_{xy}(\text{ref. surf.}) + zk_{xy}(\text{ref. surf.}). \tag{7.2}$$

For cylindrical panels, positive curvature means that the panel skin in the module shown in Fig. 9 is concave downward, that is, Segments 1, 2 and 5 in Fig. 9 are concave downward. The generators of the cylinder are normal to the screen. Figure 8 shows the sign convention for curvature and pressure. The user always supplies

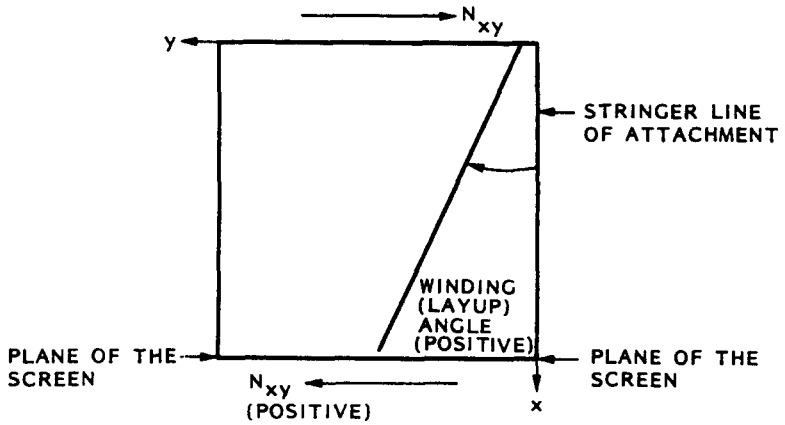

Fig. 11. Positive in-plane shear, winding (layup) angle.

a positive number for radius of curvature, and the sign of the curvature in the PANDA2 model depends upon whether the user specifies 'external' or 'internal' for stringers. If there are no stringers, the curvature is positive.

Positive normal deflection in each panel module segment is in the same direction as positive z. Positive u is in the same direction as positive s. These two displacement components lie in the plane of the screen or parallel to the plane of the screen. Positive axial displacement v is normal to the screen, and is out of the screen (toward the viewer), in the same direction as positive x. The kinematic expressions for each panel module segment are analogous to eqns (7.1) and (7.2). The coordinate y is replaced by the coordinate s (Fig. 9).

In PANDA2 the layers of the panel skin (segments 1, 2 and 5 in Fig. 10) are numbered from the top to the bottom. In all segments of the panel module, layer no. 1 is the leftmost layer as we face in the direction of increasing s coordinate, and layer no. NLAYERS is the rightmost layer.

In the analysis of the entire panel with smeared stiffeners and discretized span (span refers to the length of panel edge in the plane of the screen), a positively curved cylindrical panel is again concave downward, with the curved edges being the edge that lies in the plane of the screen at $x = 0$ and the opposite edge at $x = L$, where L is the length of the panel in the direction of the generators of the cylinder, which is normal to the screen.

7.3 *Summary of computations required for each design modification*

The following is a list of computations which must be performed for each load combination every time the panel design is modified and when design sensitivities (gradients of design constraint conditions and objective function) are being generated:

1. Calculation of residual state of the panel after cure and before application of any load.
2. Calculation of the prebuckled state of the panel after application of the load. The goal of this step is to determine the distribution of stress resultants over the cross section of the panel module. For each of up to five combinations of (N_x, N_y, N_{xy} and p), there may exist two load sets: Load Set A, which includes all loads associated with eigenvalues (load factors for buckling), and Load Set B, which includes all constant (non-eigenvalue) loads. The static response to uniform normal pressure, p, is calculated from nonlinear geometric theory (moderately large rotations).
3. Calculation of local buckling (minimization with respect to axial wave number n is required). Two ranges of number of axial waves are checked, a high-n range and a low-n range.
4. Calculation of local post buckling behavior from Koiter theory.
5. Calculation of stress components in material coordinates and establishment of minimum stress margins (five margins required for each material type: tension and compression parallel and perpendicular to the fibers and in-plane shear).
6. Calculation of general buckling, including the deleterious effect of locally post-buckled skin (reduced tangent stiffness) and nonuniformity of stress resultants distributed over the cross section of the panel.
7. Calculation of crippling load factors for the stiffener parts.
8. Calculation of the current weight of the panel.

8. CALCULATION OF CONSTITUTIVE MATRICES $C(i,j)$ FOR EACH PANEL MODULE SEGMENT AND $C_s(i,j)$ FOR THE PANEL WITH SMEARED STIFFENERS

8.1 *Calculation of* C(i, j) *and thermal resultants in each module segment*

First, calculate the integrated constitutive coefficients, $C(i,j)$, for each segment of the panel module ($i,j = 1, 2, \ldots, 6$); 'panel module' is defined in Figs 12 and 13. Calculate thermal resultants, THERM(i), $i = 1, 2, \ldots, 6$, for each segment of the panel module; calculate $C_s(i,j)$, THERMS(i, j) for the panel with smeared stiffeners. Calculate local and general thermal strains. (first call to SUBROUTINE GETCIJ in SUBROUTINE STRUCT).

The stiffened panel is considered to be divided into several identical modules, as shown in Figs 12 and 13.

The constitutive law used in PANDA2 for all segments is based on the principle of shell theory in which the stress–strain relationship is integrated through the thickness. In SUBROUTINE GETCIJ we seek the

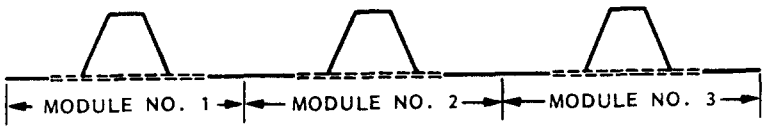

Fig. 12. Panel with three hat modules.

THIS ANALYSIS IS FOR A MODULE WITH HAT-SHAPED
(TRAPEZOIDAL) STIFFENER...

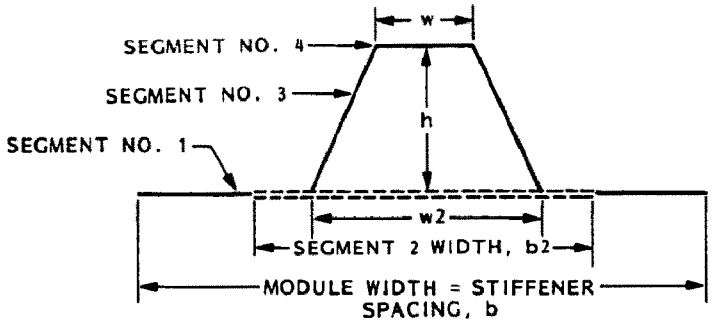

Fig. 13. Single panel module with hat stiffener.

6×6 matrix $C(i,j)$ and the six-component vector $N_T(i)$, which for each segment of the single panel module occur in the thickness-integrated stress–strain relationship thus:

$$\begin{Bmatrix} N_x \\ N_s \\ N_{xs} \\ M_x \\ M_s \\ M_{xs} \end{Bmatrix} = \begin{bmatrix} C_{11} & C_{12} & C_{13} & C_{14} & C_{15} & C_{16} \\ C_{21} & C_{22} & C_{23} & C_{24} & C_{25} & C_{26} \\ C_{31} & C_{32} & C_{33} & C_{34} & C_{35} & C_{36} \\ C_{41} & C_{42} & C_{43} & C_{44} & C_{45} & C_{46} \\ C_{51} & C_{52} & C_{53} & C_{54} & C_{55} & C_{56} \\ C_{61} & C_{62} & C_{63} & C_{64} & C_{65} & C_{66} \end{bmatrix} \begin{Bmatrix} e_x \\ e_s \\ e_{xs} \\ k_x \\ k_s \\ k_{xs} \end{Bmatrix} - \begin{Bmatrix} N_{tx} \\ N_{ts} \\ N_{txs} \\ M_{tx} \\ M_{ts} \\ M_{txs} \end{Bmatrix}, \tag{8.1}$$

in which $N = N_x, N_s, N_{xs}, M_x, M_s, M_{xs}$ are the stress and moment resultants in any panel module segment; $[C]$ is the 6×6 integrated constitutive law; $E = e_x, e_s, e_{xs}, k_x, k_s, k_{xs}$ are the strains and changes in curvature of the reference surface of the corresponding panel module segment; and $N_T = N_{tx}, N_{ts}, N_{txs}, M_{tx}, M_{ts}, M_{txs}$ are the thermal stress and moment resultants due to curing the composite material panel.

For all panel module segments PANDA2 uses the midddle surface of each segment wall as the reference surface for that segment. The same reference surface is used for all segments that comprise the panel skin.

We also need the thermal strains and changes in curvature E_T that would occur if each segment of the panel module were free to strain and warp after curing by itself. These six quantities are derived from the constitutive law above by setting $N = N_x, N_s, N_{xs}, M_x, M_s, M_{xs}$ equal to zero and solving for $E_T = e_x, e_s, e_{xs}, k_x, k_s, k_{xs}$:

$$E_T = [C]^{-1} N_T. \tag{8.2}$$

If the panel is stiffened by both stringers and rings, then $[C]$, N_T and E_T are calculated for two panel module configurations: (1) the panel module that represents a cross section normal to the x-axis, and (2) the panel module that represents a cross section normal to the y-axis.

In addition to the integrated constitutive matrix $[C]$, thermal loads N_T, and thermal deformations E_T for each segment of each panel module, the PANDA2 analysis requires analogous quantities $[C_s]$, N_{Ts} and E_{Ts}, for the panel with smeared stiffeners. These quantities are also computed in SUBROUTINE GETCIJ. Quantities are calculated for the panel with stringers smeared (between rings); for the panel with rings smeared (between stringers); and for the panel with both stringers and rings smeared. The panel deformations E_{Ts} caused by curing are calculated in SUBROUTINE STRTHM, which is called by SUBROUTINE GETCIJ. These calculations are described in Sec. 8.4.

8.2 *Reduction factors for transverse shear deformation*

In order to determine appropriate knockdown factors for the weakening effect of transverse shear deformation, integrated stiffnesses for transverse shear deformation are required. These coefficients are calculated in SUBROUTINE GETCIJ. It is assumed that the reduction factor for a plate is the same as it is for a Timoshenko beam. The equation for the reduction or knockdown factor, given by Timoshenko and Goodier [32], is:

reduction factor for axially compressed wide column =

$$K = 1/[1 + nN(\text{EULER})/(T_{eff}G_{eff})], \tag{8.3}$$

in which n is a shape factor (1.2 for homogeneous sheet); N(EULER) is the critical axial stress resultant from Kirchoff theory; T_{eff} is the effective wall thickness (simply the total wall thickness in our case); and G_{eff} is the effective transverse shear stiffness. For a layered medium, G_{eff} is assumed to be given by:

$$G_{eff} = \frac{T_{eff}}{\sum_{i=1}^{nlayers} [t(i)/G_{13}(i)]}, \tag{8.4}$$

in which $t(i)$ is the thickness of the ith layer and $G_{13}(i)$ is the transverse shear stiffness of the ith layer measured in the axial-circumferential (panel) coordinate system rather than in the material coordinate system.

For biaxial loading with or without in-plane shear loading, the 'effective' knockdown factor, KSTAR, is derived assuming that the interaction relation between the three in-plane loading components N_x, N_y, N_{xy}, is given by:

$$(N_x/N_{xcr})^2 + (N_y/N_{ycr})^2 + (N_{xy}/N_{xycr})^2 = 1. \tag{8.5}$$

We assume that the 'effective' knockdown factor for transverse shear deformation weakening, KSTAR, can by derived from:

$$(1 - \text{KSTAR})^2 = (1 - K_x)^2 + (1 - K_y)^2 + (1 - K_{xy})^2, \tag{8.6}$$

in which K_x is the transverse shear deformation weakening knockdown factor for compression in the x-direction (axial compression); K_y is the knockdown factor for compression in the y-direction; and K_{xy} is the knockdown factor for in-plane shear.

The computations for G_{eff} and T_{eff} occur in SUBROUTINE GETCIJ. The computations for KSTAR occur in SUBROUTINE SHRRED, which is called by subroutines that calculate bifurcation buckling loads neglecting transverse shear deformation effects (GENSTB and LOCAL).

8.3 *Example: The* C(i, j) *for the segments in the hat-stiffened module shown in Fig.* 13

CONSTITUTIVE MATRIX C(I,J) FOR SKIN-STRINGER MODULE — THERMAL {NT} ETHERM {ET}

UNIQUE SKIN-STRINGER MODULE SEGMENT NO. 1: PANEL SKIN — THERMAL {NT} ETHERM {ET}

7.2450E+05	2.3621E+05	-9.1024E-05	-9.7656E-04	-3.6621E-04	2.3668E-06	-3.3247E+02	-3.1369E-04
2.3621E+05	6.2738E+05	-1.1978E-02	-3.6621E-04	-7.3242E-04	-1.3759E-05	-3.5351E+02	-4.4537E-04
-9.1024E-05	-1.1978E-02	2.5017E+05	2.3668E-06	-1.3759E-05	0.0000E+00	0.0000E+00	-2.1438E-11
-9.7656E-04	-3.6621E-04	2.3668E-06	2.6910E+02	1.8285E+02	9.2078E+00	3.5763E-07	-3.9497E-10
-3.6621E-04	-7.3242E-04	-1.3759E-05	1.8285E+02	3.7425E+02	9.2078E+00	3.5763E-07	-2.9808E-11
2.3668E-06	-1.3759E-05	0.0000E+00	9.2078E+00	9.2078E+00	1.8411E+02	0.0000E+00	-8.0070E-12

UNIQUE SKIN-STRINGER MODULE SEGMENT NO. 2: STRINGER BASE — THERMAL {NT} ETHERM {ET}

1.9945E+06	2.6594E+05	-1.8197E-04	2.4414E-04	-4.8828E-04	6.6235E-06	-5.2284E+02	-1.5941E-04
2.6594E+05	9.2449E+05	-2.0046E-02	-4.8828E-04	-1.2207E-03	-2.0710E-06	-7.5466E+02	-7.7045E-04
-1.8197E-04	-2.0046E-02	3.0113E+05	6.6235E-06	-2.0710E-06	-7.3242E-04	0.0000E+00	-5.1385E-11
2.4414E-04	-4.8828E-04	6.6235E-06	3.8020E+03	7.1145E+02	9.2078E+00	1.4305E-06	2.6153E-10
-4.8828E-04	-1.2207E-03	-2.0710E-06	7.1145E+02	1.6262E+03	9.2078E+00	1.4305E-06	1.3908E-10
6.6235E-06	-2.0710E-06	-7.3242E-04	9.2078E+00	9.2078E+00	7.5111E+02	0.0000E+00	-5.6297E-12

UNIQUE SKIN-STRINGER MODULE SEGMENT NO. 3: STRINGER WEB — THERMAL {NT} ETHERM {ET}

1.5331E+05	1.1971E+05	0.0000E+00	2.4414E-04	1.8311E-04	0.0000E+00	-1.1057E+02	-4.0500E-04
1.1971E+05	1.5331E+05	0.0000E+00	1.8311E-04	2.4414E-04	0.0000E+00	-1.1057E+02	-4.0500E-04
0.0000E+00	0.0000E+00	1.1699E+05	0.0000E+00	0.0000E+00	1.8311E-04	0.0000E+00	0.0000E+00
2.4414E-04	1.8311E-04	0.0000E+00	7.3589E+00	5.7461E+00	0.0000E+00	-1.4901E-07	1.8331E-09
1.8311E-04	2.4414E-04	0.0000E+00	5.7461E+00	7.3589E+00	0.0000E+00	-1.4901E-07	1.8331E-09
0.0000E+00	0.0000E+00	1.8311E-04	0.0000E+00	0.0000E+00	5.6156E+00	0.0000E+00	0.0000E+00

UNIQUE SKIN-STRINGER MODULE SEGMENT NO. 4: STRINGER FLANGE — THERMAL {NT} ETHERM {ET}

1.4453E+06	1.5581E+05	-4.5473E-04	-9.8877E-03	-1.2207E-03	2.7285E-12	-3.9594E+02	-2.0172E-04
1.5581E+05	7.8427E+05	-2.0809E-02	-1.2207E-03	-4.5166E-03	1.1642E-10	-5.4348E+02	-6.6999E-04
-4.5473E-04	-2.0809E-02	1.7887E+05	2.7285E-12	1.1642E-10	-1.4648E-03	0.0000E+00	-7.8457E-11
-9.8877E-03	-1.2207E-03	2.7285E-12	1.3085E+03	3.2662E+02	-2.2235E-07	2.3842E-06	-1.5505E-11
-1.2207E-03	-4.5166E-03	1.1642E-10	3.2662E+02	7.0713E+02	-1.0175E-05	2.3842E-06	-1.2488E-09
2.7285E-12	1.1642E-10	-1.4648E-03	-2.2235E-07	-1.0175E-05	3.3652E+02	0.0000E+00	-1.4587E-16

8.4 *Smearing the stiffener bases and stiffeners*

Calculations now proceed inside SUBROUTINE GETCIJ, just before the first of three calls to SUBROUTINE SMRCIJ: In the first call to SUBROUTINE SMRCIJ the stringers are smeared out, and [C], N_T, E_T, T_{eff} and G_{eff} are computed as if the panel had no transverse stiffeners (rings). The smeared-stringer quantities are stored in arrays and vectors according to the following:

[C] is stored in CX(i, j, 5)

N_T is stored in THERMX(i, 5)

E_T is stored in ETHRMX(i, 5)

T_{eff} is stored in TEFF(1)

G_{eff} is stored in GTX(m, 5); m = 1 for G_{13}, m = 2 for G_{23}.

In the second call to SUBROUTINE SMRCIJ the rings are smeared out, and $[C]$, N_T, E_T, T_{eff} and G_{eff} are computed as if the panel had no axial stiffeners (stringers). The smeared-ring quantities are stored in arrays and vectors according to the following:

$[C]$ is stored in CY(i, j, 5)

N_T is stored in THERMY(i, 5)

E_T is stored in ETHRMY(i, 5)

T_{eff} is stored in TEFF(2)

G_{eff} is stored in GTY(m, 5); m = 1 for G_{13}, $m = 2$ for G_{23}.

In the third call to SUBROUTINE SMRCIJ both stringers and rings are smeared out, and $[C]$, N_T, E_T, T_{eff} and G_{eff} are stored in arrays and vectors according to the following:

$[C]$ is stored in CS(i, j)

N_T is stored in THERMS(i)

E_T is stored in ETHRMS(i)

G_{eff} is stored in GTS(m); m = 1 for G_{13}, m = 2 for G_{23}.

The smearing process is based upon the following assumptions:

(1) No in-plane shear load is carried by stiffener webs or flanges that stand out from the panel skin wall. No in-plane transverse load is carried by these segments either; they carry load only along their axes. (Note that this entire discussion about the $C(i, j)$ holds only for the models in which the stiffeners are smeared out, not for the discretized, branched single module models. Also, it holds only for the phase of the problem in which the skin between stringers is unbuckled.)

(2) The in-plane shear resultant is constant throughout the panel skin, both in the thin and in the thick parts of the skin.

(3) The axial membrane strain component, e_x, is the same in the thin part of the skin and in the part where the stringer bases exist. (This statement of course does not apply when Koiter post-local-buckling theory is being discussed. We are dealing in SUBROUTINE GETCIJ only with the unbuckled panel stiffnesses. However, it is always true that the end shortening is the same in the thin part of the skin and in the part where the stringer bases exit.)

(4) The change in axial curvature, k_x, is the same in the unbuckled thin part of the skin and in the part where the stringer bases exist.

(5) The circumferential membrane strain component, e_y, is the same in the unbuckled thin part of the skin and in the part where the ring bases exist.

(6) The circumferential change in curvature, k_y, is the same in the unbuckled thin part of the skin and in the part where the ring bases exist.

(7) Transverse shear stiffness is governed by panel module segment no. 1 (thin part of skin) and stiffener segments 3 and 4: The effect of transverse shear deformation weakening on the thickened areas under the stiffeners (segment 2) is assumed to be the same as that in segment 1.

(8) For hat stiffeners, the torsional rigidity calculated from the enclosed-area shear flow formula, valid only if there is no local deformation of the hat cross section in the buckling mode, is 'knocked down' by a factor $\phi = 0.3$. This factor was established as being reasonable during buckling analysis and tests of aluminum semi-sandwich corrugated cylindrical shells. The work is documented in [33].

The following derivation refers to a 'panel module'. A 'panel module' is defined in Figs 12 and 13. If stiffeners run both ways there are two modules:

(1) the module whose cross section is perpendicular to the x axis;
(2) the module whose cross section is perpendicular to the y axis.

In the plan view shown in Fig. 14, both 'x' and 'y' modules appear. The horizontal dimension of the figure is the stringer spacing and the vertical dimension is the ring spacing.

The starting point for derivation of the constitutive law for the panel module with stringers and rings with thickened bases is the mathematical expression of equilibrium of resultants N_x and N_y (eqns (8.7) and (8.8)

below) and of moments M_x and M_y (eqns (8.9) and (8.10) below). These equilibria are written in terms of the forces and moments in the various panel module parts:

Part (1) = panel skin.
Part (2) = stringer base and stringer web(s) and flange.
Part (3) = ring base and ring web(s) and flange.
Part (4) = the region where ring and stringer bases overlap.

A plan view of the panel module with stringer and ring bases is depicted in Fig. 14.

We know that if we 'cut' along the lower horizontal edge of the panel module sketched in Fig. 14, the average axial resultant will be equal to the applied axial resultant, N_x. The left-hand side of eqn (8.7) below expresses this average axial resultant.

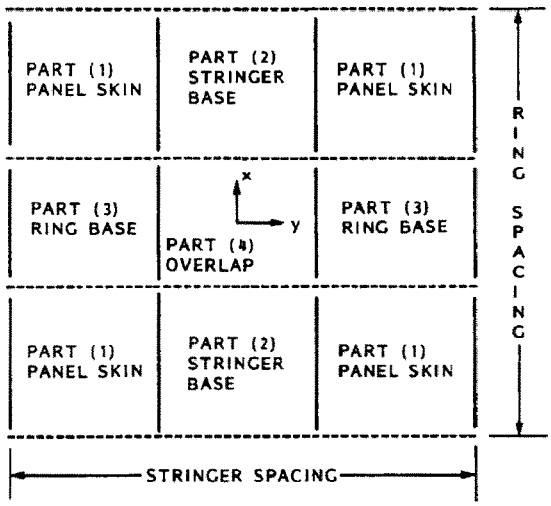

Fig. 14. Plan view of a single panel module used in the development of the integrated constitutive law C_{ij} for the panel with smeared stringers and rings.

Similarly, along the same edge the average moment resultant is equal to the applied moment resultant, M_x. The left-hand side of eqn (8.9) below expresses this average moment resultant, M_x.

Also, if we 'cut' horizontally along the y axis in Fig. 14, the average axial resultant must again be equal to the applied resultant, N_x, and the average moment must be equal to the applied moment, M_x. These average loads are expressed in the right-hand sides of eqns (8.7) and (8.9), respectively.

Now we can express analogous relationships for vertical 'cuts' along the left-hand side of the figure above and along the x-axis. The average stress resultant along both vertical 'cuts' must equal the applied hoop resultant, N_y; the average moment resultant along both vertical 'cuts' must equal the applied moment resultant, M_y. Equations (8.8) and (8.10) below express these force and moment equilibria (continuity). The four equations expressing continuity of forces and moments are as follows:

$$B_{11}N_x(1) + B_{12}N_x(2) + N_{stringer}(2) = B_{11}N_x(3) + B_{12}N_x(4) + N_{stringer}(3) \tag{8.7}$$

$$B_{22}N_y(1) + B_{21}N_y(3) + N_{ring}(3) = B_{22}N_y(2) + B_{21}N_y(4) + N_{ring}(2) \tag{8.8}$$

$$B_{11}M_x(1) + B_{12}M_x(2) + M_{stringer}(2) = B_{11}M_x(3) + B_{12}M_x(4) + M_{stringer}(3) \tag{8.9}$$

$$B_{22}M_y(1) + B_{21}M_y(3) + M_{ring}(3) = B_{22}M_y(2) + B_{21}M_y(4) + M_{ring}(2). \tag{8.10}$$

The numbers in parentheses, $N_x(1)$ for example, refer to the part or region of the panel illustrated in Fig. 14. The coefficients, B_{11}, B_{12}, B_{21}, B_{22} are given by:

$$B_{11} = (\text{stringer spacing} - \text{stringer base width})/(\text{stringer spacing})$$

$$B_{12} = (\text{stringer base width})/(\text{stringer spacing})$$

$$B_{21} = (\text{ring base width})/(\text{ring spacing})$$

$$B_{22} = (\text{ring spacing} - \text{ring base width})/(\text{ring spacing}). \tag{8.11}$$

For Parts (1), (2) and (3) the resultants and moments in terms of the strains and changes in curvature are given by:

$$N_x(i) = C_{11}(i)e_x(i) + C_{12}(i)e_y(i) + C_{14}(i)k_x(i) + C_{15}(i)k_y(i) - N_{tx}(i) \tag{8.12}$$

$$N_y(i) = C_{12}(i)e_x(i) + C_{22}(i)e_y(i) + C_{24}(i)k_x(i) + C_{25}(i)k_y(i) - N_{ty}(i) \tag{8.13}$$

$$M_x(i) = C_{14}(i)e_x(i) + C_{24}(i)e_y(i) + C_{44}(i)k_x(i) + C_{45}(i)k_y(i) - M_{tx}(i) \tag{8.14}$$

$$M_y(i) = C_{15}(i)e_x(i) + C_{25}(i)e_y(i) + C_{45}(i)k_x(i) + C_{55}(i)k_y(i) - M_{ty}(i), \tag{8.15}$$

in which (i) refers to the part number (region) of the panel and

$e_x(i)$ is the axial (x-dir.) reference surface strain

$e_y(i)$ is the transverse (y-dir.) reference surface strain

$k_x(i)$ is the change in axial curvature of the reference surface

$k_y(i)$ is the change in hoop curvature of the reference surface. (8.16)

The constitutive law for part (4), the region where the stiffener bases overlap, is:

$$N_x(4) = C_{11}(4)e_x(3) + C_{12}(4)e_y(2) + C_{14}(4)k_x(3) + C_{15}(4)k_y(2) - N_{tx}(4) \tag{8.17}$$

$$N_y(4) = C_{12}(4)e_x(3) + C_{22}(4)e_y(2) + C_{24}(4)k_x(3) + C_{25}(4)k_y(2) - N_{ty}(4) \tag{8.18}$$

$$M_x(4) = C_{14}(4)e_x(3) + C_{24}(4)e_y(2) + C_{44}(4)k_x(3) + C_{45}(4)k_y(2) - M_{tx}(4) \tag{8.19}$$

$$M_y(4) = C_{15}(4)e_x(3) + C_{25}(4)e_y(2) + C_{45}(4)k_x(3) + C_{55}(4)k_y(2) - M_{ty}(4). \tag{8.20}$$

In eqns (8.17 through 8.20) the $C_{ij}(4)$ and $N_{tx}(4)$, $N_{ty}(4)$, $M_{tx}(4)$, $M_{ty}(4)$ are assumed to be the averages of these quantities in regions 2 and 3.

The constitutive law for all stiffeners (stringers and rings) has the form:

$$N_{stringer}(i) = STFL1\, e_x(i) + STFM1\, k_x(i) - STFT1 \tag{8.21}$$

$$N_{ring}(i) = STFL2\, e_y(i) + STFM2\, k_y(i) - STFT2 \tag{8.22}$$

$$M_{stringer}(i) = STFM1\, e_x(i) + STFMM1\, k_x(i) - STFMT1 \tag{8.23}$$

$$M_{ring}(i) = STFM2\, e_y(i) + STFMM2\, k_y(i) - STFMT2, \tag{8.24}$$

in which the coefficients $STFL1$, $STFL2$, $STFM1$, $STFM2$, $STFT1$, $STFT2$, $STFMM1$, $STFMM2$, $STFMT1$, $STFMT2$ are derived in SUBROUTINE CSTIF.

It is assumed that the strains and changes in curvature in the various parts (1), (2) and (3) of the panel module are related to each other as follows:

$$\begin{aligned} e_x(\text{overall average}) &= B_{22}e_x(1) + B_{21}e_x(3) \\ e_y(\text{overall average}) &= B_{11}e_y(1) + B_{12}e_y(2) \\ e_x(2) &= e_x(1) \\ e_y(3) &= e_y(1) \end{aligned} \tag{8.25}$$

and

$$\begin{aligned} k_x(\text{overall average}) &= B_{22}k_x(1) + B_{21}k_x(3) \\ k_y(\text{overall average}) &= B_{11}k_y(1) + B_{12}k_y(2) \\ k_x(2) &= k_x(1) \\ k_y(3) &= k_y(1). \end{aligned} \tag{8.26}$$

The constitutive law for the panel with smeared stiffeners is calculated as follows.

1. Express eqns (8.7–8.10) in terms of $e_x(i)$, $e_y(i)$, $k_x(i)$, $k_y(i)$, $i = 1, 2, 3$, through use of eqns (8.12)–(8.24). Coefficients for the resulting equations are derived in SUBROUTINE EQSP67.

2. Eliminate $e_x(1)$, $e_y(1)$, $k_x(1)$, $k_y(1)$ from these equations by use of eqns (8.25) and (8.26).

3. Solve eqns (8.9) and (8.10), thus expressed, for $k_x(3)$ and $k_y(2)$ in terms of $e_x(3)$, $e_y(2)$, and average strains and changes in curvature, e_x, e_y, k_x, k_y, over the entire panel module. Obtain the coefficients D_{11}, D_{12}, D_{13}, D_{14}, D_{15}, D_{16}, D_{17} and D_{21}, D_{22}, D_{23}, D_{24}, D_{25}, D_{26}, D_{27}, which occur in the relationships:

$$\begin{aligned} k_x(3) &= D_{11} + D_{12}e_x(3) + D_{13}e_y(2) + D_{14}e_x + D_{15}e_y + D_{16}k_x + D_{17}k_y \\ k_y(2) &= D_{21} + D_{22}e_x(3) + D_{23}e_y(2) + D_{24}e_x + D_{25}e_y + D_{26}k_y + D_{27}k_y. \end{aligned} \tag{8.27}$$

4. Solve eqns (8.7) and (8.8) for $e_x(3)$ and $e_y(2)$ in terms of the average panel module strains and changes in curvature, e_x, e_y, k_x, k_y, thus obtaining the coefficients F_{11}, F_{12}, F_{13}, F_{14}, F_{15} and F_{21}, F_{22}, F_{23}, F_{24}, F_{25} which occur in the relationships:

$$e_x(3) = F_{11} + F_{12}e_x + F_{13}e_y + F_{14}k_x + F_{15}k_y$$
$$e_y(2) = F_{21} + F_{22}e_x + F_{23}e_y + F_{24}k_x + F_{25}k_y. \tag{8.28}$$

5. Plug the results from step 4 into the expressions for $k_x(3)$ and $k_y(2)$ to yield

$$k_x(3) = G_{11} + G_{12}e_x + G_{13}e_y + G_{14}k_x + G_{15}k_y$$
$$k_y(2) = G_{21} + G_{22}e_x + G_{23}e_y + G_{24}k_x + G_{25}k_y. \tag{8.29}$$

Steps 2 through 5 are performed in SUBROUTINE EPSKAP.

The constitutive law with smeared stiffeners is then derived starting from the left-hand sides of eqns (8.7)–(8.10) equated to the proper combinations of smeared-stiffener coefficients and average strains and changes in curvature and integrated thermal forces and moments:

$$B_{11}N_x(1) + B_{12}N_x(2) + N_{stringer}(2) = C_{11}e_x + C_{12}e_y + C_{14}k_x + C_{15}k_y - N_{tx} \tag{8.30}$$
$$B_{22}N_y(1) + B_{21}N_y(3) + N_{ring}(3) = C_{12}e_x + C_{22}e_y + C_{24}k_x + C_{25}k_y - N_{ty} \tag{8.31}$$
$$B_{11}M_x(1) + B_{12}M_x(2) + M_{stringer}(2) = C_{14}e_x + C_{24}e_y + C_{44}k_x + C_{45}k_y - M_{tx} \tag{8.32}$$
$$B_{22}M_y(1) + B_{21}M_y(3) + M_{ring}(3) = C_{15}e_x + C_{25}e_y + C_{45}k_x + C_{55}k_y - M_{ty}. \tag{8.33}$$

The smeared-stiffeners C_{ij} are determined with use of eqns (8.5)–(8.26) in eqns (8.30)–(8.33) above. Coefficients of e_x, e_y, k_x and k_y on the resulting left-hand sides are set equal to the corresponding coefficients on the right-hand sides. This final computation is performed in SUBROUTINE CSMEAR.

Given the C_{ij} and the thermal resultants N_{tx}, N_{ty}, M_{tx}, M_{ty}, the residual thermal strains and changes in curvature, e_{tx}, e_{ty}, e_{txy}, k_{tx}, k_{ty}, k_{txy}, are calculated in SUBROUTINE STRTHM. In this calculation the applied loads, N_x, N_y, N_{xy}, M_x, M_y, M_{xy}, are assumed to be zero, the C_{ij} matrix is inverted, and the system of six linear equations is solved for the residual strains and changes in curvature. These quantities play a role in later analyses: the residual strains affect the stress constraints in the optimization analysis; thermal resultants derived from the residual strains affect local instability of the various segments of the panel module, and changes in curvature create a bowing of the panel which increases as compressive loads are applied. An example is given later that demonstrates the complex interactions between thermal residual stresses and deformation (bowing) and local buckling and postbuckling behavior of a blade-stiffened panel.

8.4.1 *Example: results for the hat-stiffened panel*

```
C(i,j) with smeared stringers only...                                    THERMAL (NT)  ETHERM (ET)
Reference surface is at the middle surface of the skin midway between the stringers.
 1.3719E+06  2.4322E+05 -9.1024E-05  3.2855E+05 -3.8234E-04  2.3668E-06    -4.4327E+02 -2.2598E-04
 2.4322E+05  6.9742E+05 -1.1978E-02 -3.8518E-04 -8.2430E-04 -1.3759E-05    -4.4808E+02 -5.6368E-04
-9.1024E-05 -1.1978E-02  2.6414E+05  2.3668E-06 -1.3759E-05  1.2087E+04     0.0000E+00  2.3801E-10
 3.2855E+05 -3.8518E-04  2.3668E-06  4.4191E+05  2.3291E+02  9.2078E+00    -8.9077E+01  1.1698E-05
-3.8234E-04 -8.2429E-04 -1.3759E-05  2.3291E+02  4.9282E+02  9.2078E+00     5.2084E-07 -5.5283E-06
 2.3668E-06 -1.3759E-05  1.2087E+04  9.2078E+00  9.2078E+00  1.0361E+04     0.0000E+00 -5.7613E-09
```

8.5 *Calculate* C(i, j) *for smeared stiffeners with partially effective skin*

Sometimes the wide-column buckling mode calculated with use of the single panel module is characterized by bending of the stringer which is of small amplitude compared to bending of the skin midway between stringers. In PANDA2, if the skin deflects more than 10 times midway between stringers than it does directly under the stringer, then this mode is rejected as indicating wide-column buckling. It is regarded as just another local skin buckling mode, a critical load factor for which is computed elsewhere in PANDA2. Since wide-column buckling is used in PANDA2 as an indication of panel instability (buckling between rings), if the wide-column mode is rejected, then panel instability must be calculated in some other way. In PANDA2 this 'other way' is to use PANDA-type closed formulas.

However, panel instability in PANDA is ordinarily calculated by smearing the stringers and treating the skin as if it were undeformed. It is clear that if the skin deforms a great deal in the wide-column buckling mode, only some effective width of it will contribute to panel buckling. The $C(i, j)$ governing panel instability should reflect this reduced effectiveness of the skin.

This is done in PANDA2 by calculation in SUBROUTINE GETCIJ of a constitutive matrix for the panel skin with smeared stringers called $C_{swide}(i, j)$. In the generation of C_{swide}, all $C(i, j)$ of Segment 1 of the panel skin are set equal to 0.2 times their previous values, except $C(4, 4)$, $C(5, 5)$, and $C(6, 6)$, which remain at their previous values.

When the wide-column buckling mode is calculated later in PANDA2, a switch called ISKIN is set equal to 0 if the mode is accepted as a true indication of panel instability and ISKIN is set equal to 1 if the mode is rejected because there is too much relative skin motion in it. Still later in PANDA2, panel instability from the PANDA-type of analysis is calculated with use of the appropriate constitutive matrix:

$C_s(i,j)$ = constitutive matrix with use of the fully effective, undeformed panel skin if the switch ISKIN = 0, if it is known that the skin is not in its postbuckled state, if KOITER = 0, and if IWIDE = 1.

$C_s(i,j)$ = constitutive matrix calculated from Koiter post-buckling theory if the skin is in its post-buckled state, if ISKIN = 0, if KOITER = 1, and if IWIDE = 1.

$C_{SWIDE}(i,j)$ = constitutive matrix calculated with use of the undeformed panel skin, but with $C(i,j)$ of Segment 1 of the panel module reduced as described above if ISKIN = 1 or if IWIDE = 0, and if IQUICK = 0.

IWIDE = a user-determined index that has the following meaning:

IWIDE = 0 means that the user has chosen a strategy in which the wide-column buckling mode does not constrain the design, regardless of the value of ISKIN.

IWIDE = 1 means that the wide-column buckling mode does constrain the design if ISKIN = 0, that is, if PANDA 2 does not reject it as a true indication of panel instability.

IWIDE is always set equal to 1 if the run is not an optimization run and if IQUICK = 0. If the run is an optimization run, the user has previously chosen the value of IWIDE during the interactive session in MAINSETUP. If IQUICK = 1 the $C_s(i,j)$ with fully effective skin is always used.

8.5.1 *Example: The hat-stiffened panel.* $C_s(i,j)$ *with reduced skin effectiveness* (C_{swide}): $C(i,j)$ with smeared stringers and reduced stiffness for segment 1 of the panel skin. This C-matrix is called C_{swide}:

```
 8.5068E+05  3.1814E+02 -9.1024E-05  3.2855E+05 -1.3444E-05  2.3668E-06
 3.1814E+02  9.1227E+02 -1.1978E-02 -4.9940E-07 -1.0782E-06 -1.3759E-05
-9.1024E-05 -1.1978E-02  6.7666E+04  2.3668E-06 -1.3759E-05  1.2087E+04
 3.2855E+05 -4.9940E-07  2.3668E-06  4.4169E+05  6.7541E+01  9.2078E+00
-1.3444E-05 -1.0782E-06 -1.3759E-05  6.7541E+01  4.9282E+02  9.2078E+00
 2.3668E-06 -1.3759E-05  1.2087E+04  9.2078E+00  9.2078E+00  1.0361E+04
```

8.6 *Find location of neutral plane for loading in* x*-direction*

The starting point is the constitutive law for the panel with smeared stiffeners:

$$N_x = C_s(1,1)e_x + C_s(1,2)e_y + C_s(1,4)k_x + C_s(1,5)k_y \tag{8.34}$$

$$N_y = C_s(1,2)e_x + C_s(2,2)e_y + C_s(2,4)k_x + C_s(2,5)k_y \tag{8.35}$$

$$M_x = -N_x d_x = C_s(1,4)e_x + C_2s(2,4)e_y + C_s(4,4)k_x + C_s(4,5)k_y \tag{8.36}$$

$$M_y = -N_y d_y = C_s(1,5)e_x + C_s(2,5)e_y + C_s(4,5)k_x + C_s(5,5)k_y, \tag{8.37}$$

in which d_x (same as DNEUTX) is the distance from the middle surface of the thin part of the skin to the neutral plane for axial loading and d_y (same as DNEUTY) is the distance from the middle surface of the thin part of the skin to the neutral plane for hoop loading; $C_s(i,j)$ are the coefficients of the constitutive law for the panel with both sets of stiffeners smeared out; and e_x, e_y, k_x, k_y are the average strains and changes in curvature of the reference surface, which in this case is taken to be the middle surface of the thin part of the panel skin.

The objective is to determine d_x and d_y. The procedure used is as follows:

1. Solve eqns (8.34) and (8.35) for e_x and e_y.
2. Plug in the resulting expressions for e_x and e_y in eqns (8.36) and (8.37).
3. Solve for k_x and k_y in terms of d_x and d_y.
4. Determine what values of d_x and d_y yield $k_x = 0$ and $k_y = 0$.

The calculations are performed in SUBROUTINE NEUTAX, which is called from SUBROUTINE GETCIJ. DNEUTX is first calculated by setting $N_x = 1.0$ and $N_y = 0.0$ and solving for d_x. This is done in the first call to SUBROUTINE NEUTAX. DNEUTY is then calculated by setting $N_x = 0.0$ and $N_y = 1.0$ and solving for d_y. This is done in the second call to SUBROUTINE NEUTAX.

8.7 *Calculate new* $C_s(i,j)$ *corresponding to shifted reference surface*

A constitutive matrix, $C_{NEW}(i,j)$, $i = 1, 6, j = 1, 6$, is derived given the matrix $C(i,j)$ just calculated and the shift of reference surface, $D = -C(1,4)/C(1,1)$. (The shift D is chosen so that $C_{NEW}(1,4) = 0$.) The new reference surface is close to, but not exactly at, the neutral plane for loading in the x (axial) direction.

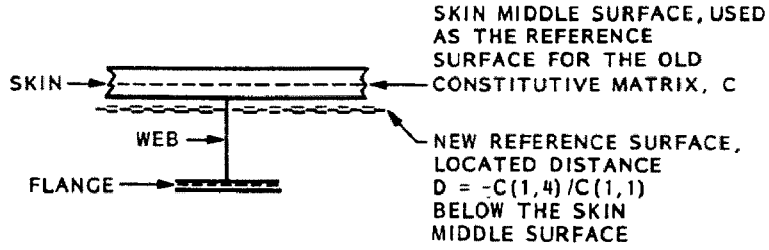

(a)

Fig. 15. (a) View of a panel module cross section, showing the old reference surface located at the skin middle surface, and the new reference surface located a distance D below the skin middle surface. (D will be positive in the figure above.)

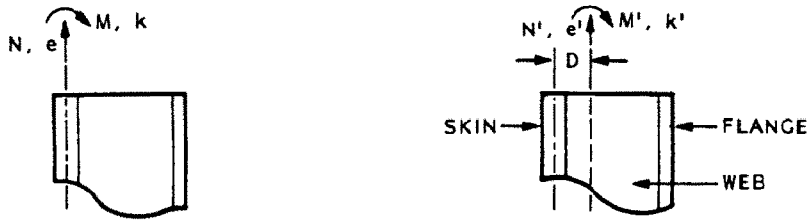

(b) (c)

Fig. 15. (b) Elevation of panel, showing reference surface at skin middle surface, axial resultant N, moment M, strain e and curvature change k. (c) Elevation of panel, showing reference surface near the neutral plane, shift D, axial resultant N', moment M', strain e' and curvature change k'.

Figures 15(a–c) show the nomenclature used in the derivation of $C_{NEW}(i, j)$. The derivation of the new constitutive matrix C_{NEW} from the old constitutive matrix C and the shift D proceeds as follows. For the original reference surface, shown in Fig. 15(b), we have

$$N = Ce \tag{8.38}$$

in which N represents the vector of six loads

$$N = \{N_x, N_y, N_{xy}, M_x, M_y, M_{xy}\} \tag{8.39}$$

e represents the vector of six strains and changes in curvature

$$e = \{e_x, e_y, e_{xy}, k_x, k_y, k_{xy}\} \tag{8.40}$$

and C represents the original 6×6 matrix derived for the reference surface located at the middle surface of the part of the panel module skin midway between stiffeners. For the new reference surface, located a distance D from the skin middle surface, we have

$$N' = C_{NEW}e'. \tag{8.41}$$

If classical Kirchhoff thin shell deformations are assumed (plane sections remain plane, normals remain normal), we can relate the forces N and N' and the strains e and e' as follows:

$$N = \{N'_x, N'_y, N'_{xy}, M'_x - N'_xD, M'_y - N'_yD, M'_{xy} + N'_{xy}D\} \tag{8.42}$$

$$e = \{e'_x + k'_xD, e'_y + k'_yD, e'_{xy} - k'_{xy}D, k'_x, k'_y, k'_{xy}\}. \tag{8.43}$$

We now insert the right-hand sides of eqns (8.42) and (8.43) into eqn (8.38), perform the indicated multiplications and additions, and equate coefficients in the result to like terms in eqn (8.41) in order to obtain the new constitutive matrix C_{NEW}. These computations are performed in SUBROUTINE CSHIFT, which is called near the end of SUBROUTINE GETCIJ.

```
INPUT TO SUBROUTINE CSHIFT...

  C = Old constitutive matrix.
  D = Reference surface shift.

OUTPUT FROM SUBROUTINE CSHIFT...

  CNEW = New constitutive matrix.
```

```
FORMULAS FOR NEW C(i,j) IN TERMS OF OLD C(i,j) AND SHIFT, D:

   CNEW(i,j), i = 1,3, j=1,3  are unchanged by reference
                              surface shift, D.

   CNEW(1,4) = C(1,4) + D*C(1,1)
   CNEW(1,5) = C(1,5) + D*C(1,2)
   CNEW(1,6) = C(1,6) - D*C(1,3)

   CNEW(2,4) = C(2,4) + D*C(1,2)
   CNEW(2,5) = C(2,5) + D*C(2,2)
   CNEW(2,6) = C(2,6) - D*C(2,3)

   CNEW(3,4) = C(3,4) + D*C(1,3)
   CNEW(3,5) = C(3,5) + D*C(2,3)
   CNEW(3,6) = C(3,6) - D*C(3,3)                                    (8.44)

   CNEW(4,4) = C(4,4) + 2.*D*C(1,4) + D*D*C(1,1)
   CNEW(4,5) = C(4,5) + D*(C(2,4)+C(1,5)) + D*D*C(1,2)
   CNEW(4,6) = C(4,6) + D*(C(1,6)-C(3,4)) - D*D*C(1,3)

   CNEW(5,5) = C(5,5) + 2.*D*C(2,5) + D*D*C(2,2)
   CNEW(5,6) = C(5,6) + D*(C(2,6)-C(3,5)) - D*D*C(2,3)

   CNEW(6,6) = C(6,6) - 2.*D*C(3,6) + D*D*C(3,3)
```

8.7.1 *Example: Hat-stiffened panel:* Cs(i, j) *with shifted reference surface.* For the following, the reference surface is $d = -C_{14}/C_{11}$ from the middle surface of the thin part of the panel skin. In this case $d = -2.3948\text{E-}01$. (Positive d corresponds to a reference surface that lies below the panel skin.) Note that the neutral surface is located at DNEUTX = −2.5527E-01.

```
 1.3719E+06  2.4322E+05 -9.1024E-05  0.0000E+00 -5.8247E+04 -1.9432E-05
 2.4322E+05  6.9742E+05 -1.1978E-02 -5.8247E+04 -1.6702E+05 -2.8823E-03
-9.1024E-05 -1.1978E-02  2.6414E+05  2.4166E-05  2.8548E-03  7.5344E+04
 0.0000E+00 -5.8247E+04  2.4166E-05  3.6323E+05  1.4182E+04  9.2078E+00
-5.8247E+04 -1.6702E+05  2.8548E-03  1.4182E+04  4.0492E+04  9.2085E+00
-1.9432E-05 -2.8823E-03  7.5344E+04  9.2078E+00  9.2085E+00  3.1299E+04
 ***** END OF CONSTITUTIVE C(i,j) CALCUL. *****

   ******** END OF CONSTITUTIVE C(i,j) CALCUL. ********
```

Next, find overall bending of panel (smeared stiffeners) under uniform pressure, $p = 1.0000\text{E} + 00$. Nonlinear theory is used.

9. NONLINEAR STATIC RESPONSE TO UNIFORM NORMAL PRESSURE

9.1 *Introduction*

It is well known that monocoque flat plates exhibit a nonlinear stiffening effect under pressure, and that even for rather low design pressures one must account for the membrane stretching that builds up as the plate deflects. Boitnott *et al.* [21] demonstrate that nonlinearities significantly affect the behavior of curved, internally pressurized panels clamped along their straight edges. In this section, which deals with a more complex problem, a stiffened panel, geometric nonlinearities must be included in the model.

Stiffened panels under normal pressure exhibit two types of response, identified here and in the following paragraphs as Problem 1 and Problem 2.

Problem 1. The panel bends overall. This behavior can be captured with a model in which the stiffeners are smeared out.

Problem 2. The panel bends locally around each stringer. This behavior can be captured with a single module model of the type shown in Fig. 1.

The strategy in PANDA2 is to obtain a reasonably good solution with little computer time by separation of these two behaviors, and analysis of each as a nonlinear problem. The total state of the pressurized panel is obtained by adding the results of the two separate analyses.

Immediately one might object that since the problem is nonlinear, one cannot superpose these results. The PANDA2 strategy would be incorrect if it were not for the fact that the membrane stresses obtained from Problem 1, the overall bending model, occur as prestresses in Problem 2, the local 'wrap-around' problem. In this way the essential nonlinear contribution of the first problem to the second is included.

9.2 *Nonlinear theory used in PANDA2*

For both the overall (Problem 1) and the local (Problem 2) behavior, the static response to uniform normal pressure is determined from the theory outlined next. The governing equations are derived by minimization of the total potential,

$$P = U - W = \int_{surface} [\mathbf{e}^T[\mathbf{C}]\mathbf{e} - \mathbf{W}]ds = 0, \tag{9.1}$$

with respect to each of the degrees of freedom q_i of the discretized panel or panel module cross section. Thus, the ith equilibrium equation ($i = 1, 2, 3, \ldots, N$, where N is the number of degrees of freedom in the discretized model of the panel or panel module cross section) is given by:

$$\partial P/\partial q_i = \int_s [\mathbf{e}^T[\mathbf{C}]\partial \mathbf{e}/\partial q_i - \partial \mathbf{W}/\partial q_i]ds = 0, \tag{9.2}$$

in which U is the strain energy, W is the work done by external forces, C is the 6×6 constitutive law, e is the strain vector consisting of three in-plane reference surface strain components and three reference surface curvature change components, and q_i is the ith degree of freedom. (Most q_i are nodal displacement components, u_i, v_i, w_i. A few of the q_i are Lagrange multipliers corresponding to boundary and juncture constraint conditions.) The quantity ds is an elemental area of the reference surface.

After integration, eqn (9.2) represents a set of N nonlinear equations which can be solved by the Newton method. The governing linear equation for each Newton iteration is obtained by expanding the terms in eqn (9.2) in a Taylor series about a given point in q-space. Call this point $\mathbf{q}_0$. Only linear terms in $\Delta\mathbf{q}$ are retained in the Taylor series expansion. The resulting equation for the ith degree of freedom has the form:

$$\sum_{j=1}^{N} \left\{ \int_s [\mathbf{e}^T[\mathbf{C}]\partial^2\mathbf{e}/\partial q_i \partial q_j + \partial \mathbf{e}^T/\partial q_j[\mathbf{C}]\partial \mathbf{e}/\partial q_i]ds \right\} \Delta q_j = \int_s [\partial \mathbf{W}/\partial q_i - \mathbf{e}^T[\mathbf{C}]\partial \mathbf{e}/\partial q_i]\, ds. \tag{9.3}$$

Equation (9.3) represents an integro-differential equation. Before solutions can be obtained, it must be converted into an algebraic equation. This can easily be done, because all quantities are assumed to vary trigonometrically in one coordinate direction and the other coordinate is discretized.

After each Newton iteration, the new equilibrium state is

$$\mathbf{q} = \mathbf{q}_0 + \Delta\mathbf{q}, \tag{9.4}$$

in which $\mathbf{q}_0$ is the known state after the previous Newton iteration.

Newton iterations continue until the Δq_i, $i = 1, 2, \ldots, N$, are less than, say, 1% of the respective q_i for all q_i larger than 10% of the largest nodal degree of freedom. (Lagrange multipliers are not included in this convergence criterion.) Actually, in order to save time, only the largest normal deflection $|w_{max}|$ is monitored for convergence. When $\Delta|w_{max}|$ is less than 0.001 $|w_{max}|$, the Newton iterations are considered converged.

In this analysis the displacement components, U, V, W, are assumed to have the form:

$$\begin{aligned} U(x, y) &= u(y) \sin(\bar{n}x) \\ V(x, y) &= v(y) \sin(2\bar{n}x) \\ W(x, y) &= w(y) \sin(\bar{n}x), \end{aligned} \tag{9.5}$$

in which x is the axial coordinate (normal to the plane of the screen) and y is the coordinate along each segment of the panel or panel module cross section (in the plane of the screen). The quantity $\bar{n}$ is given by

$$\bar{n} = \pi/L, \tag{9.6}$$

where L is the axial length presently being considered. (L may be the entire panel length or the length between adjacent rings.) The strain vector $\mathbf{e}$ is given by

$$\mathbf{e} = (e_x, e_y, e_{xy}, k_x, k_y, k_{xy}). \tag{9.7}$$

The in-plane strain components, e_x, e_y, e_{xy}, are given by

$$\begin{aligned} e_y &= (u' + w/R_1)s + 0.5(\chi^2)s^2 + e_{y0} \\ e_x &= 2\bar{n}vc_2 + (w/R_2)s + 0.5(\psi^2)c^2 + e_{x0} \\ e_{xy} &= \bar{n}uc + v's_2 + \chi\psi sc, \end{aligned} \tag{9.8}$$

and the changes in curvature, k_x and k_y, and twist, k_{xy}, are given by

$$k_y = \chi' s$$

$$k_x = -\bar{n}\psi s$$

$$k_{xy} = -4\bar{n}\chi c. \tag{9.9}$$

In eqns (9.8) and (9.9), $(\ )' = \partial(\ )/\partial y$, $s = \sin(\bar{n}x)$, $c = \cos(\bar{n}x)$, $s_2 = \sin(2\bar{n}x)$, $c_2 = \cos(2\bar{n}x)$, R_1 and R_2 are the radii of curvature in the plane of the screen and normal to the plane of the screen, respectively, χ is the rotation about an axis normal to the plane of the screen, and ψ is the rotation about an axis in the plane of the screen. These rotations are given by

$$\chi = w' - u/R_1$$

$$\psi = \bar{n}w. \tag{9.10}$$

The total strain vector e consists of a linear part e_L, a nonlinear part e_{NL}, and an initial part e_0. The initial part e_0 arises from the thermal curing of the panel and the applied in-plane load sets, N_x, N_y, N_{xy} and N_{x0}, N_{y0}, N_{xy0}. The radii of curvature, R_1 and R_2, are considered to be the initial curvatures plus any changes due to thermal curing and in-plane loading which is independent of that generated by the uniform normal pressure. Hence, the curvature changes and twist in eqns (9.9) do not contain k_{y0} or k_{x0} terms.

The work done by external forces is simply

$$W = \int_{surface} [pw] ds. \tag{9.11}$$

Equation (9.3) is converted into an algebraic equation by use of eqns (9.8)–(9.10), replacement of derivatives $(\ )'$ and $(\ )''$ with appropriate three-point central difference formulas (same as used in BOSOR4), and analytical integration over the axial coordinate x. The calculations are performed in SUBROUTINE BUCKLE. SUBROUTINE BUCKLE calls SUBROUTINE ARRAYS, in which the stiffness matrix and right-hand-side vector are set up, SUBROUTINE FACTR, in which the stiffness matrix is decomposed, and SUBROUTINE SOLVE, in which back-substitution is performed. Newton iterations continue until the largest nodal displacement converges to within 0.1%. The computational path in SUBROUTINE BUCKLE and SUBROUTINE ARRAYS is identified by a pointer INDIC having the value 3.

If the panel is stiffened, the nonlinear analysis is first performed for the entire panel with smeared stiffeners. In this analysis all four edges are supported such that $u = v = w = 0$ and rotation about each edge is permitted. Warping due to curing is included. If the entire panel is longer in the axial direction than twice the circumferential arc length, or in the case of cylindrical panels, if the axial length is greater than twice the 'boundary layer' length, considered to be 2.73 × sqrt(radius × effective thickness), then U, V, W in the panel skin are assumed to be independent of x.

Upon convergence of the nonlinear analysis of the entire panel with smeared stiffeners, the nonlinear analysis of a single panel module is begun. Here the segmented model shown in Fig. 13 is used. Symmetry conditions are applied at the two edges of the skin that are normal to the screen. Variations of displacement normal to the screen are assumed to be zero in this local branched model. The panel module is considered to be preloaded by the computed resultants due to curing, the prescribed in-plane Load Set A (N_x, N_y, N_{xy}), the prescribed Load Set B (N_{x0}, N_{y0}), and whatever average in-plane loads are predicted by the just-completed nonlinear analysis of the entire panel with smeared stiffeners.

The strains and stress resultants arising from this nonlinear analysis for static response to uniform normal pressure are evaluated only at the panel or panel module cross section midway along the x-coordinate, that is, at the symmetry plane parallel to the screen at $x = L/2$.

9.3 *Overall response from smeared stiffener discretized model of the entire panel*

The following analysis obtains the nonlinear static response of the entire panel to uniform normal pressure. Both stringers and rings, if any, are assumed to be smeared out in this analysis.

The panel edge in the plane of the screen is discretized. All edges are supported such that $u = v = w = 0$ and the rotation about each edge is permitted. The panel is preloaded by prescribed in-plane resultants N_x, N_y, N_{xy} from Load Set A and prescribed in-plane resultants N_{x0} and N_{y0} from Load Set B.

9.3.1. *Stability check.* First, an analysis is performed to see if curvature should be neglected in the global static nonlinear response to uniform pressure. This branch is entered only if PANDA2 senses the presence

of pressure applied to the convex surface of the panel. Some results follow.

```
General instability load factor        EIGPRS=  1.2839E+01
Uniform normal pressure (positive upward)   p=  1.0000E+00
Radius of curvature  (positive down)        R= -1.9400E+02
Resultants in Load Set A: (includes p*R)   Nx=   0
                                           Ny= -1.9716E+02

Wave numbers in critical buckling pattern:axial = 1
                                          circ. = 8
```

If the general instability load factor, EIGPRS, is less than unity, and if the number of half waves in the circumferential direction is greater than one, then the curvature, $1/R$, is neglected in the following nonlinear static analysis of the entire panel and the hoop tension generated by the deformation of the flat panel is set equal to zero in subsequent analyses of this panel.

9.3.2. *Nonlinear analysis for overall static response*

```
OVERALL PANEL DEFORMATION UNDER NORMAL PRESSURE HAS CONVERGED.
   Newton iterations required                =   3
   Last increment in normal displacement
            midway between stiffeners, DW =  -1.6906E-07
   Final  value  for normal displacement
            midway between stiffeners,  W =  -1.8562E-02
```

At this point we have reached the end of nonlinear equilibrium calculations for the entire panel with smeared stiffeners under uniform normal pressure, $p = 1.0000\text{E} + 00$.

9.4 *Nonlinear analysis for local static response*

Next, find bending of a single panel module under uniform normal pressure, $p = 1.0000\text{E} + 00$. Nonlinear theory is used.

The following analysis obtains the nonlinear static response of a single panel module to uniform normal pressure. Symmetry conditions are applied at the generators midway between stringers. If the panel module is longer than it is wide, axial bending in the skin is ignored.

```
LOCAL PANEL DEFORMATION UNDER NORMAL PRESSURE HAS CONVERGED.
            Newton iterations required    =   3
  Last Increment in normal displacement
            midway between stiffeners, DW =  -4.1447E-06
  Final  value  for normal displacement
            midway between stiffeners,  W =  -1.1111E-02
```

At this point we have reached the end of nonlinear equilibrium calculations for a single panel module with uniform normal pressure, $p = 1.0000\text{E} + 00$. The rather complex, two-phase nonlinear analysis for the static response of the stiffened panel to uniform normal pressure has been completed.

10. CALCULATION OF AVERAGE STRAIN AND FORCE DISTRIBUTIONS IN VARIOUS PARTS OF THE PANEL

10.1 *Preliminary general instability calculation for bowing growth*

First, calculate general instability load factor from a PANDA- type of analysis. Neglect any postbuckling effects in this preliminary calculation, the purpose of which is to obtain a rough estimate of the critical load to be used next when the additional bowing of the cured and pressurized, therefore warped, panel under the applied load set, N_x, N_y and N_{xy}, is computed. (This calculation occurs in the first call to SUBROUTINE BUCPAN in SUBROUTINE STRUCT, immediately following CALL GETCIJ.)

We are now in SUBROUTINE GENSTB, which is called from SUBROUTINE BUCPAN. PANDA-type 'closed form' analysis is performed. In this particular call to SUBROUTINE GENSTB we obtain a buckling load factor for buckling of the following type: General buckling (simple support at all boundaries).

DIMENSIONS, LOADS, C(i, i), AND TRANSVERSE SHEAR PROPERTIES OF THE PORTION OF THE PANEL NOW BEING ANALYZED:

```
Axial, circumferential lengths, this buckling model=  1.5289E+01  2.4000E+01
Eigenvalue in-plane loads/length of edge, Nx,Ny,Nxy= -3.0000E+03 -3.1623E+00  1.0000E+03
Fixed      in-plane loads/length of edge, Nxo, Nyo =  2.7196E+01 -4.8256E+01
Constitutive matrix diagonal, [C(i,i), i=1,6]      =  1.3719E+06  6.9742E+05  2.6414E+05  4.4191E+05  4.9282E+02  1.0361E+04
Effective thickness, x-face, transverse shearing   =  1.4370E+00
Effective thickness, y-face, transverse shearing   =  8.1209E-02
Transverse shear stiffness components, G13, G23    =  3.3717E+04  3.4235E+05
Is transverse shear deformation weakening included?= YES

Buckling load factors and no. of halfwaves (M = axial, N = circumferential):
  Neglecting transverse shear deformation weakening= 5.3164E+00 (M =  1, N =  1) halfwaves. Nodal line slope=  7.0000E-02
  Including  transverse shear deformation weakening= 3.5134E+00 (M =  1, N =  1) halfwaves. Nodal line slope=  7.0000E-02
```

GENERAL INSTABILITY EIGENVALUE (PANDA) = 3.5134
GROWTH FACTOR OF PANEL CURING BOW DUE TO LOAD = 1.3979

10.2 *Strain and force distributions from all loads except pressure*

```
POSITIONS OF STIFFENER SEGMENT CENTROIDS BELOW THE REFERENCE SURFACE OF THE PANEL SKIN...

  STRINGER PARTS...ZPARTX(I), I=1,4=       0.0000E+00  0.0000E+00 -7.3511E-01 -1.3568E+00
  RING     PARTS...ZPARTY(I), I=1,4=       0.0000E+00  0.0000E+00  0.0000E+00  0.0000E+00

BOWING AMPLITUDES DUE TO CURING AND PRESSURE...
AXIAL BOWING DUE TO CURING              =  -1.0667E-03
CIRCUMFERENTIAL BOWING DUE TO CURING    =   3.2284E-04
BOWING, ENTIRE PANEL UNDER EXT. PRESSURE=  -1.8662E-02
BOWING, PANEL MODULE UNDER EXT. PRESSURE=   0.0000E+00
```

```
APPLIED RESULTANTS: AXIAL, Nx = -3.0000E+03, CIRC., Ny = -3.1623E+00,  IN-PLANE SHEAR, Nxy =  1.0000E+03 (LOAD SET A)
APPLIED RESULTANTS: AXIAL, Nxo=  0.0000E+00, CIRC., Nyo=  0.0000E+00,  IN-PLANE SHEAR, Nxyo=  0.0000E+00 (LOAD SET B)
REDUCTION FACTOR FOR AXIAL LENGTH OF PANEL ( LESS THAN 1.0 ONLY IF PANEL IS CLAMPED) =  5.0965E-01
DISTANCE FROM MIDDLE SURFACE OF PANEL MODULE SEGMENT 1 (SKIN) TO NEUTRAL SURFACES (Positive for external stiffeners):
   X-DIRECTION :     DNEUTX = -2.5527E-01
   Y-DIRECTION :     DNEUTY =  1.1571E-09
```

REFERENCE SURFACE (SKIN MIDDLE SURFACE) STRAINS, CHANGES IN CURVATURE, AND TWIST CAUSED BY APPLIED IN-PLANE LOADS, Nx, Ny, Nxy AND Nxo, Nyo, Nxyo AND CAUSED BY THERMAL CURING

REFERENCE SURFACE	CAUSED BY APPLIED LOADS, Nx,Ny,Nxy (LOAD SET A)			CAUSED BY APPLIED LOADS, Nxo,Nxo,Nxyo (LOAD SET B)			CAUSED BY THERMAL CURING (Considered part of load set B)		
QUANTITIES	SKIN	STRINGER BASE	RING BASE	SKIN	STRINGER BASE	RING BASE	SKIN	STRINGER BASE	RING BASE
AXIAL STRAIN	-2.388E-03	-2.388E-03	0.000E+00	0.000E+00	0.000E+00	0.000E+00	-2.260E-04	-2.260E-04	0.000E+00
TRAN. STRAIN	8.942E-04	6.837E-04	0.000E+00	0.000E+00	0.000E+00	0.000E+00	-4.784E-04	-7.513E-04	0.000E+00
SHEAR STRAIN	3.997E-03	3.321E-03	0.000E+00	0.000E+00	0.000E+00	0.000E+00	2.380E-10	2.380E-10	0.000E+00
AXIAL KAPPA	2.291E-04	2.291E-04	0.000E+00	0.000E+00	0.000E+00	0.000E+00	1.170E-05	1.170E-05	0.000E+00
TRAN. KAPPA	2.183E-04	-2.425E-05	0.000E+00	0.000E+00	0.000E+00	0.000E+00	-5.715E-06	-5.117E-06	0.000E+00
TWIST	-4.666E-03	-4.666E-03	0.000E+00	0.000E+00	0.000E+00	0.000E+00	-5.761E-09	-5.761E-09	0.000E+00

CAUSED BY ALL LOADS EXCEPT NORMAL PRESSURE

STRAINS IN VARIOUS PARTS OF THE PANEL SKIN AND STIFFENERS

ITEM	CAUSED BY APPLIED LOADS, Nx,Ny,Nxy (LOAD SET A)			CAUSED BY APPLIED LOADS, Nxo,Nxo,Nxyo (LOAD SET B)			CAUSED BY THERMAL CURING (Considered part of load set B)		
	SKIN	STRINGER	RING	SKIN	STRINGER	RING	SKIN	STRINGER	RING
SKIN AXIAL	-2.388E-03	-	-	0.000E+00	-	-	-2.260E-04	-	-
SKIN CIRC.	8.942E-04	-	-	0.000E+00	-	-	-4.784E-04	-	-
SKIN SHEAR	3.997E-03	-	-	0.000E+00	-	-	0.000E+00	-	-
		STRINGER	RING		STRINGER	RING		STRINGER	RING
STIFFENER BASE ALONG AXIS		-2.388E-03	8.942E-04		0.000E+00	0.000E+00		-2.260E-04	0.000E+00
STIFFENER BASE TRANSVERSE		6.837E-04	-2.895E-03		0.000E+00	0.000E+00		-7.513E-04	0.000E+00
STIFFENER BASE SHEAR		3.321E-03	-3.997E-03		0.000E+00	0.000E+00		0.000E+00	0.000E+00
ALONG STIFFENER WEB AXIS		-2.220E-03	0.000E+00		0.000E+00	0.000E+00		-2.174E-04	0.000E+00
TRANSVERSE TO WEB AXIS		1.733E-03	0.000E+00		0.000E+00	0.000E+00		-5.515E-04	0.000E+00
IN-PLANE SHEARING OF WEB		0.000E+00	0.000E+00		0.000E+00	0.000E+00		0.000E+00	0.000E+00
ALONG STIFF. FLANGE AXIS		-2.078E-03	0.000E+00		0.000E+00	0.000E+00		-2.101E-04	0.000E+00
TRANSVERSE TO FLANGE AX.		4.236E-04	0.000E+00		0.000E+00	0.000E+00		-6.683E-04	0.000E+00
IN-PLANE SHEAR OF FLANGE		0.000E+00	0.000E+00		0.000E+00	0.000E+00		0.000E+00	0.000E+00

CAUSED BY ALL LOADS EXCEPT NORMAL PRESSURE

RESULTANTS IN VARIOUS PARTS OF THE PANEL SKIN AND STIFFENERS

ITEM	CAUSED BY APPLIED LOADS, Nx,Ny,Nxy (LOAD SET A)			CAUSED BY APPLIED LOADS, Nxo,Nxo,Nxyo (LOAD SET B)			CAUSED BY THERMAL CURING (Considered part of load set B)		
	SKIN	STRINGER	RING	SKIN	STRINGER	RING	SKIN	STRINGER	RING
SKIN AXIAL	-1.519E+03	-	-	0.000E+00	-	-	5.575E+01	-	-
SKIN CIRC.	-3.162E+00	-	-	0.000E+00	-	-	0.000E+00	-	-
SKIN SHEAR	1.000E+03	-	-	0.000E+00	-	-	0.000E+00	-	-
		STRINGER	RING		STRINGER	RING		STRINGER	RING
STIFFENER BASE ALONG AXIS		-4.582E+03	0.000E+00		0.000E+00	0.000E+00		-1.277E+02	0.000E+00
STIFFENER BASE TRANSVERSE		-3.162E+00	0.000E+00		0.000E+00	0.000E+00		-1.831E-04	0.000E+00
STIFFENER BASE SHEAR		1.000E+03	0.000E+00		0.000E+00	0.000E+00		0.000E+00	0.000E+00

ALONG STIFFENER WEB AXIS	-1.328E+02	0.000E+00		0.000E+00	0.000E+00		1.123E+01	0.000E+00
TRANSVERSE TO WEB AXIS	0.000E+00	0.000E+00		0.000E+00	0.000E+00		0.000E+00	0.000E+00
IN-PLANE SHEARING OF WEB	0.000E+00	0.000E+00		0.000E+00	0.000E+00		0.000E+00	0.000E+00
ALONG STIFF. FLANGE AXIS	-2.937E+03	0.000E+00		0.000E+00	0.000E+00		-1.186E+01	0.000E+00
TRANSVERSE TO FLANGE AX.	0.000E+00	0.000E+00		0.000E+00	0.000E+00		0.000E+00	0.000E+00
IN-PLANE SHEAR OF FLANGE	0.000E+00	0.000E+00		0.000E+00	0.000E+00		0.000E+00	0.000E+00

CAUSED BY ALL LOADS EXCEPT NORMAL PRESSURE

EQUILIBRIUM OF RESULTANTS FROM APPLIED LOADS AND CURING

ITEM	CAUSED BY APPLIED LOADS, Nx,Ny,Nxy (LOAD SET A)			CAUSED BY APPLIED LOADS, Nxo,Nxo,Nxyo (LOAD SET B)			CAUSED BY THERMAL CURING (Considered part of load set B)		
	Nx	Ny	Nxy	Nx	Ny	Nxy	Nx	Ny	Nxy
DERIVED	-3.000E+03	-3.162E+00	1.000E+03	0.000E+00	0.000E+00	0.000E+00	3.576E-07	0.000E+00	0.000E+00
APPLIED	-3.000E+03	-3.162E+00	1.000E+03	0.000E+00	0.000E+00	0.000E+00	0.000E+00	0.000E+00	0.000E+00
ERROR	0.000E+00	5.913E-05	0.000E+00	0.000E+00	0.000E+00	0.000E+00	3.576E-07	0.000E+00	0.000E+00

10.3 *Strain and force distributions from uniform normal pressure*

APPLIED UNIFORM NORMAL PRESSURE, P= 1.0000E+00

IN-PLANE RESULTANTS DEVELOPED FROM MODEL OF ENTIRE PANEL WITH SMEARED STIFFENERS (considered part of Load Set B):

Nx(created by normal pressure) = 3.2518E+01
Ny(created by normal pressure) = -3.2951E+01
Nxy(created by normal pressure) = 0.0000E+00

IN-PLANE RESULTANTS DEVELOPED FROM MODEL OF PANEL MODULE WITH BRANCHED STRINGER (considered part of Load Set B):

Nx(created by normal pressure) = -5.3222E+00
Ny(created by normal pressure) = -1.5305E+01
Nxy(created by normal pressure) = 0.0000E+00

REFERENCE SURFACE (skin middle surface) STRAINS, CHANGESIN CURVATURE, AND TWIST CAUSED BY UNIFORM NORMAL PRESSURE (entire panel, smeared stiffener model)

REFERENCE SURFACE QUANTITIES	CAUSED BY UNIFORM NORMAL PRESSURE, P (considered part of Load Set B) SKIN	STRINGER BASE	RING
AXIAL STRAIN	1.114E-06	1.114E-06	0.000E+00
TRAN. STRAIN	-5.294E-05	-3.596E-05	0.000E+00
SHEAR STRAIN	0.000E+00	0.000E+00	0.000E+00
AXIAL KAPPA	1.296E-04	1.296E-04	0.000E+00
TRAN. KAPPA	6.563E-05	-2.702E-05	0.000E+00
TWIST	0.000E+00	0.000E+00	0.000E+00

CAUSED BY UNIFORM PRESSURE

STRAINS IN VARIOUS PARTS OF THE PANEL SKIN AND STIFFENERS

ITEM	FROM MODEL OF ENTIRE PANEL(smeared) (LOAD SET B) SKIN	STRINGER	RING	FROM MODEL OF PANEL MODULE(branched) (LOAD SET B) SKIN	STRINGER	RING	SUM OF STRAINS FROM BOTH MODELS (Considered part of load set B) SKIN	STRINGER	RING
SKIN AXIAL	1.114E-06	-	-	1.300E-07	-	-	1.244E-06	-	-
SKIN CIRC.	-5.294E-05	-	-	-2.444E-05	-	-	-7.739E-05	-	-
SKIN SHEAR	0.000E+00	-	-	0.000E+00	-	-	0.000E+00	-	-
		STRINGER	RING		STRINGER	RING		STRINGER	RING
STIFFENER BASE ALONG AXIS		1.114E-06	-5.294E-05		-1.845E-25	0.000E+00		1.114E-06	-5.294E-05
STIFFENER BASE TRANSVERSE		-3.596E-05	1.116E-06		-1.648E-06	0.000E+00		-5.245E-05	1.116E-06
STIFFENER BASE SHEAR		0.000E+00	0.000E+00		0.000E+00	0.000E+00		0.000E+00	0.000E+00
ALONG STIFFENER WEB AXIS		9.638E-05	0.000E+00		1.075E-10	0.000E+00		9.638E-05	0.000E+00
TRANSVERSE TO WEB AXIS		-7.525E-05	0.000E+00		-1.281E-06	0.000E+00		-7.653E-05	0.000E+00
IN-PLANE SHEARING OF WEB		0.000E+00	0.000E+00		0.000E+00	0.000E+00		0.000E+00	0.000E+00
ALONG STIFF. FLANGE AXIS		1.769E-04	0.000E+00		2.068E-09	0.000E+00		1.769E-04	0.000E+00
TRANSVERSE TO FLANGE AX.		-3.607E-05	0.000E+00		9.056E-09	0.000E+00		-3.606E-05	0.000E+00
IN-PLANE SHEAR OF FLANGE		0.000E+00	0.000E+00		0.000E+00	0.000E+00		0.000E+00	0.000E+00

CAUSED BY UNIFORM PRESSURE

RESULTANTS IN VARIOUS PARTS OF THE PANEL SKIN AND STIFFENERS

ITEM	FROM MODEL OF ENTIRE PANEL(smeared) (LOAD SET B) SKIN	STRINGER	RING	FROM MODEL OF PANEL MODULE(branched) (LOAD SET B) SKIN	STRINGER	RING	SUM OF RESULTANTS FROM BOTH MODELS (Considered part of load set B) SKIN	STRINGER	RING
SKIN AXIAL	-1.170E+01	-	-	-5.680E+00	-	-	-1.738E+01	-	-
SKIN CIRC.	-3.295E+01	-	-	-1.531E+01	-	-	-4.826E+01	-	-
SKIN SHEAR	0.000E+00	-	-	0.000E+00	-	-	0.000E+00	-	-
		STRINGER	RING		STRINGER	RING		STRINGER	RING
STIFFENER BASE ALONG AXIS		-7.343E+00	0.000E+00		-4.384E+00	0.000E+00		-1.173E+01	0.000E+00
STIFFENER BASE TRANSVERSE		-3.295E+01	0.000E+00		-1.524E+01	0.000E+00		-4.819E+01	0.000E+00
STIFFENER BASE SHEAR		0.000E+00	0.000E+00		0.000E+00	0.000E+00		0.000E+00	0.000E+00
ALONG STIFFENER WEB AXIS		5.767E+00	0.000E+00		-1.534E-01	0.000E+00		5.613E+00	0.000E+00
TRANSVERSE TO WEB AXIS		0.000E+00	0.000E+00		-1.964E-01	0.000E+00		-1.964E-01	0.000E+00
IN-PLANE SHEARING OF WEB		0.000E+00	0.000E+00		0.000E+00	0.000E+00		0.000E+00	0.000E+00

```
ALONG STIFF. FLANGE AXIS   2.501E+02  0.000E+00        4.401E-03  0.000E+00        2.501E+02  0.000E+00
TRANSVERSE TO FLANGE AX.   0.000E+00  0.000E+00        7.243E-03  0.000E+00        7.243E-03  0.000E+00
IN-PLANE SHEAR OF FLANGE   0.000E+00  0.000E+00        0.000E+00  0.000E+00        0.000E+00  0.000E+00
*****************************************************************************
                    CAUSED BY UNIFORM PRESSURE
     E Q U I L I B R I U M   O F   R E S U L T A N T S   F R O M   A P P L I E D   N O R M A L   P R E S S U R E, P
    ITEM        FROM MODEL OF ENTIRE PANEL(smeared)  FROM MODEL OF PANEL MODULE(branched)  SUM OF RESULTANTS FROM BOTH MODELS
                          (LOAD SET B)                        (LOAD SET B)                  (Considered part of load set B)
                     Nx          Ny          Nxy         Nx          Ny          Nxy         Nx          Ny          Nxy

FROM EQUFCE    3.252E+01 -3.296E+01  0.000E+00   -5.322E+00 -1.531E+01  0.000E+00   2.720E+01 -4.826E+01  0.000E+00
FROM EQUILIB   3.252E+01 -3.296E+01  0.000E+00   -5.322E+00 -1.531E+01  0.000E+00   2.720E+01 -4.826E+01  0.000E+00
  ERROR        0.000E+00  0.000E+00  0.000E+00    0.000E+00  0.000E+00  0.000E+00   3.815E-06  0.000E+00  0.000E+00
*****************************************************************************
*****************************************************************************
```

11. CALCULATION OF KNOCKDOWN FACTORS TO ACCOUNT FOR THE EFFECT OF IN-PLANE SHEAR LOAD N_{xy} ON GENERAL AND LOCAL BUCKLING LOAD FACTORS CALCULATED WITH BOSOR4-TYPE OF DISCRETIZED MODELS

11.1 *Method used in PANDA2*

Next, PANDA2 calculates knockdown factors for the effect of in-plane shear loads on general buckling, wide column buckling, and on local buckling. These knockdown factors are obtained from PANDA-type analysis in which general, panel and local buckling load factors are calculated with and without the in-plane shear load, N_{xy}. The knockdown factors are given by:

$$\text{KNOCKDOWN} = \text{EIGENCRIT(with shear)/EIGENCRIT(no shear)}. \tag{11.1}$$

The shear knockdown factor for general instability calculated with the smeared stiffener model is stored in FKNOCK(1); the shear knockdown factor for wide-column instability calculated with the single panel module model is stored in FKNOCK(4); and shear knockdown factors for local instability are stored in FKNOCK(2) and FKNOCK(3). These factors are later applied to critical loads obtained with BOSOR4-type of discretized panel module models because buckling loads for these models are obtained neglecting in-plane shear. FKNOCK(1) is applied to the BOSOR4-type model in which the entire width of the panel with smeared rings and stringers is discretized; FKNOCK(4) is applied to the discretized single panel module model that is used to predict wide-column buckling (see Figs 20(c) and 22(c)); FKNOCK(2) is applied to the discretized single panel module model that is used to predict local buckling (see Figs 20(a) and 22(a)); and FKNOCK(3) is applied to buckling of the panel skin under a hat stiffener. It is emphasized that these four knockdown factors are for the effect of in-plane shear loading N_{xy} not for transverse shear deformation. The transverse shear deformation knockdown factors are obtained from Timoshenko beam theory, and they are discussed in Sec. 8.2.

11.2 *Example: the hat-stiffened panel*

Results from the PANDA-type of analysis:

```
Preliminary general buckling (from PANDA)=   3.5134E+00
 (axial,circ.) waves with shear=(1,1); without shear=(1,1)
Preliminary local buckling (from PANDA)  =   2.2605E-01
 Simply-supported edges. No. of axial waves, MLOCAL= 4
 Slope of local buckling nodal lines, CSLOPE=3.2846E-01
Knockdown factors to account for the effect of in-plane shear load:
 Knockdown factor for general instabilty =   9.1580E-01
 Knockdown factor for local instabilty   =   8.1278E-01
 Knockdown factor (under hat crippling)  =   9.4494E-01
 Knockdown factor for inter-ring buckling=   9.1580E-01 (wide-column)
```

```
Resultants in prebuckled panel module segments: SEG. 1     SEG. 2     SEG. 3     SEG.4     Nave(calc.) Nave(given)
          Axial resultant,   Nx =  -1.4809E+03 -4.7215E+03 -1.1600E+02 -2.6985E+03 -2.9728E+03 -2.9728E+03
  Circumferential resultant,  Ny =  -5.1418E+01 -5.1353E+01 -1.9842E-01  7.2433E-03 -5.1418E+01 -5.1419E+01
   In-plane shear resultant,  Nxy =   1.0000E+03  1.0000E+03  0.0000E+00  0.0000E+00  1.0000E+03  1.0000E+03
```

12. TYPES OF BUCKLING ANALYSES PERFORMED IN PANDA2

12.1 *Summary of types of buckling analysis in PANDA2*

(a) All types of buckling covered by the original PANDA code. These are listed in [1, Table 1]. Included are: general instability (rings and stringers participate), local buckling (between adjacent stringers and adjacent rings), panel buckling (between rings with smeared stringers and between stringers with smeared rings), rolling

of stiffeners (no web deformation) with skin participation, rolling of stiffeners (with web deformation) without skin participation, and crippling of stiffener parts.

(b) Local buckling predicted from a model in which the cross section of a single panel module is discretized. Two modes may be calculated, depending on results: a 'high-axial-wavenumber' mode and a 'low-axial-wavenumber' mode. The 'high-axial-wavenumber' mode corresponds roughly to buckling of the thin part of the skin (part excluding the width b_2 of the faying flange of the stringer). The 'low-axial-wavenumber' mode may correspond roughly to local buckling between stringer centerlines or it may correspond to a mode involving sidesway of the stringers between rings. A constraint is introduced into the optimization problem that the 'low-axial-wavenumber' mode shall correspond to a load factor that is 20% higher than the load factor corresponding to the 'high-axial-wavenumber' mode. This tends to prevent stiffener popoff for panels loaded into the post-local-buckling regime. Local buckling is enforced by introduction of constraints in the stiffness matrix that force the mode to be antisymmetric about the panel module centerline and symmetric midway between stringers. For both 'high' and 'low'-axial-wavenumber modes, ranges of number of axial halfwaves are searched until minimum buckling load factors are found with respect to the number of axial halfwaves.

(c) Wide column buckling predicted from the model in which the cross section of a single panel module is discretized. This mode is obtained in the same way as are the local buckling modes in (b), except that wide-column buckling is enforced by introduction of constraints in the stiffness matrix that force the mode to be symmetric about the panel module centerline as well as symmetric midway between stringers. The number of axial half-waves is fixed at $n = 1$, rather than a search being conducted for a critical load factor by varying n, as is done in (b). If there are transverse stiffeners (rings) present, both the local and the wide-column loads correspond to the panel being simply supported along ring centerlines and rings are neglected in the stability phase of the calculations. (Of course the rings are accounted for in the calculations of prebuckling strain and force distributions in the various parts of the panel.)

(d) general instability (rings and stringers smeared out) of the entire panel from a simple discretized model (no branches for stiffeners, since they are smeared out). The purposes of this model are:

(1) to provide buckling loads in cases for which the axial load varies along the edge of the panel;
(2) to provide a check on both the PANDA calculations for general instability and on the wide column calculation for the case of uniform axial compression.

Such a check is especially useful for the wide column buckling load from (c) because curvature is neglected in the calculation in (c) and included in the calculation in (d). Note, however, that in this general instability calculation:

(1) The stiffeners are smeared out. Hence local stringer cross section deformation is not accounted for, and local skin bending in the general instability mode is not possible.
(2) The actual (spanwise varying) axial load distribution in the post-locally-buckled panel is not used; only the uniform prebuckling axial load distribution determined in SUBROUTINE FORCES is used.

Approximation (1) yields an unconservative result (buckling load too high); approximation (2) could cause either plus or minus error.

12.2 *Local buckling predicted from a discretized module*

Local buckling as predicted from the discretized model of the single panel module is performed by SUBROUTINE LOCAL. The first call to SUBROUTINE LOCAL corresponds to determination of the 'high-axial-wavenumber' local buckling load factor. If panel module local modes have been determined previously in a given run (for example, for a previous design iteration), the starting axial wavenumber and eigenvector are the values corresponding to the previous critical condition.

If the structural analysis is being conducted for a small design perturbation for the purpose of determining gradients of constraint conditions for optimization (IMOD = 1), new buckling load factors may be calculated from Rayleigh's quotient, in which the eigenmode is that corresponding to the unperturbed design. This is what happens if post-local-buckling effects are neglected (KOITER = 0). If post-local-buckling effects are included, a new mode is calculated even for each small design perturbation because this mode is used to calculate the changes in post-local-buckling stresses due to the design perturbation. These changes must be computed accounting for changes in the local buckling mode shape in order to obtain accurate stress constraint gradients, and therefore appropriate design modifications during optimization cycles.

Eigenvalues corresponding to local buckling of the skin obtained from the BOSOR4-discretized panel module model are calculated for a range of axial wavenumbers. All four edges of the panel are assumed to be simply supported, even if you indicated 'clamped' in your input, and the in-plane loading is assumed to be uniform (N_1, N_2, N_{12}), even if you provided for axial load N_x varying in the L2 (circumferential) direction.

If KOITER = Y (local postbuckling effects wanted), the state of the locally postbuckled panel is determined

at the applied load and at the critical axial wavenumber determined from the local bifurcation buckling analysis.

Local buckling load factors from the discretized model of a single panel module for design iteration no. 0, load set no. 1, material iteration no. 0, follow. These load factors include the knockdown factor, 0.813, that accounts for the effect of in-plane shear loading. Resultants are uniform and given by:

```
LOAD SET A: axial, Nx = -3.00E+03; circ., Ny = -3.16E+00;
  in-plane shear, Nxy =  1.00E+03
LOAD SET B: axial, Nxo=  0.00E+00; circ., Nyo=  0.00E+00;
  in-plane shear, Nxyo=  0.00E+00 (Not from pressure)
LOAD SET B: Uniform normal pressure, P =   1.0000E+00
  Resultants from global (smeared stiffener) model:
    Nxo(p)= 32.5  Nyo(p)= -33.0,  Nxyo(p)= 0.0
  Resultants from local (discrete stiffener) model:
    Nxo(p)= -5.32,  Nyo(p)= -15.3,  Nxyo(p)= 0.0 :

HIGH AXIAL WAVENUMBER LOAD FACTORS FOR LOCAL BIFURCATION BUCKLING
   Axial     Eigenvalue    Knockdown Factors:       Final
 Halfwaves                 Transverse   in-plane    Value
                           shear def.  shear load
     9        0.494          0.964       0.813      0.387
    10        0.513          0.962         "        0.401
     8        0.484          0.964         "        0.379
     7        0.487          0.964         "        0.382
```

Buckling modal displacements and derivatives of displacements with respect to s, the arc length along the discretized panel module segments, are computed from the eigenvector for the 'high-axial-wavenumber' local buckling. These computations are performed by SUBROUTINE MODE, which follows the first call to SUBROUTINE LOCAL. These quantities are used in the post-local-buckling stress analysis and for later plotting.

'Low-axial-wavenumber' local panel module buckling is next calculated. In the search for the critical buckling load factor with respect to the number of axial waves, the maximum number of axial waves is restricted to be less than MHIGH-1, so that computations for the 'high-axial-wavenumber' will not be repeated. The local buckling load factor and mode are determined in the second call to SUBROUTINE LOCAL in SUBROUTINE STRUCT.

```
LOW AXIAL WAVENUMBER LOAD FACTORS FOR LOCAL BIFURCATION BUCKLING
   Axial     Eigenvalue    Knockdown Factors:       Final
 Halfwaves                 Transverse   in-plane    Value
                           shear def.  shear load
     1        1.34           0.906       0.813      0.964
     2        0.836          0.939         "        0.639
     3        0.742          0.946         "        0.570
     4        0.635          0.953         "        0.492
     5        0.555          0.959         "        0.432
     6        0.508          0.962         "        0.397
```

13. LOCAL POSTBUCKLING ANALYSIS IN PANDA2

13.1 *Introduction*

There is a section of code in SUBROUTINE STRUCT identified as the 'KOITER = 1 BRANCH'. KOITER is a control indicator (0 or 1) whereby the user chooses whether (KOITER = 1) or not (KOITER = 0) he or she wants the analysis to include the effect of local postbuckling of the panel skin between stiffeners. If KOITER = 1 the post-local-buckling state of the panel is calculated. The postbuckling theory used in PANDA2 is similar to a theory originally formulated by Koiter [4] (see [34]).

13.2 *Local postbuckling theory used in PANDA2*

According to this theory the local buckling mode in the skin changes shape during the post-local-buckling loading phase: for applied loads slightly above the bifurcation buckling load corresponding to local buckling, the post-buckling deformation pattern closely resembles the local bifurcation buckling mode. However, as the

applied load is further increased, a region develops midway between two adjacent stringers in which there is little curvature change in the transverse (y) direction. Thus, the post-locally-buckled skin has one-half wave between stringers, but the top of the wave is 'chopped off'—nearly flat—midway between stringers. This nearly flat region develops only after the load has risen somewhat above the bifurcation buckling load.

If KOITER = 1 the following calculations are performed.

(a) The post-local buckling normal deflection, $w(x, y)$, is assumed to have the form:

$$\begin{aligned} w(x, y) &= f(\phi + a\phi^3)\sin[(\pi/\mathrm{L})(x - my)] \\ &= W(y)\sin[(\pi/L)(x - my)], \end{aligned} \tag{13.1}$$

in which ϕ is the bifurcation buckling mode, f and a are undetermined coefficients, L is the half wavelength in the axial direction of the critical bifurcation buckling mode and m is the slope of the nodal lines of the post-local buckling pattern.

This post-local-buckling pattern differs from that proposed by Koiter [4]. Koiter assumed that $W(y)$ was constant in a central region away from the stiffeners. He introduced an edge parameter, α, that determined the extent of this region. Energy minimization with respect to α yielded the extent of the flat region.

In other respects, however, the local postbuckling theory used in PANDA2 is similar to Koiter's 1946 theory.

(b) Certain wave shape parameters, $A_1, A_2, \ldots, A_{25}$, are calculated once the bifurcation buckling mode shape ϕ is known. These calculations, involving numerical integration of various products of the buckling modal normal displacement and its first and second derivatives, take place in SUBROUTINE INTEG, which is called from SUBROUTINE MODE.

The heart of the Koiter theory is contained in SUBROUTINE KOIT2, in which the post-locally-buckled state of the panel is derived. The following computations occur in KOIT2.

(c) The average in-plane strains in the panel, e_1, e_2 and e_{12}, are obtained in terms of f, a and m, which appear above in the expression for $w(x, y)$. This calculation occurs in SUBROUTINE EPSAVE, which is called from SUBROUTINE KOIT2.

The purpose of SUBROUTINE EPSAVE is to calculate certain coefficients, $G_{11}, G_{12}, \ldots, G_{16}$, and $G_{21}, G_{22}, \ldots, G_{26}$, as described next.

The average in-plane strains in the post-buckling range are given by:

$$\begin{aligned} e_1 &= F_{10} + f^2[G_{11} + aG_{12} + a^2G_{13} + m^2(G_{14} + aG_{15} + a^2G_{16})] \\ e_2 &= F_{20} + f^2[G_{21} + aG_{22} + a^2G_{23} + m^2(G_{24} + aG_{25} + a^2G_{26})] \\ e_{12} &= N_{xy}/C_x(3, 3, 5) + mf^2(G_{31} + aG_{32} + a^2G_{33}), \end{aligned} \tag{13.2}$$

in which $C_x(3, 3, 5)$ is the shear stiffness identified in Sec. 8.4; F_{10}, F_{20} and G_{ij} are derived in EPSAVE; m is the slope of the buckling nodal lines; and a is an as yet undetermined coefficient that appears in the expression for the y-variation of the post-local-buckling pattern:

$$W(y) = f(\phi + a\phi^3), \tag{13.3}$$

where y is the coordinate across the panel, measured from midway between stringers, and ϕ is the normalized buckling mode shape determined by the BOSOR4-type of analysis for the discretized panel module cross section.

The quantity e_1 is the average axial strain in the locally post-buckled panel, $e_{2r} = e_2 + C(y)$, where e_2 is the average circumferential strain in the locally post-buckled panel; $C(y)$ is a nonlinear function of $W(y)$ given in SUBROUTINE EPSAVE; e_{12} is the average in-plane shear strain in the post-buckled panel; and f is the amplitude of the local buckling pattern.

The starting point for this derivation is the relation between given applied loads, N_x, N_y, N_{xy}, and average loads in the panel skin, N_1, N_2, N_{12}:

$$\begin{aligned} N_x &= N_1 + N_{stringer} \\ N_y &= N_2 + N_{ring} \\ N_{xy} &= N_{12}, \end{aligned} \tag{13.4}$$

in which N_1, N_2, N_{12} are given by

$$N_1 = \int_0^{2L} \left\{ \int_0^b [A^i_{11}e_x + A^i_{12}e_y + N^i_{x0}]\mathrm{d}y \right\} \mathrm{d}x/(2bL)$$

$$N_2 = \int_0^{2L} \left\{ \int_0^b [A^i_{12} e_x + A^i_{22} e_y + N^i_{y0}] \mathrm{d}y \right\} \mathrm{d}x/(2bL)$$

$$N_{12} = \int_0^{2L} \left\{ \int_0^b [A^i_{33} e_{xy}] \mathrm{d}y \right\} \mathrm{d}x/(2bL), \tag{13.5}$$

where the coefficients $A^i_{11} = C_x(1, 1, i)$; $A^i_{12} = C_x(1, 2, i)$; $A^i_{22} = C_x(2, 2, i)$; $A^i_{33} = C_x(3, 3, i)$, where C_x are the membrane stiffnesses of the segments of an 'x-oriented' panel module; i is the module segment number; e_x, e_y, e_{xy} are the local membrane strains; and N^i_{x0}, N^i_{y0} are the known thermal resultants from curing. L is the half-wavelength of the local buckle pattern, and b is the stringer spacing.

The axial load in each stringer is

$$N_{stringer} = \int_0^L \left\{ \sum_{i=1}^{NSEGS} \left[\int_0^{S_i} (A^i_{11} e_x + A^i_{12} e_y + N^i_{x0}) \mathrm{d}s \right] \right\} \mathrm{d}x/(2bL), \tag{13.6}$$

in which S_i is the width of the ith stringer segment. The expression for N_{rings} is analogous. '*NSEGS*' above refers to the segments of the stringer cross section (e.g. web, flange).

The local membrane strains, e_x, e_y, e_{xy}, can be expressed in terms of average strains, e_1, e_2, e_{12}, plus nonlinear terms arising from local buckling deformations:

$$e_x = e_1 + NW^2$$

$$e_y = e_2 + C(y) - \nu_{12} NW^2$$

$$e_{xy} = e_{12} + (\text{local buckling terms}), \tag{13.7}$$

in which the parameter N is given by

$$N = [0.5\,\pi n/(\text{ring spacing})]^2. \tag{13.8}$$

(d) The local bifurcation buckling load factor, EKOITR, is calculated in SUBROUTINE EIGKOI. In this calculation the amplitude of the local postbuckling deformations, f, is assumed to be zero, and the flattening of the bifurcation buckling mode shape, a, is assumed to be zero.

The eigenvalue, EKOITR, is computed in the following way:

(1) The total potential, $U - W$, [strain energy minus the work done by the applied load set (N_x, N_y, N_{xy})], is written in terms of f and m.
(2) This total potential is minimized with respect to f and m.
(3) In the resulting two equations, all terms with f^2 are neglected, since the amplitude of the bifurcation buckling mode f is infinitesimal.
(4) The equation resulting from $\partial(U - W)/\partial f = 0$ yields an expression for the eigenvalue EKOITR in terms of m, the slope of the buckling nodal lines. This expression is 'plugged into' the equation resulting from $\partial(U - W)/\partial m = 0$.
(5) The nonlinear equation for m resulting from step (4) is solved by Newton's method.
(6) The value of m determined in step (5) is 'plugged into' the expression for EKOITR derived in step (4).

(e) The locally post-buckled state is calculated through solution of three simultaneous nonlinear algebraic equations for: f^2, the square of the amplitude of the local buckles; a, the measure of the flattening of the bifurcation buckling mode midway between stringers; and m, the slope of the buckling nodal lines (nonzero due to in-plane shear and/or unbalanced laminate). These equations are easy to solve because both a and m can be expressed in terms of f^2. The resulting two simultaneous nonlinear algebraic equations are solved by Newton's method in SUBROUTINE NEWTON.

(f) The average strains, e_1, e_2, e_{12}, and average stress resultants, N_1, N_2, N_{12}, in the panel skin are computed in SUBROUTINE NEWTON. These quantities are needed for computation of the tangent stiffness matrix of the locally post-buckled skin. Both the thin and thick portions of the panel skin are included.

(g) The tangent membrane stiffness of the locally post buckled skin is computed. This 3×3 matrix called C_{TAN} is needed for later calculation of general instability and wide column buckling of the locally post-buckled panel. This computation takes place in SUBROUTINE KOIT2. Each of the applied resultants, N_x, N_y, N_{xy}, is perturbed in turn, and new values for e_1, e_2, e_{12} and N_1, N_2, N_{12} are recomputed. The tangent stiffness matrix C_{TAN} is calculated knowing the rates of change of N_1, N_2 and N_{12} with respect to e_1, e_2 and e_{12}.

(h) Local membrane strain components, e_x, e_y, e_{xy}, and stress resultants, N_{1var}, N_{2var}, N_{12var}, are next calculated in SUBROUTINE STRMID. These quantities are calculated for all segments in the x-cross section

of the single panel module. Particularly important is the accurate computation of the new axial load distribution, since this of course affects the predicted load factors for crippling of the various segments of the stringer cross section. Also, new computations of the stress resultants in the ring cross section are performed.

(i) The stresses in material coordinates are computed in all the layers and at the midwidth and end points of all the segments in the discretized panel module. The stresses are calculated for both sine and cosine amplitudes of the locally post-buckled panel. Stress constraint conditions are set up based on the minimum margins for each type of failure in each type of material. The stress failure criteria used in PANDA2 are:

(1) maximum tension along fibers;
(2) maximum compression along fibers;
(3) maximum tension transverse to fibers;
(4) maximum compression transverse to fibers;
(5) maximum in-plane shear stress.

If the user has indicated in BEGIN that certain material types are composite material unidirectional tape, then for these layers the failure criterion (3) maximum tension transverse to fibers, is ignored. Instead, if transverse failure (cracking) has been detected at certain points in the panel module, at those points the panel is not considered to have failed. However, the allowable in compression along the fibers of cracked layers is reduced by as much as 50%, depending upon by what margin the transverse tensile stress exceeds the threshold value.

The stress constraints of the locally post-buckled panel are calculated in SUBROUTINE STRTHK, which is the last subroutine called in the KOITER = 1 branch of SUBROUTINE STRUCT.

(j) a stringer popoff constraint is also calculated in SUBROUTINE STRTHK. This constraint is based on tensile forces that develop in parts of the stringer web adjacent to the faying flange. These tensile forces tend to peel the faying flange from the panel skin to which it is attached. Results from a peel test may be necessary in order to establish an allowable value for the maximum web force permitted at the root of the stringer web. This maximum permitted force/(axial length) is required as input in BEGIN. The phenomenon and appropriate peel test specimen are shown in Figs 5–7.

(k) If rings are present the stresses in the various parts of the 'ring panel module' (module cross section that is normal to the y-axis) are calculated. This calculation is performed in SUBROUTINE STRCON.

Modifications to the post-buckling theory just described, including the effect of initial local imperfections in the form of the bifurcation buckling mode, are described in detail in [34].

13.3 *Example: the hat-stiffened panel*

Corresponding to N = 8 waves from the skin buckling and local post-buckling analysis above, the distributions of N_{1var}, N_{2var} and N_{12var} in the locally post-buckled panel are next calculated. The maximum stress components in the buckled skin as well as in the stiffener segments are also computed. In addition, the tangent membrane stiffness C_{TAN} in the locally buckled skin is calculated. C_{TAN} is needed for subsequent calculation of the load factor corresponding to wide column panel buckling.

Local bifurcation buckling load factor estimates: No. of axial half-waves = 8; Load Factor from Koiter Theory = 4.08E-01; Load Factor from BOSOR4-type panel module model = 3.80E-01 NOTE: The load factor from Koiter theory is computed for a flat panel. If the actual panel is curved, or if normal pressure is present, or if there exist significant prescribed in-plane resultants N_{x0}, N_{y0} from Load Set B, or if there is significant applied in-plane shear, N_{xy}, the load factor computed from Koiter theory will not necessarily agree with that computed from the BOSOR4-type module model.

```
RESULTS FOR  8  AXIAL WAVES...POSTBUCKLING PARAMETERS:
   SLOPE, a, f**2 =  6.6279E-01 -2.1436E-01  3.3451E-02
APPLIED STRESS RESULTANTS (Load set A):
   Nx, Ny, Nxy = -3.0000E+03 -3.1623E+00  1.0000E+03
STRESS RESULTANTS GENERATED BY NORMAL PRESSURE (Load set B):
   Nxo,Nyo,Nxyo=  2.7200E+01 -4.8256E+01  0.0000E+00
STRAIN AND STRESS FROM APPLIED LOADS (curing not included):
 AVERAGE STRAIN COMPONENTS :
   EPS1,   EPS2,   EPS12   = -3.06E-03 -1.36E-04  5.58E-03
 AVERAGE RESULTANTS IN SKIN:
   N1SKIN, N2SKIN, N12SKIN = -2.32E+03 -5.14E+01  1.00E+03
 TANGENT STIFFNESS MATRIX, CTAN...
     8.0878E+05  6.1842E+04  0.0000E+00
     6.1842E+04  4.8862E+05  0.0000E+00
     0.0000E+00  0.0000E+00  1.4446E+05
**** END OF POSTBUCKLING EQUILIBRIUM CALCULATIONS****
```

14. CALCULATION OF MAXIMUM STRESSES IN EACH LAMINA OF EACH SEGMENT AND CALCULATION OF THE STRINGER POP-OFF FORCE

14.1 *Geometry of this case, showing (segment, node) and layer numbering*

INTERNAL STIFFENER
MODULE WITH HAT-SHAPED (TRAPEZOIDAL) STIFFENER...

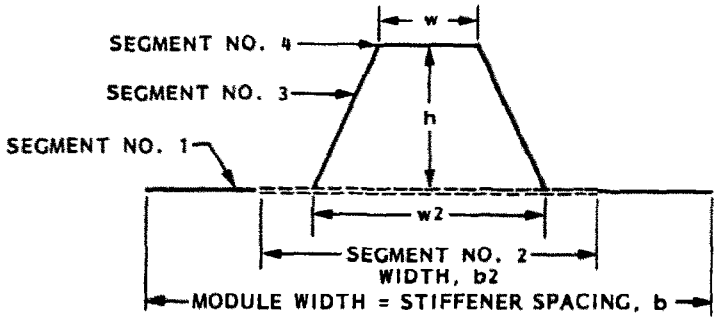

Fig. 16. Segment numbering in this sketch corresponds to numbering used for purposes of providing input data. The number of discretized BOSOR4-type segments into which the panel module is divided depends on whether or not the length b_2 is greater than w_2.

MODULE WITH b2 > w2
MODULE WITH HAT-SHAPED (TRAPEZOIDAL) STIFFENER ...

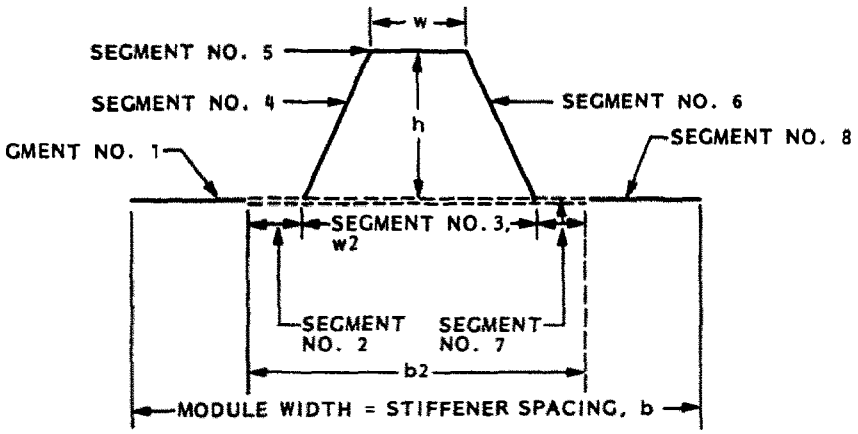

Fig. 17. Segment numbering for discretized single module models of the hat-stiffened panel for the case for which $b_2 > w_2$.

MODULE FOR CASE WHEN b2 > w2...
EXPLODED VIEW, SHOWING LAYERS and (SEGMENT, NODE) NUMBERS

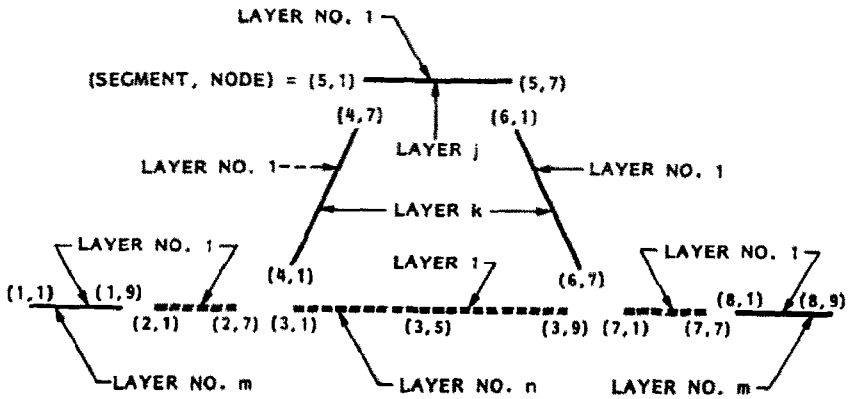

Fig. 18. (Segment, node) pairs for stress output for hat-stiffened panel module for the case for which $b_2 > w_2$.

14.2 *Post-local-buckling stresses in the panel module*

Start calculation of stresses in the panel module depicted above . . . (segment numbering below refers to that shown in Fig. 18). Stresses are calculated in each of the lamina through the thickness only at the nodes shown in Fig. 18 because computation of these stresses requires quite a bit of computer time, especially if there are many layers. The critical stresses are most likely to be at these points in the panel module cross section because these points correspond to the maximum skin buckling amplitude or bending stress concentrations which occur where the thickness changes or where the webs intersect the panel skin or the stringer flange.

There are components of stress that vary in the axial direction as $\sin n\pi x/L$ as well as those that vary as $\cos n\pi x/L$. The values of stress corresponding to the axial locations where $\sin n\pi x/L = 1$ are listed in the rows of the following table in which the leftmost entry is SIN. Those corresponding to axial locations where $\cos n\pi x/L = 1$ are listed in the rows in which the leftmost entry is COS.

Sometimes four entries are given for each layer, two for SIN and two for COS. Notice that each (SIN, COS) pair is for a different value of the coordinate, Z, through the thickness. These two pairs of entries correspond to the stresses at the extreme fibers of the layer. Only one pair is given for any layer that was originally designated by the user as being composite tape. This is because composite tape layers are usually very thin, and it is not necessary to compute the stresses at more than one location through the thickness of a thin layer. Sometimes layers are missing from the list. These are layers the thicknesses of which either the user or PANDA2 has set equal to zero.

Stress components in the post-locally-buckled panel module:

BUCK. MODE	LOCATION SEG.	NODE	IN LAYER	PANEL Z	WINDING ANGLE	IN-PLANE STRESSES IN MATL COORDS. SIG1	SIG2	SIG12	MODE OF FAILURE	TRANSVERSE CRACKING (1.0 means inactive)	ALLOWABLE STRESS	MATERIAL TYPE
SIN	1	1	1	-4.06E-02	45.0	-4.0651E+04	-2.6702E+04	5.3684E+02	no failure	1.0000E+00		2
COS	1	1	1	-4.06E-02	45.0	2.0006E+04	-1.8965E+04	-9.8749E+02	no failure	1.0000E+00		2
SIN	1	1	1	-3.46E-02	45.0	-3.1066E+04	-2.4937E+04	3.8921E+02	no failure	1.0000E+00		2
SIN	1	1	2	-3.46E-02	-45.0	-2.4937E+04	-3.1066E+04	-3.8921E+02	no failure	1.0000E+00		2
COS	1	1	1	-3.46E-02	45.0	1.9864E+04	-1.9107E+04	-1.0038E+03	no failure	1.0000E+00		2
COS	1	1	2	-3.46E-02	-45.0	-1.9107E+04	1.9864E+04	1.0038E+03	no failure	1.0000E+00		2
SIN	1	1	2	-2.86E-02	-45.0	-2.3172E+04	-2.1481E+04	-2.4157E+02	no failure	1.0000E+00		2
SIN	1	1	3	-2.86E-02	90.0	-4.3163E+04	1.6156E+03	-1.2137E+02	no failure	1.0000E+00		1
COS	1	1	2	-2.86E-02	-45.0	-1.9249E+04	1.9722E+04	1.0202E+03	no failure	1.0000E+00		2
COS	1	1	3	-2.86E-02	90.0	-2.0213E+04	6.1200E+03	-2.7981E+03	no failure	1.0000E+00		1
SIN	1	1	4	-2.34E-02	45.0	-2.9116E+04	2.1397E+03	1.1351E+02	no failure	1.0000E+00		1
COS	1	1	4	-2.34E-02	45.0	3.3321E+04	3.3733E+03	-1.0344E+03	no failure	1.0000E+00		1
SIN	1	1	6	-1.82E-02	-45.0	-4.4223E+04	4.1417E+03	1.4441E+01	no failure	1.0000E+00		1
COS	1	1	6	-1.82E-02	-45.0	-4.5687E+04	7.3506E+03	1.0485E+03	no failure	1.0000E+00		1
SIN	1	1	7	-1.30E-02	0.0	-1.7928E+04	4.0434E+03	1.5816E+03	no failure	1.0000E+00		1
COS	1	1	7	-1.30E-02	0.0	8.4464E+03	4.5735E+03	2.7981E+03	no failure	1.0000E+00		1
SIN	1	1	8	-2.60E-03	90.0	-7.7906E+03	6.0004E+03	-2.5548E+03	no failure	1.0000E+00		1
COS	1	1	8	-2.60E-03	90.0	-2.2319E+04	6.0726E+03	-2.7981E+03	no failure	1.0000E+00		1
SIN	1	1	9	6.98E-10	90.0	-4.2540E+03	6.4388E+03	-2.7981E+03	no failure	1.0000E+00		1
COS	1	1	9	6.98E-10	90.0	-2.2529E+04	6.0678E+03	-2.7981E+03	no failure	1.0000E+00		1
SIN	1	1	10	2.60E-03	0.0	1.4100E+04	6.1255E+03	3.0414E+03	no failure	1.0000E+00		1
COS	1	1	10	2.60E-03	0.0	8.3801E+03	4.4844E+03	2.7981E+03	no failure	1.0000E+00		1
SIN	1	1	11	1.30E-02	-45.0	-3.2080E+04	1.0939E+04	7.8215E+02	90 deg. tension	7.1667E-01	7.8400E+03	1
COS	1	1	11	1.30E-02	-45.0	-4.7016E+04	7.2329E+03	1.1336E+03	no failure	1.0000E+00		1
SIN	1	1	13	1.82E-02	45.0	9.6686E+04	5.6429E+03	-9.1010E+02	no failure	1.0000E+00		1
COS	1	1	13	1.82E-02	45.0	3.1549E+04	3.2165E+03	-1.1477E+03	no failure	1.0000E+00		1
SIN	1	1	14	2.34E-02	90.0	2.7575E+04	1.0384E+04	-4.9878E+03	90 deg. tension	9.4372E-01	9.8000E+03	1
COS	1	1	14	2.34E-02	90.0	-2.4424E+04	6.0251E+03	-2.7981E+03	no failure	1.0000E+00		1
SIN	1	1	15	2.86E-02	-45.0	-6.3427E+03	6.9908E+04	1.1661E+03	no failure	1.0000E+00		2
COS	1	1	15	2.86E-02	-45.0	-2.0600E+04	1.8371E+04	1.1761E+03	no failure	1.0000E+00		2
SIN	1	1	15	3.46E-02	-45.0	-4.5777E+03	7.9493E+04	1.3137E+03	no failure	1.0000E+00		2
SIN	1	1	16	3.46E-02	45.0	7.9493E+04	-4.5777E+03	-1.3137E+03	no failure	1.0000E+00		2
COS	1	1	15	3.46E-02	-45.0	-2.0741E+04	1.8230E+04	1.1924E+03	no failure	1.0000E+00		2
COS	1	1	16	3.46E-02	45.0	1.8230E+04	-2.0741E+04	-1.1924E+03	no failure	1.0000E+00		2
SIN	1	1	16	4.06E-02	45.0	8.9078E+04	-2.8127E+03	-1.4614E+03	no failure	1.0000E+00		2
COS	1	1	16	4.06E-02	45.0	1.8088E+04	-2.0883E+04	-1.2088E+03	no failure	1.0000E+00		2
SIN	1	9	1	-4.06E-02	45.0	3.3205E+04	-4.6359E+02	6.5584E+03	no failure	1.0000E+00		2
COS	1	9	1	-4.06E-02	45.0	2.7843E+04	-3.2952E+04	3.6550E+03	no failure	1.0000E+00		2
SIN	1	9	1	-3.46E-02	45.0	2.9519E+04	-4.9328E+03	5.9728E+03	no failure	1.0000E+00		2
SIN	1	9	2	-3.46E-02	-45.0	-4.9328E+03	2.9519E+04	-5.9728E+03	no failure	1.0000E+00		2
COS	1	9	2	-3.46E-02	-45.0	-3.2429E+04	2.5142E+04	-3.5220E+03	no failure	1.0000E+00		2

-------- MORE RESULTS GIVEN BY PANDA2 BUT NOT LISTED TO SAVE SPACE --------

MAXIMUM STRESS COMPONENTS AND LOCATIONS OF THEM

ALLOWABLE STRESS	MAXIMUM STRESS	STRESS MARGIN	THRU THICKNESS LOCATION, Z	TYPE OF STRESS	LOCATION IN PANEL MODULE
9.1400E+04	-7.5472E+04	2.1104E-01	-6.5004E-02	compression along fiber	seg=2 , node=1 , layer=3 , matl=1
8.0000E+03	4.8333E+03	6.5519E-01	-6.5004E-02	in-plane shear stress	seg=2 , node=1 , layer=3 , matl=1
5.0000E+01	4.0749E+01	2.2703E-01	-1.2000E-02	stringer popoff stress margin	seg=4 , node=1 , layer=1 , matl=AD
5.0000E+01	4.8867E+01	2.3191E-02	-1.2000E-02	stringer popoff stress margin	seg=6 , node=7 , layer=1 , matl=AD
8.0000E+03	4.8333E+03	6.5519E-01	-6.5004E-02	in-plane shear stress	seg=7 , node=7 , layer=3 , matl=1

```
1.0500E+05 -6.3093E+04  6.6422E-01 -4.0604E-02    compression transverse to fiber seg=8 , node=1 , layer=1 , matl=2
1.0385E+05 -5.8307E+04  7.8099E-01 -3.4604E-02    compression along fiber         seg=8 , node=1 , layer=2 , matl=2
2.5060E+04 -1.3302E+03  1.7839E+01 -2.3400E-02    compression transverse to fiber seg=8 , node=1 , layer=4 , matl=1
7.0000E+03  6.8363E+03  2.3939E-02  4.0604E-02    in-plane shear stress           seg=8 , node=1 , layer=16, matl=2
9.1035E+04  9.0996E+04  4.2951E-04 -4.0604E-02    tension along fiber             seg=8 , node=9 , layer=1 , matl=2
8.9880E+04  8.1128E+04  1.0788E-01 -3.4604E-02    tension transverse to fiber     seg=8 , node=9 , layer=2 , matl=2
1.9000E+05  1.1441E+05  6.6076E-01 -2.3400E-02    tension along fiber             seg=8 , node=9 , layer=4 , matl=1
```

14.3 *Results of stringer pop-off calculations*

```
*** STRINGER POPOFF MARGIN FOR FIRST WEB OF HAT ****
Maximum in-plane tensile force in stringer web
tending to peel the faying flange from the skin:
 Peel force that varies axially as cos(nx)=   4.059
 Peel force that varies axially as sin(nx)=  40.75
 Peel force used in popoff constraint,FPOP=  40.75
Maximum allowable peel force, FPOPMAX      =  50.00
Stringer popoff margin=FPOP/FPOPMAX - 1.0 =   0.227


*** STRINGER POPOFF MARGIN FOR SECOND WEB OF HAT ***
Maximum in-plane tensile force in stringer web
tending to peel the faying flange from the skin:
 Peel force that varies axially as cos(nx)=   4.059
 Peel force that varies axially as sin(nx)=  48.87
 Peel force used in popoff constraint,FPOP=  48.87
Maximum allowable peel force, FPOPMAX      =  50.00
Stringer popoff margin=FPOP/FPOPMAX - 1.0 =   0.0232
******* END OF STRINGER POPOFF CALCULATIONS *******
***** END OF POSTBUCKLING STRESS CALCULATIONS *****
```

14.4 *Some miscellaneous data about the hat-stiffened panel*

```
BOWING DUE TO CURING, WRESID= -1.0667E-03  3.226E-04
BOWING DUE TO NORMAL PRESSURE (GLOBAL MODEL), -1.856E-02
DEPTH OF LOCAL BUCKLE =   0.1437
```

15. CRIPPLING OF STIFFENER PARTS

Crippling of stiffener parts is calculated next in SUBROUTINE STFEIG. Proper account is of course made here for redistribution of the applied in-plane loads, N_x, N_y, N_{xy}, due to post-local buckling. After local skin buckling less load is carried by the skin and more by the stringers. The coding in SUBROUTINE STFEIG is essentially the same as that in the original PANDA code [1, 8]. There are two types of crippling:

(a) Crippling of so-called 'internal' segments, that is stiffener segments that do not have free edges. Crippling loads for these interior segments are calculated as if they are infinitely long axially compressed plates simply supported along their two opposite long edges.

(b) Crippling of so-called 'end' segments, that is stiffener segments with one free edge. Crippling loads are computed assuming that the stiffener end cross section does not deform and the number of axial half-weaves is the same as that for the interior segment to which the end segment is attached.

```
                  *** CRIPPLING (short wavelength buckling) ***
               *** of parts of the panel module cross section ***
                  *** perpendicular to the panel generator  ***
STIFF.   MODULE  PRELOAD      APPLIED     CRIPPLING     CRIPPLING     HALFWAVES
TYPE      SEG.  RESULTANT     RESULTANT   LOAD FACTOR   LOAD FACTOR   BETWEEN
                                                                      RINGS
                (from curing                  (no          (with
                    and                   transverse     transverse
                load set B)                  shear          shear
                                          deformation)  deformation)

stringer  2  -1.3941E+02  -5.8633E+03  5.8513E+00   3.6526E+00      14
stringer  3   1.6840E+01  -1.4528E+02  2.2179E+00   2.0952E+00      23
stringer  4   2.3826E+02  -3.8811E+03  5.8492E+00   3.8468E+00      19
                  *** END OF CRIPPLING CALCULATIONS ***
```

16. WIDE COLUMN BUCKLING

16.1 *PANDA2 model and philosophy*

Next, the wide column buckling load (an approximation of the panel instability load, that is, buckling between rings) is calculated. The proper tangent stiffness of the locally post-buckled skin is included in this model. Also, redistribution of the axial load due to local buckling of the skin between stringers is accounted for. The wide column load factor is computed by SUBROUTINE BUCKLE. It is called 'wide column' because instability of only a single panel module is considered. Therefore, the boundary conditions along the two edges of the complete panel normal to the screen are not considered. Instead, symmetry conditions are imposed along the analogous two edges of the single panel module.

The number of axial halfwaves is restricted to one. The length of panel normal to the screen depends on whether or not there are stiffeners in the transverse direction (rings). If there are not, this length is taken as the length of the entire panel multiplied by a factor that is unity if the actual panel is simply supported along the two edges that lie in the plane of the screen and parallel to it. If the actual panel is clamped along these two edges, the length of panel normal to the screen is taken as the length of the actual panel divided by $3.85^{1/2}$. If the panel is stiffened by transverse stiffeners (called 'rings' in PANDA2) the length normal to the screen is taken to be the spacing between ring attachment lines and the panel is assumed to be simply supported along these attachment lines and the rings are neglected in the stability phase of the calculations.

Wide column buckling with use of the discretized single panel module model is included as a constraint because it accounts for local deformations of the stiffener whose axis is normal to the screen in the panel (inter-ring) buckling mode, and it accounts for local deformation of the skin between stringers. In contrast, the PANDA-type of panel instability calculation with the smeared stiffeners does not include these local deformations. The local deformation of the stringer cross section is particularly significant in the case of J-shaped stiffeners and sometimes in the case of hat-shaped stiffeners. Some examples given later show the importance of local deformation of the skin between stringers in the wide column buckling mode.

The wide column buckling model uses the same discretized single panel module as does the local skin buckling model. However, in the case of wide column buckling the number of axial half waves between rings is unity, and the normal modal deflection at the right-hand symmetry plane in the single module model is constrained to be equal to that at the left-hand symmetry plane. In contrast, in the local skin buckling model the number of axial halfwaves between rings varies until a minimum buckling load factor has been found, and the normal modal deflection at the right-hand symmetry plane is constrained to be equal to minus that at the left-hand symmetry plane.

The wide column buckling analysis takes into account the reduced effective stiffness of the panel skin due to local post-buckling of the skin between stringers if you have chosen KOITER = Y. The applied average axial load N_x is assumed to be uniform (equal to N_1), even if you provided for N_x varying in the L2 (circum.) direction.

16.2 *Results from the hat-stiffened panel example*

Next, PANDA2 calculates the wide column buckling factor from a discretized model of a single panel module for design iteration No. 0, load set No. 1, material iteration No. 0. This load factor includes the knockdown factor, 9.158E-01, that accounts for the effect of in-plane shear loading. The effective axial length of the wide column is 1.5289E + 01. Resultants are uniform and given by:

```
LOAD SET A: axial, Nx = -3.00E+03; circ., Ny = -3.16E+00;
            in-plane shear, Nxy =  1.00E+03
LOAD SET B: axial, Nxo=  0.00E+00; circ., Nyo=  0.00E+00;
            in-plane shear, Nxyo=  0.00E+00:
LOAD SET B: induced by uniform normal pressure, P =   1.0000E+00
            Resultants from global (smeared stiffener) model:
            Nxo(p)=  3.25E+01,  Nyo(p)= -3.30E+01,  Nxyo(p)= 0.0
            Resultants from local (discrete stiffener) model:
            Nxo(p)= -5.32E+00,  Nyo(p)= -1.53E+01,  Nxyo(p)= 0.0 :

WIDE COLUMN PANEL BUCKLING LOAD FACTOR =        2.64E+00

ISKIN = 0. (WIDE COLUMN BUCKLING IS IGNORED IF ISKIN = 1.)
IWIDE = 1. (WIDE COLUMN BUCKLING IS IGNORED IF IWIDE = 0.)
    *** END OF WIDE COLUMN BUCKLING CALCULATIONS ***
```

17. PANDA[1]-TYPE BUCKLING ANALYSIS

17.1 *Introduction*

Next, local, panel and general instability load factors and load factors corresponding to rolling of the stiffeners with and without participation of the skin are calculated in SUBROUTINE BUCPAN. (Calcu-

lations including rolling of the stiffeners are not performed for hat-stiffened panels. However, the torsional rigidity derived from the area enclosed within the hat is accounted for correctly, as previously described in the section of smeared stiffener analysis.) If KOITER = 1 (local post-buckling effects included in the analysis) the proper constitutive law for the locally post buckled skin is used in generation of panel and general instability load factors. The following represents a PANDA-type of buckling analysis of the entire panel. It does not involve the discretized model of the panel module.

17.2 *Explanation and results for the hat-stiffened panel*

Next, various types of buckling (general, panel, local, rolling) are calculated with use of subroutines from the original PANDA program. See [1] and [8] for details on methods used.

In the list below, 'simp-support' means that the region of the panel being considered is assumed to be simply-supported along all four edges and there are no stiffeners along these edges; 'local buck', indicates the region being considered is that bounded by adjacent rings and stringers; 'smear string' indicates the region is that bounded axially by adjacent rings and bounded circumferentially by the panel longitudinal edges, with stringers smeared out; 'smear rings' indicates the region is that bounded axially by the panel lateral edges and circumferentially by adjacent stringers, with rings smeared out in the model; 'rolling with' means that both stiffeners and skin participate in the buckling deflections; 'rolling only' means that only the stiffener cross sections deform—the panel skin does not participate; M is the number of axial half-waves in the region being considered; N is the number of circumferential half-waves in the region being considered; and 'slope' is the slope of the nodal lines in the buckling modal pattern (non-zero for panels with unbalanced laminates and panels with applied in-plane shear loading). Loading is assumed to be uniform (N_1, N_2, N_{12}) even if you provided for N_x varying in the L2 (circumferential) direction. Clamping is taken into account by doing the analysis for a panel that is shorter in the axial direction by the factor $3.85^{1/2}$ than the dimension that you originally provided as input.

Buckling load factors from PANDA-type models for design iteration no. 0, load set no. 1, material iteration no. 0. These load factors include the effect of in-plane shear loading. M = axial half-waves; N = circ. half-waves. Loading is uniform, with resultants given by:

```
LOAD SET A: axial, Nx = -3.00E+03; circ., Ny = -3.16E+00;
            in-plane shear, Nxy =  1.00E+03
LOAD SET B: axial, Nxo=  0.00E+00; circ., Nyo=  0.00E+00;
            in-plane shear, Nxyo=  0.00E+00....
LOAD SET B: induced by uniform normal pressure, P =   1.0000E+00
            Resultants from global (smeared stiffener) model:
            Nxo(p)=  3.25E+01,  Nyo(p)= -3.30E+01,  Nxyo(p)= 0.0
            Resultants from local (discrete stiffener) model:
            Nxo(p)= -5.32E+00,  Nyo(p)= -1.53E+01,  Nxyo(p)= 0.0 :
```

We are now in SUBROUTINE GENSTB, which is called from SUBROUTINE BUCPAN. PANDA-type 'closed form' analysis. In this particular call to SUBROUTINE GENSTB we obtain a buckling load factor for buckling of the following type.

General buckling (simple support at all boundaries). Rolling of non-smeared stiffeners is not included.

```
Axial, circumferential lengths, this buckling model=
  1.5289E+01  2.4000E+01
Eigenvalue in-plane loads/length of edge,
  Nx,Ny,Nxy= -3.0000E+03 -3.1623E+00  1.0000E+03
Fixed       in-plane loads/length of edge,
  Nxo, Nyo =  2.7200E+01 -4.8260E+01
Effective thick, x-face, transverse shearing = 1.437E+00
Effective thick, y-face, transverse shearing = 8.1209E-02
Transverse shear stiffness components =
  G13, G23 =  3.3717E+04  3.4233E+05
Is transverse shear deformation weakening included?=  YES

Buckling load factors, no. of halfwaves, nodal line slope
  (M = axial, N = circumferential):
  Neglecting transverse shear deformation weakening=
    Buckling load factor = 5.3164E+00 (M =  1, N =  1)
    Nodal line slope     = 7.0000E-02
  Including  transverse shear deformation weakening=
    Buckling load factor = 3.5134E+00 (M =  1, N =  1)
    Nodal line slope     = 7.0000E-02
   **** END OF PANDA-TYPE (CLOSED FORM) *****
  *** CALCS. FOR A VARIETY OF BUCKLING MODES ***
```

18. FINAL LISTING OF WEIGHT, DESIGN MARGINS, AND DESIGN FOR THE HAT-STIFFENED PANEL

After all behavioral constraints (buckling load factors and stresses) have been calculated in SUBROUTINE STRUCT, the objective function, which in this case is the weight of the panel, is computed in SUBROUTINE OBJECT.

```
**************************************************************
************************** PANEL WEIGHT **************************
*****************                                  *****************

     CURRENT VALUE OF THE OBJECTIVE FUNCTION:  WEIGHT OF PANEL
VAR.  STR/  SEG.  LAYER  CURRENT
NO.   RNG   NO.    NO.    VALUE              DEFINITION

                          5.239E+00   WEIGHT OF THE ENTIRE PANEL

*****************                                  *****************
************************** PANEL WEIGHT **************************
```

Next are listed the design margins, the values of current design parameters with an indication of the role of these parameters in an optimization process and lower and upper bounds of the decision variables, fixed parameters and allowables. Finally, the thicknesses and winding angles of each layer of each segment in the panel module are listed. The sample case ends with a list of files used and generated during execution of the PANDA2 mainprocessor.

```
        CURRENT VALUES OF MARGINS CORRESPONDING TO CURRENT DESIGN
SEG.  CURRENT
NO.    VALUE                      DEFINITION
     6.608E-01  tensile fiber: (allowable stress)/(actual stress)-1, matl 1
     2.110E-01  compressive fiber: (allowable stress)/actual-1, matl type 1
     1.784E+01  compres. transverse stress margin: (allow./actual)-1, matl 1
     6.552E-01  in-plane shear stress margin: (allowable/actual)-1, matl 1
     2.270E-01  stringer popoff stress margin:(allowable/actual)-1, web  1
     4.295E-04  tensile fiber: (allowable stress)/(actual stress)-1, matl 2
     7.810E-01  compressive fiber: (allowable stress)/actual-1, matl type 2
     1.079E-01  tensile transverse stress marg.:(allowable/actual)-1, matl 2
     6.642E-01  compres. transverse stress margin: (allow./actual)-1, matl 2
     2.394E-02  in-plane shear stress margin: (allowable/actual)-1, matl 2
     2.319E-02  stringer popoff stress margin:(allowable/actual)-1, web  2
  2  2.653E+00  crippling margin for stringer segment. 14  local halfwaves
  3  1.095E+00  crippling margin for stringer segment. 23  local halfwaves
  4  2.847E+00  crippling margin for stringer segment. 19  local halfwaves
     1.647E+00  (Wide column panel buck. factor)/(factor of safety) - 1
                ***********  ALL 1 LOAD SETS PROCESSED  ***********
                ******************************************************
```

Summary of information from optimization analysis

VAR. NO.	DEC. VAR.	ESCAPE VAR.	LINK. VAR.	LINKED TO	LINKING CONSTANT	LOWER BOUND	CURRENT VALUE	UPPER BOUND	DEFINITION
1	N	N	N	0	0.00E+00	0.00E+00	8.0000E+00	0.00E+00	stiffener spacing, b
2	Y	N	N	0	0.00E+00	1.50E+00	2.5000E+00	2.50E+00	width of stiffener base, b2
3	Y	N	N	0	0.00E+00	8.00E-01	1.2434E+00	1.50E+00	height of stiffener (type H to see sketch), h
4	N	N	Y	5	8.00E-01	0.00E+00	1.3129E+00	0.00E+00	width of outer flange of stiffener, w
5	Y	N	N	0	0.00E+00	8.00E-01	1.6411E+00	2.00E+00	width of hat base, w2
6	N	N	N	0	0.00E+00	0.00E+00	6.0000E-03	0.00E+00	thickness for layer index no.(1)
7	N	N	N	0	0.00E+00	0.00E+00	6.0000E-03	0.00E+00	thickness for layer index no.(2)
8	N	N	N	0	0.00E+00	0.00E+00	5.2045E-03	0.00E+00	thickness for layer index no.(3)
9	N	N	N	0	0.00E+00	0.00E+00	5.2000E-03	0.00E+00	thickness for layer index no.(4)
10	N	N	N	0	0.00E+00	0.00E+00	0.0000E+00	0.00E+00	thickness for layer index no.(5)
11	N	N	N	0	0.00E+00	0.00E+00	5.2000E-03	0.00E+00	thickness for layer index no.(6)
12	N	N	N	0	0.00E+00	0.00E+00	1.0400E-02	0.00E+00	thickness for layer index no.(7)
13	N	N	N	0	0.00E+00	0.00E+00	2.6000E-03	0.00E+00	thickness for layer index no.(8)
14	N	N	N	0	0.00E+00	0.00E+00	1.5600E-02	0.00E+00	thickness for layer index no.(9)
15	N	N	N	0	0.00E+00	0.00E+00	5.2000E-03	0.00E+00	thickness for layer index no.(10)
16	N	N	N	0	0.00E+00	0.00E+00	1.0400E-02	0.00E+00	thickness for layer index no.(11)

PARAMETERS WHICH ARE ALWAYS FIXED. NONE CAN BE DECISION VARIAB.

VAR. NO.	STR/ RNG	SEG. NO.	LAYER NO.	CURRENT VALUE	DEFINITION
1		0	0	3.000E+01	Panel length normal to the plane of the screen, L1
2		0	0	2.400E+01	Panel length in the plane of the screen, L2
3	STR	0	0	HAT	Identify type of stiffener along L1 (N, T, J, R, A)
4	STR	0	0	1.000E+00	Are the stringers cocured with the skin?
5	STR	1	1	4.500E+01	winding angle (deg.) for layer index no.(1)
6	STR	1	2	-4.500E+01	winding angle (deg.) for layer index no.(2)
7	STR	1	3	9.000E+01	winding angle (deg.) for layer index no.(3)
8	STR	1	4	4.500E+01	winding angle (deg.) for layer index no.(4)
9	STR	1	5	0.000E+00	winding angle (deg.) for layer index no.(5)
10	STR	1	6	-4.500E+01	winding angle (deg.) for layer index no.(6)
11	STR	1	7	0.000E+00	winding angle (deg.) for layer index no.(7)
12	STR	1	8	9.000E+01	winding angle (deg.) for layer index no.(8)
13	STR	2	3	0.000E+00	winding angle (deg.) for layer index no.(9)
14	STR	2	4	9.000E+01	winding angle (deg.) for layer index no.(10)
15	STR	4	3	0.000E+00	winding angle (deg.) for layer index no.(11)
16	STR	0	0	1.000E+00	choose external (0) or internal (1) stiffeners
17	RNG	0	0	NONE	Identify type of stiffener along L2 (N, T, J, R, A)
18		0	0	-1.940E+02	Radius of curvature in the plane of screen, R
19		0	0	3.842E+05	Radius of curvature normal to plane of screen, R2
20		0	0	2.000E+07	modulus in the fiber direction, E1(1)
21		0	0	1.400E+06	modulus transverse to fibers, E2(1)
22		0	0	7.000E+05	in-plane shear modulus, G(1)
23		0	0	2.030E-02	small Poisson's ratio, NU(1)
24		0	0	7.000E+05	out-of-plane shear modulus, G13(1)
25		0	0	4.000E+05	out-of-plane shear modulus, G23(1)
26		0	0	5.000E-08	thermal expansion along fibers, A1(1)
27		0	0	1.600E-05	transverse thermal expansion, A2(1)
28		0	0	2.700E+02	residual stress temperature (positive),TEMPTUR(1)
29		0	0	5.600E-02	weight density (gtr than 0!) of material type(1)
30		0	0	5.200E-03	Thickness of a single lamina of matl type(1)
31		0	0	1.050E+07	modulus in the fiber direction, E1(2)
32		0	0	1.050E+07	modulus transverse to fibers, E2(2)
33		0	0	7.000E+05	in-plane shear modulus, G(2)
34		0	0	7.700E-02	small Poisson's ratio, NU(2)
35		0	0	7.000E+05	out-of-plane shear modulus, G13(2)
36		0	0	4.000E+05	out-of-plane shear modulus, G23(2)
37		0	0	1.500E-06	thermal expansion along fibers, A1(2)
38		0	0	1.500E-06	transverse thermal expansion, A2(2)
39		0	0	2.700E+02	residual stress temperature (positive),TEMPTUR(2)
40		0	0	5.600E-02	weight density (gtr than 0!) of material type(2)
41		0	0	0.000E+00	Thickness of a single lamina of matl type(2)
42		0	0	1.000E+00	Choose 0=simple support or 1=clamping

PARAMETERS WHICH ARE CLASSIFIED AS ALLOWABLES (e.g. max. stress)

VAR. NO.	STR/ RNG	SEG. NO.	LAYER NO.	CURRENT VALUE	DEFINITION
1	STR	0	0	5.000E+01	What force/(axial length) will cause web peel-off?
2		0	0	2.000E+07	Maximum allowable stress in material type(1)
3		0	0	1.900E+05	maximum tensile stress along fibers, matl(1)
4		0	0	1.828E+05	max compressive stress along fibers, matl(1)
5		0	0	9.800E+03	max tensile stress normal to fibers, matl(1)
6		0	0	2.506E+04	max compress stress normal to fibers,matl(1)
7		0	0	1.000E+04	maximum shear stress in material type(1)
8		0	0	1.050E+07	Maximum allowable stress in material type(2)
9		0	0	9.104E+04	maximum tensile stress along fibers, matl(2)
10		0	0	1.038E+05	max compressive stress along fibers, matl(2)
11		0	0	8.988E+04	max tensile stress normal to fibers, matl(2)
12		0	0	1.050E+05	max compress stress normal to fibers,matl(2)
13		0	0	7.000E+03	maximum shear stress in material type(2)
14		0	0	1.000E+00	maximum value of local/general buckling

PANEL GEOMETRY IN THE AXIAL (L1) DIRECTION
MODULE WITH HAT-SHAPED (TRAPEZOIDAL) STIFFENER

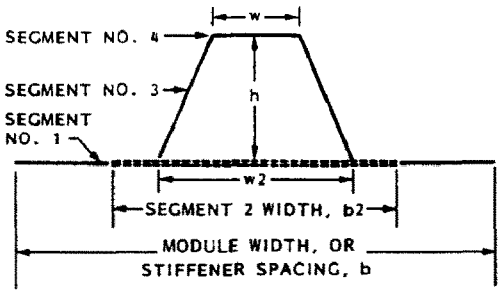

Fig. 19. Segment numbering for wall construction list that follows.

STR/ RNG	TYPE	SEG. NO.	LAYER NO.	LAYER TYPE	THICKNESS	WINDING ANGLE	MATERAL TYPE	CRACKING RATIO
STR	HAT	1	1	1	6.0000E-03	4.5000E+01	2	1.0000E+00
STR	HAT	1	2	2	6.0000E-03	-4.5000E+01	2	1.0000E+00
STR	HAT	1	3	3	5.2000E-03	9.0000E+01	1	1.0000E+00
STR	HAT	1	4	4	5.2000E-03	4.5000E+01	1	1.0000E+00
STR	HAT	1	5	5	0.0000E+00	0.0000E+00	1	1.0000E+00
STR	HAT	1	6	6	5.2000E-03	-4.5000E+01	1	1.0000E+00
STR	HAT	1	7	7	1.0400E-02	0.0000E+00	1	1.0000E+00
STR	HAT	1	8	8	2.6000E-03	9.0000E+01	1	1.0000E+00
STR	HAT	1	9	8	2.6000E-03	9.0000E+01	1	1.0000E+00
STR	HAT	1	10	7	1.0400E-02	0.0000E+00	1	1.0000E+00
STR	HAT	1	11	6	5.2000E-03	-4.5000E+01	1	1.0000E+00
STR	HAT	1	12	5	0.0000E+00	0.0000E+00	1	1.0000E+00
STR	HAT	1	13	4	5.2000E-03	4.5000E+01	1	1.0000E+00
STR	HAT	1	14	3	5.2000E-03	9.0000E+01	1	1.0000E+00
STR	HAT	1	15	2	6.0000E-03	-4.5000E+01	2	1.0000E+00
STR	HAT	1	16	1	6.0000E-03	4.5000E+01	2	1.0000E+00
STR	HAT	2	1	1	6.0000E-03	4.5000E+01	2	1.0000E+00
STR	HAT	2	2	2	6.0000E-03	-4.5000E+01	2	1.0000E+00
STR	HAT	2	3	9	1.5600E-02	0.0000E+00	1	1.0000E+00
STR	HAT	2	4	10	5.2000E-03	9.0000E+01	1	1.0000E+00
STR	HAT	2	5	9	1.5600E-02	0.0000E+00	1	1.0000E+00
STR	HAT	2	6	3	5.2000E-03	9.0000E+01	1	1.0000E+00
STR	HAT	2	7	4	5.2000E-03	4.5000E+01	1	1.0000E+00
STR	HAT	2	8	5	0.0000E+00	0.0000E+00	1	1.0000E+00
STR	HAT	2	9	6	5.2000E-03	-4.5000E+01	1	1.0000E+00
STR	HAT	2	10	7	1.0400E-02	0.0000E+00	1	1.0000E+00
STR	HAT	2	11	8	2.6000E-03	9.0000E+01	1	1.0000E+00
STR	HAT	2	12	8	2.6000E-03	9.0000E+01	1	1.0000E+00
STR	HAT	2	13	7	1.0400E-02	0.0000E+00	1	1.0000E+00
STR	HAT	2	14	6	5.2000E-03	-4.5000E+01	1	1.0000E+00
STR	HAT	2	15	5	0.0000E+00	0.0000E+00	1	1.0000E+00
STR	HAT	2	16	4	5.2000E-03	4.5000E+01	1	1.0000E+00
STR	HAT	2	17	3	5.2000E-03	9.0000E+01	1	1.0000E+00
STR	HAT	2	18	9	1.5600E-02	0.0000E+00	1	1.0000E+00
STR	HAT	2	19	10	5.2000E-03	9.0000E+01	1	1.0000E+00
STR	HAT	2	20	9	1.5600E-02	0.0000E+00	1	1.0000E+00
STR	HAT	2	21	2	6.0000E-03	-4.5000E+01	2	1.0000E+00
STR	HAT	2	22	1	6.0000E-03	4.5000E+01	2	1.0000E+00
STR	HAT	3	1	1	6.0000E-03	4.5000E+01	2	1.0000E+00
STR	HAT	3	2	2	6.0000E-03	-4.5000E+01	2	1.0000E+00
STR	HAT	3	3	2	6.0000E-03	-4.5000E+01	2	1.0000E+00
STR	HAT	3	4	1	6.0000E-03	4.5000E+01	2	1.0000E+00
STR	HAT	4	1	1	6.0000E-03	4.5000E+01	2	1.0000E+00
STR	HAT	4	2	2	6.0000E-03	-4.5000E+01	2	1.0000E+00
STR	HAT	4	3	11	1.5600E-02	0.0000E+00	1	1.0000E+00
STR	HAT	4	4	10	5.2000E-03	9.0000E+01	1	1.0000E+00
STR	HAT	4	5	11	1.5600E-02	0.0000E+00	1	1.0000E+00
STR	HAT	4	6	10	5.2000E-03	9.0000E+01	1	1.0000E+00
STR	HAT	4	7	11	1.5600E-02	0.0000E+00	1	1.0000E+00
STR	HAT	4	8	10	5.2000E-03	9.0000E+01	1	1.0000E+00
STR	HAT	4	9	11	1.5600E-02	0.0000E+00	1	1.0000E+00

```
STR   HAT   4     10     10   5.2000E-03  9.0000E+01     1        1.0000E+00
STR   HAT   4     11     11   1.5600E-02  0.0000E+00     1        1.0000E+00
STR   HAT   4     12     10   5.2000E-03  9.0000E+01     1        1.0000E+00
STR   HAT   4     13     11   1.5600E-02  0.0000E+00     1        1.0000E+00
STR   HAT   4     14      2   6.0000E-03 -4.5000E+01     2        1.0000E+00
STR   HAT   4     15      1   6.0000E-03  4.5000E+01     2        1.0000E+00

 DESCRIPTION OF FILES USED AND GENERATED IN THIS RUN:
  HAT.NAM = This file contains only the name of the case.
  HAT.OPT = Input data generated by MAINSETUP.
  HAT.OPM = Output data. Please list this file and inspect
            carefully before proceeding.
  HAT.CBL = Labelled common blocks for PANDA2 analysis.
            (This is an unformatted sequential file.)
  HAT.BL1 = Labelled common blocks for BOSOR4-type discretized
            model of single panel module.
            (This is an unformatted sequential file.)
  HAT.BL2 = Labelled common blocks for BOSOR4-type discretized
            model of entire panel with smeared stiffeners.
            (This is an unformatted sequential file.)
  HAT.RN1 = Direct access file for data base pertaining to
            BOSOR4-type discretized model of single module.
            (This is an unformatted direct access file.)
  HAT.RN2 = Direct access file for data base pertaining to
            BOSOR4-type discretized model of entire panel
            with smeared stiffeners.
            (This is an unformatted direct access file.)
  HAT.003 = Scratch file similar to the .OPT file.
  PROMPT.DAT = Prompt file for interactive input for PANDA2.
  TUTORMAIN.DAT = File containing rather detailed explanations
                  of theories on which PANDA2 is based.

  For further information about files used and generated
  during operation of PANDA2, give the command HELPAN FILES.

  Menu of commands: PANDAOPT, PLOTTER, MAINSETUP, CHANGE,
                    DECIDE, PANEL
```

18.1 *Plots of discretized, segmented panel module model*

Figure 20(b) shows a discretized model of a single module of the hat-stiffened panel. This module consists of eight segments, each of which is discretized via the BOSOR4-type of finite-difference element [2]. Figure 20(a) shows the predicted bifurcation buckling mode corresponding to local buckling of the skin between stiffeners, and Fig. 20(c) shows the predicted wide-column buckling mode. These plots were obtained via execution of the PANDA2 processor called PLOTTER.

18.2 *BOSOR4 run of entire panel with all skin and stringer segments modeled as discretized branches*

Figure 21 shows the discretized model and the six lowest eigenvalues and eigenmodes. These plots were generated after the optimum design of the hat-stiffened panel had been obtained, and after PLOTTER had been executed to obtain plots of the single module models of local and wide-column buckling. The results shown in Fig. 21 were obtained by means of the following runstream:

PANEL	(The user first answers a few simple questions. Then the PANDA2 system sets up a BOSOR4 input file for a multi-module panel.)
BOSOR4LOG	(You activate the BOSOR4 command set.)
BOSORALL	(You launch a batch run of BOSOR4 to get general bifurcation buckling of the multi-module model.)
BOSORPLOT	(The BOSOR4 system generates a multi-module panel plot file.)
PLOT	(You give a command that generates plots at your facility.)

The PANDA2 processor called PANEL uses current dimensions, properties and loading of the single panel module model to set up a multi-segment model of the entire panel. The processor PANEL asks the user how wide the panel is, whether or not there are stringers at the edges (or are the edges midway between stringers?), and whether or not the boundaries of the panel normal to the screen are constrained other than by stringers, and if they are constrained, are they simply-supported or is there a symmetry condition there?

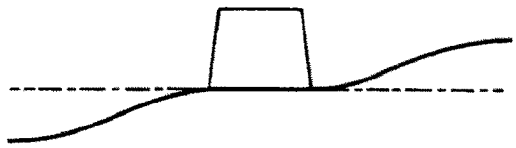

(a) LOCAL BUCKLING AT LOAD FACTOR = 0.380
n = 7 HALFWAVES NORMAL TO THE PLANE OF THE PAPER

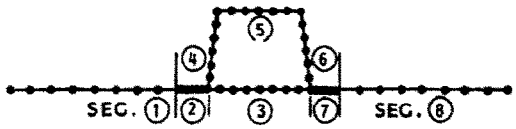

(b) DISCRETIZED CROSS SECTION OF PANEL MODULE

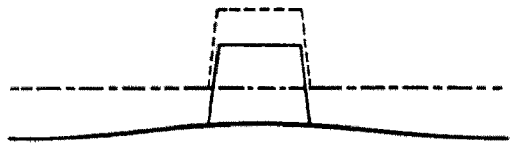

(c) WIDE COLUMN BUCKLING AT LOAD FACTOR = 2.65

Fig. 20. Discretized model of hat-stiffened module with local bifurcation buckling mode and wide column buckling mode.

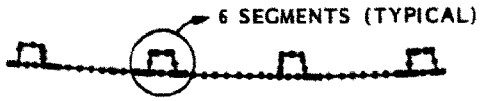

(a) Discretized 27-SEGMENT BOSOR4 MODEL

(b) MODE 1: $\lambda = 1.801$

(e) MODE 4: $\lambda = 2.488$

(c) MODE 2: $\lambda = 1.996$

(f) MODE 5: $\lambda = 2.912$

(d) MODE 3: $\lambda = 2.298$

(g) MODE 6: $\lambda = 2.991$

Fig. 21. (a) Twenty-seven-segment BOSOR4 model of the entire hat-stiffened panel. This model was automatically generated with use of the PANEL processor. (b–g) Buckling modes and load factors λ corresponding to buckling between rings (in this case buckling over the entire length of the panel, since there are no rings). Only the fifth and sixth modes represent general instability. The in-plane shear load of 1000 lb/in. is neglected in the calculation of these buckling load factors and modes. The fifth mode load factor, $\lambda = 2.912$, times the knockdown factor for in-plane shear, FKNOCK(4) = 0.916, should be compared to the wide column buckling load predicted by PANDA2: $\lambda_{WIDECOLUMN} = 2.65$.

Given the output from this short interactive session, and given the current state of the panel module, including any variation of load due to post-local buckling of the skin, PANDA2 sets up a file called NAME.ALL which is suitable without modification for use as input to BOSOR4.

The discretized model shown in Fig. 21(a) was generated after the user responded to PANEL that the panel is 24 in. wide, has stringers at the edges, and is not further supported there. The discretized model has 27 shell segments, six in each of the hat stiffeners (segments 2–7 in Fig. 20(b)), and three skin segments forming the bays between the stringers. The model is subjected to axial load that varies across the panel in a periodic fashion because the skin is in its post-locally-buckled state and has therefore shed axial load to the stringers. The stiffness of the skin between stringers is the tangent stiffness C_{TAN} determined as described above. The stiffness of the stringer segments is $Cx(i,j,k)$, $k = 2, 3, 4$, where k is the segment number in Fig. 3.

The length of the panel normal to the plane of the paper is equal to the length between adjacent rings. If there are no rings, the length is equal to the 'effective' length of the panel provided by PANDA2. (This 'effective' length is either the user-provided length L if the panel is simply-supported along the edges at $x = 0$ and at $x = L$, or it is $L/3.85^{1/2}$ if the panel is clamped along these two edges.)

To be able to analyze this complex structure with BOSOR4 requires treating it as a shell of revolution. This is done using the 'trick' described in detail in [30, Ch. 7]: essentially the axial and circumferential coordinates are interchanged; the panel is treated as a section of a torus of large diameter. The coordinate along the axis of the panel is the same as the coordinate around the circumference of the torus; the coordinate along the circumference of the panel (transverse to the stringers) is the same as the coordinate along the meridian of the torus. In applying the PANEL and BOSOR4 processors as described above, the user does not need to worry about coordinates, however. This is taken care of internally.

It is important to remember at this point that BOSOR4 does not have the capability to predict buckling in the presence of in-plane shear loading. Therefore, the applied in-plane shear load of 1000 lb/in. is ignored in the BOSOR4 analysis. One must multiply all load factors obtained with BOSOR4 by the knockdown factor FKNOCK(4) pertaining to inter-ring buckling and given by PANDA2.

Figures 21(b–g) show bifurcation buckling modes predicted by BOSOR4. It is clear that the first four modes represent skin buckling, and therefore are not of much interest. The fifth and sixth modes, however, represent general instability of at least one stringer. The buckling load factor, $\lambda_5 = 2.912$ multiplied by the knockdown factor for in-plane shear loading, FKNOCK(4) = 0.916 (from the final PANDA2 run), should be compared with the PANDA2 prediction of wide column buckling and/or general instability.

19. COMPARISONS BETWEEN TESTS, PANDA2 AND RESULTS FROM OTHER SOURCES

19.1 *Comparison with results from PANDA*

PANDA2 has been exercised for most of the cases given in [1]. Since much of the coding in PANDA2 is taken directly from PANDA [1], agreement with PANDA is good.

19.2 *Axially compressed, graphite-epoxy, tee-stiffened panel*

Figure 22 shows the geometry and local and wide-column bifurcation buckling modes predicted by PANDA2. Graphite-epoxy, flat panels 32 in. long and 24 in. wide were tested under pure axial compression at the NASA Langley Research Center. Complete descriptions of the panels and test and computer models and results are presented by Starnes *et al.* [5].

The panel to which Fig. 22 corresponds carried an ultimate axial load about three times the local bifurcation buckling load, $P(cr)$. Figure 23 shows back-to-back axial strains at the peak of a local buckle. Figure 24 demonstrates the load redistribution that occurs from the skin to the stringers as the panel is loaded further into the post-local-buckling region. In view of the approximate nature of the PANDA2 analysis, it is felt that the agreement between PANDA2 results and STAGSC-1 [17] results is reasonably good.

19.3 *Predictions of bifurcation buckling of isotropic and orthotropic plates under various combinations of* N_x, N_y *and* N_{xy}

Leissa [6] has written a long survey on buckling of laminated composite plates and shells. Some results presented in [6] are compared with PANDA2 results in the following paragraphs.

Table 1 lists comparisons between PANDA2 and the results of calculations by Chamis [7], who used a trigonometric series and the Galerkin method to compute buckling loads of isotropic and orthotropic plates under combined N_x, N_y and N_{xy}. Inspection of Table 1 reveals that the agreement between PANDA2 and Chamis' results is excellent if no in-plane shear load is present, is good if N_{xy} is considerably less than N_x or N_y, and in every case underestimates the buckling load factor in instances in which the agreement with Chamis' results is not very good: PANDA2 errs on the safe side.

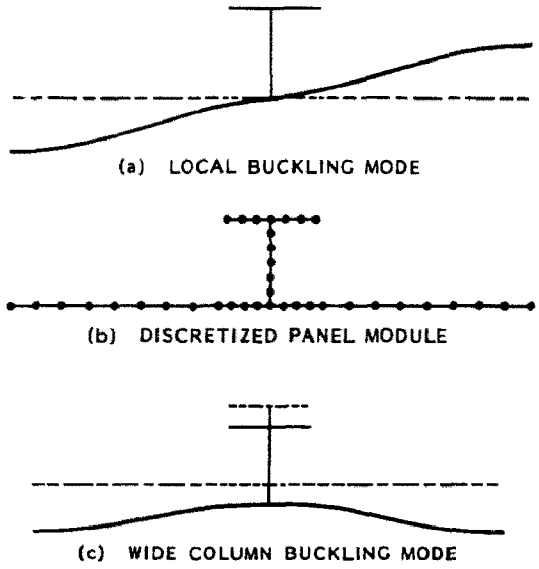

Fig. 22. Discretized model of tee-stiffened module with (a) local bifurcation buckling mode and (c) wide column buckling mode. These results correspond to a test performed at NASA [5] on a flat, graphite-epoxy panel under pure axial compression.

The theory by which buckling load factors are obtained for cases involving in-plane shear and/or unbalanced laminates is explained in [8, pp. 40–41, Fig. 14]. PANDA2 uses a one-term Rayleigh–Ritz method, rather than a trigonometric series expansion, as did Chamis. It appears that the quality of the results obtained justifies the greatly improved efficiency on the computer. This efficiency is required for the practical solution of optimization problems of the complex sort solved by PANDA2. Anderson and Stroud [9] and Stroud and Anderson [10] use a strategy that is similar to that used in PANDA2 for obtaining improved results with their optimization code, PASCO, for cases involving in-plane shear loading.

19.4 *Transverse shear deformation effects*

Leissa [6] includes examples originally presented in [11–13]. Figure 25 shows PANDA2 results compared with results from classical plate theory and results obtained by Whitney [12] for a uniformly axially compressed plate with an infinite number of layers with fibers at plus and minus 45°. Whitney's theory represents an extension of Ambartsumyan's [11] valid for angle-ply laminates. Table 2 lists comparisons of

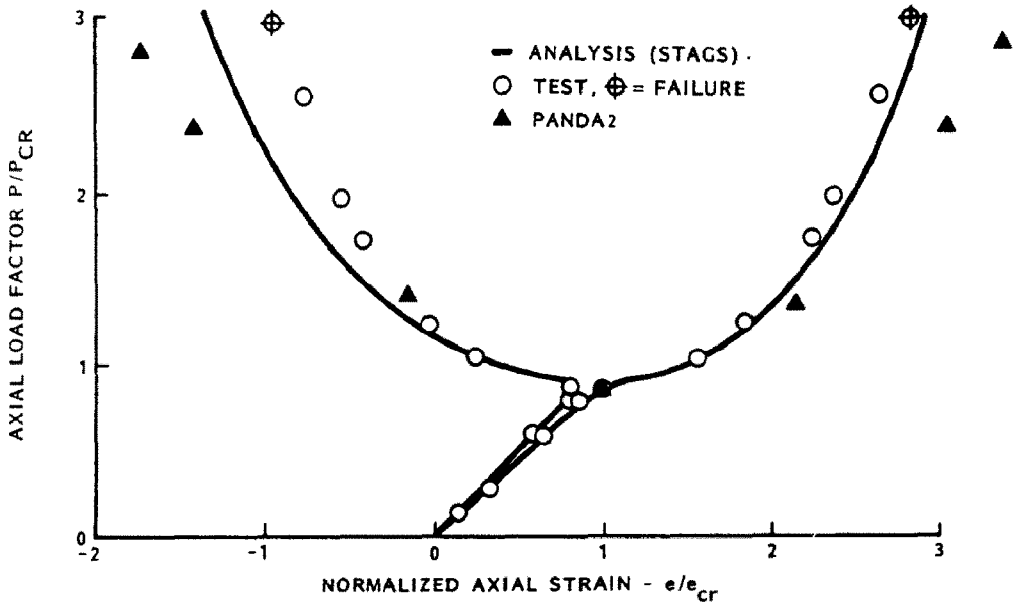

Fig. 23. Comparison axial strain at a local buckle peak from test [5], STAGSC-1 analysis [5], and PANDA2 analysis for axially compressed, tee-stiffened, graphite-epoxy flat panel (adapted from [5, Fig. 13c]).

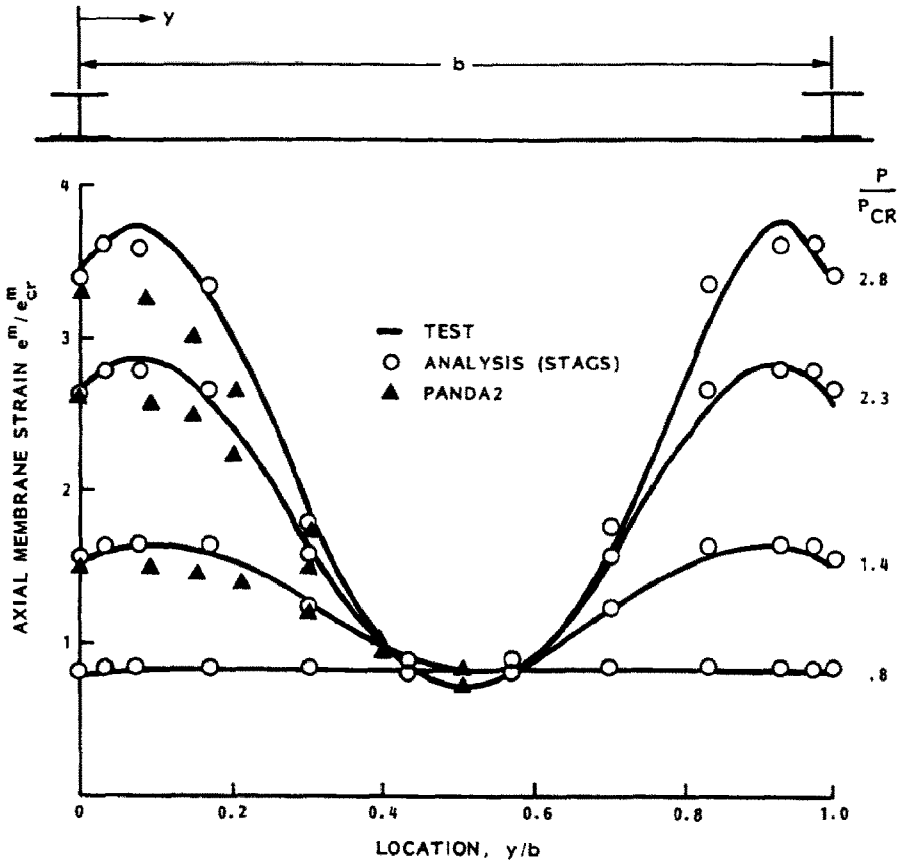

Fig. 24. Comparison of membrane axial strain from test [5], STAGSC-1 analysis [5], and PANDA2 analysis for axially compressed, tee-stiffened, graphite-epoxy flat panel (adapted from [5, Fig. 14]).

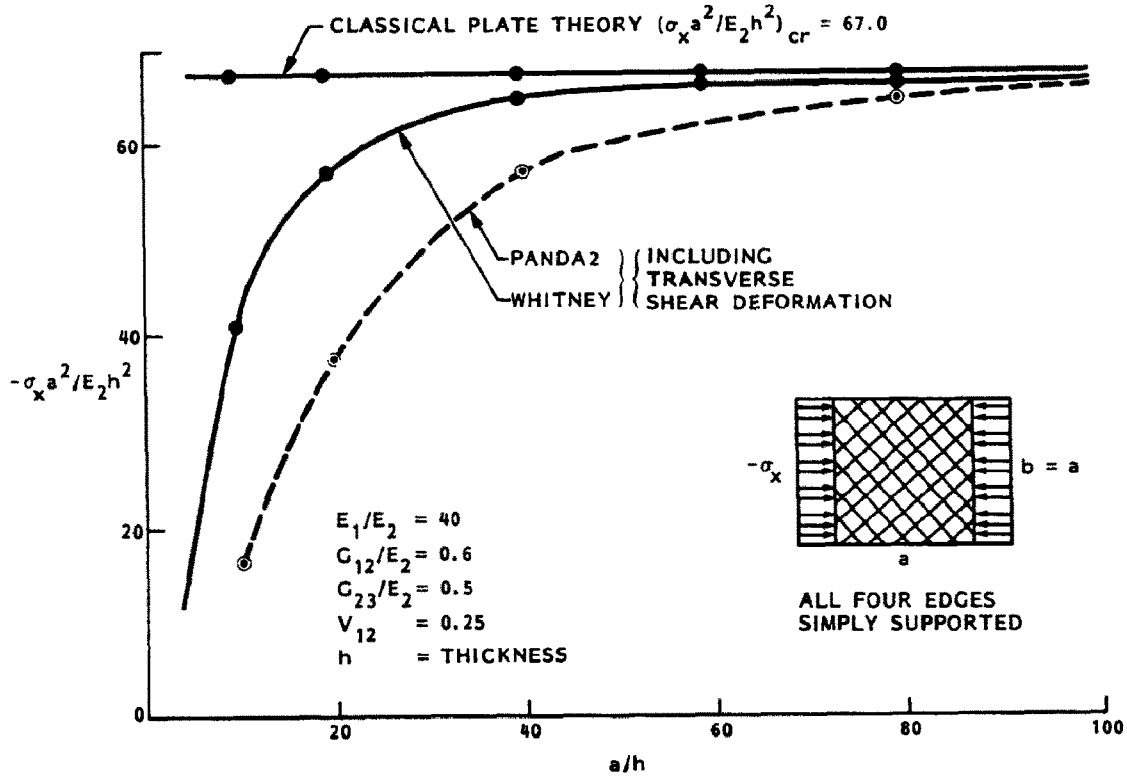

Fig. 25. Buckling of uniformly axially compressed, simply supported, plus-and-minus 45° angle-ply square plate with an infinite number of layers, with and without accounting for transverse shear deformation.

Table 1. Buckling load factors N_{cr} for simply supported plates

Plate Dim. X x Y (in.)	Loading Combination Nx (lb/in)	Ny (lb/in)	Nxy (lb/in)	Buckling Load Factors, Ncr — Orthotropic — Fibers along x PANDA2	Fibers along x Chamis	Fibers along y PANDA2	Fibers along y Chamis	Isotropic PANDA2	Isotropic Chamis
5x10	-1	0	0	996	998	145	145	499	500
"	0	-1	0	578	581	576	581	1278	1279
"	-1	-1	0	463	465	116	116	400	400
"	-1	0	1	949	948	132	114	466	479
"	0	-1	1	532	619	300	395	940	998
"	-1	-1	1	437	446	109	113	383	389
"	-.001	0	1	1949	2185	487	700	1858	2104
10x10	-1	0	0	285	286	145	145	320	320
"	0	-1	0	145	145	285	286	320	320
"	-1	-1	0	116	116	116	116	160	160
"	-1	0	1	239	246	133	136	214	277
"	0	-1	1	133	136	239	246	235	277
"	-1	-1	1	109	111	109	136	140	153
"	-.001	0	1	487	531	487	531	464	752
"	-1	-0.75	0	145	145	122	122	183	183
"	-1	-0.50	0	190	191	129	129	213	213
"	-1	-0.25	0	228	229	136	137	256	256
"	-1	+0.25	0	378	381	154	155	427	426
"	-1	+0.50	0	570	572	165	166	571	571
"	-1	+1.00	0	1328	1330	193	194	666	666
"	-1	-0.50	0.25	189	190	128	129	209	212
"	-1	+0.50	0.25	532	549	164	165	482	562
"	-1	-0.50	0.50	190	187	126	127	199	209
"	-1	+0.50	0.50	470	496	161	163	384	539
20x10	-1	0	0	144	145	145	145	320	320
"	0	-1	0	36.4	36	249	249	125	125
"	-1	-1	0	29.1	29	116	116	100	100
"	-1	0	1	74.9	99	133	155	235	250
"	0	-1	1	33.6	35	237	237	117	120
"	-1	-1	1	27.4	28	109	111	96	97
"	-.001	0	1	122	175	487	491	464	528

Matl Props:Orthotropic: E11, E12, G = 32.9, 1.8, 0.88 x 10**6 psi
large nu = 0.24; fibers along E11
Isotropic: E = 10.0 x 10**6 psi, nu = 0.3
Plate thickness, t = 0.096 in.; B.C.s: all edges simply supported

Table 2. Buckling load factors $N_x\pi^2/(G_{13}h)$ for simply supported, orthotropic plates

Plate Aspect Ratio a/b	Classical Plate Theory PANDA2	Classical Plate Theory REF. [13]	Including Transverse Shear Deformation PANDA2	Including Transverse Shear Deformation REF. [13]
0.33	4.18	4.15	2.77	2.76
0.50	4.25	4.22	2.80	2.80
1.00	4.80	4.78	3.03	3.32
1.50	6.27	6.28	3.56	4.95
2.00	9.56	9.60	4.41	9.20

Material Properties:
E1, E2, G12, G13, G23 = 32.5, 1.84, 0.642, 0.642, 0.361 x 10**6 psi
large nu = 0.256
Geometry: Axial length a; Width b; Thickness h; h/a = 0.1

Table 3. Buckling load factors k_0 for orthotropic plates subjected to pure in-plane bending

Stiffness Ratio, D	Buckling Load Factor ko	
	PANDA2	REF. [14]
0.0	12.11	12.87
0.4	15.89	17.39
1.0	23.68	23.90

PANDA2 results with results from a theory for orthotropic plates given by Vinson and Smith [13]. In both cases PANDA2, which is based on Timoshenko beam theory, yields conservative buckling loads when transverse shear deformation is taken into account.

19.5 *Nonuniformly axially compressed orthotropic plates*

Table 3 lists results from PANDA2 and from a theory given by Brunelle and Oyibo in [14] for orthotropic flat plates subjected to a membrane stress field corresponding to pure in-plane axial bending in the prebuckling phase, and simply supported on all four edges in the buckling phase. The buckling load factor,

$$k_0 = N_x b^2/[\pi^2(D_{11}D_{22})^{1/2}], \tag{19.1}$$

is determined by a single parameter,

$$D = (D_{12} + 2D_{66})/(D_{11}D_{22})^{1/2}, \tag{19.2}$$

in which b is the panel width and D_{11}, D_{12}, D_{22}, D_{66} are the bending and twisting stiffnesses previously called C_{44}, C_{45}, C_{55} and C_{66} in the sections on PANDA2 theory.

The PANDA2 results, which are conservative, are computed from a BOSOR4-type of model in which the panel width b is discretized and buckling modal displacements are assumed to vary harmonically in the axial direction.

19.6 *Stiffened panels under combined axial compression and in-plane shear*

Figures 26–29 pertain to six stiffened panels analyzed by Stroud *et al.* [15]. They obtained results using PASCO [10], EAL [16] and STAGS [17]. Figure 26 gives the properties of the four panels stiffened by blades. The sketches in Fig. 26 show a single module only. All of the panels had six equally spaced stiffeners and were 30 in. square. They were simply supported on all four edges.

In Fig. 27 results from PANDA2 are compared with those from EAL. In the EAL model the panel and stringers were discretized into a rather fine grid of finite elements. The EAL results agreed very well with those obtained with STAGS. Therefore, these results are regarded here as the correct, converged standard with which to compare the results obtained with PANDA2.

The coordinates in each of the four frames in Fig. 27 are the ratios of the applied loads to critical loads calculated by the EAL program for pure axial compression $[N_{xcr}(N_{xy} = 0)]$ and pure in-plane shear $[N_{xycr}(N_x = 0)]$.

Interaction curves for several PANDA2 models are plotted in each frame of Fig. 27. In example 1 the local buckling load factor far exceeds that for general buckling; in examples 2 and 3 local and general buckling load factors are fairly close to each other; and in example 4 the local buckling load factor is much smaller than that for general buckling.

In PANDA2 general or panel (between rings) buckling load factors are calculated with use of three models:

1. A wide column model, based on results obtained with use of a single discretized panel module. Examples of buckling modes obtained with this model are shown in Figs 20(c) and 22(c). The wide column model simulates panel buckling, that is, buckling between rings in which both panel skin and stringers participate in the buckling mode. If there are no rings, the wide column model simulates general instability.

2. A smeared stiffener model, based on the closed form theory used in PANDA [1] and based on the assumption that the panel skin between stringers is fully effective in resisting buckling. Panel instability is predicted by a model in which the stringers are smeared out and buckling occurs between rings, with simple support boundary conditions being applied at the ring lines of attachment and rings neglected. General instability is predicted by a model in which both stringers and rings are smeared out, with simple support boundary conditions being applied on all four edges of the panel and the axial length of the panel being modified as previously described to simulate clamping.

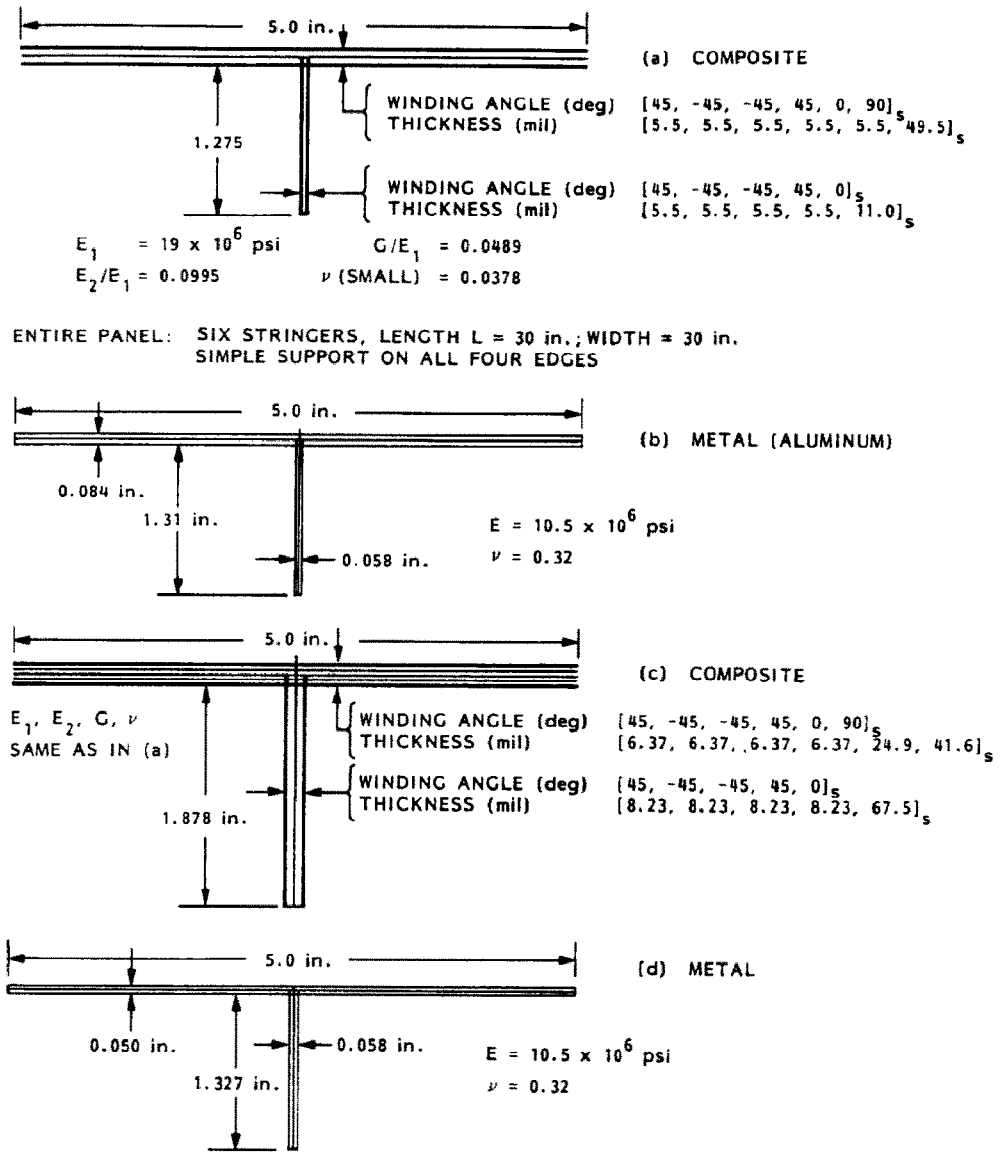

Fig. 26. Blade-stiffened panel modules that comprise the 30-in.-square simply supported panels under axial compression and in-plane shear analyzed by Stroud *et al.* [15] at NASA Langley.

3. A smeared stiffener model, based on the closed form theory used in PANDA [1] and based on the assumption that the skin is only partially effective in resisting buckling (called 'reduced skin stiffness' in Fig. 27). In this model the reduced skin stiffness is used for both panel (between rings) and general (overall) instability predictions.

During optimization runs with PANDA2, buckling constraint conditions corresponding to general or panel instability are generated with use of the wide column criterion because it is generally conservative. However, there are two circumstances in which the wide column buckling load factor does not constrain the design:

1. if the user indicates that he or she does not want it to constrain the design; and

2. if the wide column buckling mode resembles a local skin buckling mode. To identify precisely what is meant by 'resembles': if the amplitude of the wide column buckling modal normal deflection midway between stiffeners is more than ten times the normal deflection directly under a stiffener, then this mode is rejected by PANDA2 as an indicator of wide column buckling. For example, the buckling modes in Figs 20(c) and 22(c) were both accepted by PANDA2 as indicators of panel instability because the normal deflection of the panel skin where the stiffener is attached is about 25% of the maximum normal deflection shown in Fig. 20(c) and is about 50% of the maximum normal deflection shown in Fig. 22(c). An example is given later of a 'wide column' buckling mode that was rejected by PANDA2 as an indicator of panel instability.

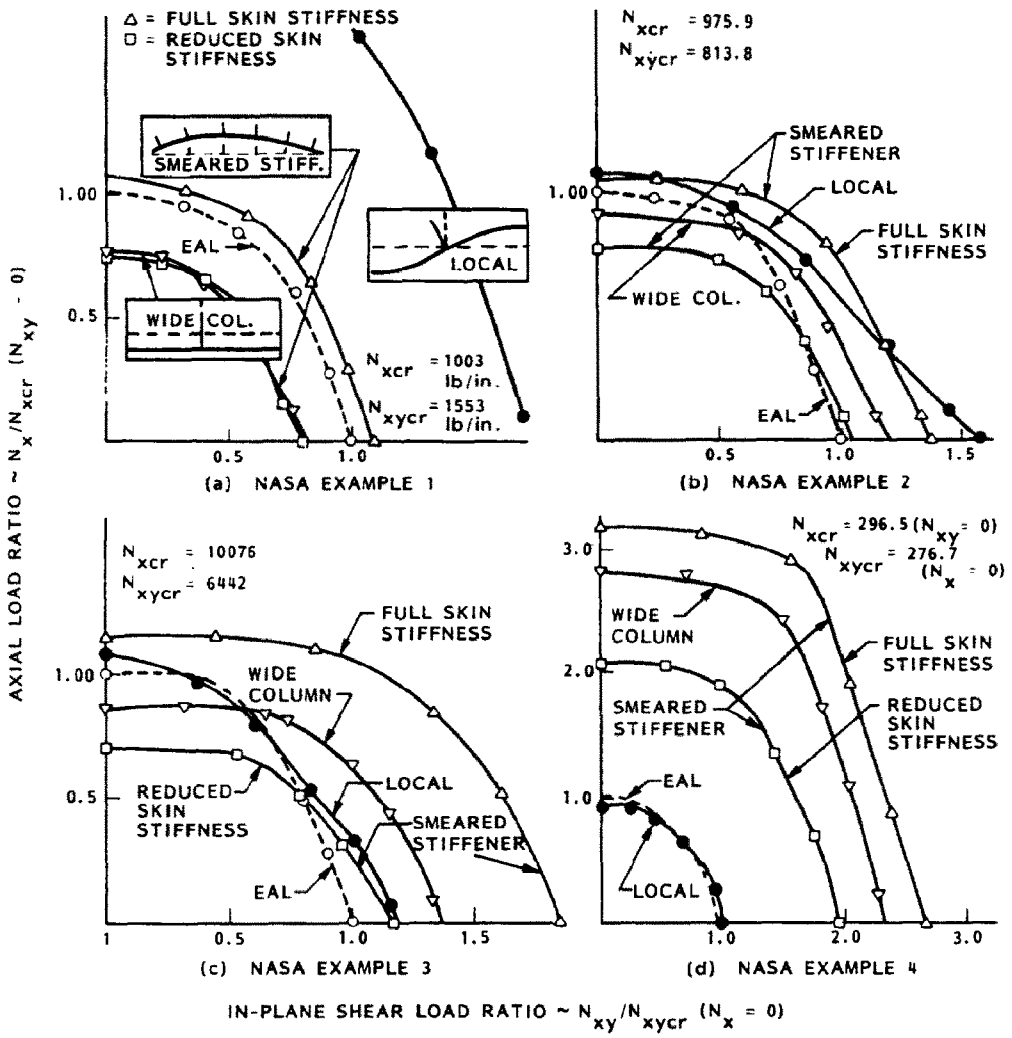

Fig. 27. Bifurcation buckling load–interaction curves obtained from PANDA2 and from a finite element model (EAL) for the four blade stiffened panels identified in the previous figure.

If either circumstance 1 or 2 pertains, PANDA2 uses as a constraint condition in the optimization process the buckling load factor from the closed form PANDA analysis with skin stiffness reduced as described in Sec. 8.5.

An important observation from Fig. 27 is that the wide column buckling load factor does not necessarily yield a conservative estimate of the general instability load. Wide column buckling loads overestimate the general instability load as predicted from EAL when the loading is predominantly in-plane shear and local and general buckling occur at loads that are fairly close to each other. This result is most noticeable in Fig. 27(c), NASA example 3.

Figure 28 depicts two additional panel modules treated in the NASA paper [15], and Fig. 29 shows the corresponding load–interaction curves. The statement just made with regard to conservativeness of buckling load factors obtained for panels loaded predominantly in shear holds in these cases also, the more noticeable being NASA example 7.

In view of these results, the user should probably apply a factor of safety of something like 1.5 to load factors for general instability in cases when the loading is predominantly in-plane shear and local and general instability loads factors are fairly close to each other.

Figure 30 shows interaction curves obtained for two optimized designs. The starting design corresponding to Fig. 30(a) was the NASA example 2 shown in Fig. 26(b). The starting design corresponding to Fig. 30(b) was the final design in Fig. 30(a). The decision variables during optimization were the skin thickness, stiffener thickness, and stiffener height. In each case the panel was considered to be subjected to five independent combinations of axial load N_x and in-plane shear load N_{xy}:

$$(N_x, N_{xy}) = (-1000, 0), (-866, 500), (-707, 707), (-500, 866), (-100, 950),$$

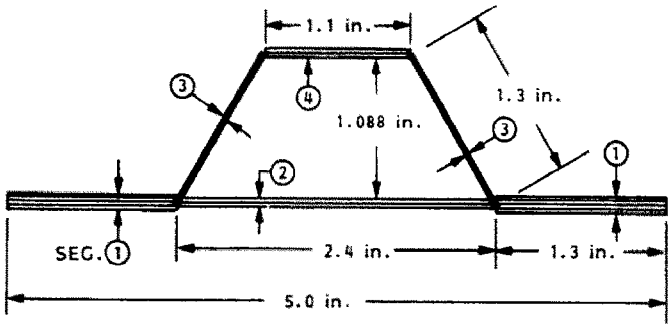

(a) COMPOSITE

E_1, E_2, G, ν SAME AS IN FIG. 20 (a)

SEG. ① WINDING ANGLES (deg) $[45, -45, -45, 45, 0]_s$
THICKNESS (mil) $[10.315, 10.315, 10.315, 10.315, 9.953]_s$

SEG. ② WINDING ANGLES (deg) $[45, -45, 0]_s$
THICKNESS (mil) $[10.315, 10.315, 16.955]_s$

SEG. ③ WINDING ANGLES (deg) $[45, -45]_s$
THICKNESS (mil) $[10.315, 10.315]_s$

SEG. ④ WINDING ANGLES (deg) $[45, -45, 0]_s$
THICKNESS (mil) $[10.315, 10.315, 25.383]_s$

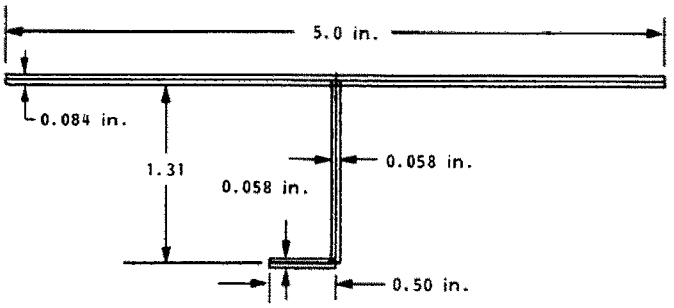

(b) METAL

$E = 10.5 \times 10^6$ psi
$\nu = 0.32$

Fig. 28. Hat- and J-stiffened panel modules that comprise the 30-in.-square simply supported panels under axial compression and in-plane shear analyzed by Stroud *et al.* [15] at NASA Langley.

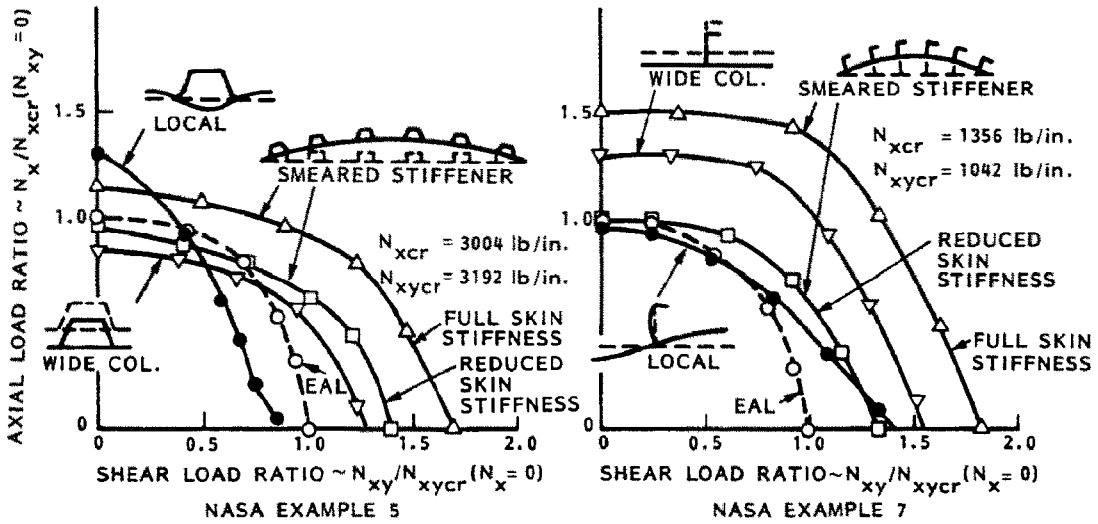

Fig. 29. Bifurcation buckling load–interaction curves obtained from PANDA2 and from a finite element model (EAL) for the hat- and J-stiffened panels identified in Fig. 28.

in which the units of N_x and N_{xy} are lb/in. In each case five design iterations were used. Approximately 14 min of VAX 11/780 (VMS operating system version 4.2) were required for the five iterations. The option IQUICK = 0 was used, that is, the optimum designs were obtained with use of discretized single panel module models as well as PANDA closed-form models.

The results in Fig. 30(a) were obtained via a strategy that required the use of the wide column buckling load factor as a design constraint. Therefore, the smeared stringer model with skin stiffness reduced as described in Sec. 8.5 was not active in this run. The load–interaction curve for the reduced skin stiffness model is shown in Fig. 30(a) so that it can be compared to that for the wide column model, which was active during the optimization process.

The results in Fig. 30(b) were obtained via a strategy that ignored the wide column buckling load factor but used the smeared stringer model with reduced skin stiffness instead.

In this case there is very little difference between the results. It is slightly more conservative to use the reduced skin stiffness model rather than the wide column buckling model in this case, but the difference is insignificant. As a general rule, it is probably good practice to run cases of particular importance both ways and choose the more conservative design.

19.7 *Optimization, tests and comparison of test and theory for axially compressed, graphite-epoxy, hat-stiffened panels*

PANDA2 was used to find the minimum weight design of a graphite-epoxy curved panel, 30 in. long, 24 in. wide, with a radius of curvature of 194 in. (hat stiffeners on the inside), and clamped along the curved edges. The panel was optimized for 3000 lb/in. uniform axial compression. All factors of safety were set equal to unity.

Local skin buckling did not constrain the design. That is, the panel was designed so that the skin was permitted to go far into its post-buckled state. Rather than the load factor corresponding to local bifurcation of the panel skin constraining the design, the maximum stresses generated in certain of the laminae as the skin stretches, compresses, and bends in its locally post-buckled state constrained the design instead.

The procedure for optimization was as follows.

1. A starting design was established via the BEGIN processor. This design is listed in the section on BEGIN. Notice that the force/(axial length) required to cause web peel-off is given as 50 lb/in. This number was used after some peel tests had been conducted on graphite-epoxy samples with thicknesses and fiber angles similar to those obtained in previously optimized designs. In these T-tests, peeling occurred between 50 and 100 lb/in.

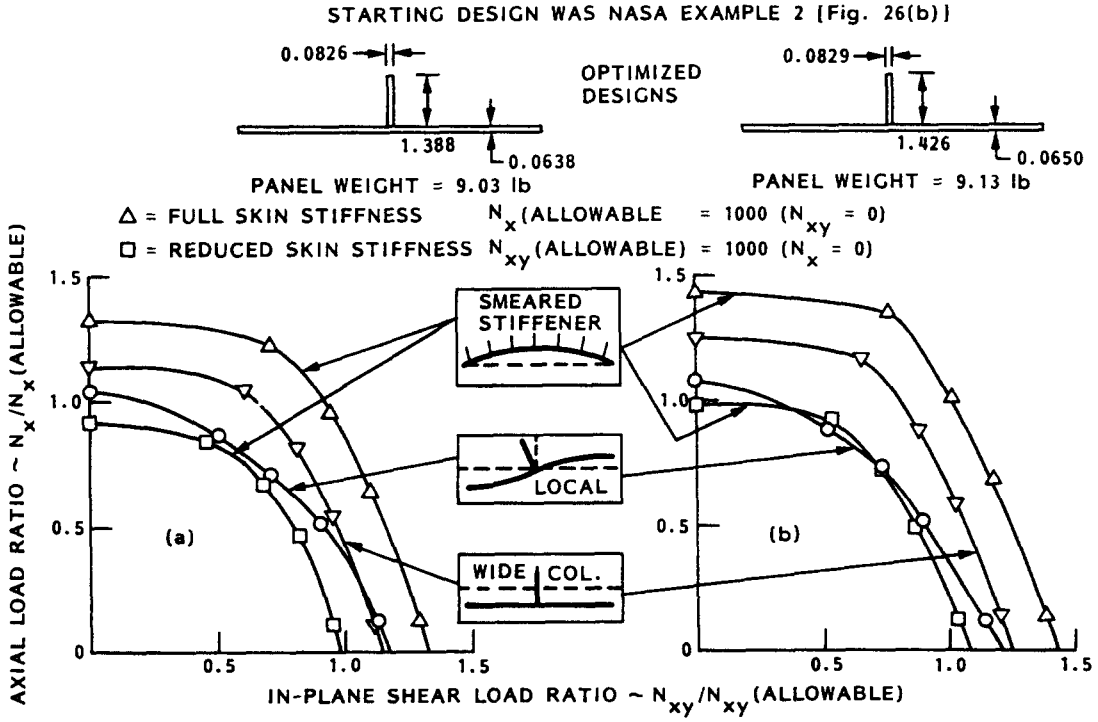

Fig. 30. Bifurcation buckling load–interaction curves obtained from designs optimized with use of PANDA2: (a) optimum design with use of the wide column buckling load factor as a design constraint; (b) optimum design with neglect of the wide column buckling load factor as a design constraint.

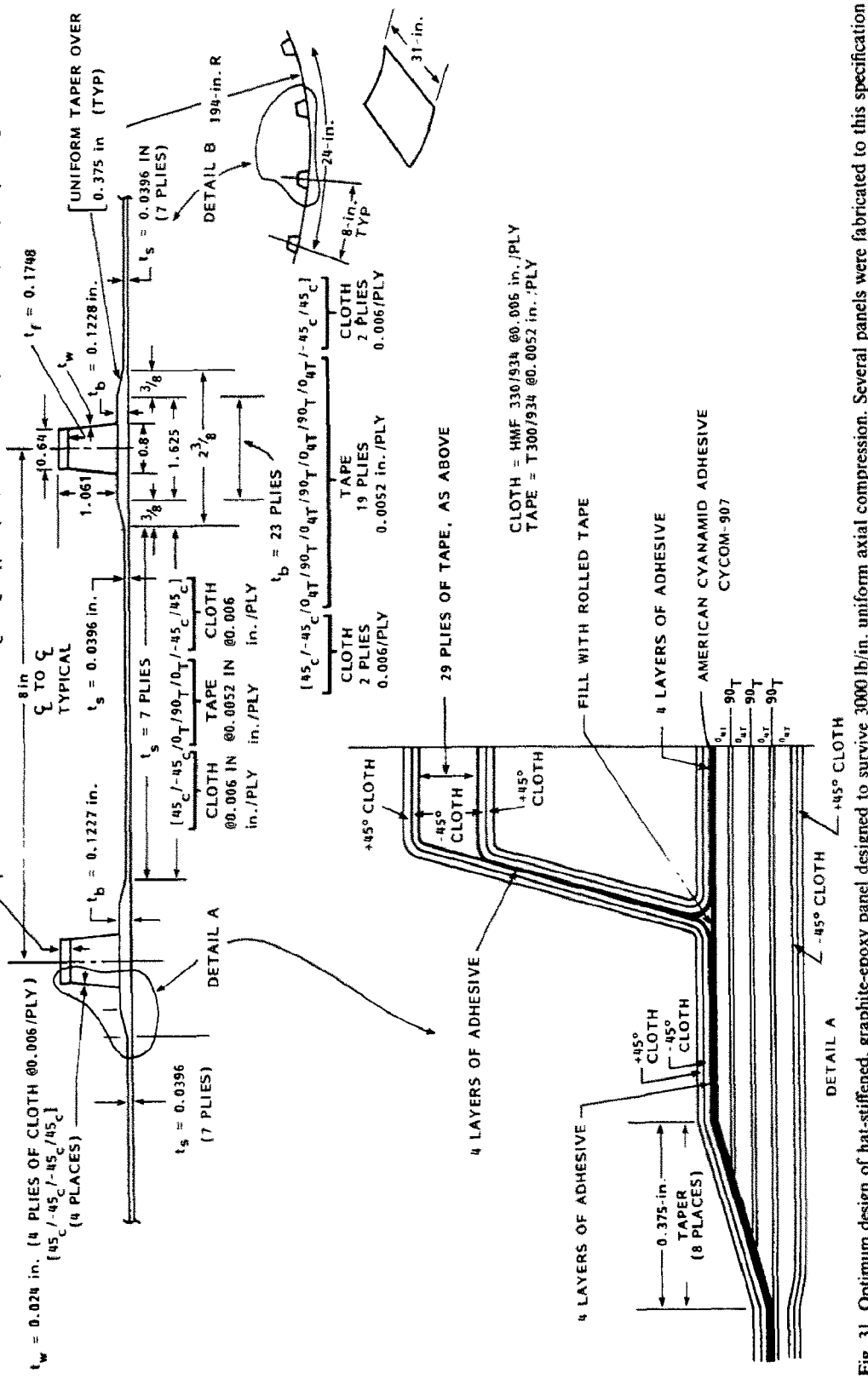

Fig. 31. Optimum design of hat-stiffened, graphite-epoxy panel designed to survive 3000 lb/in. uniform axial compression. Several panels were fabricated to this specification and tested.

tension. One of the peel text specimens after failure is shown in Fig. 7, and the origin of the stiffener 'pop-off' constraint used in PANDA2 is illustrated in Figs 5 and 6.

2. Decision variables, linked variables, and escape variables were initially selected as listed in the section on DECIDE.

3. Loading was initially selected as listed in the section, ESTABLISHING LOADS AND STRATEGY IN PANDA2, except that there was no pressure loading and the type of analysis selected was optimization (analysis type 1) rather than fixed design (analysis type 2). Note that even though we wished to load the panel only in axial compression in the test with which the results obtained with PANDA2 were to be compared, a combination of axial compression of 3000 lb/in. and in-plane shear of 1000 lb/in. was initially selected during the first interactive session in MAINSETUP. There is an interesting reason for initially using combined axial compression and in-plane shear rather than axial compression alone, a reason that becomes obvious only after trying to optimize an axially stiffened panel under pure axial compression. The optimum design of an axially stiffened panel with no applied in-plane shear load is a panel with no skin at all, just an array of columns that support the axial load! The writer has fallen into this trap more than once in giving demonstrations of PANDA2.

4. The main processor PANDAOPT was executed several times. Each time it performed five design iterations. A minimum weight design was obtained.

5. Next, DECIDE was used again. Certain of the layers in the panel skin, in particular those with plus and minus 45° fiber angles, were assigned minimum thicknesses close to those determined previously. This was done so that in optimization runs performed for axial compression only, the skin would not disappear entirely and the panel to be tested would be capable of supporting considerable in-plane shear if required.

6. MAINSETUP was used again. This time the in-plane shear load was dropped. The panel was loaded by 3000 lb/in. axial compression only.

7. PANDAOPT was exercised several times again in order to obtain a new minimum weight under the less severe loading.

8. The processor CHANGE was used in order to change thicknesses of certain of the laminae so that all laminae represented integral numbers of layers of graphite-epoxy tape of thickness 0.0052 in. or graphite-epoxy cloth of thickness 0.006 in., where appropriate (Fig. 31). The total thicknesses of all laminae were kept as close as possible to those obtained via the PANDA2 optimization in step 7.

9. DECIDE was exercised again. This time no thicknesses were chosen as decision variables. Only the height and width of the hat and the width of the base under the hat were chosen as decision variables.

10. PANDAOPT was exercised again to obtain a final optimum design. This design is shown in Fig. 31.

The predicted failure load is, of course, 3000 lb/in. pure axial compression, and the predicted failure mode is maximum shear strain in the outermost cloth layers at the twelve points shown in Fig. 32. According to PANDA2 predictions, the failure mode should be characterized by vertical tears through the wall adjacent to the stiffeners where the skin is thin.

Notice that PANDA2 causes a rather thick base to be built up under each hat stiffener. This base appears to perform three functions:

(a) It causes reduction in the forces tending to peel the hat webs from the panel skin by reducing the amplitude of the local skin buckling pattern at the lines of attachment of the hat webs to the panel skin. This reduced amplitude of the local skin buckling mode can be seen in Fig. 20(a).

(b) It maximizes the bending moment of inertia of each hat by balancing the material in the crown of the hat, thereby maximizing the wide-column buckling load factor.

(c) It minimizes the amount of axial bowing in the panel due to curing.

The predicted failure load of 3000 lb/in. corresponds to a model in which the panel is assumed to be infinitely wide with stringers spaced at 8-in. intervals. The actual test panels were 27.25 in. wide and had stringers near

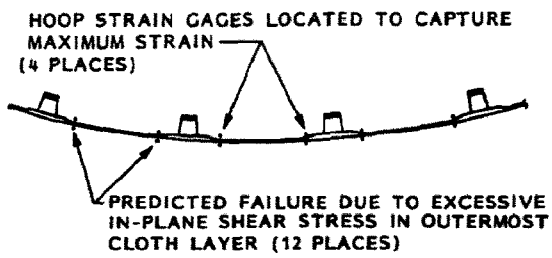

Fig. 32. Predicted locations of critical stresses in the locally postbuckled, axially compressed, hat-stiffened, graphite-epoxy panel.

each edge. Hence, the actual panel is axially stiffer than the theoretical model of it because there are four stiffeners in 27.25 in. whereas in the theoretical model there are three stiffeners in 24 in. If the PANDA2 prediction of 3000 lb/in. is multiplied by the ratio of the axial stiffness of the test panel to the axial stiffness of the theoretical panel (1.17), a new prediction of failure of the test article at an axial load/(circumferential arclength) of 3510 lb/in. is obtained.

Before any large panels were fabricated, several tests were conducted on small, flat panels, an example of which is shown in Fig. 33. The small panels were about 18 in. long and 11 in. wide. They had two stringers, one near each edge. The vertical edges were clamped lightly together to prevent delaminations from propagating in from a free edge. Many small C-clamps were applied to short aluminum tabs. Small axial gaps between each aluminum tab prevented this edge support from accepting significant axial load. The C-clamps and aluminum tabs are visible in Fig. 33, with some of the small axial gaps visible near the bottom of the panel where the failure occurred.

The purpose of testing several small panels first was to learn how best to fabricate the large panel. Should kevlar stitching be used near the hats in order to postpone stringer pop-off, a failure mode frequently encountered by other investigators? Should adhesive be used in addition to the basic epoxy? Six of the small panels were tested with various combinations of stitching and adhesive. As a result of these tests, it was found best to use adhesive alone, as specified in Fig. 31. (An interesting finding is that stitching plus adhesive seems to be worse than adhesive alone.)

Figure 34 shows one of the large, curved panels installed in a testing machine especially built for axial compression tests of panels of this type. Details about the testing machine are given by Holmes [18]. The top head of the machine can rotate and translate as a rigid body in order to accommodate any linear errors in the trim of the panel to be tested. Axial strain measurements from crown and base of each of the four stringers at their midlengths inform the operator of the test machine how to actuate the head in order to make the axial load as uniform as possible across the panel width and to minimize bending of the stringers at low load levels. The placement of the eight strain gages is indicated in Fig. 35.

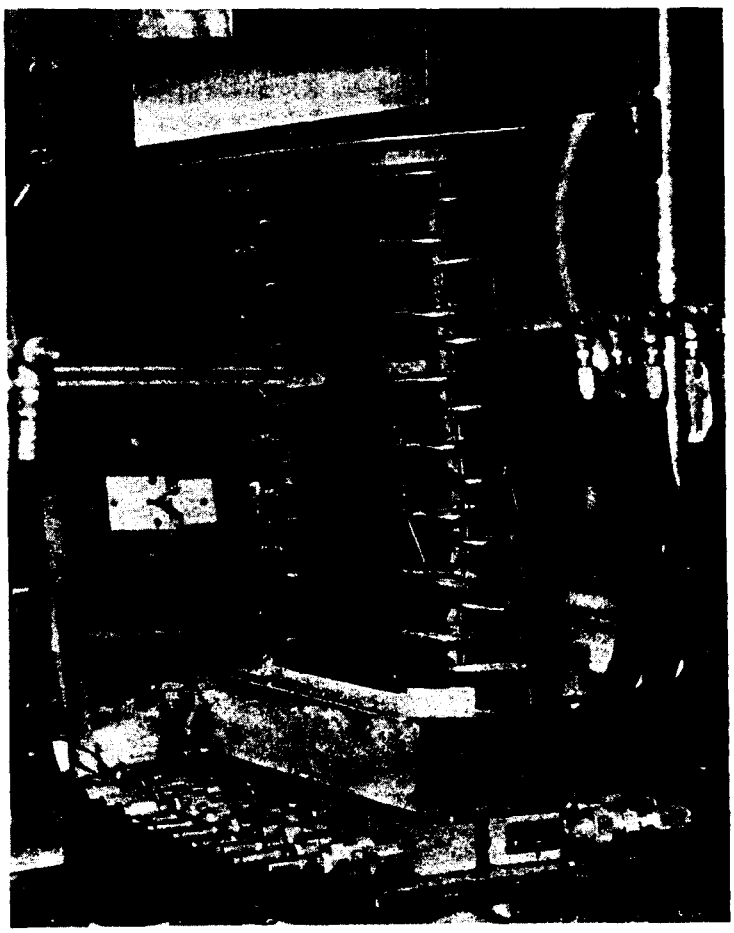

Fig. 33. Test setup for buckling of small (18 × 11 in.) flat panel under axial compression.

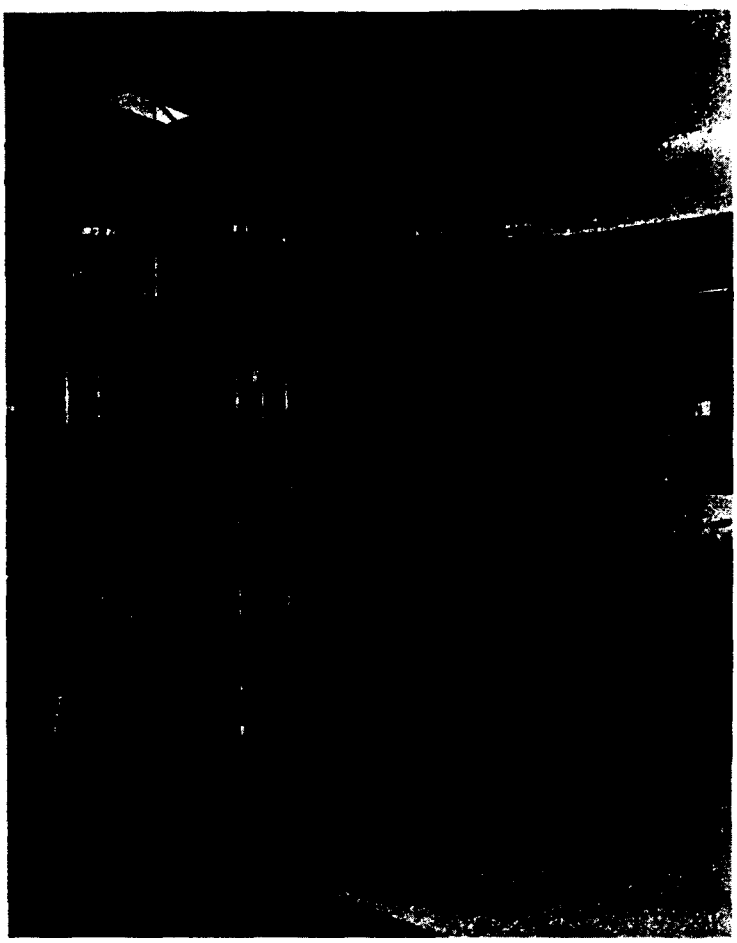

Fig. 34. Test setup for buckling of large (30 × 27 in.) curved panels under axial compression.

Three large hat-stiffened panels were tested. Figure 34 shows Panel No. 1 installed in the test fixture. Notice the C-clamps along the vertical edges. The purpose of these clamps, described previously in connection with tests on small panels, is to prevent early delaminations from propagating inward from the free edges of the panel.

The following test procedure was used for all three panels:

1. Strain gages were attached to the crown and opposite sides of each of the four stringers at the midlength of the panel, the curved ends of which had previously been carefully trimmed potted, and attached to aluminum plates.

2. The panel was installed in the test fixture.

3. Axial compression was applied, and the top head of the machine tilted front and back and side to side in order to obtain the smallest differences in the readings of front and back and side to side load cells. The eight strain gages on the stringers were carefully monitored, the goal being to minimize the differences in the strains measured by these gages, especially at low load levels.

4. The panel was loaded well into the local-post-buckling regime. For all panels, local buckling occurred at about 8000 lb total axial compression [N_{xcr}(local) = 294 lb/in.]. The panels were loaded in this preliminary phase to about 35,000 lb, at which load the local buckling pattern was clearly visible. This local buckling pattern was carefully inspected. Based on the location of the maximum buckling displacement in the middle bay of the panel, nearest the midlength, marks were made on the panel to identify locations of strain gages to be attached. Ten channels were available, and it was decided to attach gages at the following locations:

(a) back-to-back axial and hoop gages at the buckle inward peak nearest the center of the panel (four channels);

(b) back-to-back axial gages at the buckle outward peak nearest the inward peak and above it (Panels 1 and 3 only) (two channels);

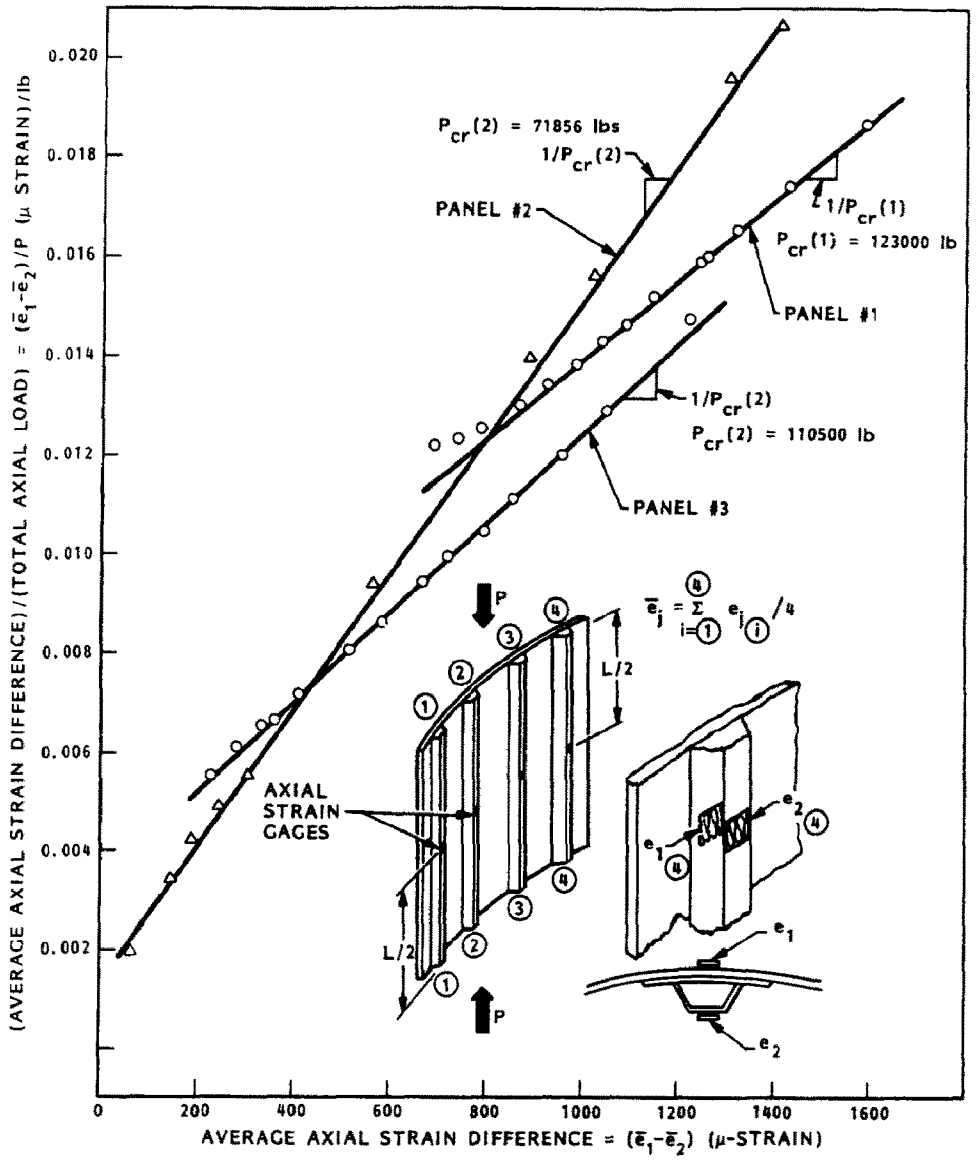

Fig. 35. Southwell plots for the three large panels tested to failure under pure axial compression.

(c) hoop gages on the outer (convex) and inner (concave) surfaces at the same axial station as the gages in (a), but located where the sharpest curvature is observed in the local inward buckle. These gages should be located where the material in the stiffener base tapers down to the skin thickness in the center bay of the panel. The positions of them are called out in Fig. 32 (four channels). These gages are important because they are located at positions where PANDA2 predicts maximum stress and failure;

(d) hoop gages on the outer (convex) surface at the same axial location as (b), located as described in (c) (Panel 2 only) (two channels).

5. The panel was unloaded and the ten gages identified in (a)–(d) above were attached.

6. The panel was reinstalled in the test fixture and loaded to failure. Strain and load data were recorded by a computerized data acquisition system.

Figures 35 through 45 give test and theoretical results for these three large panels.

Figure 35 displays Southwell plots for the three panels. The average axial strain difference between axial strain in the skin opposite the stringers and axial strain in the crown of the stringers, $\Delta\bar{e} = (\bar{e}_1 - \bar{e}_2)$, essentially represents the axial bowing of the panel. The Southwell plots, $\Delta\bar{e}/P$ vs $\Delta\bar{e}$, yield estimates of the wide-column buckling loads of the panels: the slope of the plot for each panel represents the inverse of the wide-column buckling load of that panel. (An explanation of the Southwell method with a discussion of its limitations is given in [30, pp. 357–367].)

From Fig. 35 it is seen that the wide-column buckling loads of Panel 1 and Panel 3 are within 10% of each other and are much higher than that of Panel 2. Yet all three panels were nominally identical. Since each Southwell plot represents behavior averaged over an entire panel, it is unlikely that this rather dramatic difference is caused by local flaws in any of the panels. It is much more likely to be caused by a difference in restraint at the boundaries.

In the tests Panel 1 failed at about 86,000 lb, Panel 2 at 70,000 lb and Panel 3 at 83,000 lb. The Southwell plot of Panel 2 behavior indicates that its failure was due to wide-column buckling, since the inverse of the slope of the Southwell plot, $P_{southwell}(2) = 71{,}800$ lb, is not far above the load, $P_{test}(2) = 70{,}000$ lb, at failure in the test. The Southwell plots of Panels' 1 and 3 behavior indicate that their failure was not due to wide column buckling, since the inverses of the slopes of the Southwell plots for these two panels, $P_{southwell}(1) = 123{,}000$ lb for Panel 1 and $P_{southwell}(3) = 110{,}500$ lb for Panel 3, are far above the loads, $P_{test}(1) = 86{,}000$ lb and $P_{test}(3) = 86{,}000$ lb, respectively, at which Panels 1 and 3 failed in the tests.

Figure 36 is analogous to Fig. 21. It corresponds to the design actually tested. This model yields a prediction of general instability (similar to wide-column buckling) at $P_{cr} = 125{,}000$ lb. Clamped boundaries at the loaded ends of the panel were assumed in this model. The critical general instability load, P_{cr}(BOSOR4) = 125,000 lb, corresponding to clamped ends, is not very far above the values P_{cr}(test) = 123,000 lb for Panel 1 and P_{cr}(test) = 110,500 lb for Panel 3 obtained from the Southwell plots of Fig. 35. Since wide-column buckling of axially stiffened panels is sensitive to the rotational restraint at the boundaries, it appears that in the tests Panels 1 and 3 were very nearly clamped at the loaded edges, but that Panel 2 was not.

After the tests on all three panels, it was determined that because of mislabeled aluminum stock, Panel 2 was mounted on 6061/T4 (26 ksi yield) aluminum end plates, whereas Panels 1 and 3 were mounted on significantly harder 6061/T6 (56 ksi yield) aluminum end plates. Figure 37 shows part of one of the end plates of Panel 2 after its test. There is significant 'print-through' caused by local plastic flow directly over the stringers. This 'print-through' cannot be seen in the end plates of Panels 1 and 3. It indicates that Panel 2 was freer to rotate at its loaded ends than were Panels 1 and 3.

Figure 38 shows load–axial strain curves from test, from PANDA2 predictions, and from PANDA2 predictions multiplied by a factor of 1.17 to account for the fact that the test panel had four stringers in a width of 27.25 in., whereas the PANDA2 theory applies to a panel with 3 stringers in a width of 24 in. There is some bending in the stringers from the beginning, bending which is not predicted in the PANDA2 analysis. (Bending from axial bowing of the panel caused by curing, which is predicted by PANDA2, is not significant in this case.)

In the PANDA2 model of the panel, one extra 'fake' layer was added to each side of each wall in the multi-segment model. These layers were very thin (0.0001 in.), had a modulus of unity and a Poisson's ratio of zero, and a very small density. The purpose of these fake layers was to obtain strain in the panel coordinate system (x, y) directly, rather than have to convert stresses in the material coordinate system to strains in the panel coordinate system. This 'trick' does not affect the panel behavior. It was also used in the analysis of the NASA T-stiffened panel described in the discussion associated with Figs 22–24.

The local buckling pattern observed in the test agreed qualitatively with that predicted by PANDA2 (seven axial half waves in the test, eight axial half waves predicted by PANDA2, but the predicted bifurcation buckling loads for seven and eight waves are within 1% of each other). The test panel failed at about 13% below what one might expect from the PANDA2 predictions as modified by the factor of 1.17. However, Fig. 39, which shows the failed panel removed from the test machine, indicates that the mode of failure is in agreement with that predicted by PANDA2: vertical tears exist at locations where the hat base has tapered to the thickness of the panel skin. (See Fig. 32.) There was no evidence of skin–stringer separation. No secondary bifurcation, described below, was observed during the test of this panel. The post-local-buckling axial wave pattern remained qualitatively constant throughout the test.

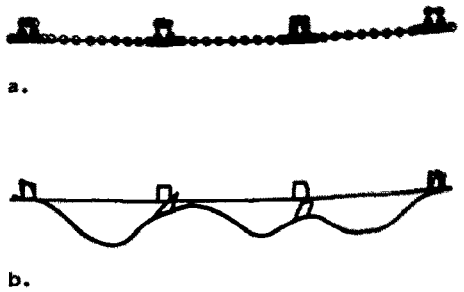

Fig. 36. (a) Twenty-seven-segment BOSOR4 model of the panels that were tested and (b) predicted general instability mode shape. The predicted critical total axial load is $P_{cr} = 125{,}000$ lb compression. This prediction should be compared with the predictions shown on the previous figure from the inverse of the slopes of the Southwell plots.

Fig. 37. Photograph of the local deformation of one of the soft aluminum end plates that occurred directly over one of the stringers in Panel 2. This end plate was fabricated from 6061T4 aluminum stock, which had a 26 ksi yield stress. No such deformations were observed in the end plates of Panels 1 and 3. These other harder end plates were fabricated from 6061T6 aluminum stock, which had a 56 ksi yield stress.

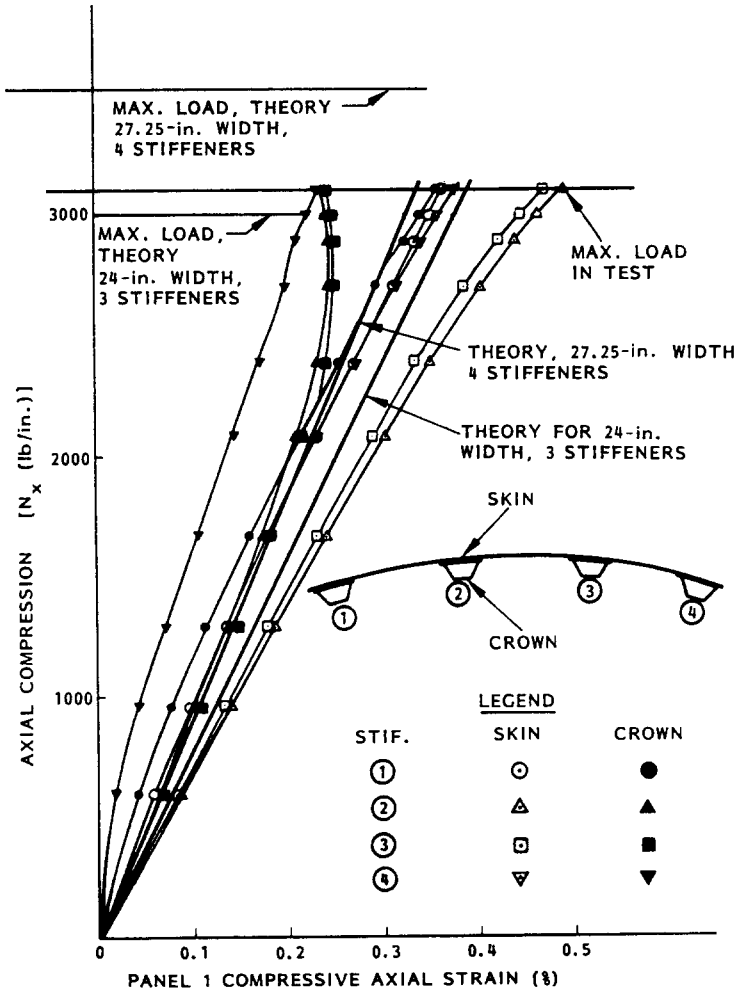

Fig. 38. Load–strain curves for axially compressed large Panel No. 1.

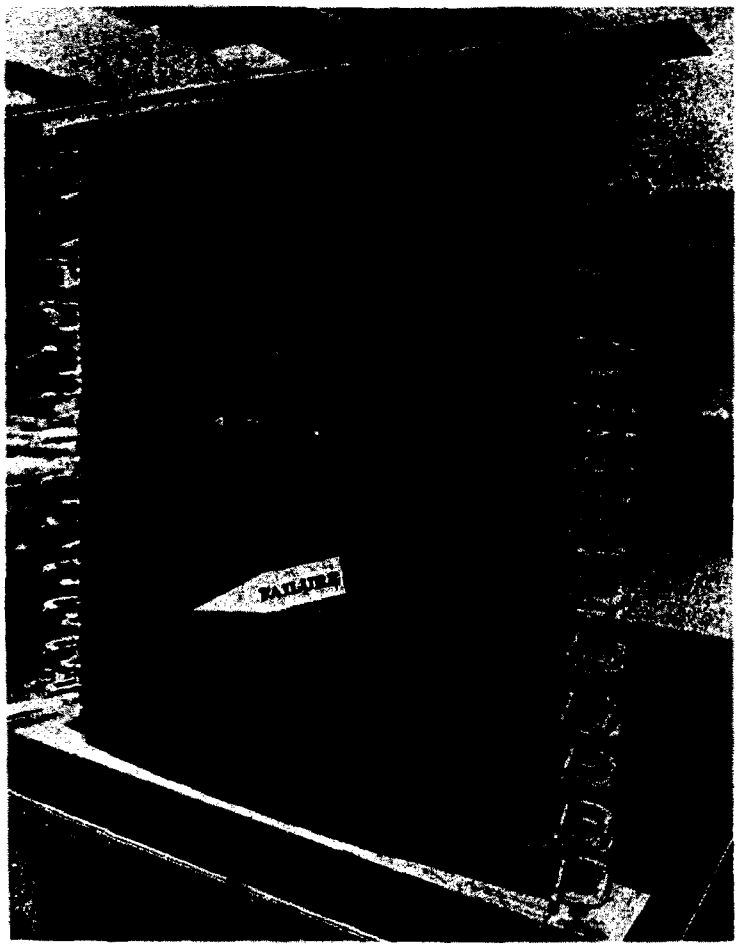

Fig. 39. Panel No. 1 after testing. The failure mode consists of vertical fractures that occur where the thickened base under the hat stiffeners tapers down to the skin thickness. Failure is due to excessive stresses caused by sharp changes in skin curvature that occur in the locally postbuckled panel. These large stresses are predicted by PANDA2.

Figures 38, 40 and 41 show the axial strains at the 4 stringer locations for Panels 1, 2 and 3, respectively. The following observations apply to these three figures.

1. There is rather a lot of bending in the stringers, especially in Panel No. 1 and Panel No. 2, even at fairly low loads. Much of this may be generated by axially nonuniform Poisson-ratio expansion of the radius of the panel as the load is increased. While Poisson ratio expansion is, of course, included in the PANDA2 theory, it is assumed to occur in the plane of the panel and not normal to it: the prebuckling state of the panel in this case (no normal pressure and insignificant axial bowing) is assumed to be uniform: it does not vary in the axial direction due to edge restraint. It is as if there were no edge restraint in the prebuckling phase, simple support or clamping conditions being applied only in the bifurcation buckling analyses.

2. It is possible (although unlikely because of the evidence supplied by the Southwell plots in Fig. 35 and the BOSOR4 prediction in Fig. 36) that all three panels failed via general instability rather than maximum stress. The PANDA2 calculations were conducted with the assumption that the curved edges of the panel were clamped, whereas in the test the support is not as rigid as clamping: in the test the zero rotation constraint is enforced only by a natural feedback mechanism: as the curved edges rotate the load shifts so as to counteract this rotation. PANDA2 predicts wide column buckling of the clamped panel at a load factor of only 1.36 times the imposed axial load of 3000 lb/in. Wide column buckling loads of panels such as these, with stringers that are very strong compared to the skin, are very sensitive to the nature of the rotational restraint at the edge. It could be that all of the test panels, bearing as they do on aluminum end plates, have end constraints weak enough to lead to wide column instability prior to or combined with material failure. As discussed above in connection with the Southwell plots, it is very likely that Panel 2 failed in general instability, but that Panels 1 and 3, because of their harder aluminum end plates, did not.

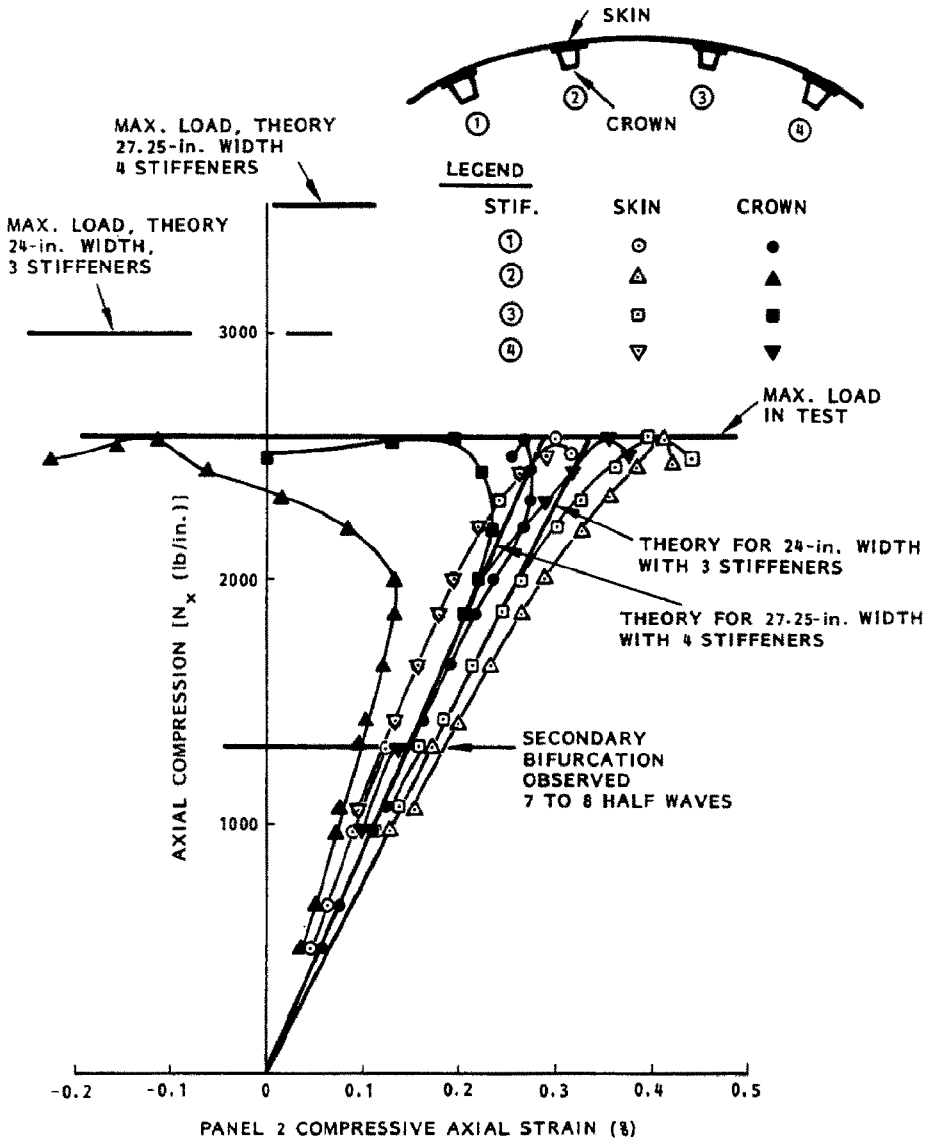

Fig. 40. Load–strain curves for axially compressed large Panel No. 2.

Figures 42–45 show various strain components from test and theory. The following observations apply:

1. The axial strains at the peaks of the inward and outward buckles are quite different (Fig. 42). PANDA2 is based on a theory that neglects this difference. While this might appear to be a serious omission at first, it is not very critical because these strains are much smaller than strains predicted elsewhere which cause material failure.

2. There is a great deal of scatter in the behavior of hoop strain, as can be seen from a comparison of Figs 43 and 44. In both figures the hoop strains are generally greater than those predicted by PANDA2. However, the comment given in 1 applies here also: These strains do not come close to generating material failure, and so do not govern the evolution of the optimum design.

3. The comparison between test and theory for the most important strain, the hoop strain at the interface between the thickened stringer base and the thin skin, indicates reasonably good agreement (Fig. 45).

4. Panel No. 2 exhibited a sudden change in the buckle pattern at a load of about 35,000 lb. The change was accompanied by a rather loud noise. The redistribution of energy caused the applied load to decrease abruptly to about 29,000 lb. It appeared that the number of axial half-waves in the center bay of the panel increased from seven to eight. (Eight agrees with the PANDA2 prediction, although the critical bifurcation buckling loads corresponding to seven waves and eight waves are within one percent of each other.) While the strain gages were located based on the seven-wave pattern, it seems that, fortuitously, the gage locations remained

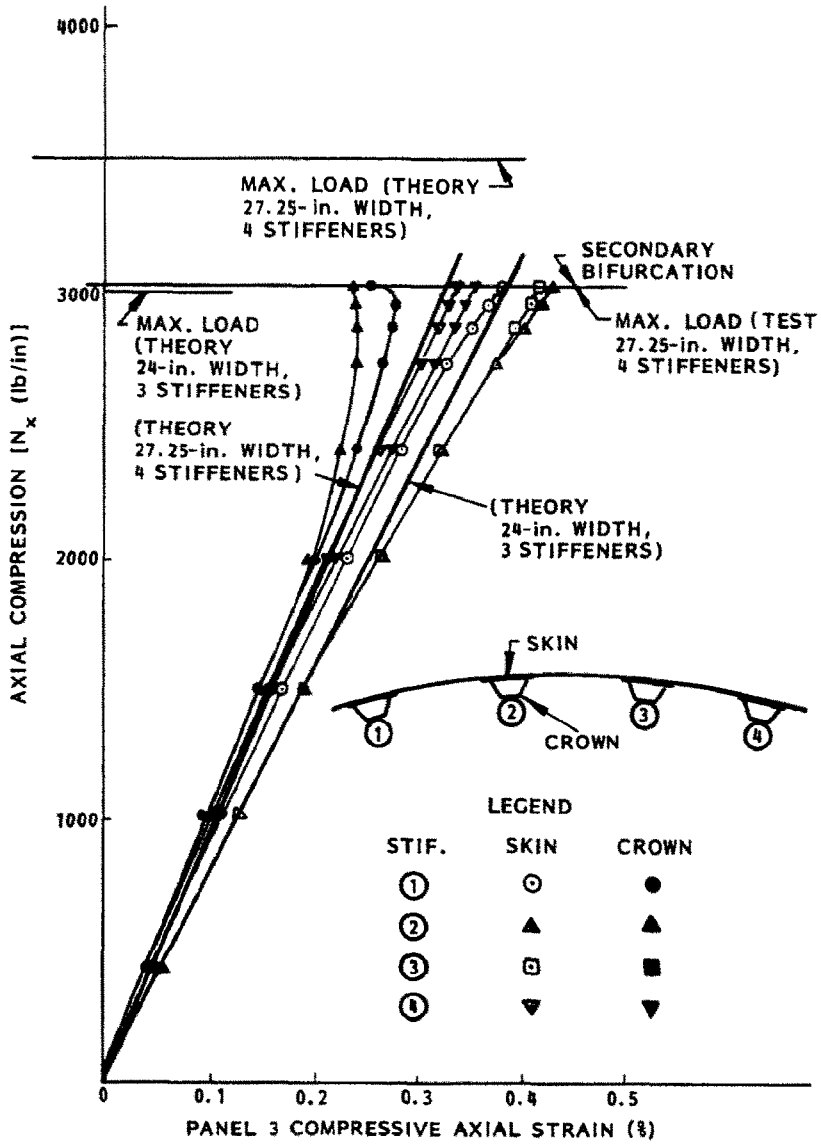

Fig. 41. Load–strain curves for axially compressed large Panel No. 3.

appropriate for the eight-wave pattern: the gages initially located at the peak of an inward buckle in the seven-wave pattern became located at the peak of an outward buckle in the eight-wave pattern. Hence, in Figs 44 and 45, the locations of the gages are called out as if they were in different bays of the panel. Actually, only the middle bay had gages and it was the buckle pattern that changed during loading. As seen from Fig. 45, curves 2 and 4 and 5 and 7, the continuity of strain measurement in the neighborhood of the load at which the buckle pattern changed is extraordinarily good.

Unfortunately, only in Panel 2 were the hoop gages located properly to catch the maximum strains. In Panel 1 they were located too far away from the tapered section to capture the very sharp, local change in circumferential curvature of the locally buckled skin of the middle bay. In Panel 3 the gages were applied in the correct positions according to observations during the preliminary loading phase, but when the panel was reinstalled in the test machine and reloaded, the local buckle pattern shifted enough to destroy completely the usefulness of these as well as the other strain gages placed on the panel skin! Apparently the local buckle pattern can rather freely 'slide' in the axial direction, and the locations of peak buckling displacements depend on very small load eccentricity effects.

It is clear that more tests of this type should be conducted and that there should be many more gages applied to a panel in order to ensure capture of the peak strains. The conclusion from tests conducted so far is that PANDA2 agrees reasonably well with test results. The difficulty seems to lie mainly in obtaining repeatability in tests with regard to uniformity of load and determination of proper locations for strain gages. There may also be considerable scatter in the quality of composite panels of this type with rather complex cross sections.

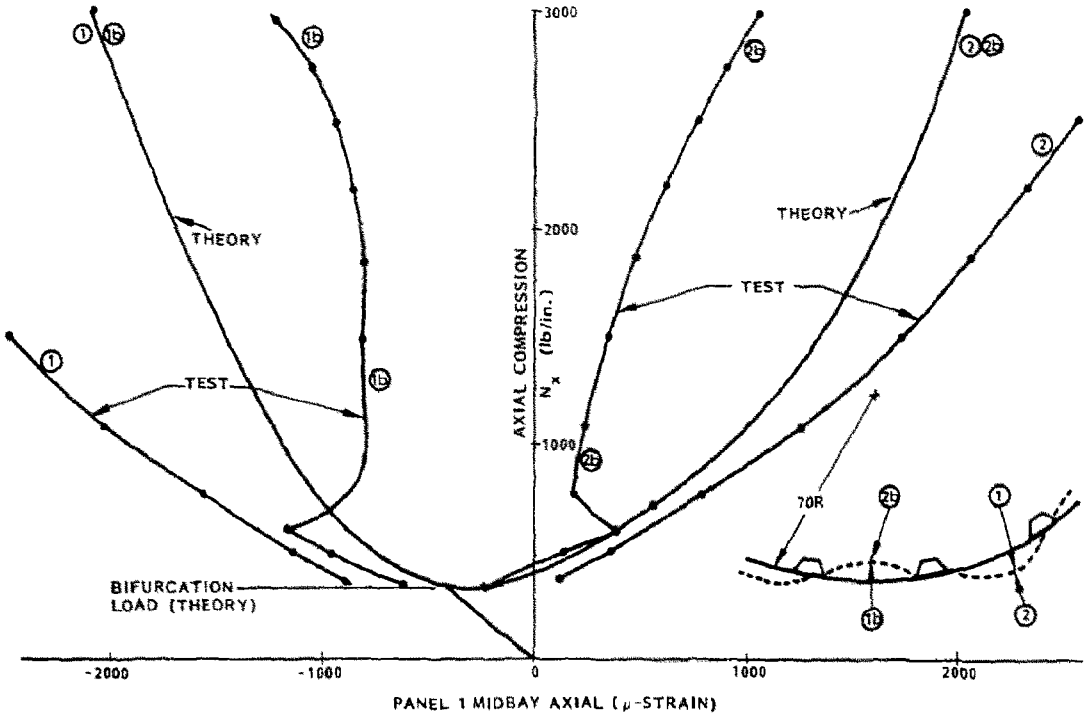

Fig. 42. Axial strain at inward and outward buckles midway between stringers 2 and 3 in Panel No. 1.

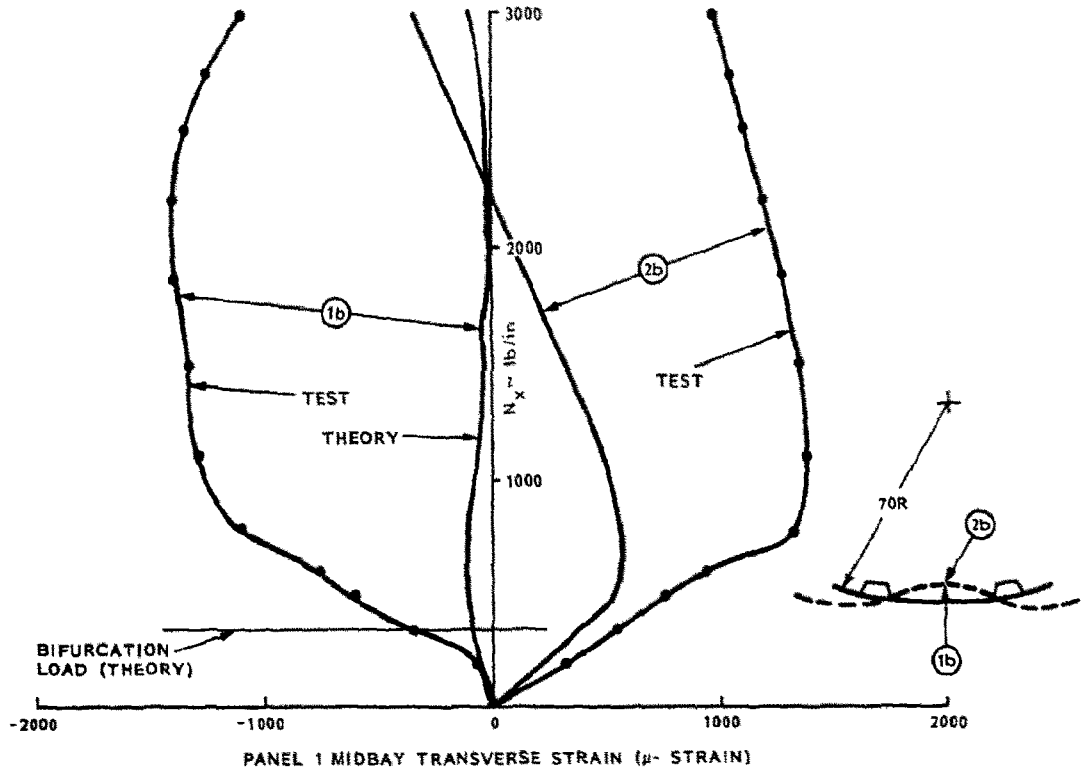

Fig. 43. Hoop strain at an inward buckle midway between stringers 2 and 3 in Panel No. 1.

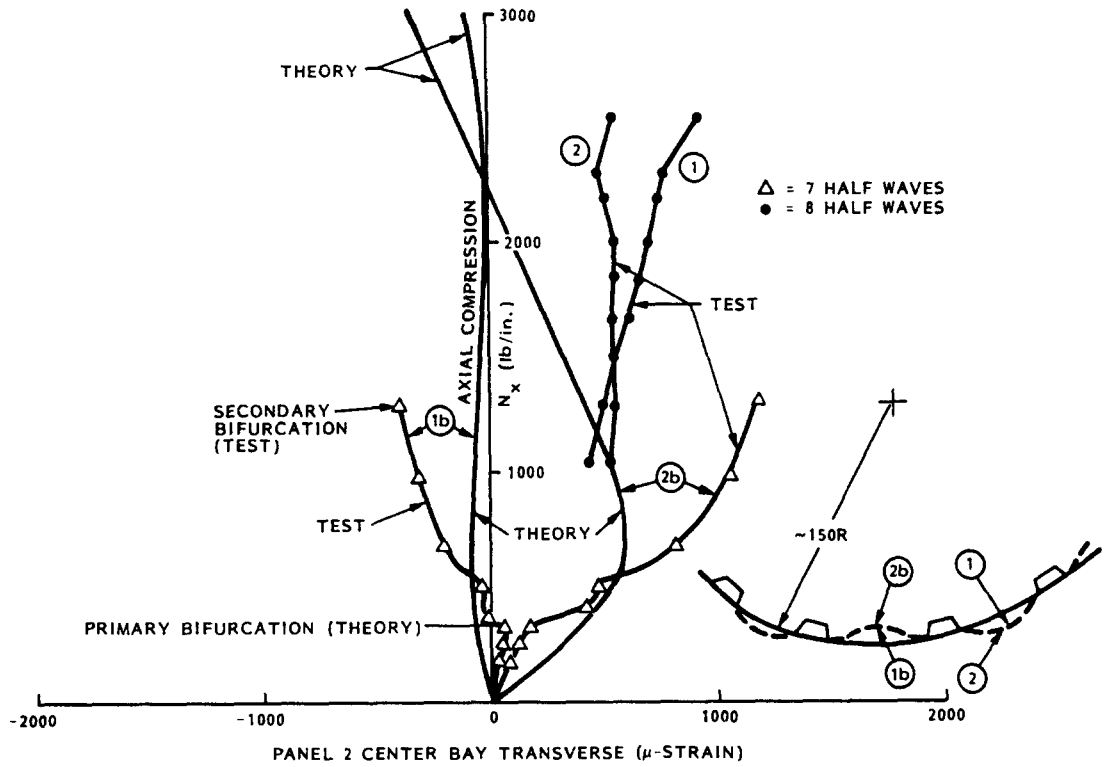

Fig. 44. Hoop strain at an inward buckle midway between stringers 2 and 3 prior to secondary bifurcation and at an outward buckle at the same location after secondary bifurcation, Panel No. 2.

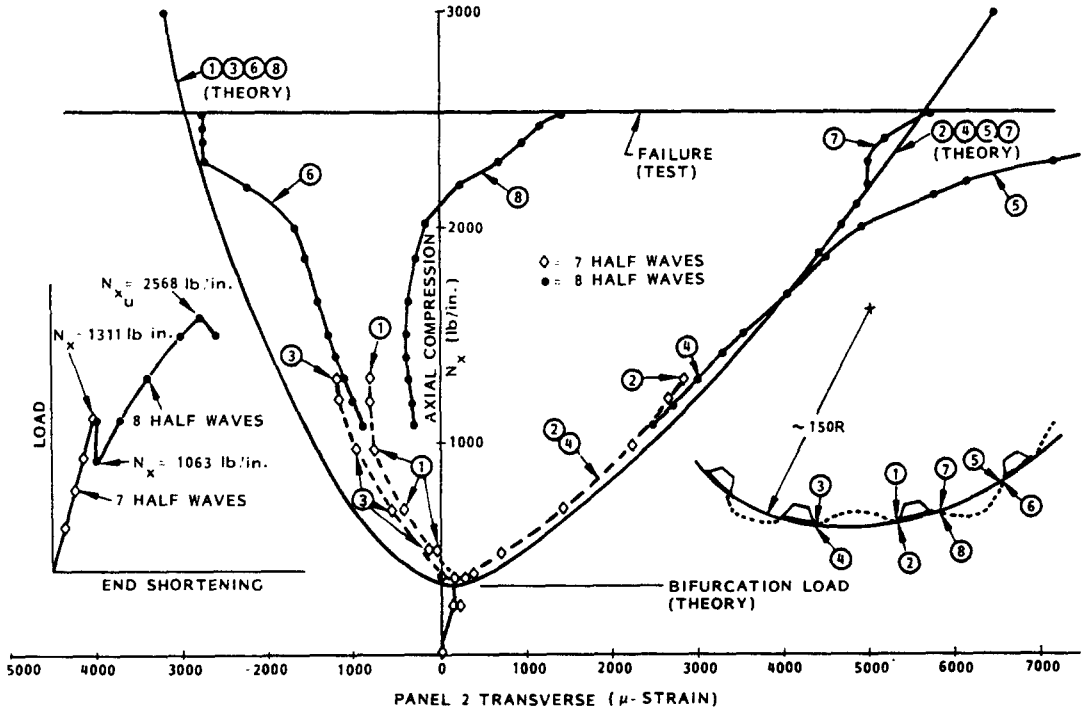

Fig. 45. Hoop strain next to the stringer bases in the middle bay at an inward buckle prior to secondary bifurcation and at an outward buckle after secondary bifurcation, Panel No. 2.

20. INVESTIGATION OF BLADE-STIFFENED PANEL WITH AXIAL COMPRESSION, PRESSURE AND THERMAL LOADING

20.1 *Introduction*

In this section is described a variety of phenomena for a stiffened elastic plate with geometry and linear material shown in Fig. 46. The plate is designed so that it buckles locally between the stringers at an axial load well below the wide column buckling load. This case does not represent a good engineering design. Its purpose is to demonstrate many interesting and sometimes rather subtle and complex phenomena that occur when the plate is loaded in pure axial compression far into its locally post-buckled regime, when it is loaded by pure normal pressure far into the nonlinear regime (geometric, not material nonlinearity), and when it is loaded by combinations of axial compression and normal pressure or axial compression and nonuniform temperature that simulates curing of a composite panel.

20.2 *Summary of this section*

Figures 48–54 pertain to the case of pure axial compression with neither pressure nor thermal effects. The main purpose of this section is to obtain comparisons with results from a new version of the STAGSC-1 program [19] which contains a new algorithm called the 'Thurston Processor', or 'TP' for short [20]. This algorithm mitigates difficulties encountered during a nonlinear process when load–deflection curves are tracked in the neighborhood of single or multiple bifurcation points. Through certain transformations, the Thurston Process eases the transition from pre-buckling to post-buckling load–deflection curves, and from primary post-buckling to secondary post-buckling load–deflection curves, etc.

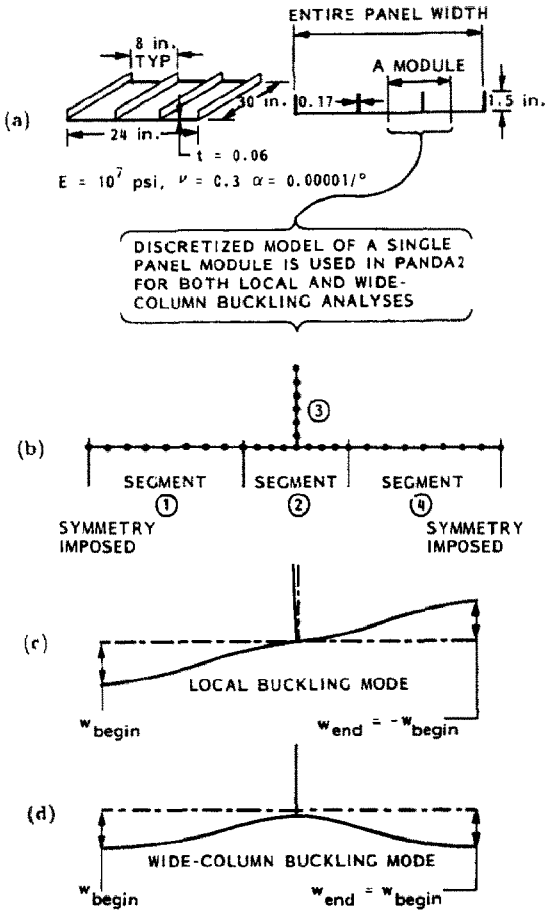

Fig. 46. (a) Blade-stiffened aluminum panel. Loading is uniform axial compression N_x or uniform pressure p or combinations of axial compression and pressure. (b) Discretized model of a single panel module. (c) Local buckling mode is induced by imposing antisymmetrical normal displacement w about the attachment line of the stringer to the panel skin. (d) Wide column (general) instability is induced by imposing symmetrical w about the attachment line of the stringer to the panel skin.

Figures 55–64 pertain to the case of pure normal pressure, with neither axial compression nor thermal effects. The purposes here are:

1. to demonstrate the approximate method used in PANDA2 to obtain reasonably accurate predictions for nonlinear behavior of a stiffened panel under uniform normal pressure;
2. to obtain comparisons with results from STAGSC-1;
3. to describe some interesting phenomena.

Figures 65–71 pertain to the case of axial compression combined with normal pressure. The purpose is to describe some interesting phenomena. Figures 72–77 pertain to the case of axial compression combined with thermal loading that simulates curing of a composite panel. The purpose is to describe some interesting phenomena.

20.3 *Computer models*

Figure 46(b) shows the discretized panel module used in the PANDA2 analysis throughout. Figure 46(c) shows the local buckling mode and Fig. 46(d) shows the wide column buckling mode. In PANDA2 both local and wide column buckling load factors are obtained with use of the same discretized model. The local mode is singled out by enforcing equal and opposite normal displacements at the symmetry planes at either end of the single module model depicted in Fig. 46(b). The wide column mode is singled out by imposing equal normal displacements at either end of the single module model. As mentioned previously, the wide column mode is rejected by PANDA2 as an indicator of general instability if the normal displacement under the stiffener is less than 10% of that midway between stiffeners.

Figure 47 shows the STAGS finite element model used for the study of the behavior of the panel under

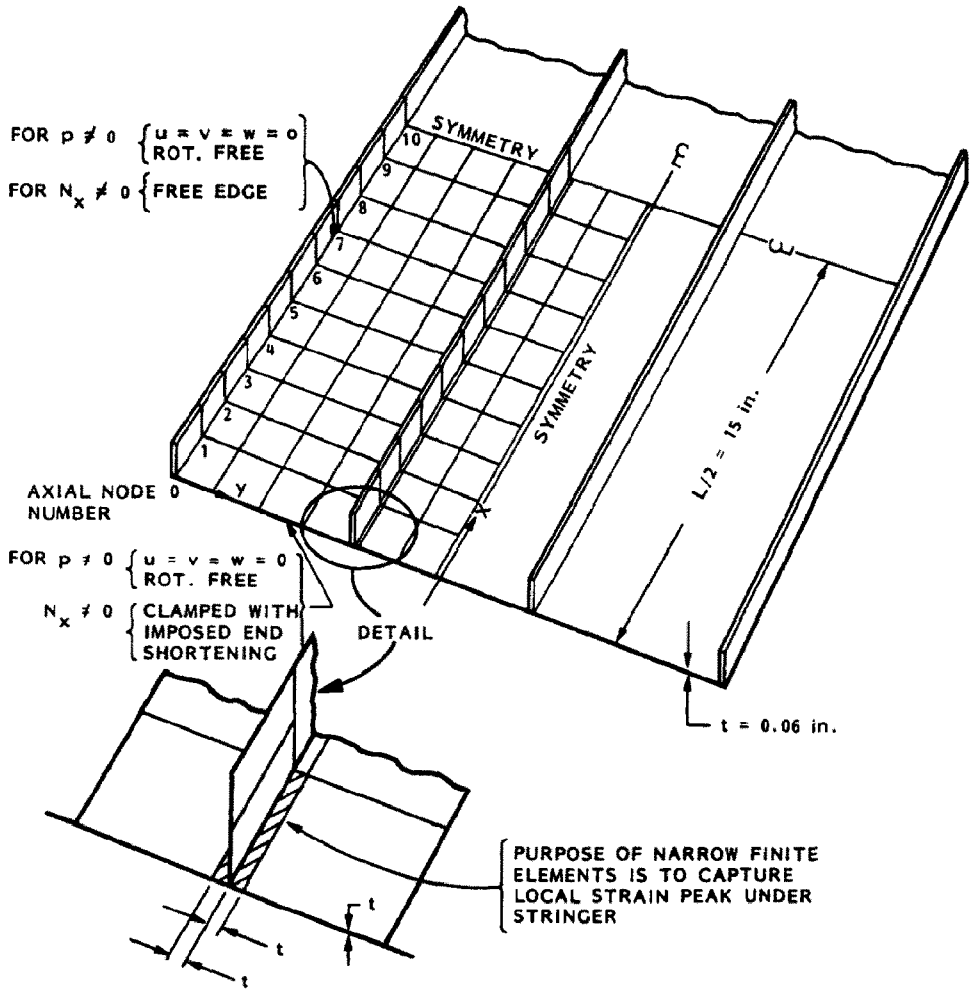

Fig. 47. Discretized model used for the STAGSC-1 analysis of the panel under uniform normal pressure p. The STAGSC-1 model for the case with uniform axial compression N_x is analogous, although the compression model has an extra finite element on either side of the stringer not at the edge and runs the entire 30-in. length rather than having a symmetry plane at midlength.

normal pressure. One fourth of the plate is included, with symmetry planes at midlength and midwidth. The STAGS model for pure axial compression is twice as large: the symmetry plane at the panel midwidth is retained, but the entire length of 30 in. is included for two reasons:

1. It is not known *a priori* (except from PANDA2 results, which are being checked!) whether the local skin bifurcation buckling pattern has an odd or an even number of axial halfwaves.

2. It is possible that the number of axial halfwaves in the local buckling pattern will change by one as the panel is loaded far into the post-local-buckling regime. A symmetry plane introduced at the panel midlength would artificially preclude this from happening. Recall that in the test of hat-stiffened Panel No. 2, described in the previous section, the number of axial halfwaves in the local skin buckling pattern increased from seven to eight at an axial load somewhat less than half of that for which the panel was optimally designed. (See Fig. 45.)

In addition, the STAGS finite element model for the case of pure axial compression contained additional rather small elements near the stringer not at the panel edge in order better to capture the fairly localized inflection behavior of the local buckling mode seen in Fig. 46(c).

The boundary conditions in the STAGS model for pure axial compression differed from that in the STAGS model for pure normal pressure:

1. In the axial compression case the stiffened edges were free, except for the presence of the stiffener, of course, and the loaded edges were subjected to uniform end shortening with no rotation allowed.

2. In the normal pressure case the three displacement components u, v, w were restrained at the stiffened edge and at the other edge not at a symmetry plane, and the edge rotation was free. The other two edges were symmetry planes.

20.4 *Results for pure axial compression*

Figure 48 shows load–axial strain curves from PANDA2 and STAGS. The STAGS model shows higher axial stiffness at low axial load because there are four stringers in 24 in. in the STAGS model, whereas there are only three in the PANDA2 model. (Recall the similar difference in the case of the hat-stiffened test panels and the PANDA2 models of them; see Fig. 38, for example.) The slope of the post-local-buckling curve is essentially constant in the PANDA2 model because the number of axial half waves is fixed at that predicted for the critical bifurcation buckling mode. Changes in the number of axial halfwaves after primary bifurcation are not accounted for by PANDA2. This slope decreases slightly in the STAGS model because the post-buckling mode of deformation changes during loading, as will be described later.

The load coordinate in Fig. 48 is normalized by the local bifurcation buckling load predicted by PANDA2. This normalizing factor is used throughout this study.

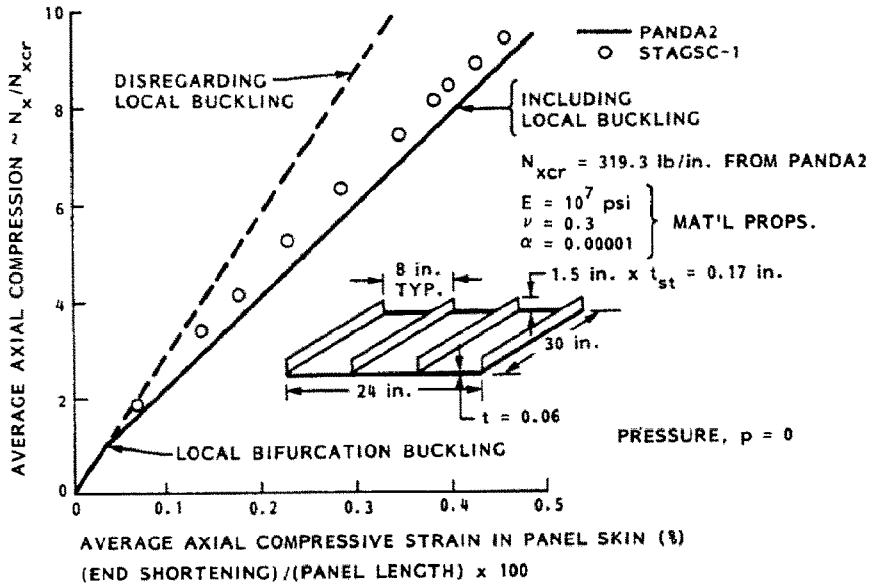

Fig. 48. Load-end-shortening for uniformly axially compressed panel. Local buckling pattern has five axial half-waves. The STAGS result shows more axial stiffness because the STAGS model has stringers at each edge (four stringers in a width of 24 in.), whereas the PANDA2 model has three stringers in the width of 24 in.

Figure 49 depicts the normal deflection at the center of the panel as a function of normalized axial load. The STAGS and PANDA2 models agree extraordinarily well up to a load factor $N_x/N_{xcr} = 5.22$. At an axial load slightly higher than that, STAGS has difficulty converging. Use of the Thurston processor, however, aids convergence. As the axial load is further increased, STAGS predicts maximum normal displacements that exceed those predicted with PANDA2. The number of axial waves in the post-locally-buckled panel does not change throughout the load range, but the distribution of displacement changes. For axial loads that are less than $N_x/N_{xcr} = 5.22$ both STAGS and PANDA2 predict normal displacements that have equal inward and outward maxima and uniform wavelengths. For higher axial loads, however, the waviness predicted by STAGS becomes more nonuniform. STAGS and PANDA2 predictions of normal displacement distributions at the maximum axial load, which coresponds to an imposed average axial compression of 3000 lb/in., are plotted in Figs 50 and 51. The STAGS results indicate a kind of alternating discrepancy with PANDA2 results, in which the maximum normal deflection in one buckle is more than that predicted by PANDA2, whereas that in a neighboring buckle is less than than predicted by PANDA2.

Figure 52 shows a plot of the largest strain anywhere in the panel. STAGS predicts considerably more strain than does PANDA2, possibly because the STAGS model is a bit freer in the y-direction than is the PANDA2 model. In the PANDA2 model symmetry conditions are imposed midway between stringers in the local buckling mode [Fig. 46(c)]. Since the post-buckling behavior is represented in the PANDA2 model as a series expansion of the local buckling mode, the entire panel is not free to become narrower as the skin goes deeper into its post-buckled regime. Possibly this restraint prevents bending about each stringer to the degree that STAGS predicts. However, note that according to STAGS the maximum normal deflection in some of the buckles in the edge bay is considerably less than that predicted by PANDA2, a result that argues against this reasoning. Note also that STAGS predicts some overall axial bowing of the panel which PANDA2 cannot predict in this case (zero pressure, zero curing deformations) because PANDA2 is based on the assumption that the post-local buckling pattern is antisymmetric about all lines of attachment of stringers to the panel skin.

Figure 53 shows that the STAGS and PANDA2 predictions of midbay axial strain at the midlength of the panel agree very well for the entire axial load range.

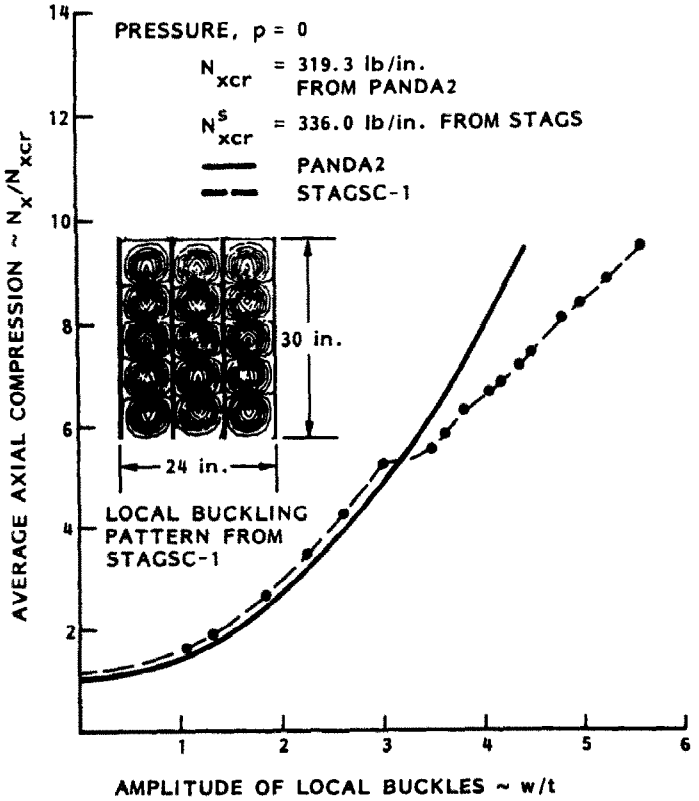

Fig. 49. Normal deflection w at the center of the panel. The bifurcation buckling load factor predicted from STAGSC-1 is 336 lb/in., compared with PANDA2's prediction of 319 lb/in. The difference is due to the axial restraint at the loaded end of the panel, present in the local bifurcation buckling problem in the STAGS model but absent in the local bifurcation buckling problem in the PANDA2 model.

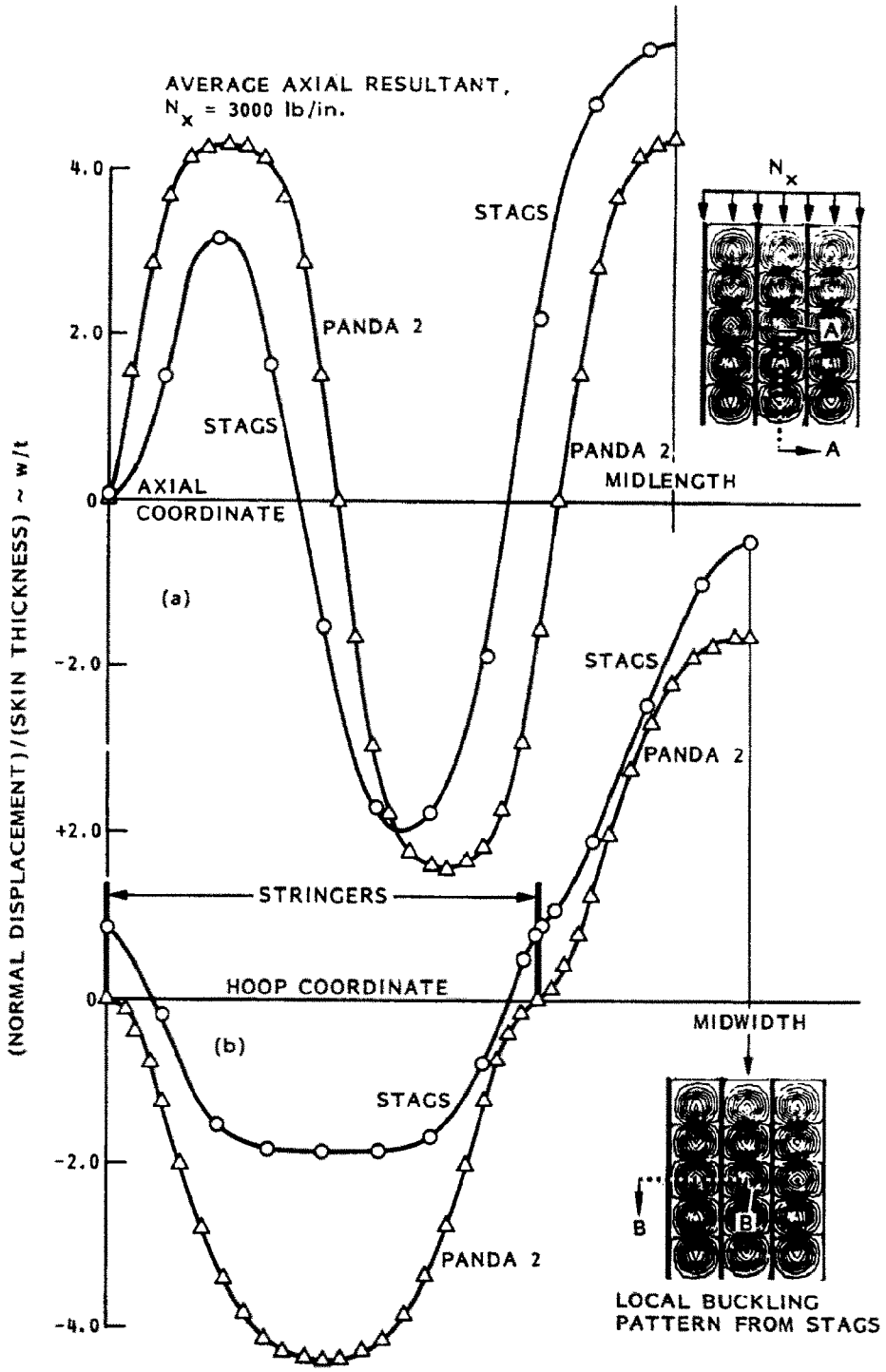

Fig. 50. Normal deflection w as predicted by STAGS and PANDA2 (a) along half the length of the panel in the middle bay and (b) across half the width at the midlength symmetry plane.

Figure 54 demonstrates the redistribution of axial load from skin to stiffeners as the panel is loaded into the post-local buckling regime. For high axial compression, STAGS predicts that N_{xloc} falls off more steeply with distance from a stringer than does N_{xloc} predicted by PANDA2.

The main conclusion from the results shown in Figs 49–54 is that, with the possible exception of prediction of maximum transverse strain in the immediate neighborhood of a stringer, PANDA2 agrees well enough with STAGS to ensure that it can be used to generate reasonably good minimum weight designs of panels in which the skin is permitted to buckle during service. The discrepancy in maximum hoop strain can be compensated by application of a suitable factor of safety, FSSTR.

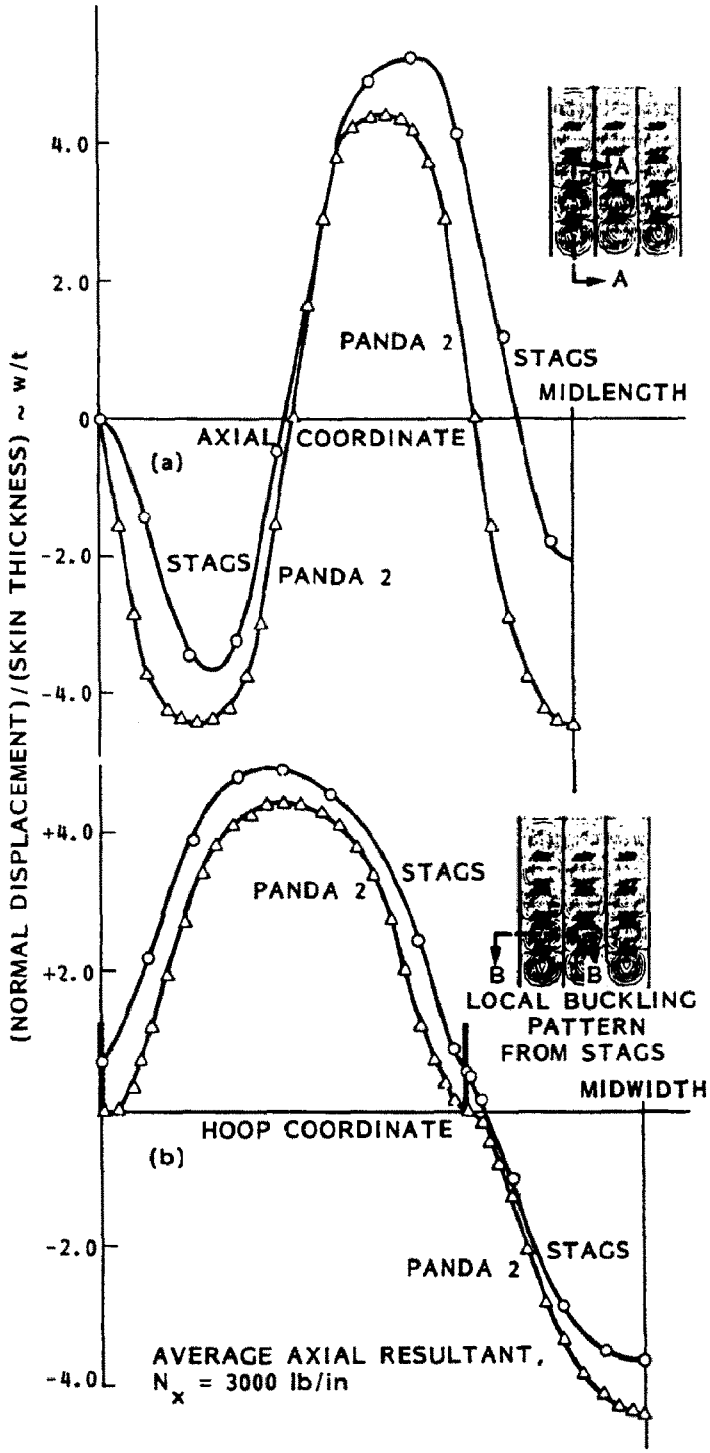

Fig. 51. Normal deflection w as predicted by STAGS and PANDA2 (a) along half the length of the panel in one of the side bays and (b) across half the width at one quarter of the length.

20.5 *Results for pure uniform normal pressure*

As described in the analysis section, nonlinear theory is used in the PANDA2 analysis. It is well known that monocoque flat plates exhibit a nonlinear stiffening effect under pressure, and that even for rather low design pressures one must account for the membrane stretching that builds up as the plate deflects. Boitnott *et al.* [21] demonstrate that nonlinearities significantly affect the behavior of curved, internally pressurized panels clamped along their straight edges. In this section, which deals with a more complex problem, a stiffened panel, it is shown that geometric nonlinearities must be included in the model.

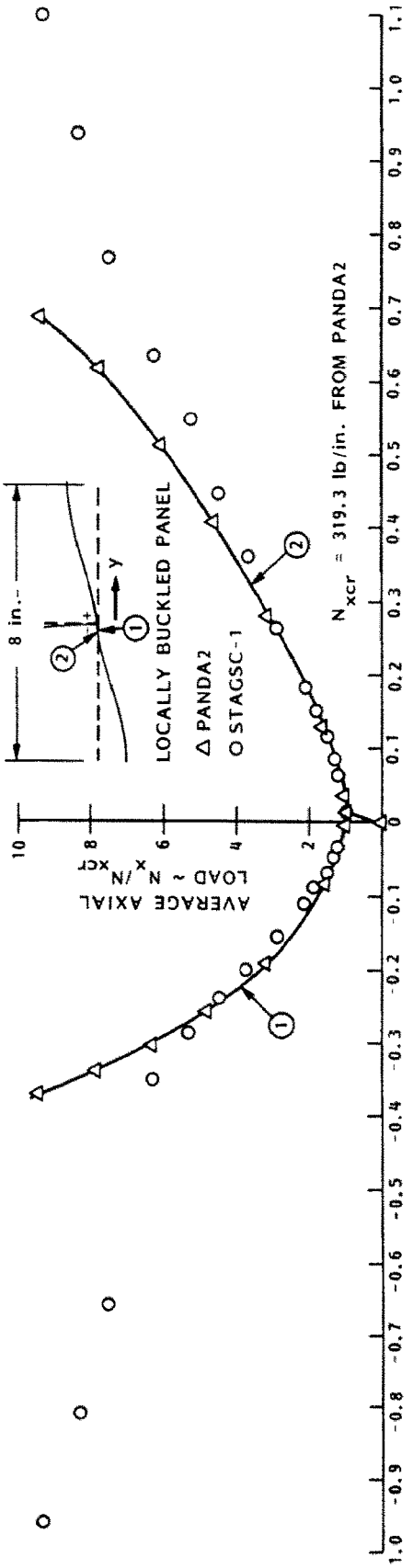

Fig. 52. Maximum transverse ('hoop') strain in the panel skin under the stringer that is not at the edge of the panel, at axial node No. 10. The strains plotted here correspond to the 'minus' side of the stringer. These include the largest strain anywhere in the panel.

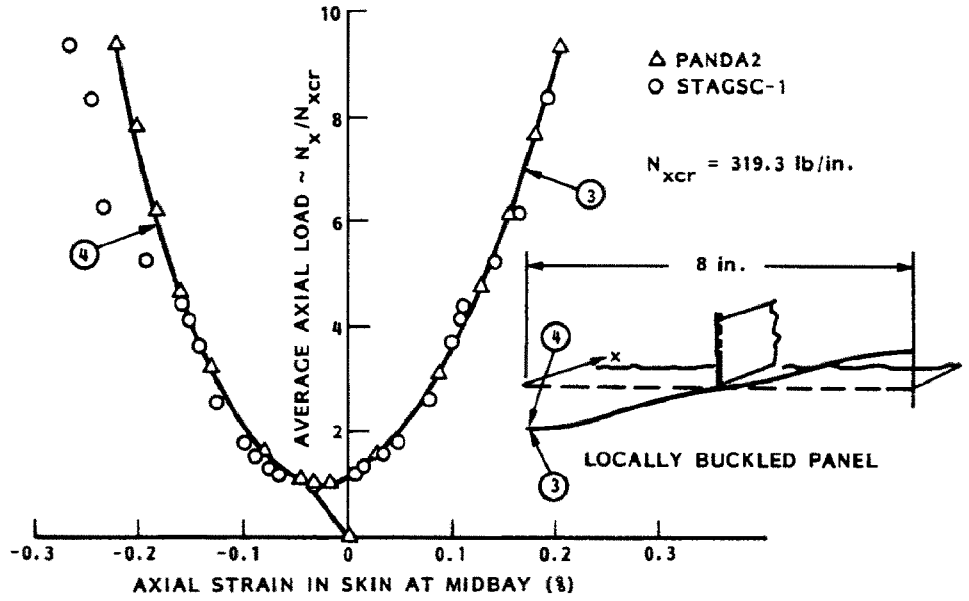

Fig. 53. Maximum axial strain in the panel skin at the midwidth of the panel. The STAGSC-1 results correspond to a point at axial node No. 10.

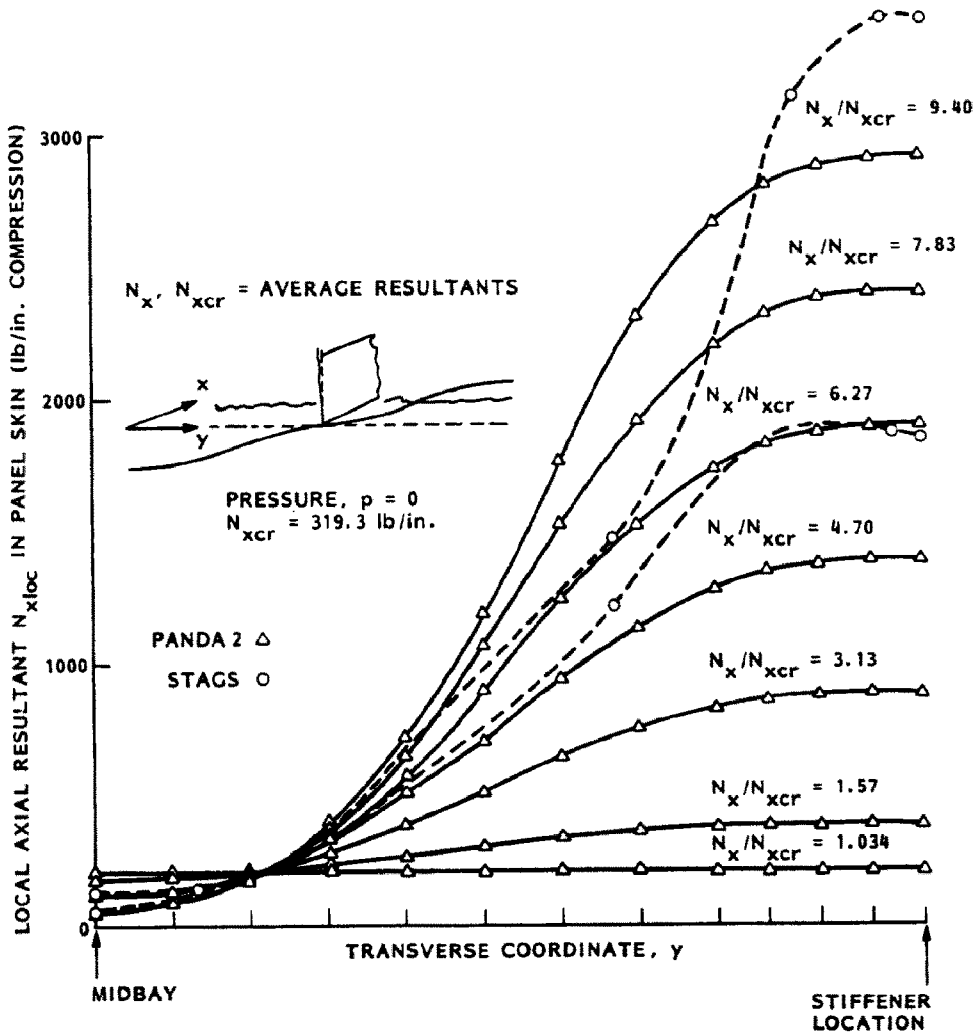

Fig. 54. Local axial resultant, N_x(local), in panel skin for various average axial loads N_x/N_{xcr}. STAGS results correspond to values at the axial symmetry line in the bay that includes the center of the panel.

Stiffened panels under normal pressure exhibit two types of response, identified here and in the following paragraphs as Problem 1 and Problem 2:

Problem 1. The panel bends overall, as shown in Fig. 55. This behavior can be captured with a model in which the stiffeners are smeared out.

Problem 2. The panel bends locally around each stringer, as shown in Fig. 56. This behavior can be captured with a single module of the type shown in Fig. 46(b).

As described in the analysis section, the strategy in PANDA2 is to obtain a reasonably good solution with little computer time by separation of these two behaviors and analysis of each as a nonlinear problem. The total state of the pressurized panel is obtained by adding the results of the two separate analyses.

Immediately one might object that since the problem is nonlinear, one cannot superpose these results. The PANDA2 strategy would be incorrect if it were not for the fact that the membrane stresses obtained from Problem 1, the overall bending model, occur as prestresses in Problem 2, the local 'wrap-around' problem. In this way the essential nonlinear contribution of the first problem to the second is included. As shown in the following, this strategy leads to reasonably good agreement with a rigorous nonlinear finite element solution [19] in the only case explored as of this writing.

Figure 55 shows the results from Problem 1, overall bending, obtained with PANDA2 for a range of pressures from +20 psi to −20 psi. The stringers are smeared out and the panel is assumed to be supported in the plane of the skin. For positive pressures the panel continuously stiffens as the pressure increases. This

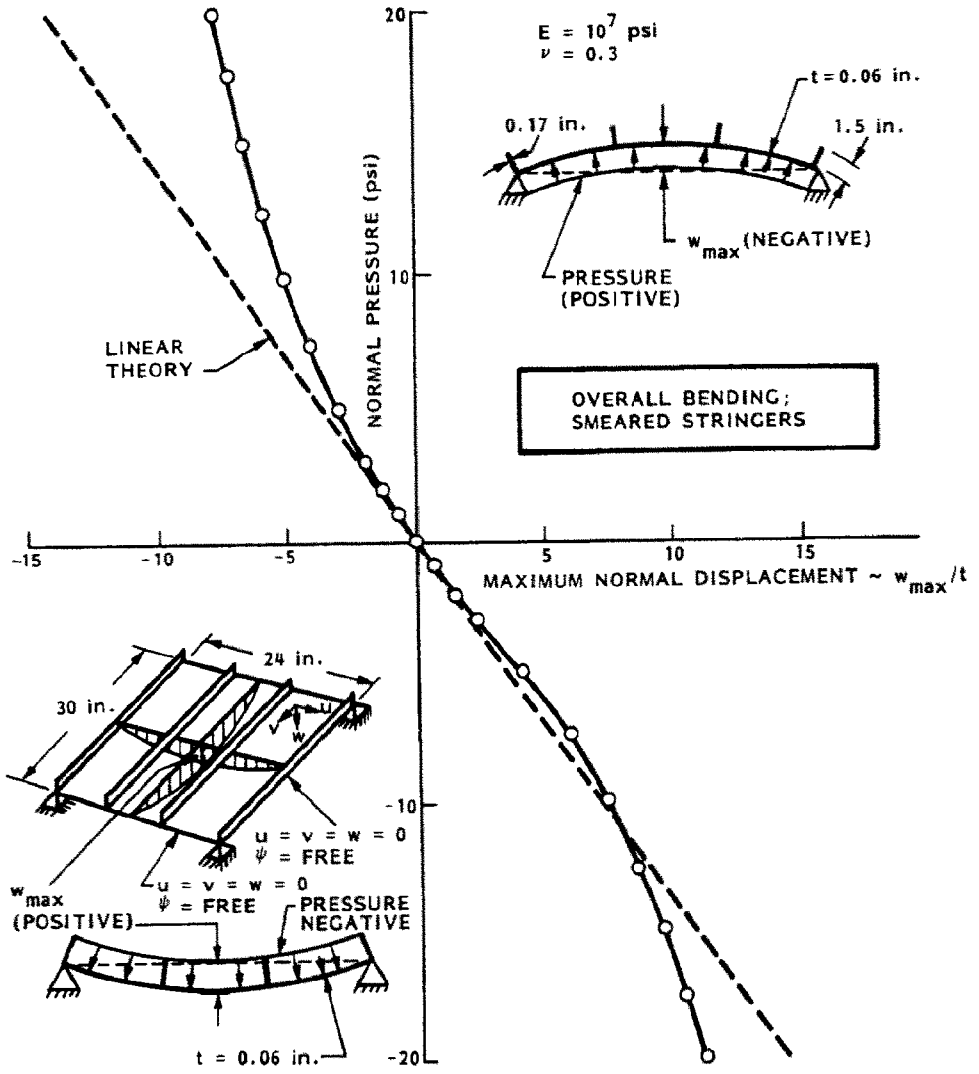

Fig. 55. PANDA2 prediction for the normal deflection w at the center of the panel loaded only by uniform pressure p. In this PANDA2 model the stringers are smeared out, the panel width (y coord.) is discretized with 36 nodes, and displacements are assumed to vary along the length (x coord.) as follows:

$$U(x, y) = u(y)\sin(n\pi x/L); \quad V(x, y) = v(y)\sin(2n\pi x/L); \quad W(x, y) = w(y)\sin(n\pi x/L).$$

is because both the induced axial forces and transverse (hoop) forces are tensile and monotonically increase with increasing pressure. For positive pressures, therefore, the stiffened panel behaves in a manner qualitatively similar to that of a monocoque panel.

For negative pressures the panel initially softens and then stiffens. The initial softening is caused by induced axial compressive forces that initially increase. For negative pressures greater than about five psi, however, the induced axial compression decreases. At a negative pressure above 12.5 psi the induced axial force becomes tensile and increases at an increasing rate as the negative pressure is further increased. (The behavior of the induced axial force is shown in Fig. 66, which is used later to discuss wide column buckling as a function of pressure.)

Figure 56 shows results from Problem 2, local bending around a stringer. The results are not skew symmetric for plus and minus pressures because the prestress in the panel skin obtained from the solution of Problem 1 is not symmetric (see Fig. 66). Notice the small range of applicability of linear theory.

Figure 57 shows the total displacement from the solutions of Problem 1 plus Problem 2 compared with the results from the STAGS finite element model depicted in Fig. 47. STAGS predicts a somewhat stiffer behavior, both in the linear and nonlinear range, probably because the STAGS model contains four stringers in the 24-in. panel width, whereas the PANDA2 model contains three.

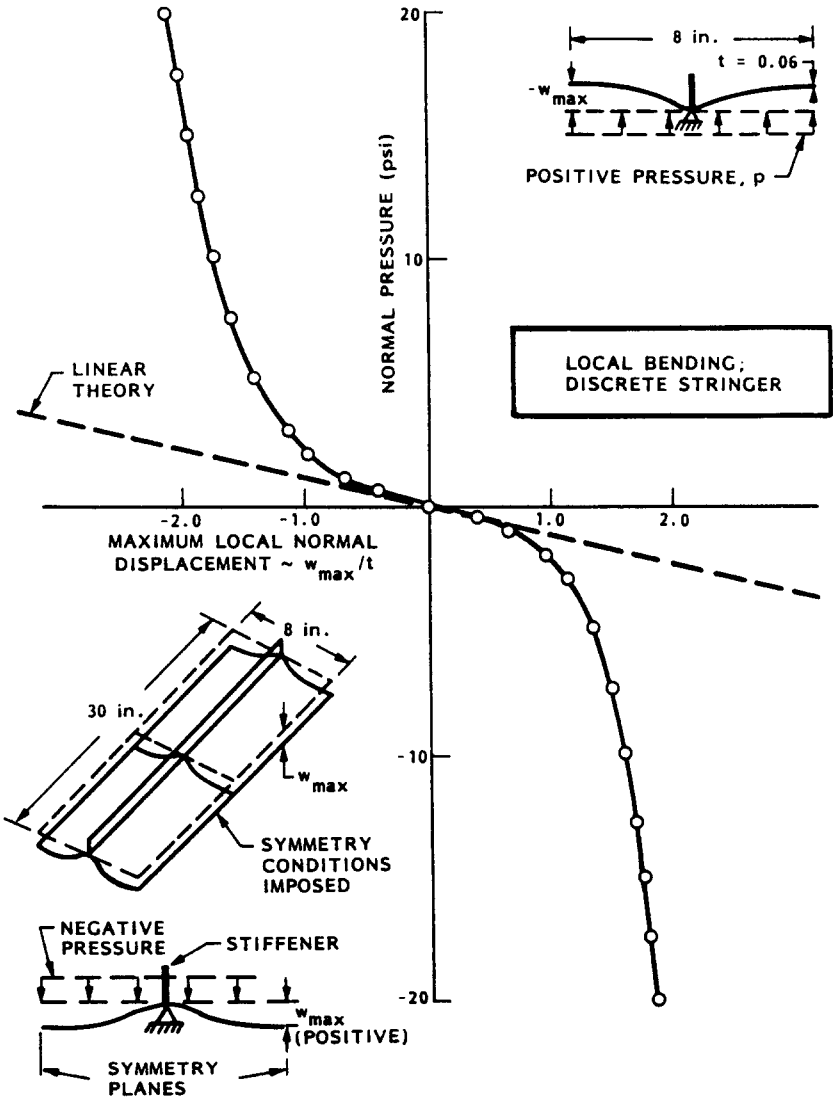

Fig. 56. PANDA2 prediction for the normal deflection w at the symmetry plane midway between stringers for a single-module (discrete stringer) model of a panel loaded only by uniform pressure. In this model the single panel module is discretized as shown in Fig. 46(b); bending of the stringer in its plane is prevented; the panel module is assumed to be infinitely long normal to the plane of the paper; and the membrane prestress state at the center of the panel calculated from the model shown in the previous figure is included in the nonlinear equilibrium analysis.

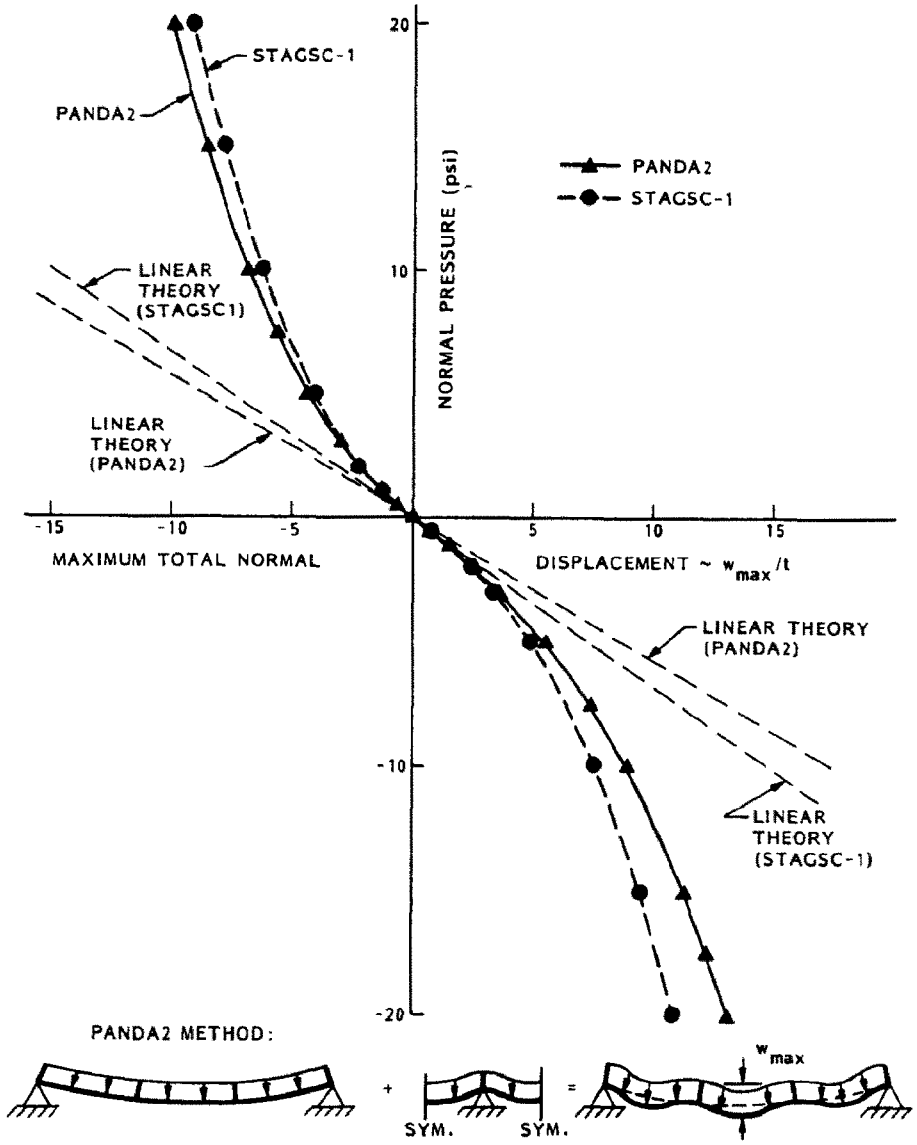

Fig. 57. PANDA2 and STAGS predictions of the normal displacement w at the center of the panel. The PANDA2 prediction is obtained by adding results shown in the previous two figures.

Figures 58 and 59 show the distributions of normal displacement across the panel width at the midlength symmetry line and along the length at the midwidth symmetry line. Agreement between STAGS and PANDA2 seems good enough to justify the use of PANDA2 for preliminary design optimization.

Figure 60 shows the largest strains anywhere in the panel predicted by PANDA2 and by STAGS. PANDA2 indicates that the largest strains are in the y-direction in the panel skin at the attachment line of any stringer at the midlength of the panel. They are due mostly to local bending of the panel skin around the hard stiffener. STAGS gives a similar result, except that at high pressures these transverse 'wrap-around' strains are greater at about one quarter of the way along the panel than they are at the midlength line of symmetry. This is probably because there is less transverse (hoop) tension in the panel skin one quarter of the way along the panel than there is at the midlength plane of symmetry. Therefore, the skin between stringers is freer to deflect more before large local tensile forces build up in it.

Figure 61 demonstrates this effect. The top frame shows the distributions of normal displacement across half of the panel width at various nodal lines in the STAGS model shown in Fig. 47. The bottom frame shows the lengthwise distribution of axial (N_x) and hoop (N_y) resultants in the panel skin at the midwidth line of symmetry. It is clear that in the STAGS model the amount of local 'wrap-around' transverse bending decreases as N_y increases. The maximum extreme fiber transverse strain is a sum of membrane plus bending contributions which turns out to be maximum at about nodal line 4 in the STAGS model. In the PANDA

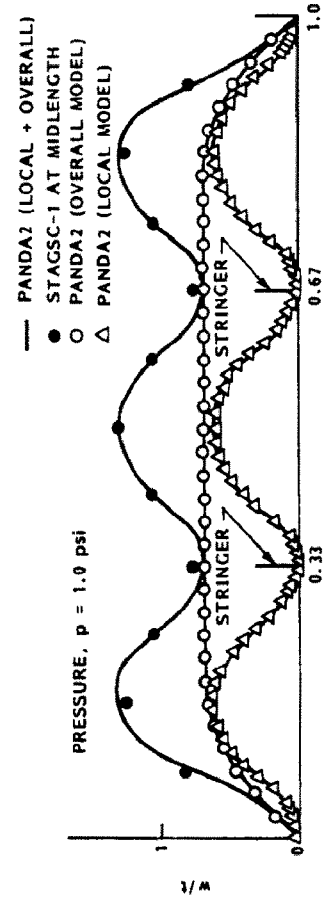

Fig. 58. Comparison between predictions of PANDA2 and STAGS for the normal displacement w (a) across the panel at the axial symmetry plane and (b) along the panel at its midwidth at a pressure $p = 1.0$ psi.

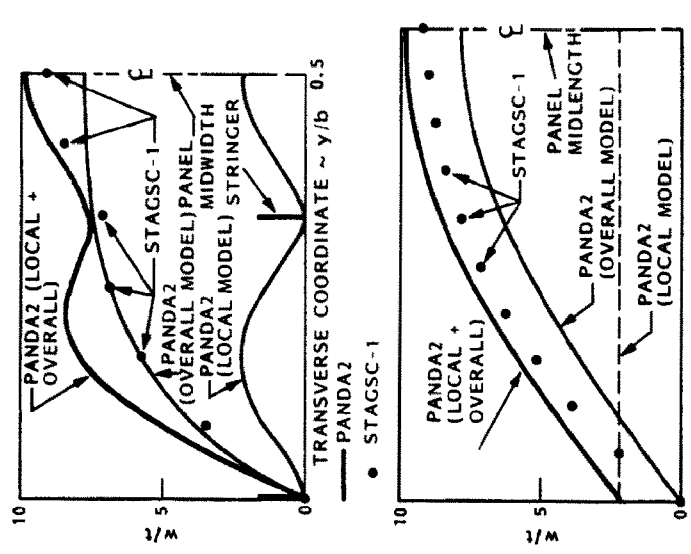

Fig. 59. Comparison between predictions of PANDA2 and STAGS for the normal displacement w (a) across the panel at the axial symmetry plane and (b) along the panel at its midwidth at a pressure $p = 20.0$ psi.

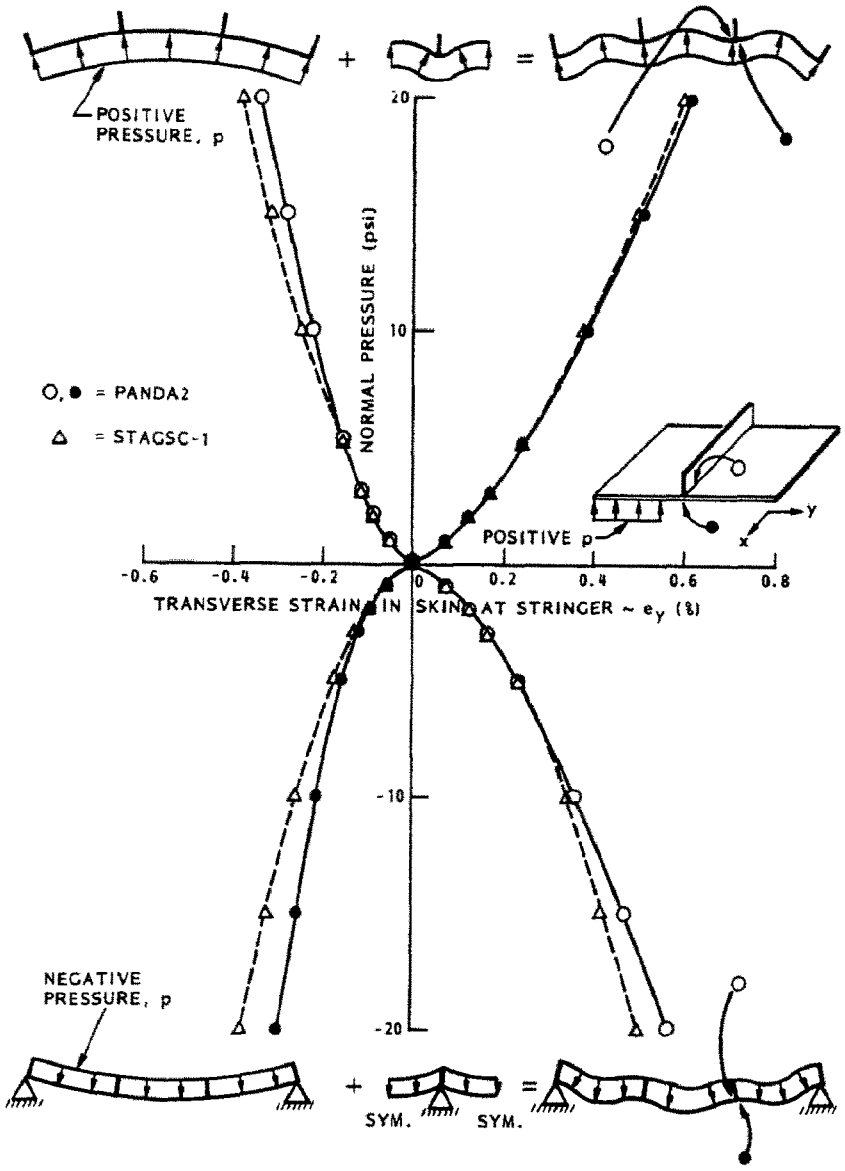

Fig. 60. Comparison of the maximum strains in the panel predicted by PANDA2 and STAGS.

model only the prestress at the midlength of the panel from Problem 1 is used in the solution of Problem 2, since in Problem 2 it is assumed that there is no variation in behavior along the length of the panel module. Perhaps it is only fortuitous that the maximum strains anywhere in the panel predicted by PANDA2 are in reasonably good agreement with those predicted by STAGS, even though the locations of them are different. One would need to run more cases to find out.

Figures 62 through 64 show certain stress resultants predicted by PANDA2 and by STAGS. These are important because they affect the local bifurcation buckling and post-local-buckling behavior, to be described next.

20.6 *Results for combined axial compression and normal pressure*

Figures 65–71 pertain to this section. The behavioral characteristics of primary importance arise from the following:

1. The normal pressure bows the panel, and a bowed panel under axial compression behaves differently from a straight panel.

2. The normal pressure prestresses the panel skin and stiffeners, which affects the local bifurcation buckling load factor, mode shape and post-buckling behavior.

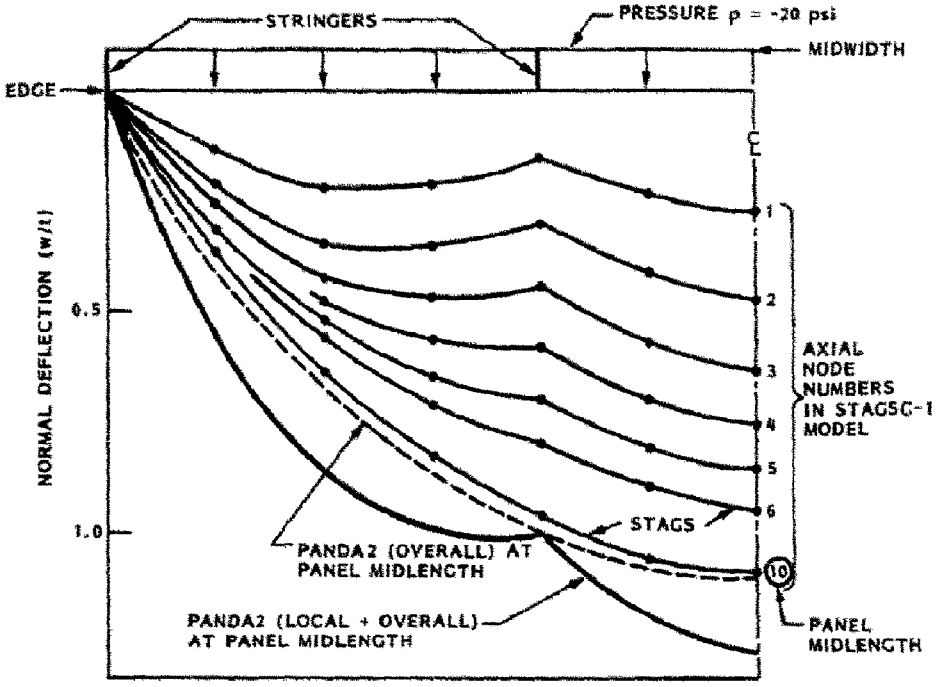

(a) PANDA2 AND STAGS RESULTS

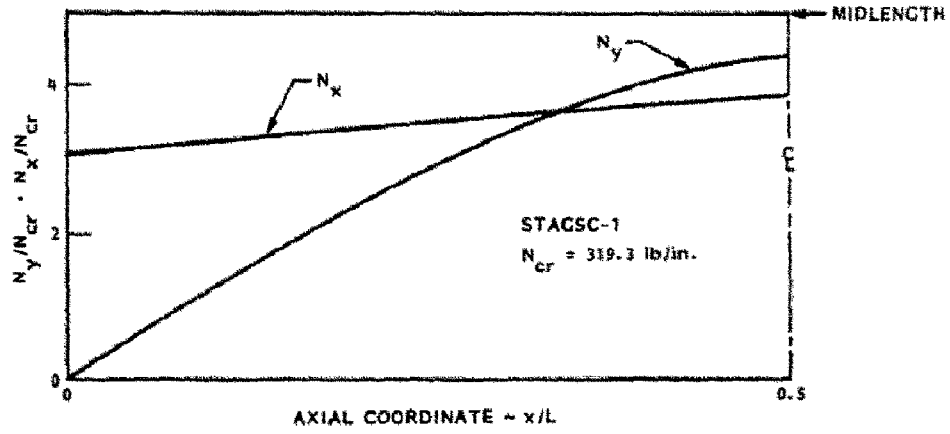

(b) STAGS RESULTS

Fig. 61. (a) Distribution of normal displacement w across the width of the panel for pressure $p = -20$ psi; (b) STAGS prediction of axial distributions of axial resultant N_x and hoop resultant N_y at the panel midwidth.

3. The change in post-buckling behavior due to pressure, especially the change in post-buckling skin stiffness and the change in the share of total axial load carried by the skin cause changes in the wide column buckling load factor and mode shape.

Figure 65 demonstrates the effect of pressure on the share of unit axial load carried by the panel skin and the local bifurcation buckling load factor and mode shape. For positive and increasing pressure the panel bows upward to an increasing degree. Hence, an increasing share of the applied axial load passes through the skin. By itself, this trend would lead to decreasing load factors for local buckling. However, the skin also becomes prestressed by the pressure, especially in the direction transverse to the stringers. This by itself would postpone local buckling and would cause the critical buckling mode to have more halfwaves in the axial direction than the critical mode for the unpressurized panel. A membrane tensile stress field also develops in the stringers. This effect postpones local buckling because the pretensioned stringer, especially the fibers of it farthest from the skin, will not want to rotate in the local buckling mode. Therefore, the pretensioned stringer will act more

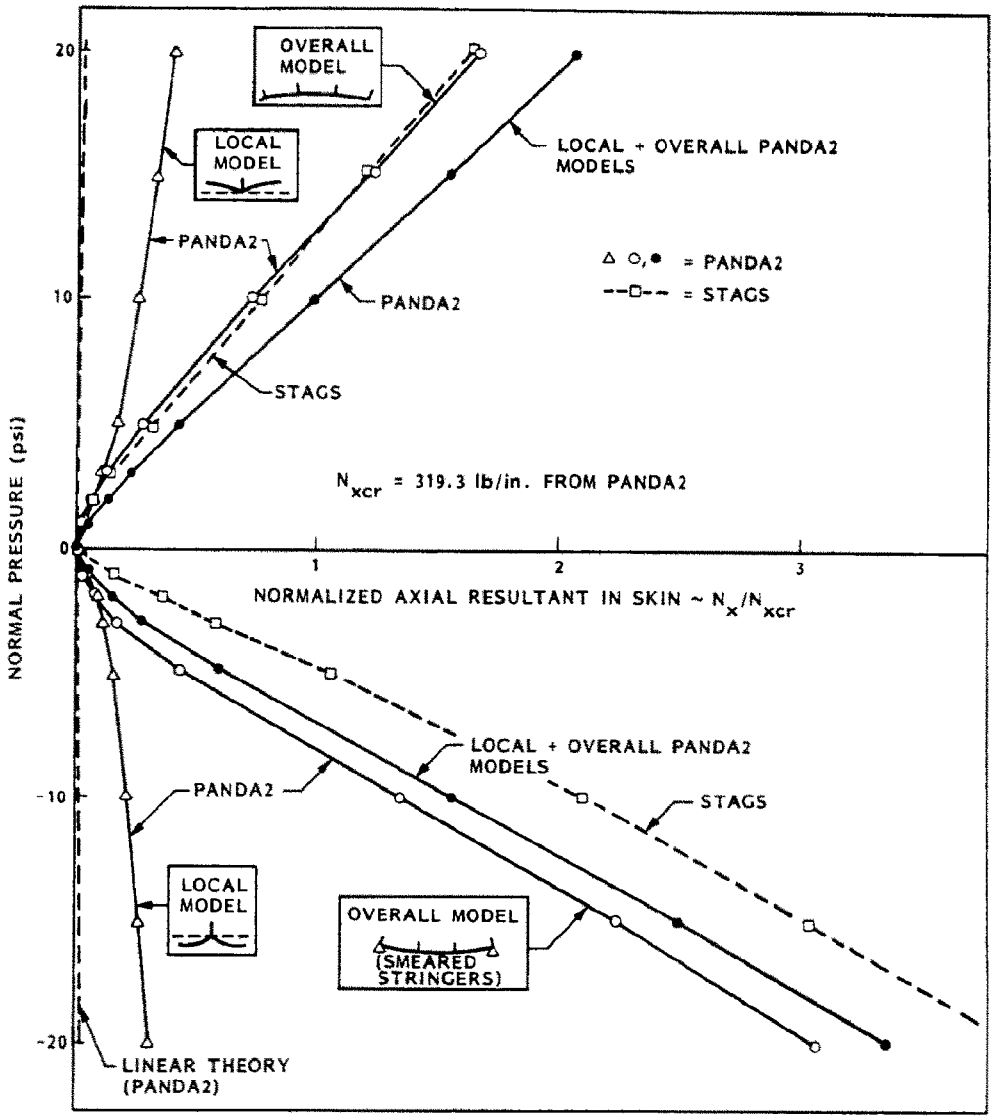

Fig. 62. PANDA2 and STAGS predictions of the axial resultant N_x at the center of the panel.

like a line along which the panel is clamped that it would if it were not pretensioned. The bowing and the prestressing therefore have opposite effects. In this case, the tensile prestress field predominates, so that for positive and increasing pressure the local bifurcation buckling load factor increases even though the skin carries an increasing percentage of the applied axial load.

For increasingly negative pressure, bowing leads to a smaller share of applied load going through the panel skin, which by itself would lead to higher bifurcation buckling load factors than that for the unpressurized panel. Negative pressure also generates a tensile stress field in the panel skin, which additionally postpones local bifurcation buckling. Therefore, unlike the case of positive pressure, for negative pressure these two factors have the same effect. However, the extreme fibers of the stringer become compressed, a factor that would by itself reduce the local bifurcation buckling load factor because it tends to make the stringer want to roll over. This tendency is small for small negative pressures, but predominates for large negative pressures, as seen from the change in direction of curve (2) in Fig. 65 and the change in the local buckling mode shape as the negative pressure increases above 10 psi.

Whereas Fig. 65 demonstrates the effect of pressure on local bifurcation buckling behavior, Figs 66 and 67 demonstrate the effect of pressure on wide column and general instability. There is much information in Figs 66 and 67. It may help to list items of primary importance:

1. For increasing positive pressure the overall axial tension induced by the pressure increases, as seen from curve (1). This increase gives rise to the slopes of curves (2a), (2b) and (3).

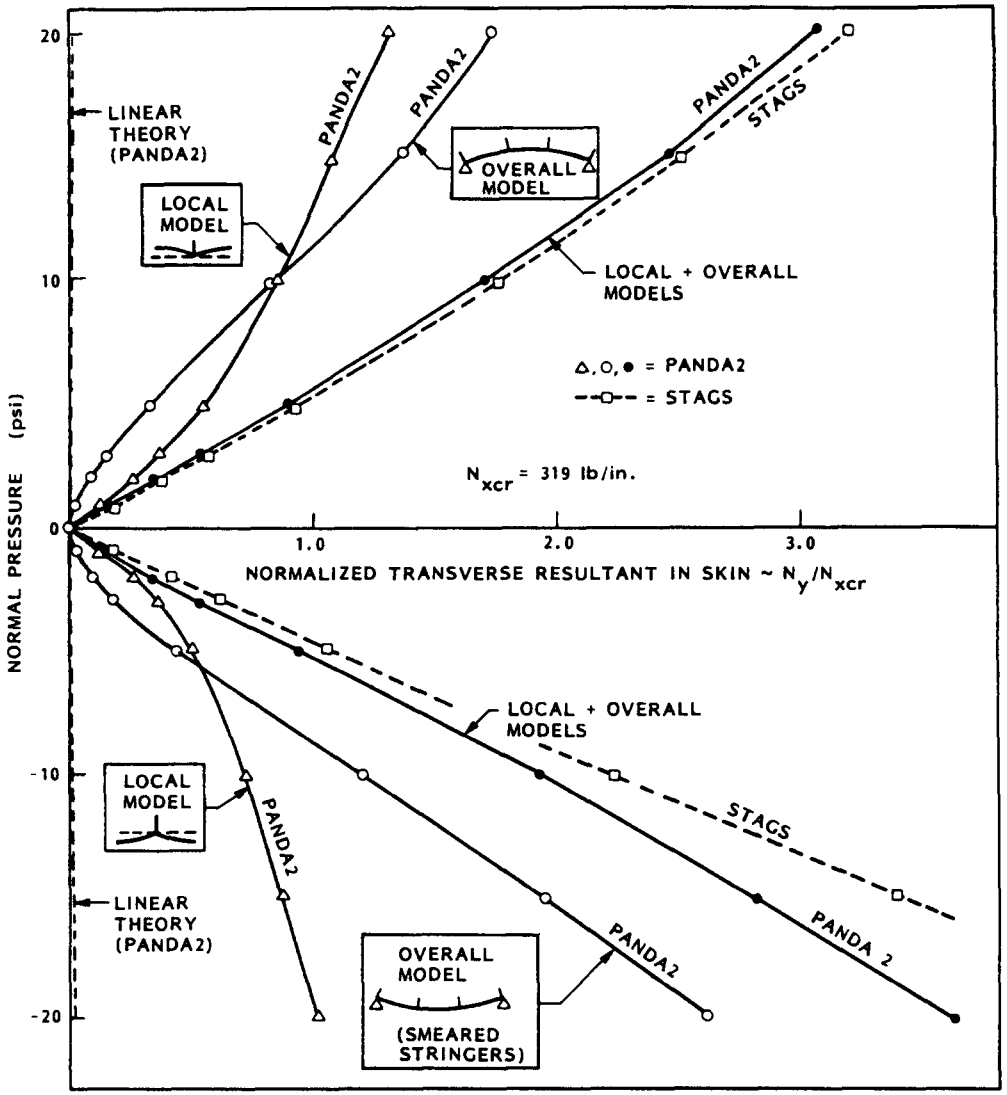

Fig. 63. PANDA2 and STAGS predictions of the transverse ('hoop') resultant N_y at the center of the panel.

2. The wide column buckling load factor is very sensitive to the amount of skin deformation present in the wide column buckling mode, as seen from the sketches in Fig. 67. The more skin deformation, the lower is the wide column buckling mode.

3. If there is little or no local skin deformation in the wide column buckling mode, as is the case in Fig. 67, bottom left, then the wide column buckling load factor should be approximately equal to the load factor from the PANDA-type closed form analysis corresponding to zero pressure.

The fact that for positive pressure the curve for N_{xcr} neglecting local post-buckling (curve 2a) lies to the left of that for N_{xcr} including local post-buckling (curve 2b) requires explanation because this result at first runs counter to intuition. One would think that including local post-buckling effects means using reduced axial skin stiffness in the buckling analysis, which would naturally lead to reduced wide column buckling load factors.

However, one must remember that the pre-buckling loads in the skin are much smaller in the theory that includes local post-buckling than they are in the theory that neglects local post-buckling. This difference in load distribution over the cross section of the wide column causes the differences in the wide column buckling modes and load factors listed in the top part of Fig. 67. Notice that for all pressures greater than $p = -3$ there is much more movement of the relatively heavy stiffener in the buckling modes corresponding to 'local post-buckling included' than there is for those corresponding to 'local post-buckling neglected'. This is because relatively more axial load passes through the stringer in the 'local post-buckling included' case, giving rise to buckling modes that reflect general instability behavior rather than local skin buckling. In fact, the mode corresponding to $p = 0$ on the left-hand side of Fig. 67 was rejected by PANDA2 as an indicator of general instability. Therefore, the eigenvalue of 0.306 would not have represented a violated constraint in an

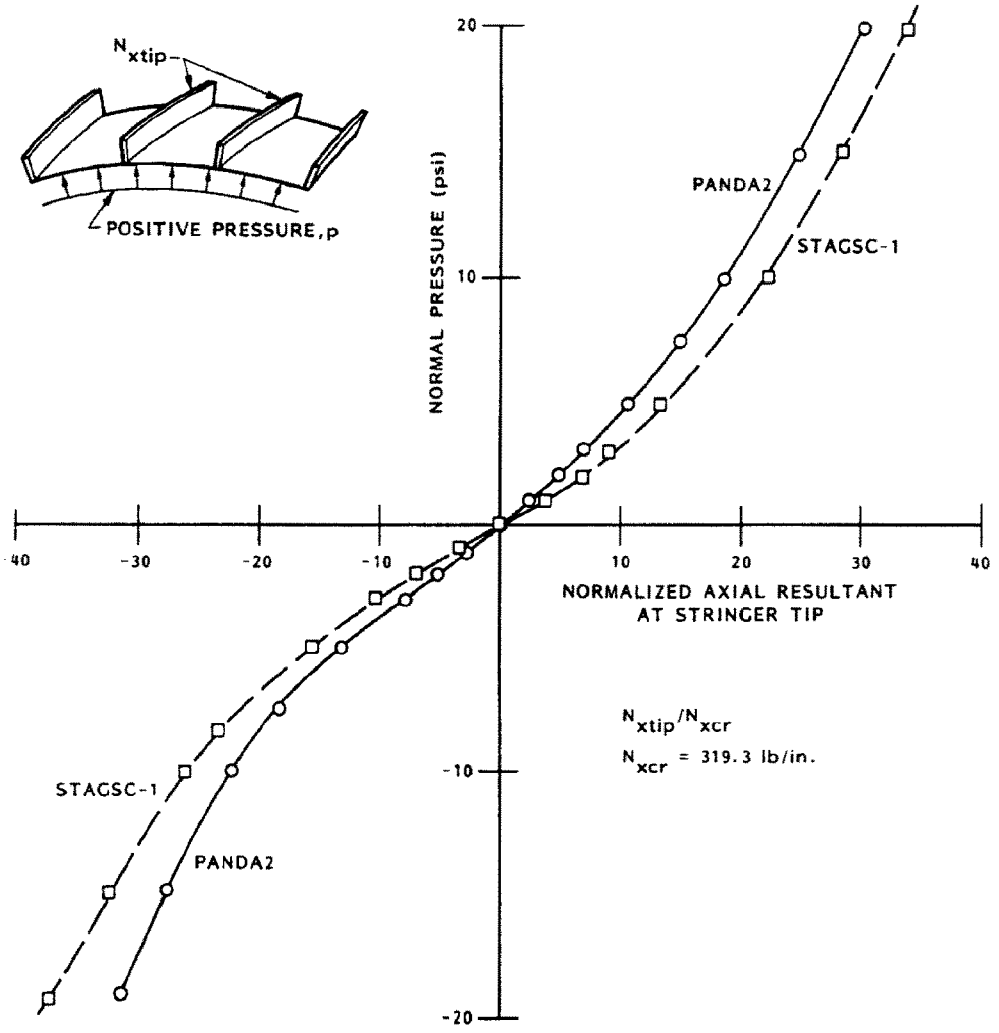

Fig. 64. PANDA2 and STAGS predictions of the axial resultant N_{xtip} at the tips of the stringers that are not at the panel edges, at the midlength of the panel.

optimization analysis of this panel. The mode shape just above the rejected mode was barely accepted. (It is felt that the acceptance of such modes, which actually represent local skin buckling more than general instability, is a good practice, since it helps to yield conservative results for general instability, a mode of failure that is more likely to be sensitive to unknown imperfections than is the local instability mode of failure.)

Figure 68 shows the effect of pressure on (axial load)–(axial strain) curves. Those for positive pressure lie to the right of those for negative pressure for two reasons:

1. The axial bowing induced by pressure increases as the axial load increases, and if the pressure is positive this bowing is of such a sign as to give rise to average decreases in distance betweeen the two loaded ends of the panel skin reference surface, at which the average axial end shortening is measured.

2. As seen from Fig. 65, positive pressure leads to local bifurcation buckling modes that have more axial halfwaves than is the case for no pressure or negative pressure. The tangent stiffness of post-buckled panel skin decreases with increasing number of axial halfwaves in the post-buckled modal pattern.

Figures 69 and 70 show the effect of pressure on post-buckling normal deflection and maximum strain in the panel. From Fig. 69 one can see that negative pressure leads to a higher local bifurcation load than does a positive pressure. This is for the reasons explained in connection with Fig. 65. The growth of the local buckles is faster with increasing axial load in the case of positive pressure than it is with negative pressure. This is because a relatively larger share of axial compression passes through the skin, as shown in Fig. 65.

From Fig. 70 one can see that positive pressure leads to much higher strains than negative pressure. This is obviously related to the much faster growth of the local buckles in the case of positive pressure.

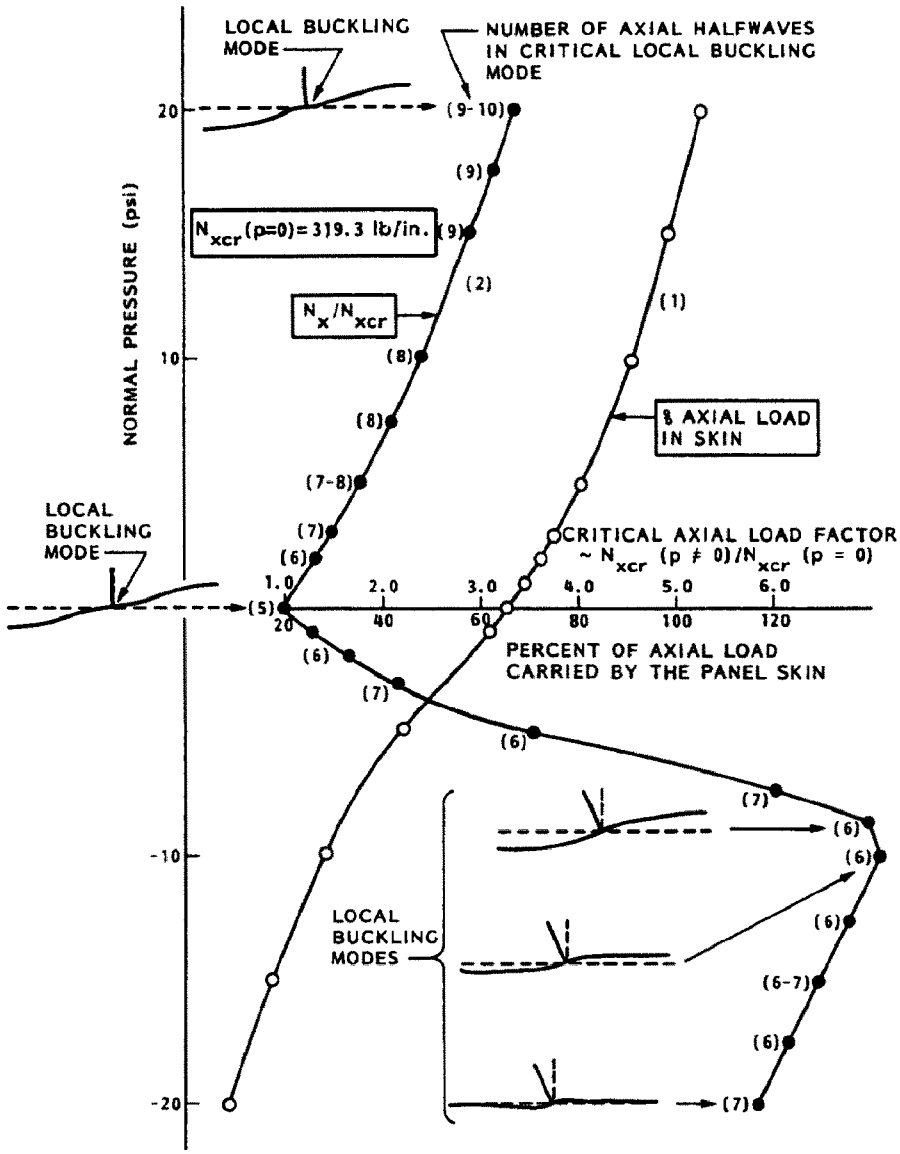

Fig. 65. PANDA2 predictions of the effect of pressure p on: (1) how much of the average applied axial load N_x is carried by the skin; and (2) local bifurcation buckling load factor and number of axial half waves.

Figure 71 shows the effect of pressure on the pre- and post-local-buckling axial strain in the panel skin midway between stringers. The PANDA2 results are explained by the faster growth of local buckles in the case of positive pressure.

20.7 *Results for combined axial compression and simulated curing*

In panels similar to the isotropic blade stiffened panel being studied here, but fabricated from composite materials, optimum designs would be characterized by stringers with predominantly axial fibers and a skin which may be predominantly plus and minus 45° fibers. If the skin and stiffeners are cocured, thermal stresses and deformations build up as the panel cools from the temperature at which the composite material sets to ambient temperature. If the stringers have mostly zero fibers while the skin has mostly plus and minus 45° fibers, the skin will try to shrink more than the stringers, and the panel will bow axially so that the side of the skin farthest from the stringers is concave. This thermally induced residual state can be predicted with PANDA2.

In the case of the isotropic material of this example, there would not be any overall residual stresses or deformations in an actual cases because the stringers and skin would shrink equally during post-cure cool-down from a uniform temperature. However, this rather unrealistic example involving skin and stringers

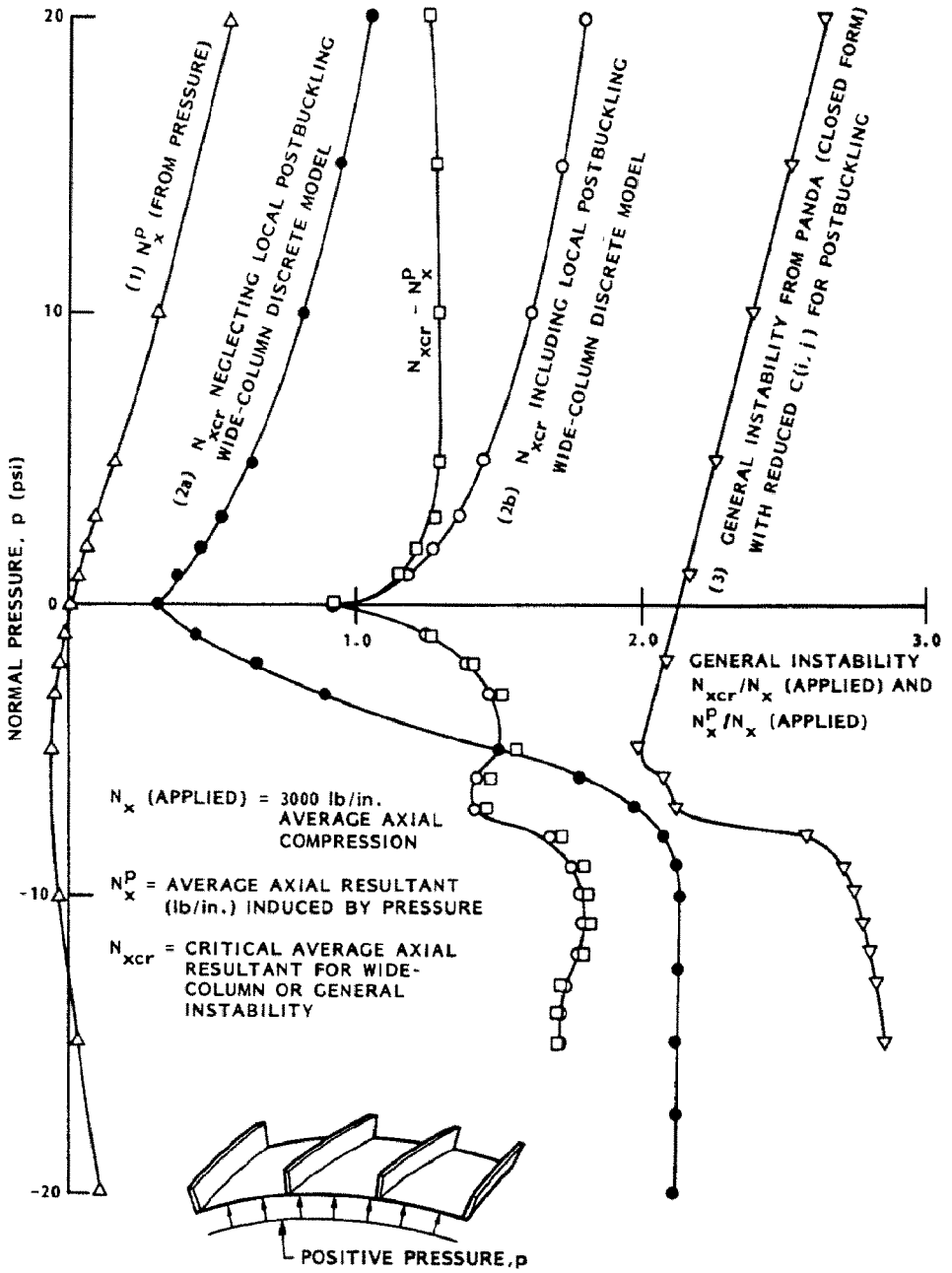

Fig. 66. PANDA2 predictions of the effect of pressure p on: (1) average axial membrane prestress, N_x^p; (2) wide column buckling load factors N_{xcr} obtained from theories in which: (a) local post-buckling of the skin is neglected, (b) local post-buckling of the skin is included; (3) general instability as predicted by a PANDA-type (closed form) analysis.

at different temperatures is introduced for demonstration purposes. The phenomena described next would occur in realistic cases also, although they probably would be a lot less pronounced, even in a non-optimally designed panel.

The results are shown in Figs 72–77. The axial load–strain curves in Fig. 72 have qualitatively the same shape as those in Fig. 68 for plus and minus pressure, respectively, because the important effect, axial bowing of the panel, has the same sign and approximately the same amplitude, as seen from comparison of Figs 57 and 76.

Figure 73 demonstrates that following local bifurcation buckling, the amplitude of the local buckles increases at the fastest rate when the panel bows so that the side of the skin away from the stringers becomes concave (curve labelled $T = -290$). This happens because a higher share of the axial load goes through the skin, as shown in Fig. 77, than is the case with bowing of the opposite sign. The same effect was obtained

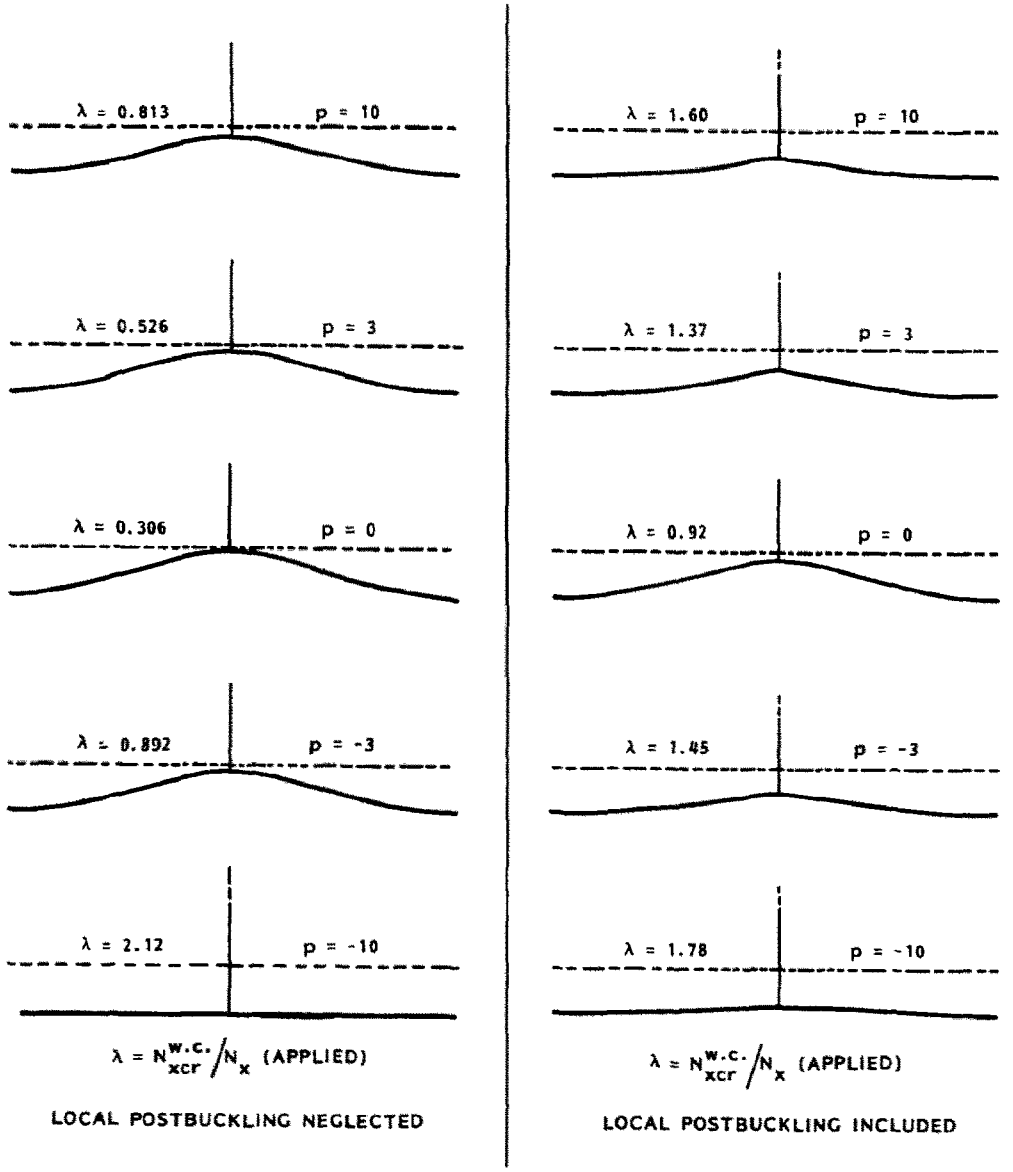

Fig. 67. PANDA2 predictions of the effect of pressure on the wide column buckling modes and load factors obtained with use of the discretized model of the single panel module.

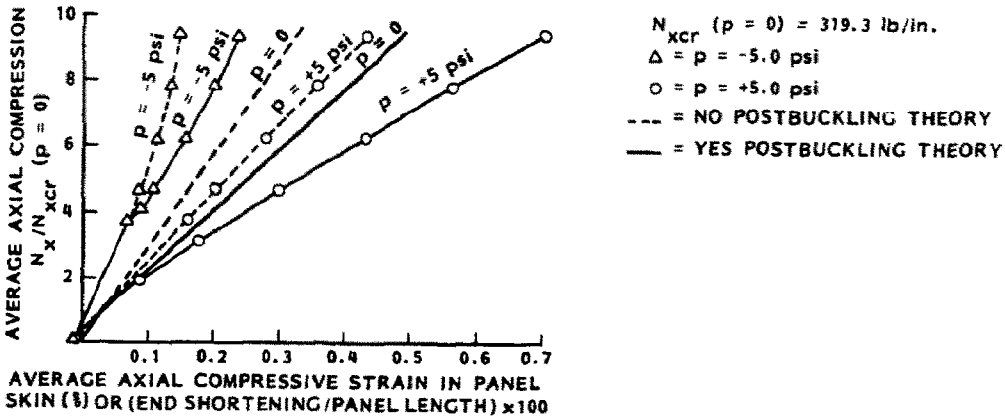

Fig. 68. PANDA2 predictions of the effect of pressure on load-end-shortening curves for the uniformly axially compressed blade-stiffened panel.

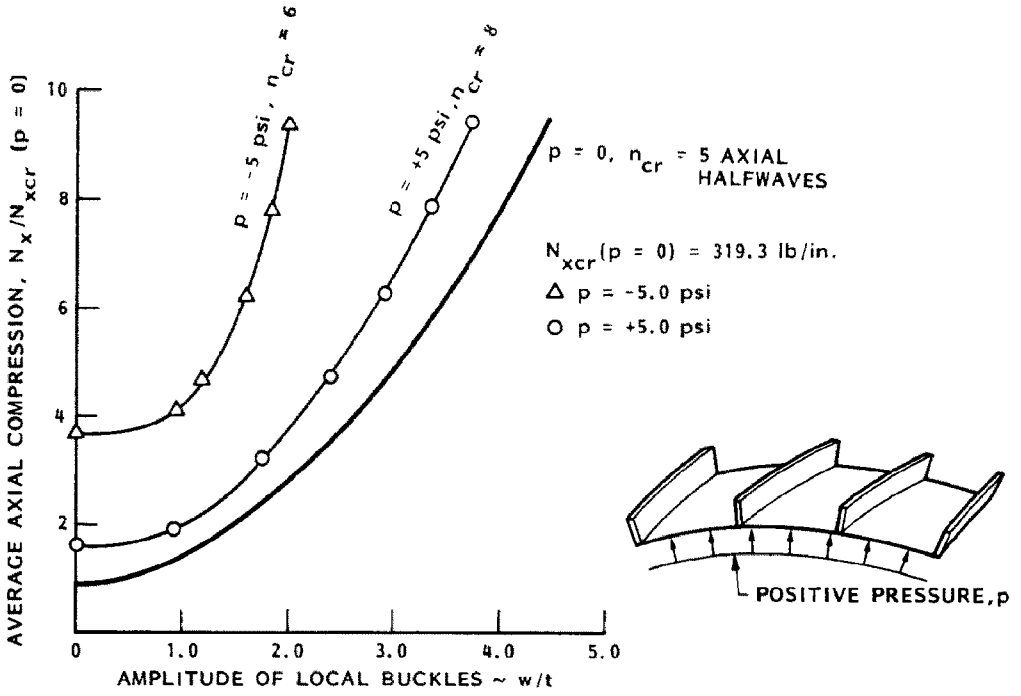

Fig. 69. PANDA2 predictions of the effect of pressure on local bifurcation and growth of the local normal displacement pattern in the post-buckling regime.

with positive pressure (see Figs 65 and 69). The bifurcation buckling load is higher than those for $T = 0$ and $T = +290$ because the residual resultant is tensile in the skin. The local bifurcation buckling load factor is nearly zero for the panel with the heated skin because the residual state of the 'cured' panel almost causes local buckling by itself.

The maximum transverse strains in the locally post-buckled panel, shown in Fig. 74, exhibit behavior analogous to that in the pressurized axially compressed panel for the same reason: the local buckles grow faster for the panel bowed so that the highest percentage of applied axial load is absorbed by the skin. However, the effect is much less dramatic in the case of thermal residual strains than it is for strains due to pressure because there is no thermal strain concentration in the pre-buckling phase analogous to the 'wrap-around' strain concentration described in the section on panels subjected to normal pressure alone.

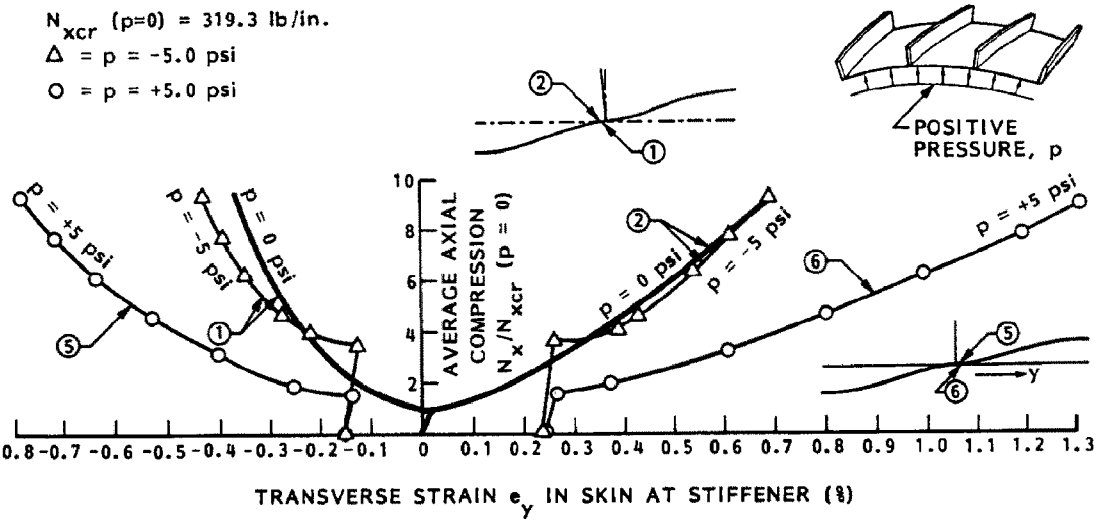

Fig. 70. PANDA2 predictions of the effect of pressure on the maximum transverse strain e_y in the panel skin next to the stringer.

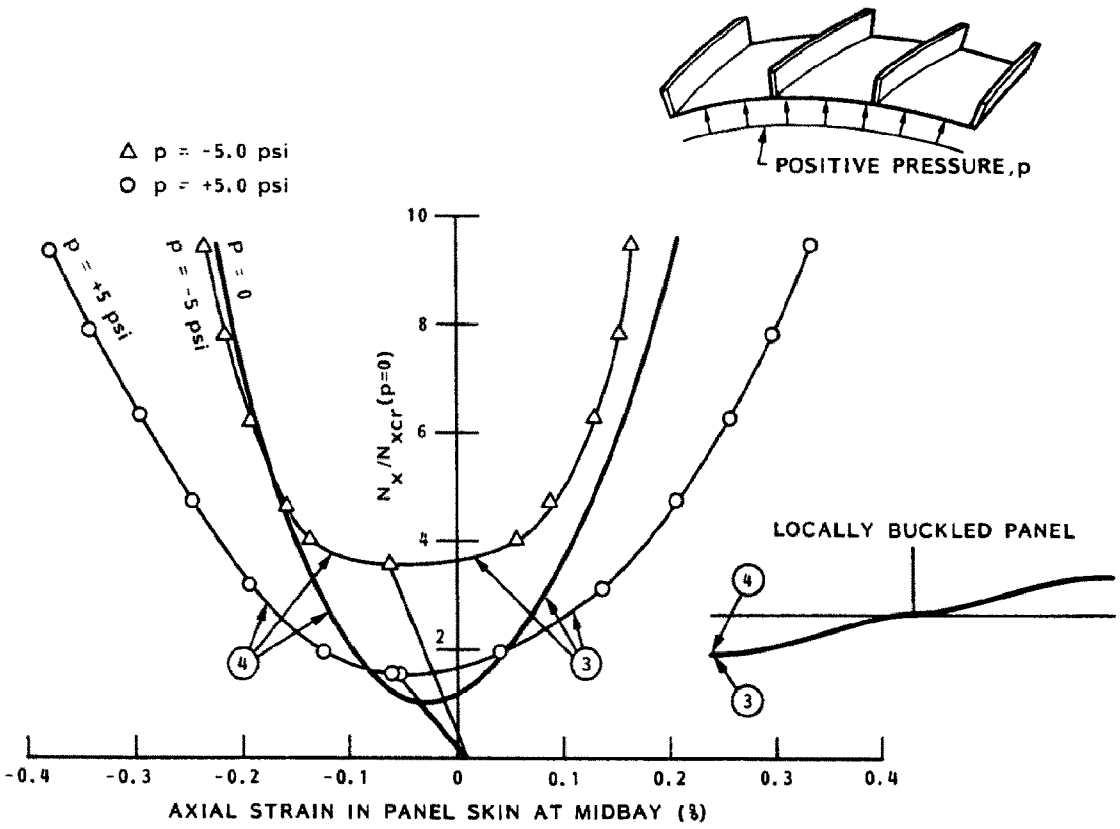

Fig. 71. PANDA2 predictions of the effect of pressure on the maximum axial strain e_x in the panel skin midway between stringers.

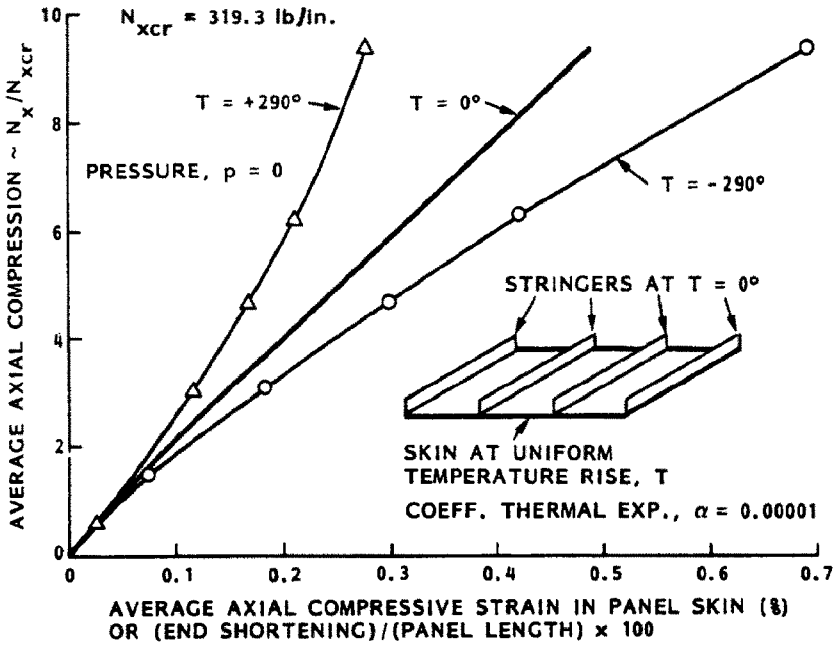

Fig. 72. PANDA2 predictions of the effect of curing on load-end-shortening curves for the uniformly axially compressed blade-stiffened panel. Curing is simulated by heating or cooling the panel skin relative to the stringers, which in this example are kept at ambient temperature ($T = 0$).

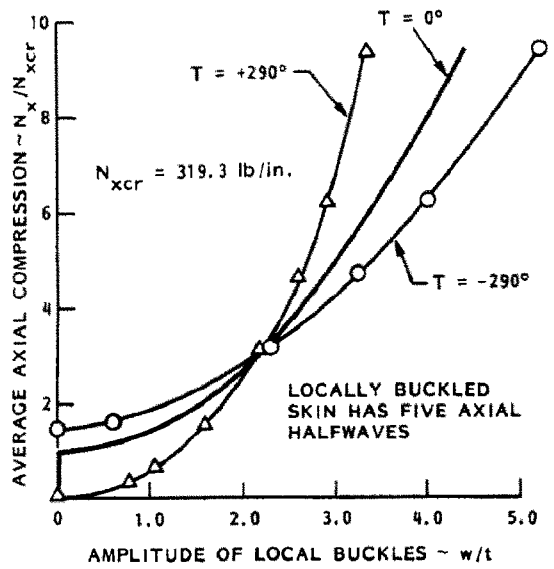

Fig. 73. PANDA2 predictions of the effect of curing on local bifurcation and growth of the local normal displacement pattern in the post-buckling regime.

Figure 75 shows the extreme fiber axial strain in the panel skin midway between stringers. This behavior is also explained by the later bifurcation of the panel in which the residual axial resultant is tensile but the buckles of this panel grow faster than do those in the panel that is thermally bowed the opposite way.

Figure 76 shows the linear dependence of axial bowing and axial residual stress resultant on temperature. Figure 77 shows the effect of temperature on share of axial load carried by the skin and on the local bifurcation buckling load factor. In this case the local bifurcation buckling load factor is influenced by two counteracting factors:

1. For increasing skin temperature (note: positive temperatures are plotted downward to preserve the analogy with the normal pressure case!) the smaller share of axial load carried by the panel skin would lead to higher bifurcation load factors if there were no residual stress resultant in the skin.
2. For increasing skin temperature there is increasing compressive residual stress resultant in the skin, which would lead to lower bifurcation load factors. This is the dominant effect.

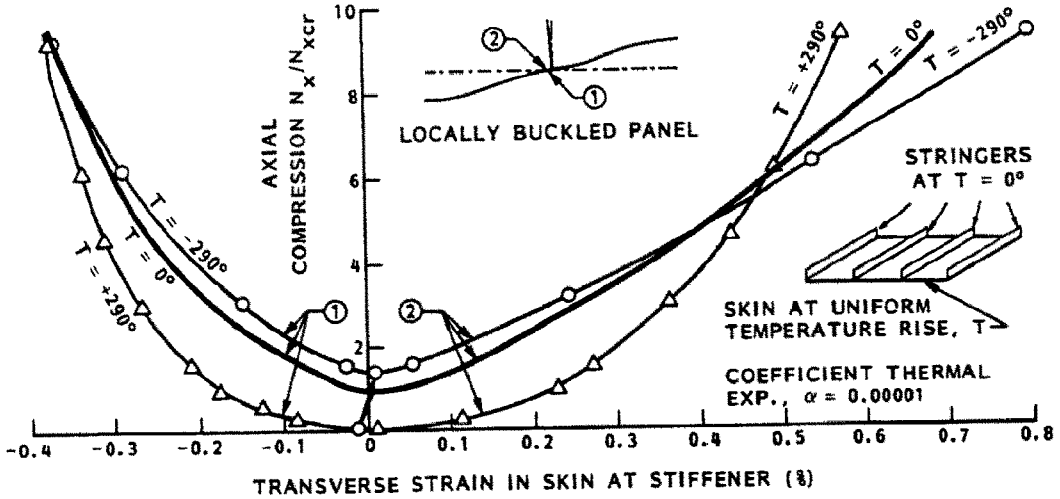

Fig. 74. PANDA2 predictions of the effect of curing on the maximum transverse strain e_y in the panel skin next to the stringer.

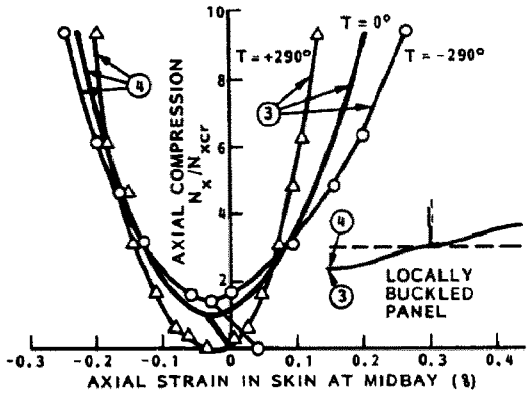

Fig. 75. PANDA2 predictions of the effect of curing on the maximum axial strain e_x in the panel skin midway between stringers.

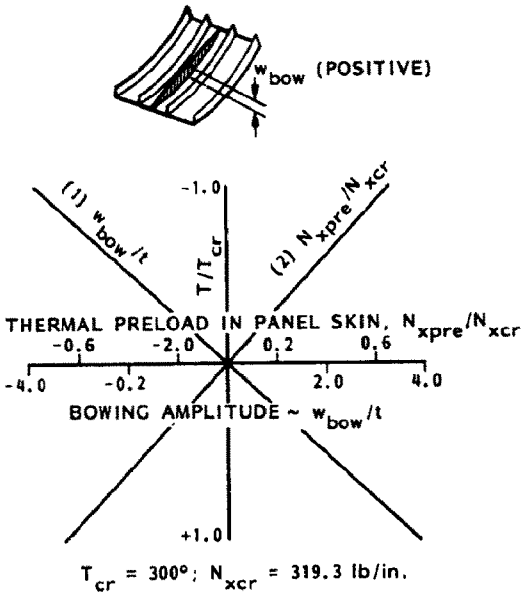

Fig. 76. PANDA2 predictions of the effect of curing temperature on: (1) the amount of axial bowing; (2) the average thermal resultant in the panel skin. Note that the temperature scale is inverted: minus at the top.

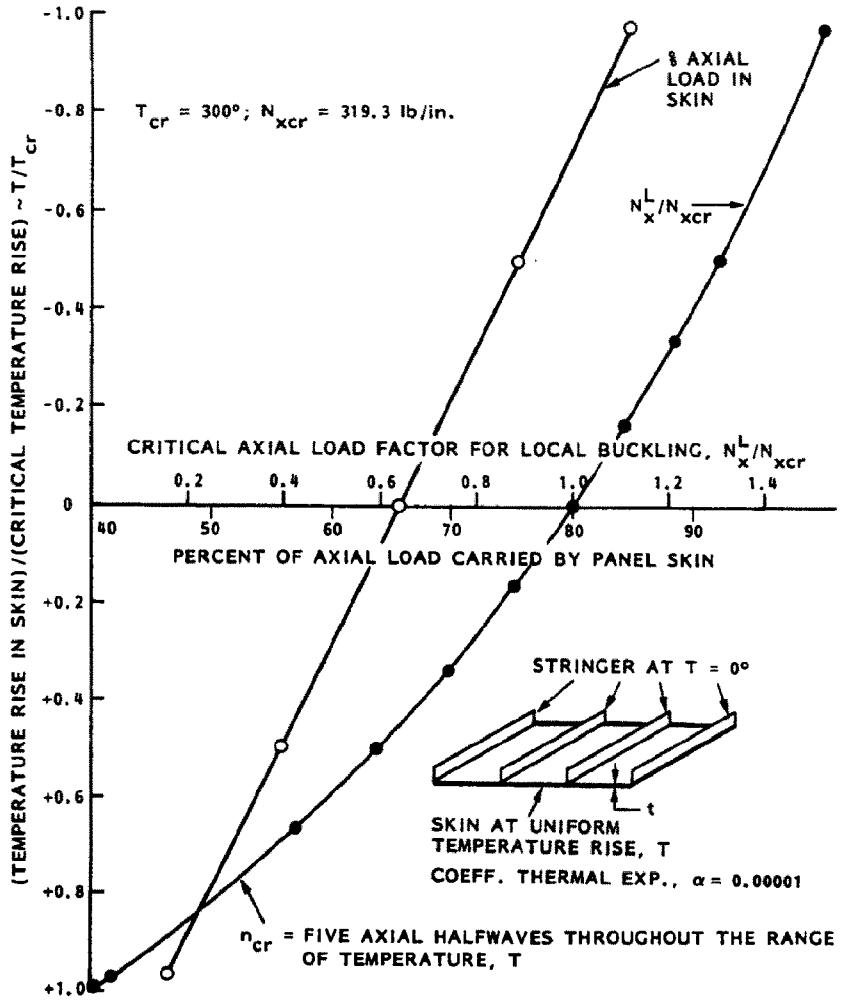

Fig. 77. PANDA2 predictions of the effect of curing temperature on: (1) the percentage of applied axial load carried by the panel skin; (2) the bifurcation buckling load factor for local buckling of the bowed, thermally pre-stressed panel. Note that the temperature scale is inverted: minus at the top.

21. OPTIMUM DESIGN OF ARIANE4 INTERSTAGE

21.1 *Procedure for designing with PANDA2*

Section 19.7 contains a brief description of the steps leading to an optimum design of a graphite-epoxy, hat-stiffened panel loaded in axial compression. That panel is subjected to only one set of loads, and results are not given for the evolution of the design during iterations.

In this section the design procedure is explained more fully. Minimum weight designs are obtained for the ARIANE4 interstage between the second and third stages of the ARIANE4 booster. Blaas and Wiggenraad call it 'Interstage 2/3' [31]. This example is employed to illustrate a typical use of PANDA2 to solve a practical, rather large, design problem. Two design concepts are explored: (1) T-shaped stringers, for which two 'sub-concepts' are investigated—(1.1) all-graphite-epoxy and (1.2) graphite-epoxy with an aluminum insert inside the stringers and stringer bases; and (2) Hat-shaped stringers. Table 4 lists the tasks required during the design process.

Table 4. Procedure for designing a stiffened shell with PANDA2

TASK	EXAMPLE
1. Decide what part of a structure to optimize.	ARIANE4 2/3 interstage (Fig. 78).
2. Decide how to model the part.	Entire cylindrical shell with spatially varying loads is modeled as a 40-inch-wide panel with multiple sets of uniform loads (Fig. 79).
3. Decide what load sets to use.	Load sets are shown in Fig. 79: 3.1. Uniform axial compression of 3000 lb/in. 3.2. Uniform axial compression of 1000 lb/in. combined with uniform in-plane shear of 1000 lb/in. 3.3. Uniform axial tension of 2000 lb/in.
4. Decide what design concept to use.	Concept is shown in Fig. 80: 4.1. Graphite-epoxy (GR/EP), external, T-shaped, stringers. 4.2. Aluminum, internal, rectangular rings spaced 26.75 inches apart. 4.3. Balanced laminates throughout. 4.4. 45-degree, GR/EP "isotropic" cloth outer layers (layer type 1 in Fig. 80). 4.5. Web of stringer formed by extension of top cloth layer. 4.6. In addition to the outer cloth layers, default group of 12 GR/EP tape layers for panel skin: [90/45/0/-45/0/90]s 4.7. 3-layer insert [0(m2)/90/0(m2)] within stringer base. 4.8. 3-layer insert [0(m4)/90/0(m4)] within stringer flange.
5. Choose starting design and material properties	Starting design and material properties are listed in Table 5, which represents input for the BEGIN processor.
6. Choose decision, linked, escape variables, and lower and upper bounds of decision variables.	Decision variables, linked variables, escape variables and lower and upper bounds of decision variables are listed in Table 7. Table 6 represents input for the DECIDE processor.

Table 4—*cont.*

7. Decide what optimization strategy to use, and whether or not to permit local buckling. Choose factors of safety.	Sequence of optimization runs: 7.1. Several runs with IQUICK=1 in order to get approximate approximate design quickly. (Figs. 84-89). Factor of safety for general and panel buckling = 2.0 for Load Set 1 (pure axial compression); F.S. = 1.5 for general and panel buckling for Load Set 2 (combined axial compression and in-plane shear). All other F.S.'s = 1.0. 7.2. Several runs with IQUICK=0 and with KOITER=1 (local buckling allowed). Factors of safety for general and panel buckling that were 2.0 and 1.5 in the IQUICK=1 runs are reduced to 1.5 and 1.2, respectively (Figs. 84-90). 7.3. Several runs with IQUICK=0 and with KOITER=0 (no local buckling permitted). Factors of safety remain as in 2 (Figs. 92-95).
8. Evaluate final design by running PANEL followed by BOSOR4LOG and BOSORALL.	Results from the KOITER = 1 design are shown in Fig. 91. Results from KOITER = 0 design are shown in Fig.96.

21.1.1 *Step* 1: *Identify the structure to be optimized.* Step 1 is to identify the structure to be optimized. Figure 78 shows the ARIANE4 2/3-interstage, which is initially assumed to be a cylindrical shell reinforced by external T-shaped stringers and internal rectangular rings. (In the PANDA2 analysis special end fittings and doublers are of course neglected. The weights of the panels designed by PANDA2 do not include any structure, such as large end rings, that would be required to provide end support for the interstage.)

21.1.2 *Steps* 2 *and* 3: *How much and what load sets?* Steps 2 and 3 are to decide how much of the structure to include in the optimization analysis and how many and what load sets to optimize this portion to withstand. The very important decisions that the user makes in steps 2 and 3 depend on whether or not the loading varies along the length and around the circumference of the structure selected in step 1.

In this case the cylindrical shell is subjected to overall bending, axial compression, and shear loads, **M**, **P** and **S**, as shown in the top part of Fig. 79. The bending moment **M** is assumed to be represented by an axial line load $N_x(\theta)$ that is distributed around the circumference of the cylindrical shell as $\cos\theta$, and the shear load **S** is represented by a shear line load $N_{xy}(\theta)$ distributed as $\sin\theta$. In order to determine the in-plane shear N_{xy} at $\theta = 90°$ generated by the cosinusoidally varying axial load $N_x(\theta)$, an initial run was made with BOSOR4 with use of its INDIC = 3 analysis branch [2]. The design used for this preliminary analysis was that obtained by Blaas and Wiggenraad [31]. This shear line load plus that generated from the applied shear load **S** constitute the total maximum N_{xy}. In this analysis it is assumed that the maximum axial compression from bending **M** is $N_x(\text{from } \mathbf{M}) = 2000$ lb/in.; the uniform axial compression from **P** is $N_x(\text{from } P) = 1000$ lb/in.; and the maximum in-plane shear at $\theta = 90°$ from both **M** and **S** is $N_{xy} = 1000$ lb/in.

The actual problem is to find the minimum weight of a complete cylindrical shell with axial line load N_x and shear line load N_{xy} both varying around the circumference. PANDA2 allows only N_x to vary along the panel edge. Therefore, this problem was approached by assuming that the complete cylindrical shell is divided into identical panels, each spanning 40 in. of circumference and each subjected to uniform loads. Three such panels are depicted in the bottom of Fig. 79. The optimum design of the complete cylindrical shell with loads varying over its surface can be determined by optimizing one of the identical 40-in.-wide panels subjected to multiple sets of uniform loads. Initially the three load sets shown at the bottom of Fig. 79 were chosen. However, it was soon determined that the uniform tension load, $N_x = 2000$ lb/in., did not generate any critical behavioral constraint conditions. Therefore, this load set was dropped.

21.1.3 *Step* 4: *Decide what design concept to use.* Step 4 is to decide what design concept to use. In this case the skin and stringers are initially assumed to be fabricated of graphite-epoxy cloth and tape, as depicted

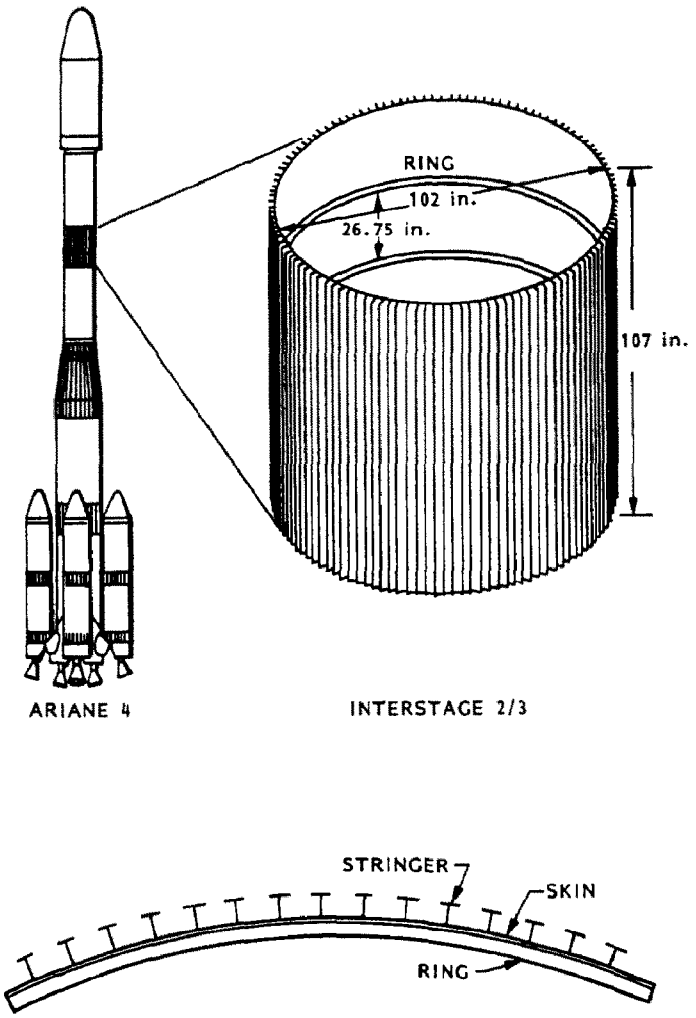

Fig. 78. ARIANE4 interstage between stage 2 and stage 3. The cylindrical shell is reinforced by external stringers and internal rings.

in Fig. 80. The spacing of the stringers is to be determined. The internal rings are of aluminum and are equally spaced 26.75 in. apart.

Details of the design concept with the T-shaped stringers appear in Fig. 80. The graphite-epoxy cloth and tape (material types 1 and 3) have the same properties as those listed in the file HAT.BEG given at the end of Sec. 3. The Default Group of 12 layers of graphite-epoxy tape has layup angles fixed but thicknesses to be determined during optimization. The graphite-epoxy cloth has the same modulus along the fibers in the two orthogonal directions ('pseudo-isotropic') but low shear modulus. The fiber directions are oriented at plus and minus 45° from the axis of the stringers. Only one layer is given because this cloth is considered to be homogeneous material with the same properties in the plus and minus 45° directions. The thickness of this cloth is a decision variable.

Both tape and cloth are made in certain ply thicknesses. It is not possible to fabricate a structure with layer thicknesses that are not integral numbers of plies of this tape or cloth. However, PANDA2 treats all decision variables as continuous. If the user indicates that a certain material is composite tape, then PANDA2 sets the thickness of any layer of this material that is less than a quarter of the thickness of a single ply of the tape equal to zero. Hence, if the user indicates that material type 1 is composite tape with ply thickness of 0.005 in., then any layer consisting of this material becoming less than 0.00125 in. in thickness during optimization iterations is dropped from further consideration unless the user reinserts it via the CHANGE processor. PANDA2 does not eliminate any layers not designated by the user as being made of composite tape.

After several sets of design iterations are performed, a panel will doubtless consist of many layers that are not integral numbers of plies of tape or cloth. It is up to the user to decide which layers to eliminate, which

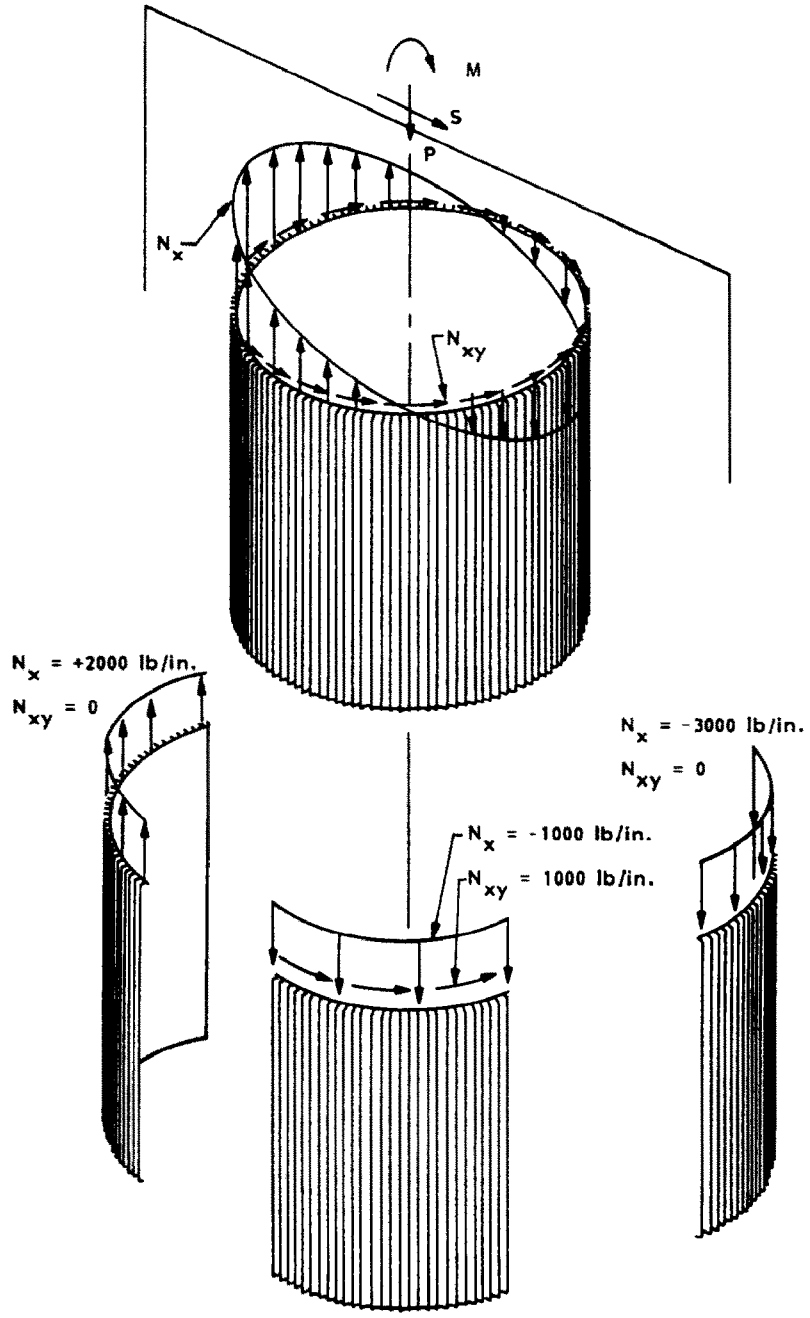

Fig. 79. Applied moment M, axial compression P and shear S; assumed resulting distribution of line loads N_x and N_{xy} in the shell; and replacement of the actual complete cylindrical shell with circumferentially varying line loads by a single cylindrical panel spanning 40 in. of circumference with three separate load sets, each of which acts alone and each of which has uniform line loads N_x and N_{xy}.

to increase in thickness, and which to decrease in thickness in order to make them integral numbers of plies of tape or cloth. These changes can be made via the CHANGE processor. Lower and upper bounds should then be reset at values equal to integral numbers of plies, and certain of the thickness variables should doubtless be eliminated as decision variables. Then more design iterations should be made. The user should continue this cycle until all thicknesses in the panel and stiffeners are integral numbers of plies of tape or cloth. The examples given here demonstrate this strategy.

Note that the design concept drawn in Fig. 80 allows for three extra layers $[0_{m_2}/90/0_{m_2}]$ in the base under the stringer. The role of the extra 0° layers is described in Sec. 19.7. The 0° layers are divided into two groups separated by a 90° layer in both the stringer base and in the stringer flange because tests have shown that

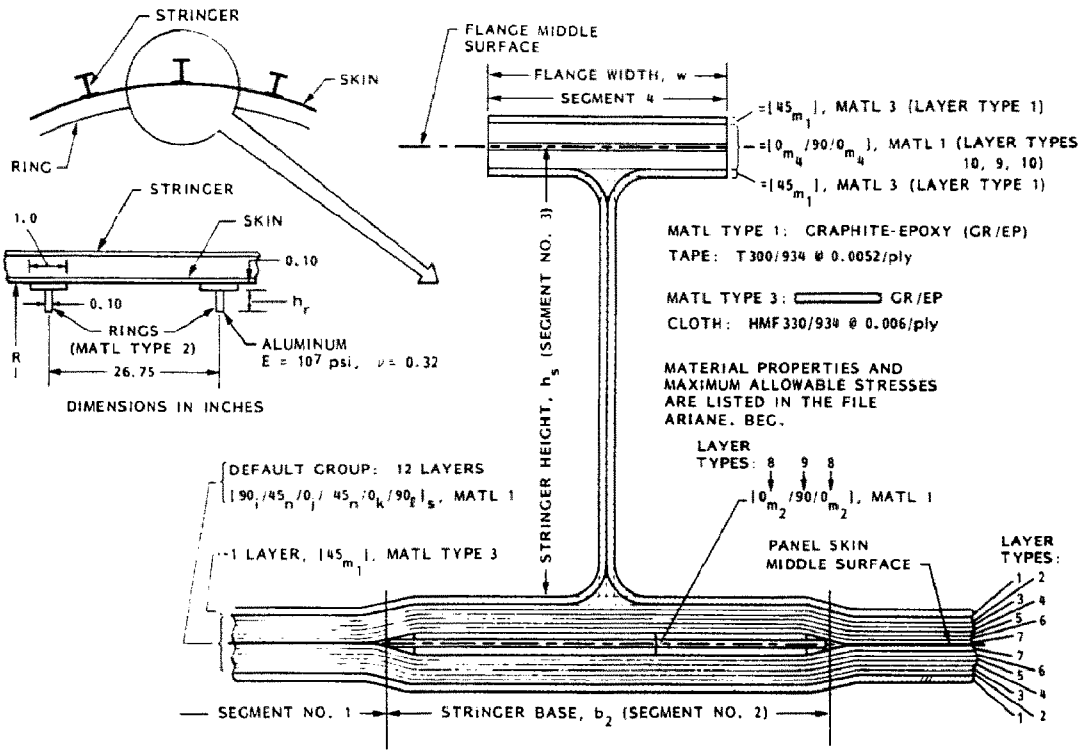

Fig. 80. Design concept to be optimized: external T-shaped stringers made of graphite-epoxy cloth and tape with thickened areas under the stringer web, and internal aluminum rings with spacing fixed at 26.75 in. The spacing of the stringers is to be determined, as well as the cross section dimensions and thicknesses of the various composite laminae.

large numbers of uniaxially oriented layers have less ultimate strength than do small numbers of such layers. Hence, it is wise to break up these 'blocks' of material by inserting 90° layers of a single thickness of tape.

Note that although the aluminum rings indicated in Fig. 80 have T-shaped cross sections, they are considered to be rectangular by PANDA2. This is because the faying flanges of the rings (flanges next to the panel skin) are considered by PANDA2 to be part of the skin, not part of the stiffener. These flanges are one of the layers in segment 2 of the ring module. The outstanding leg of the ring is segment 3 of the ring module.

21.1.4 *Steps* 5–8: *Starting design, optimization parameters, optimization strategy, final evaluation.* Table 4 lists the remaining steps (steps 5–8) in the design procedure. Once the starting design is selected and decision, linked and escape variables are chosen, a certain design strategy or sequence of design strategies are pursued. The final optimum design is partially checked via the PANEL processor, which sets up a BOSOR4 model of the entire panel width with all stringers treated as shell branches. The BOSOR4 model considers only buckling between rings in modes with one half axial wave between rings. In an actual design process, the user should of course fully check the optimum design obtained with PANDA2 by performing detailed multi-dimensional finite element analyses and tests.

21.2 *Starting design with all-composite, T-shaped stringers (step* 5)

Table 5 lists the input data for the BEGIN processor. Note that as input for segment 2 of the ring module (Table 5 following the entries 'R' and 26.75) there are several new layer types, 11, 12, 13, 14 and 15. Layer index 15 really does represent a new layer type, the faying flange of the aluminum ring, but layer types 11, 12, 13 and 14 are simply layer types 2, 4, 6 and 7 for the stringer module as seen from the perspective of a ring cross section. They must be introduced as new layer types because the 90° layup angle for layer type 2 of the stringer module becomes a 0° layup angle from the perspective of a ring module; the 0° layup angle for layer type 4 of the stringer module becomes a 90° layup angle for the ring module, and so on. Later, in DECIDE, the thicknesses of these new layer types must be linked to the thicknesses of layer types 2, 4, 6 and 7, respectively.

Note also, that layer type 1 of the stringer module remains layer type 1 in the ring module. Although the +45° layup angle in the stringer module becomes a −45° layup angle from the perspective of the ring module,

Table 5. Input data for starting design of ARIANE4 2/3-Interstage

This file is called ARIANE.BEG

```
   N          $ Do you want a tutorial session and tutorial output?
  107         $ Panel length normal to the plane of the screen, L1
   40         $ Panel length in the plane of the screen, L2
   T          $ Identify type of stiffener along L1    (N, T, J, R, A)
    5         $ stiffener spacing, b
    1         $ width of stiffener base, b2 (must be > 0, see Help)
    1         $ height of stiffener (type H to see sketch), h
    1         $ width of outer flange of stiffener, w
   N          $ Are the stringers cocured with the skin?
  100         $ What force/(axial length) will cause web peel-off?
   N          $ Is the next group of layers to be a "default group"?
    1         $ number of layers in the next group in Segment no.( 1)
   N          $ Can winding (layup) angles ever be decision variables?
    1         $ layer index (1,2,...), for layer no.( 1)
   Y          $ Is this a new layer type?
0.1200000E-01 $ thickness for layer index no.( 1)
   45         $ winding angle (deg.) for layer index no.( 1)
    3         $ material index (1,2,...) for layer index no.( 1)
   Y          $ Any more layers or groups of layers in Segment no.( 1)
   Y          $ Is the next group of layers to be a "default group"?
   N          $ Is this default group identical to a previous group?
0.5200000E-02 $ thickness of each layer of the default group
    1         $ material type in the default group
   Y          $ Any more layers or groups of layers in Segment no.( 1)
   N          $ Is the next group of layers to be a "default group"?
    1         $ number of layers in the next group in Segment no.( 1)
   N          $ Can winding (layup) angles ever be decision variables?
    1         $ layer index (1,2,...), for layer no.(14)
   N          $ Is this a new layer type?
   N          $ Any more layers or groups of layers in Segment no.( 1)
   N          $ Is the next group of layers to be a "default group"?
    7         $ number of layers in the next group in Segment no.( 2)
   N          $ Can winding (layup) angles ever be decision variables?
    1         $ layer index (1,2,...), for layer no.( 1)
   N          $ Is this a new layer type?
    2         $ layer index (1,2,...), for layer no.( 2)
   N          $ Is this a new layer type?
    3         $ layer index (1,2,...), for layer no.( 3)
   N          $ Is this a new layer type?
    4         $ layer index (1,2,...), for layer no.( 4)
   N          $ Is this a new layer type?
    5         $ layer index (1,2,...), for layer no.( 5)
   N          $ Is this a new layer type?
    6         $ layer index (1,2,...), for layer no.( 6)
   N          $ Is this a new layer type?
    7         $ layer index (1,2,...), for layer no.( 7)
   N          $ Is this a new layer type?
   Y          $ Any more layers or groups of layers in Segment no.( 2)
   N          $ Is the next group of layers to be a "default group"?
    3         $ number of layers in the next group in Segment no.( 2)
   N          $ Can winding (layup) angles ever be decision variables?
    8         $ layer index (1,2,...), for layer no.( 8)
   Y          $ Is this a new layer type?
0.1040000E-01 $ thickness for layer index no.( 8)
    0         $ winding angle (deg.) for layer index no.( 8)
    1         $ material index (1,2,...) for layer index no.( 8)
    9         $ layer index (1,2,...), for layer no.( 9)
   Y          $ Is this a new layer type?
0.5200000E-02 $ thickness for layer index no.( 9)
   90         $ winding angle (deg.) for layer index no.( 9)
    1         $ material index (1,2,...) for layer index no.( 9)
    8         $ layer index (1,2,...), for layer no.(10)
   N          $ Is this a new layer type?
   Y          $ Any more layers or groups of layers in Segment no.( 2)
   N          $ Is the next group of layers to be a "default group"?
    7         $ number of layers in the next group in Segment no.( 2)
   N          $ Can winding (layup) angles ever be decision variables?
```

Table 5—*cont.*

```
      7       $ layer index (1,2,...), for layer no.(11)
    N         $ Is this a new layer type?
      6       $ layer index (1,2,...), for layer no.(12)
    N         $ Is this a new layer type?
      5       $ layer index (1,2,...), for layer no.(13)
    N         $ Is this a new layer type?
      4       $ layer index (1,2,...), for layer no.(14)
    N         $ Is this a new layer type?
      3       $ layer index (1,2,...), for layer no.(15)
    N         $ Is this a new layer type?
      2       $ layer index (1,2,...), for layer no.(16)
    N         $ Is this a new layer type?
      1       $ layer index (1,2,...), for layer no.(17)
    N         $ Is this a new layer type?
    N         $ Any more layers or groups of layers in Segment no.( 2)
    N         $ Is the next group of layers to be a "default group"?
      2       $ number of layers in the next group in Segment no.( 3)
    N         $ Can winding (layup) angles ever be decision variables?
      1       $ layer index (1,2,...), for layer no.( 1)
    N         $ Is this a new layer type?
      1       $ layer index (1,2,...), for layer no.( 2)
    N         $ Is this a new layer type?
    N         $ Any more layers or groups of layers in Segment no.( 3)
    N         $ Is the next group of layers to be a "default group"?
      1       $ number of layers in the next group in Segment no.( 4)
    N         $ Can winding (layup) angles ever be decision variables?
      1       $ layer index (1,2,...), for layer no.( 1)
    N         $ Is this a new layer type?
    Y         $ Any more layers or groups of layers in Segment no.( 4)
    N         $ Is the next group of layers to be a "default group"?
      3       $ number of layers in the next group in Segment no.( 4)
    N         $ Can winding (layup) angles ever be decision variables?
     10       $ layer index (1,2,...), for layer no.( 2)
    Y         $ Is this a new layer type?
0.1040000E-01 $ thickness for layer index no.(10)
      0       $ winding angle (deg.) for layer index no.(10)
      1       $ material index (1,2,...) for layer index no.(10)
      9       $ layer index (1,2,...), for layer no.( 3)
    N         $ Is this a new layer type?
     10       $ layer index (1,2,...), for layer no.( 4)
    N         $ Is this a new layer type?
    Y         $ Any more layers or groups of layers in Segment no.( 4)
    N         $ Is the next group of layers to be a "default group"?
      1       $ number of layers in the next group in Segment no.( 4)
    N         $ Can winding (layup) angles ever be decision variables?
      1       $ layer index (1,2,...), for layer no.( 5)
    N         $ Is this a new layer type?
    N         $ Any more layers or groups of layers in Segment no.( 4)
      0       $ choose external (0) or internal (1) stringers
    R         $ Identify type of stiffener along L2  (N, T, J, R, A)
 26.75000     $ stiffener spacing, b
      1       $ width of stiffener base, b2 (must be > 0, see Help)
      1       $ height of stiffener (type H to see sketch), h
    N         $ Are the rings cocured with the skin?
    N         $ Is the next group of layers to be a "default group"?
      7       $ number of layers in the next group in Segment no.( 2)
    N         $ Can winding (layup) angles ever be decision variables?
      1       $ layer index (1,2,...), for layer no.( 1)
    N         $ Is this a new layer type?
     11       $ layer index (1,2,...), for layer no.( 2)
    Y         $ Is this a new layer type?
0.5200000E-02 $ thickness for layer index no.(11)
      0       $ winding angle (deg.) for layer index no.(11)
      1       $ material index (1,2,...) for layer index no.(11)
      5       $ layer index (1,2,...), for layer no.( 3)
    N         $ Is this a new layer type?
     12       $ layer index (1,2,...), for layer no.( 4)
    Y         $ Is this a new layer type?
```

Table 5—*cont.*

```
0.5200000E-02 $ thickness for layer index no.(12)
      90      $ winding angle (deg.) for layer index no.(12)
       1      $ material index (1,2,...) for layer index no.(12)
       3      $ layer index (1,2,...), for layer no.( 5)
   N          $ Is this a new layer type?
      13      $ layer index (1,2,...), for layer no.( 6)
   Y          $ Is this a new layer type?
0.5200000E-02 $ thickness for layer index no.(13)
      90      $ winding angle (deg.) for layer index no.(13)
       1      $ material index (1,2,...) for layer index no.(13)
      14      $ layer index (1,2,...), for layer no.( 7)
   Y          $ Is this a new layer type?
0.5200000E-02 $ thickness for layer index no.(14)
       0      $ winding angle (deg.) for layer index no.(14)
       1      $ material index (1,2,...) for layer index no.(14)
   Y          $ Any more layers or groups of layers in Segment no.( 2)
   N          $ Is the next group of layers to be a "default group"?
       7      $ number of layers in the next group in Segment no.( 2)
   N          $ Can winding (layup) angles ever be decision variables?
      14      $ layer index (1,2,...), for layer no.( 8)
   N          $ Is this a new layer type?
      13      $ layer index (1,2,...), for layer no.( 9)
   N          $ Is this a new layer type?
       3      $ layer index (1,2,...), for layer no.(10)
   N          $ Is this a new layer type?
      12      $ layer index (1,2,...), for layer no.(11)
   N          $ Is this a new layer type?
       5      $ layer index (1,2,...), for layer no.(12)
   N          $ Is this a new layer type?
      11      $ layer index (1,2,...), for layer no.(13)
   N          $ Is this a new layer type?
       1      $ layer index (1,2,...), for layer no.(14)
   N          $ Is this a new layer type?
   Y          $ Any more layers or groups of layers in Segment no.( 2)
   N          $ Is the next group of layers to be a "default group"?
       1      $ number of layers in the next group in Segment no.( 2)
   N          $ Can winding (layup) angles ever be decision variables?
      15      $ layer index (1,2,...), for layer no.(15)
   Y          $ Is this a new layer type?
 0.1000000    $ thickness for layer index no.(15)
       0      $ winding angle (deg.) for layer index no.(15)
       2      $ material index (1,2,...) for layer index no.(15)
   N          $ Any more layers or groups of layers in Segment no.( 2)
   N          $ Is the next group of layers to be a "default group"?
       1      $ number of layers in the next group in Segment no.( 3)
   N          $ Can winding (layup) angles ever be decision variables?
      15      $ layer index (1,2,...), for layer no.( 1)
   N          $ Is this a new layer type?
   N          $ Any more layers or groups of layers in Segment no.( 3)
       1      $ choose external (0) or internal (1) rings
   Y          $ Is the panel curved in the plane of the screen (Y for cyls.)?
      51      $ Radius of curvature (cyl. rad.) in the plane of screen, R
   N          $ Is panel curved normal to plane of screen? (answer N)
   N          $ Is this material isotropic (Y or N)?
 0.2000000E+08 $ modulus in the fiber direction, E1( 1)
  1400000.     $ modulus transverse to fibers,   E2( 1)
  700000.0     $ in-plane shear modulus,          G( 1)
 0.2030000E-01 $ small Poisson s ratio,          NU( 1)
  700000.0     $ out-of-plane shear modulus,    G13( 1)
  400000.0     $ out-of-plane shear modulus,    G23( 1)
 0.5000000E-07 $ thermal expansion along fibers, A1( 1)
 0.1600000E-04 $ transverse thermal expansion,   A2( 1)
  270.0000     $ residual stress temperature (positive),TEMPTUR( 1)
   N           $ Want to specify  maximum effective stress (N)?
  190000.0     $ maximum tensile stress along fibers, matl( 1)
   182800      $ max compressive stress along fibers, matl( 1)
    9800       $ max tensile stress normal to fibers, matl( 1)
   25060       $ max compress stress normal to fibers,matl( 1)
```

Table 5—*cont.*

```
   10000       $ maximum  shear  stress  in  material type( 1)
0.5600000E-01  $ weight density (greater than 0!) of material type( 1)
    Y          $ Is this unidirectional composite material (tape) ?
0.5200000E-02  $ Thickness of a single lamina of matl type( 1)
    Y          $ Does max. allowable stress decrease for more layers?
       0       $ Degradation (%) in max. sig1(tension) for n layers, n=( 2)
       0       $ Degradation (%) in max. sig1(comp.)   for n layers, n=( 2)
      20       $ Degradation (%) in max. sig2(tension) for n layers, n=( 2)
       0       $ Degradation (%) in max. sig2(comp.)   for n layers, n=( 2)
       0       $ Degradation (%) in max. sig12         for n layers, n=( 2)
    Y          $ Any further degradation with more layers of matl type( 1)
       0       $ Degradation (%) in max. sig1(tension) for n layers, n=( 3)
       0       $ Degradation (%) in max. sig1(comp.)   for n layers, n=( 3)
      30       $ Degradation (%) in max. sig2(tension) for n layers, n=( 3)
       0       $ Degradation (%) in max. sig2(comp.)   for n layers, n=( 3)
       0       $ Degradation (%) in max. sig12         for n layers, n=( 3)
    Y          $ Any further degradation with more layers of matl type( 1)
       0       $ Degradation (%) in max. sig1(tension) for n layers, n=( 4)
       0       $ Degradation (%) in max. sig1(comp.)   for n layers, n=( 4)
      37       $ Degradation (%) in max. sig2(tension) for n layers, n=( 4)
       0       $ Degradation (%) in max. sig2(comp.)   for n layers, n=( 4)
       0       $ Degradation (%) in max. sig12         for n layers, n=( 4)
    N          $ Any further degradation with more layers of matl type( 1)
    Y          $ Is this material isotropic (Y or N)?
0.1000000E+08  $ Young's modulus,                  E( 2)
0.3200000      $ small Poisson's ratio,           NU( 2)
 3846000       $ transverse shear modulus,       G13( 2)
       0       $ Thermal expansion coeff.,     ALPHA( 2)
       0       $ residual stress temperature (positive),TEMPTUR( 2)
    N          $ Want to supply a stress-strain "curve" for this mat'l? (N)
    Y          $ Want to specify  maximum effective stress (N)?
 50000.00      $ Maximum allowable effective stress in material type( 2)
0.1000000      $ weight density (greater than 0!) of material type( 2)
    N          $ Is this unidirectional composite material (tape) ?
    N          $ Is this material isotropic (Y or N)?
0.1050000E+08  $ modulus in the fiber direction, E1( 3)
0.1050000E+08  $ modulus transverse to fibers.   E2( 3)
 700000.0      $ in-plane shear modulus.         G( 3)
0.7700000E-01  $ small Poisson's ratio.          NU( 3)
 700000.0      $ out-of-plane shear modulus,    G13( 3)
 400000.0      $ out-of-plane shear modulus,    G23( 3)
0.1500000E-05  $ thermal expansion along fibers, A1( 3)
0.1500000E-05  $ transverse thermal expansion,   A2( 3)
 270.0000      $ residual stress temperature (positive),TEMPTUR( 3)
    N          $ Want to specify  maximum effective stress (N)?
  91035        $ maximum tensile stress along fibers, matl( 3)
 103845        $ max compressive stress along fibers, matl( 3)
  89880        $ max tensile stress normal to fibers, matl( 3)
 105000        $ max compress stress normal to fibers,matl( 3)
   7000        $ maximum  shear  stress  in  material type( 3)
0.5600000E-01  $ weight density (greater than 0!) of material type( 3)
    N          $ Is this unidirectional composite material (tape) ?
       0       $ Choose 0=simple support or 1=clamping
```

since the properties of this cloth layer are the same in both the + and $-45°$ directions, it is not necessary to introduce a new layer type. Note that the third layer in the stringer module ($+45°$ tape) becomes $-45°$ tape from the perspective of the ring module. Hence, one must either introduce a new layer type in the ring module or see if some other layer type in the stringer module will suffice. Since the thickness of the $-45°$ layer (layer no. 5) in the stringer module will be constrained later to be equal to that of the $+45°$ layer in the stringer module, this layer type can be used for the third layer of the ring module. Similarly, the fifth layer in the ring module can be designated layer type 3.

21.3 *Selection of decision, linked, escape variables (step 6)*

Tables 6 and 7 list the input to the DECIDE processor and part of the output from DECIDE. We see from these tables the linking of the thicknesses of certain of the layers in the ring module to those in the stringer

Table 6. Input data for selection of decision, linked and escape variables for minimum weight design of ARIANE4 2/3-Interstage

This file is called ARIANE.DEC

```
     N          $ Do you want a tutorial session and tutorial output?
     Y          $ Want to use default for thickness decision variables?
     1          $ Lowest layer index for default decision variable
     8          $ Highest layer index for default decision variable
     Y          $ Any more ranges of layer types for default dec. var.?
    10          $ Lowest layer index for default decision variable
    10          $ Highest layer index for default decision variable
     N          $ Any more ranges of layer types for default dec. var.?
     Y          $ Any more decision variables (Y or N) ?
     1          $ Choose a decision variable (1,2,3,...)
 2.500000       $ Lower bound of variable no.( 1)
    10          $ Upper bound of variable no.( 1)
     Y          $ Any more decision variables (Y or N) ?
     2          $ Choose a decision variable (1,2,3,...)
0.5000000       $ Lower bound of variable no.( 2)
     3          $ Upper bound of variable no.( 2)
     Y          $ Any more decision variables (Y or N) ?
     3          $ Choose a decision variable (1,2,3,...)
0.2000000       $ Lower bound of variable no.( 3)
     2          $ Upper bound of variable no.( 3)
     Y          $ Any more decision variables (Y or N) ?
     4          $ Choose a decision variable (1,2,3,...)
0.1000000       $ Lower bound of variable no.( 4)
     2          $ Upper bound of variable no.( 4)
     Y          $ Any more decision variables (Y or N) ?
    17          $ Choose a decision variable (1,2,3,...)
     1          $ Lower bound of variable no.(17)
     2          $ Upper bound of variable no.(17)
     N          $ Any more decision variables (Y or N) ?
     Y          $ Any linked variables (Y or N) ?
    18          $ Choose a linked variable (1,2,3,...)
     6          $ To which variable is this variable linked?
     1          $ Assign a value to the linking constant, C(18)
     Y          $ Any more linked variables (Y or N) ?
    19          $ Choose a linked variable (1,2,3,...)
     8          $ To which variable is this variable linked?
     1          $ Assign a value to the linking constant, C(19)
     Y          $ Any more linked variables (Y or N) ?
    20          $ Choose a linked variable (1,2,3,...)
    10          $ To which variable is this variable linked?
     1          $ Assign a value to the linking constant, C(20)
     Y          $ Any more linked variables (Y or N) ?
    21          $ Choose a linked variable (1,2,3,...)
    11          $ To which variable is this variable linked?
     1          $ Assign a value to the linking constant, C(21)
     N          $ Any more linked variables (Y or N) ?
     Y          $ Any escape variables (Y or N) ?
     Y          $ Want to have escape variables chosen by default?
```

module. The thicknesses of layer types 1–8 and layer type 10 were chosen as decision variables by use of a default option in DECIDE, as seen from the second input entry in Table 6. The thickness of layer type 9 is not a decision variable because this 90° layer is simply intended to prevent the buildup of thick blocks of 0° layers in the stringer base and flange.

21.4 *Optimization strategy (step 7)*

Figures 81 and 82 show the overall architecture of the PANDA2 mainprocessor, which is invoked via the command PANDAOPT. With the rather large number of decision variables indicated in Table 7, particularly if there are multiple sets of combined loads and if highly nonlinear, post-local buckling behavior is allowed to occur, the design of a complex panel with use of discretized models may require quite a bit of computer time. It is best therefore to begin by using the IQUICK = 1 option. The meaning of IQUICK was introduced in Sec. 6.2. With this option only the closed-form PANDA [1] type of analysis is used and local post-buckling behavior is not investigated. Following MAINSETUP, sample input for which is listed in Table 8, the user

Table 7. Part of output from the processor 'DECIDE'. Decision, linked and escape variables for minimum weight design of ARIANE4 2/3-Interstage

This list is part of the file called ARIANE.OPD

SUMMARY OF INFORMATION FOR OPTIMIZATION ANALYSIS

VAR. NO.	DEC. VAR.	ESCAPE VAR.	LINK. VAR.	LINKED TO	LINKING CONSTANT	LOWER BOUND	CURRENT VALUE	UPPER BOUND	DEFINITION
1	T	N	N	0	0.00E+00	2.50E+00	5.0000E+00	1.00E+01	stiffener spacing, b
2	T	N	N	0	0.00E+00	5.00E-01	1.0000E+00	2.00E+00	width of stiffener base, b2
3	T	N	N	0	0.00E+00	2.00E-01	1.0000E+00	2.00E+00	height of stiffener, h
4	T	N	N	0	0.00E+00	1.00E-01	1.0000E+00	2.00E+00	width of outer flange of stiffener, t
5	T	T	N	0	0.00E+00	1.20E-04	1.2000E-02	1.20E+00	thickness for layer index no.(1)
6	T	T	N	0	0.00E+00	5.20E-05	5.2000E-03	5.20E-01	thickness for layer index no.(2)
7	T	T	N	0	0.00E+00	5.20E-05	5.2000E-03	5.20E-01	thickness for layer index no.(3)
8	T	T	N	0	0.00E+00	5.20E-05	5.2000E-03	5.20E-01	thickness for layer index no.(4)
9	N	N	T	7	1.00E+00	0.00E+00	5.2000E-03	0.00E+00	thickness for layer index no.(5)
10	T	T	N	0	0.00E+00	5.20E-05	5.2000E-03	5.20E-01	thickness for layer index no.(6)
11	T	T	N	0	0.00E+00	5.20E-05	5.2000E-03	5.20E-01	thickness for layer index no.(7)
12	T	T	N	0	0.00E+00	1.04E-04	1.0400E-02	1.04E+00	thickness for layer index no.(8)
13	N	N	N	0	0.00E+00	0.00E+00	5.2000E-03	0.00E+00	thickness for layer index no.(9)
14	T	T	N	0	0.00E+00	1.04E-04	1.0400E-02	1.04E+00	thickness for layer index no.(10)
15	N	N	N	0	0.00E+00	0.00E+00	2.6750E+01	0.00E+00	stiffener spacing, b
16	N	N	N	0	0.00E+00	0.00E+00	1.0000E+00	0.00E+00	width of stiffener base, b2
17	T	N	N	0	0.00E+00	1.00E+00	1.0000E+00	2.00E+00	height of stiffener, h
18	N	N	T	6	1.00E+00	0.00E+00	5.2000E-03	0.00E+00	thickness for layer index no.(11)
19	N	N	T	8	1.00E+00	0.00E+00	5.2000E-03	0.00E+00	thickness for layer index no.(12)
20	N	N	T	10	1.00E+00	0.00E+00	5.2000E-03	0.00E+00	thickness for layer index no.(13)
21	N	N	T	11	1.00E+00	0.00E+00	5.2000E-03	0.00E+00	thickness for layer index no.(14)
22	N	N	N	0	0.00E+00	0.00E+00	1.0000E-01	0.00E+00	thickness for layer index no.(15)

should give the command PANDAOPT several times, each time allowing PANDA2 to perform from 5 to 10 design iterations with IQUICK = 1. In the current example there were three sets of five iterations each and a fourth with 10 iterations.

Why take several sets of five iterations each, instead of just one set with 15 or 20 iterations? There are two reasons. The first is that it is always a good idea for the user to monitor carefully the output as the design is evolving. Hence, after each set of five iterations the user should inspect the file NAME.OPM (in this case NAME = ARIANE) to ensure that the intermediate results seem correct and that each design looks reasonable. The second reason has to do with how the optimizer CONMIN works. Figure 83 illustrates the case of two decision variables. Given the user's lower and upper bounds of the decision variables, CONMIN establishes a more restrictive 'window' within which the decision variables are allowed to vary in any given iteration. The size of this window decreases with each design iteration. (In PANDA2 the dimensions of the window decrease by a factor 0.8 with each iteration.) These restrictions are placed upon the permitted

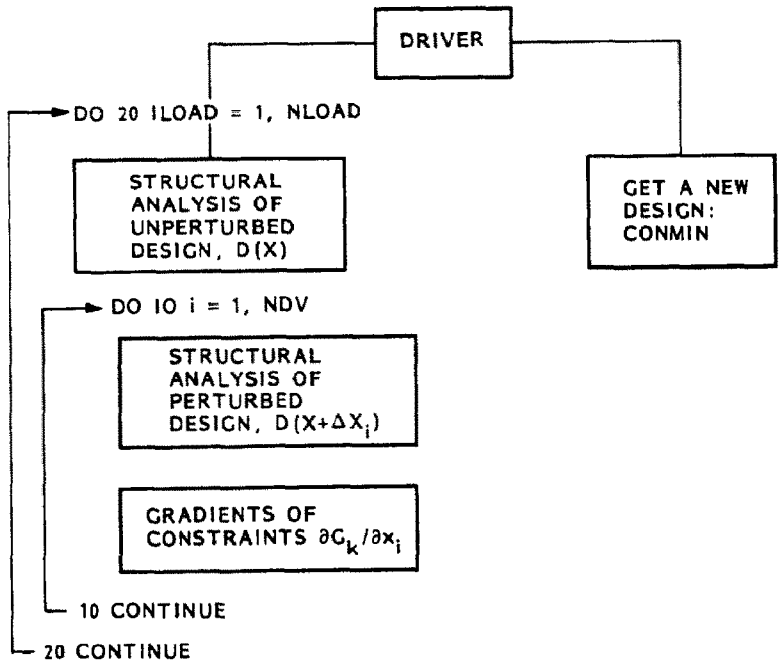

Fig. 81. Architecture of the PANDA2 mainprocessor.

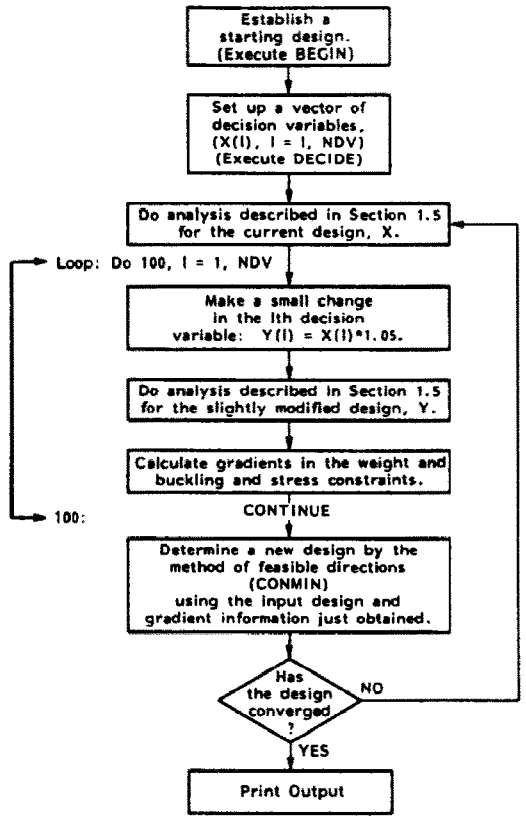

Fig. 82. Flow of calculations in the PANDA2 mainprocessor for an optimization analysis.

Table 8. Input data for PANDA2 processor 'MAINSETUP' for optimization of ARIANE4 2/3-Interstage

There are two load sets, and IQUICK=1
This file is called ARIANE.OPT

```
N          $ Do you want a tutorial session and tutorial output?
-3000      $ Resultant normal to the plane of screen, N1( 1)
   0       $ Resultant in the plane of the screen,    N2( 1)
   0       $ In-plane shear in load set A,            N12( 1)
N          $ Does the axial load vary in the L2 direction?
  2.0      $ Factor of safety for general instability, FSGEN( 1)
   1       $ Factor of safety for local instability, FSLOC( 1)
   0       $ Resultant normal to the plane of screen, N10( 1)
   0       $ Resultant in the plane of the screen,    N20( 1)
   0       $ Uniform applied pressure (positive upward), p( 1)
Y          $ Want to provide another load set (N1,N2,N12,N10,N20, p)?
-1000      $ Resultant normal to the plane of screen, N1( 2)
   0       $ Resultant in the plane of the screen,    N2( 2)
 1000      $ In-plane shear in load set A,            N12( 2)
N          $ Does the axial load vary in the L2 direction?
1.500000   $ Factor of safety for general instability, FSGEN( 2)
   1       $ Factor of safety for local instability, FSLOC( 2)
   0       $ Resultant normal to the plane of screen, N10( 2)
   0       $ Resultant in the plane of the screen,    N20( 2)
   0       $ Uniform applied pressure (positive upward), p( 2)
N          $ Want to provide another load set (N1,N2,N12,N10,N20, p)?
Y          $ Want to include effect of transverse shear deformation?
   1       $ IQUICK = quick analysis indicator (0 or 1)
   1       $ NPRINT= output index (1=good, 2=debug, 3=too much)
   1       $ Choose type of analysis (1=opt., 2=fixed design)
   5       $ How many design iterations in this run (3 to 10)?
   1       $ Index for objective (1=min. weight, 2=min. distortion)
```

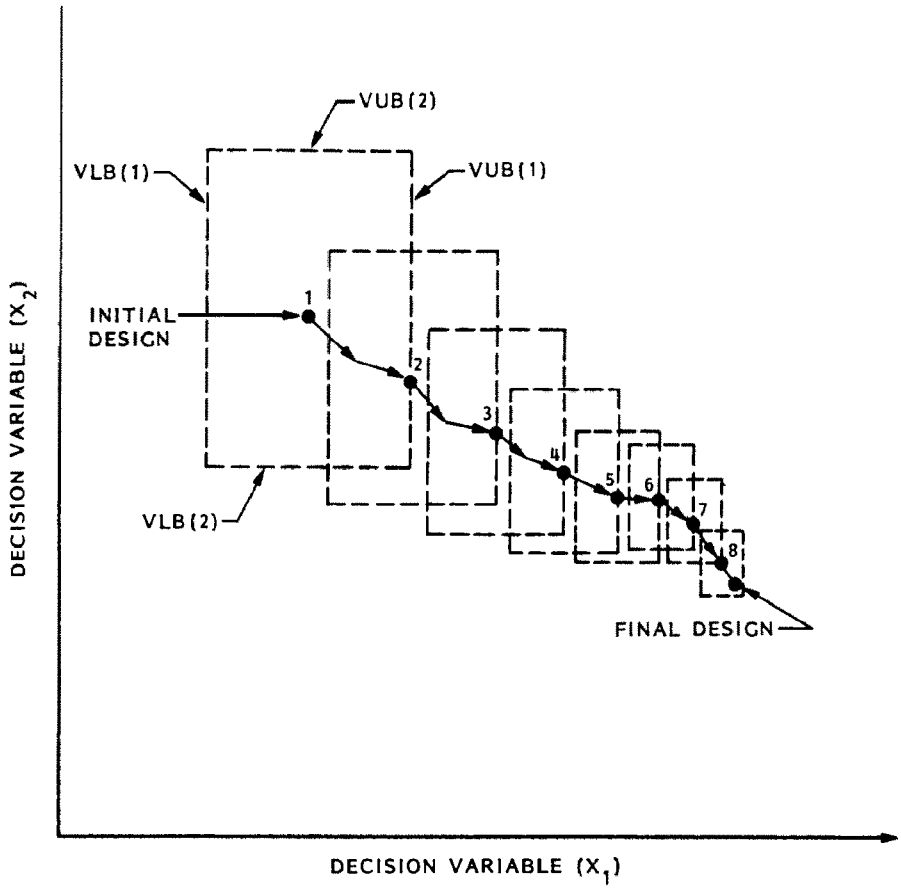

Fig. 83. Schematic of the evolution of a design with two decision variables, X_1 and X_2. With each iteration, the optimizer, CONMIN, establishes a 'window' of permitted excursion of the decision variables. In PANDA2 this 'window' shrinks by a factor of 0.8 for each design iteration. Upon re-execution of PANDAOPT the 'window' is re-expanded to its original size, which depends upon lower and upper bounds supplied by the user and certain strategies used by CONMIN.

excursions of the decision variables in order to prevent wild swings in the design as it evolves. The example shown in Fig. 83 shows eight iterations, and the last design point is labeled 'FINAL DESIGN'. Note, however, that the 'window' of permitted excursions is rather small. To the user it may appear that design iterations have converged, whereas actually they may not have. On the other hand, they really may have converged. This can easily be checked simply by executing PANDAOPT again. When this is done, the 'window' of permitted excursions is re-expanded to its original size, the new starting design is the last design obtained in the previous set of iterations, and new iterations proceed as before. The user should keep executing PANADOPT until the objective does not change very much. When the user is satisfied with the current design, he or she should then take one additional set of design iterations in which the number of iterations is larger than the number used previously, say twice or three times as many.

After the user is satisfied with the preliminary design obtained with the IQUICK = 1 option, he or she should pursue further design iterations with IQUICK = 0. Lower factors of safety can generally be used with the IQUICK = 0 option, especially for buckling between rings, because the wide column buckling model is used with this option. This model is more conservative than the smeared-stringer model used with the IQUICK = 1 option, since it neglects the curvature of the panel and it accounts for local deformations of the panel module cross section as it buckles in the wide-column mode. However, note that some factor greater than unity should generally be used because PANDA2 does not account for local initial imperfections and the important effect of these on overall buckling, particularly for cases in which local and general buckling occur at loads that are close. (See [34] for the recent addition of capability to handle initial imperfections.)

21.5 *Results with IQUICK* = 1 (*step* 7.1)

The leftmost portions of Figs 84–89 give results obtained with IQUICK = 1. The 25 iterations are performed in three sets of five each followed by one set of 10. A total of about 8 min of CPU time on the

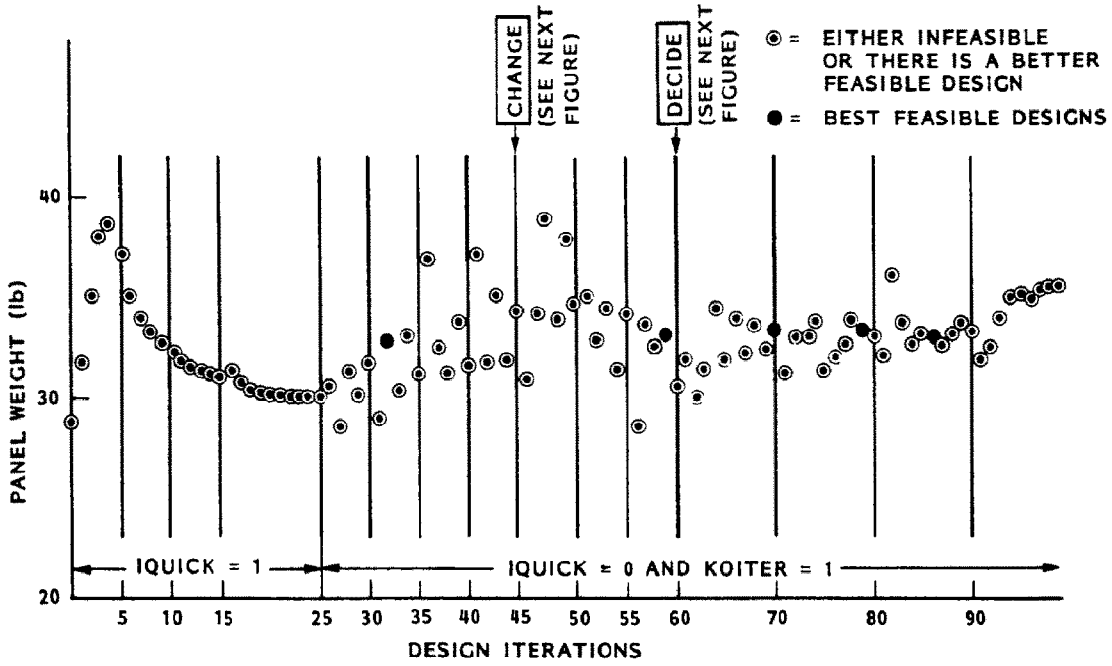

Fig. 84. Evolution of the panel weight during design iterations. There are 25 iterations with use of the closed-form PANDA-type [1] models (IQUICK = 1), followed by 75 iterations with use of the discretized BOSOR4-type panel module models plus the PANDA-type models (IQUICK = 0). In these latter iterations local post-buckling is permitted (KOITER = 1).

VAX 11/785 with the VMS 4.2 operating system are required for execution of the 25 iterations. For the first load set (pure axial compression of 3000 lb/in.) a factor of safety of 2.0 is used for general instability. For the second load set (axial compression of 1000 lb/in. combined with in-plane shear of 1000 lb/in.) a factor of safety of 1.5 is used. The behavior of the decision variables and design margins is reasonably smooth.

21.6 *Results with IQUICK = 0, post-local-buckling permitted (step 7.2)*

The remaining portions of Figs 84 through 89, Tables 9 through 11, and Figures 90 and 91 pertain to optimization with use of the discretized panel module models and with local buckling of the panel skin permitted. The factors of safety for general instability are now 1.5 for load set 1 and 1.2 for load set 2. The computer time required for 5 design iterations varied from 15 minutes to half an hour of VAX 11/785 time, depending on how much local post-buckling analysis was required. (The PANDA2 system decides this, not the user!)

Note that the decision variables and the design margins no longer vary smoothly with design iterations, as they did with the IQUICK = 1 option. It appears that an optimum design corresponds to early post-buckling, a domain in which the state of the panel is very sensitive to small changes in stringer spacing and thickness. From Fig. 88, which corresponds to load set 1, one can see that the behavioral constraints most often violated (violated behavioral constraint = negative design margin) are the stringer pop-off constraint and the wide column buckling constraint. Also violated is the 'long wavelength local buckling' constraint, the purpose of which is described in Sec. 12.1(b), where it is called 'low-axial-wavenumber' local buckling. From Fig. 89, which corresponds to load set 2, one can see that the constraints most often violated are stringer pop-off, wide column buckling, and maximum tensile stress in the cloth. (This maximum tensile stress occurs at the peaks of the buckles midway between stringers.)

In Fig. 84 five of the points are blackened. These five designs, all quite different, correspond to feasible designs, or designs that are almost feasible. (Check the margins in Figs 88 and 89!) Points at the corresponding iterations are also blackened in Figs 85 and 87. (This code is NOT used in Figs 86, 88 or 89, in which blackened points have different meanings.) Although these feasible designs are all quite different, they all correspond to weights that are close to 33 lb. There are other feasible designs encountered during the approximately 100 iterations, but these correspond to somewhat heavier panels.The designs corresponding to iterations 32 and 59 are not in their locally post-buckled states for either of the two load sets; that at iteration 70 is not in its locally post-buckled state for load set 1 but is for load set 2; and those at iterations 79 and 86 are in their locally post-buckled states for both load sets.

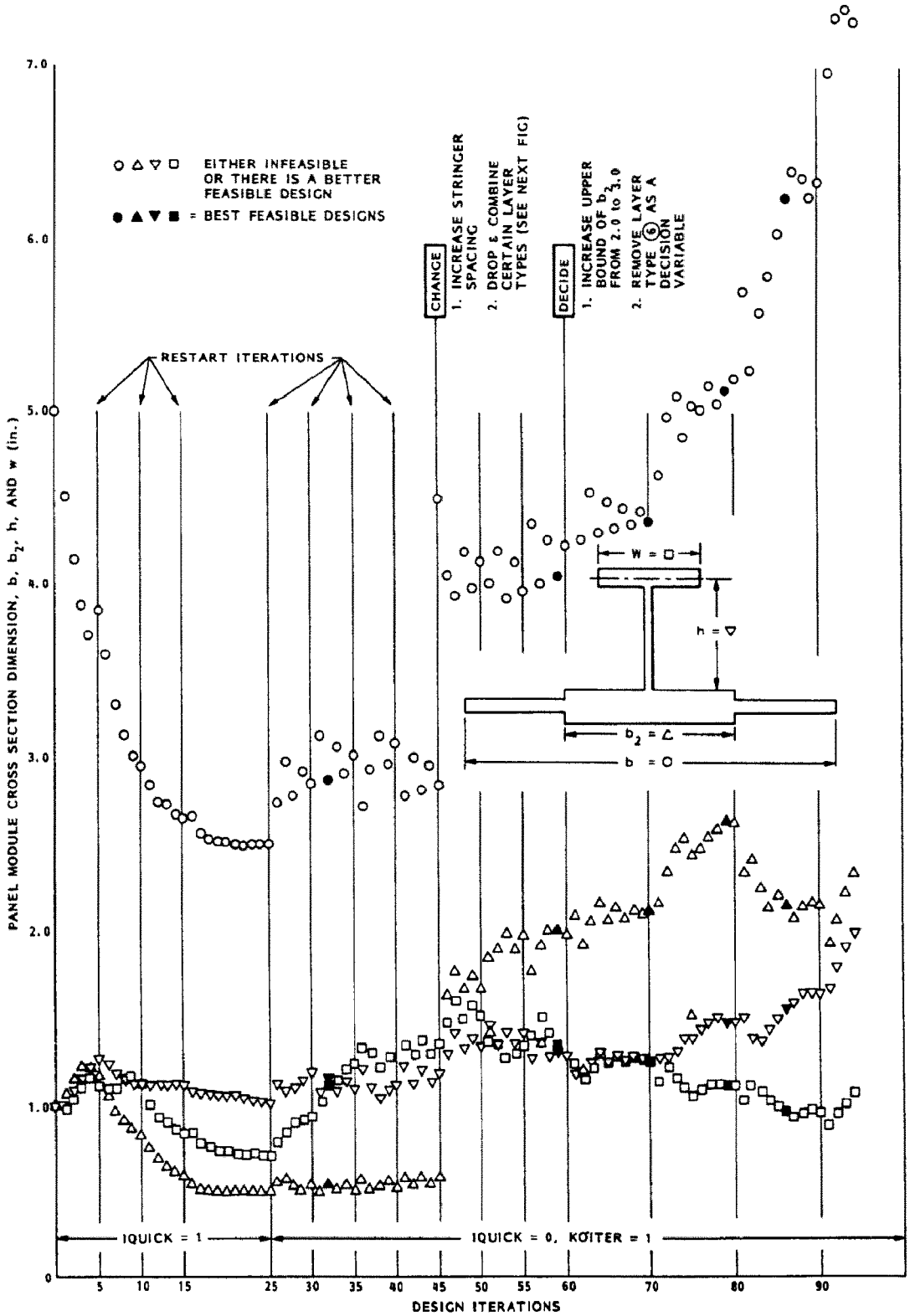

Fig. 85. Evolution of the cross section dimensions in the all-composite T-shaped stringers during design iterations. Local post-buckling is permitted (KOITER = 1). The rather unstable behavior in the IQUICK = 0 regime results from optimum designs being sought in the early post-buckling regime, in which the behavior of the panel (stress, internal load distribution) changes steeply with change in panel dimensions.

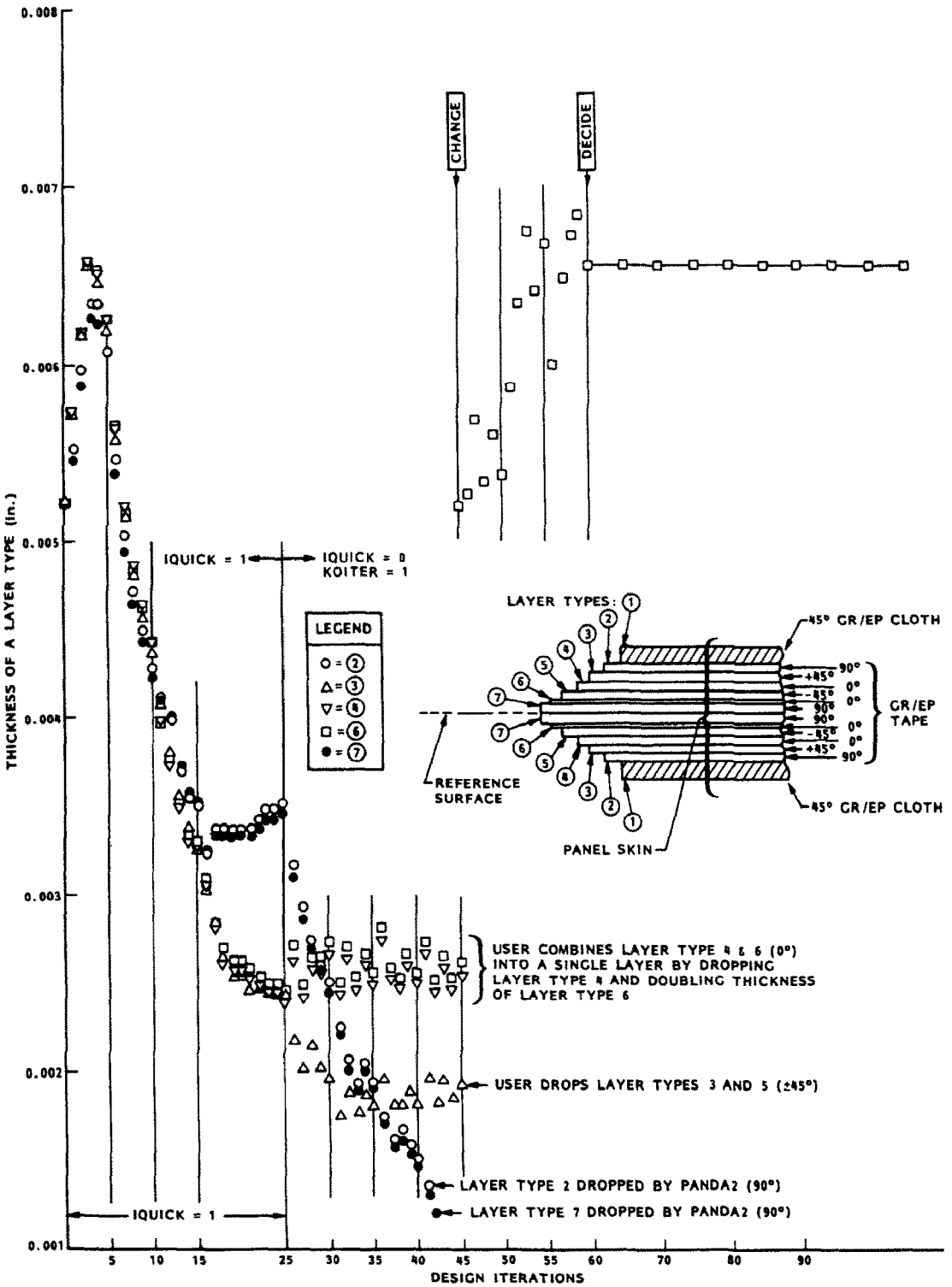

Fig. 86. Evolution of the thicknesses of the 12-layer default stacking sequence [90/45/0/ – 45/0/90]$_s$ during design iterations. Local post-buckling is permitted (KOITER = 1).

Figures 85, 86 and 87 illustrate the use of the PANDA2 processors, CHANGE and DECIDE in the midst of design iterations. These figures show that the design was 'bobbing around' during iterations 35–45. At iteration 45 it was decided to increase the stringer spacing and drop and combine certain layer types, as depicted in Fig. 85. At iteration 60 it was observed that a pre-established upper bound of 2.0 in. on the width of the stringer base was limiting design opportunities, and this upper bound was increased to 3.0 in. Also, it was judged beneficial to remove layer type 6 as a decision variable.

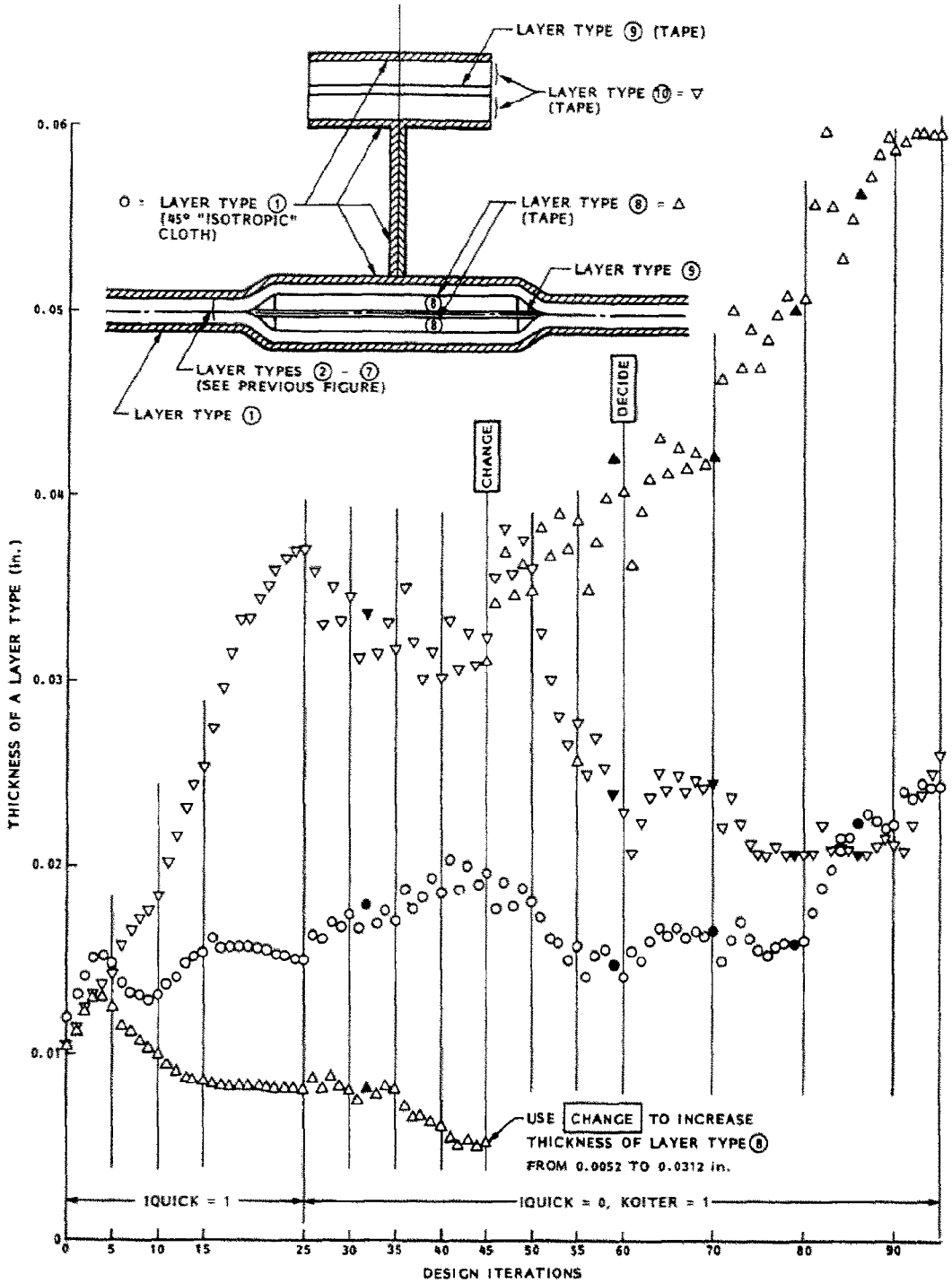

Fig. 87. Evolution of the thickness of the graphite-epoxy cloth and of the 0° layers in the stringer base and in the flange during design iterations. Local post-buckling is permitted (KOITER = 1). Blackened points represent feasible or almost feasible designs.

After 100 iterations a decision was made to use the design at iteration 70 as a starting design, to change the thicknesses so that all thicknesses represented integral numbers of plies of cloth or tape (the cloth is 0.006 in. per ply and the tape is 0.0052 in. per ply), to eliminate all thicknesses as decision variables, and to perform more design iterations. The results after 15 iterations performed in a single set are listed in Tables 9, 10 and 11. It turns out that the panel is not in its post-locally-buckled state for either of the two load sets. Figure 90 gives plots of the discretized optimum panel module and the local and wide column buckling modes and load factors λ_{LOCAL} and $\lambda_{WIDECOLUMN}$ corresponding to load set 1, pure axial compression of 3000 lb/in. Please note that the BOSOR4-type of analysis yields a local buckling load factor $\lambda_{LOCAL} = 0.9151$, indicating

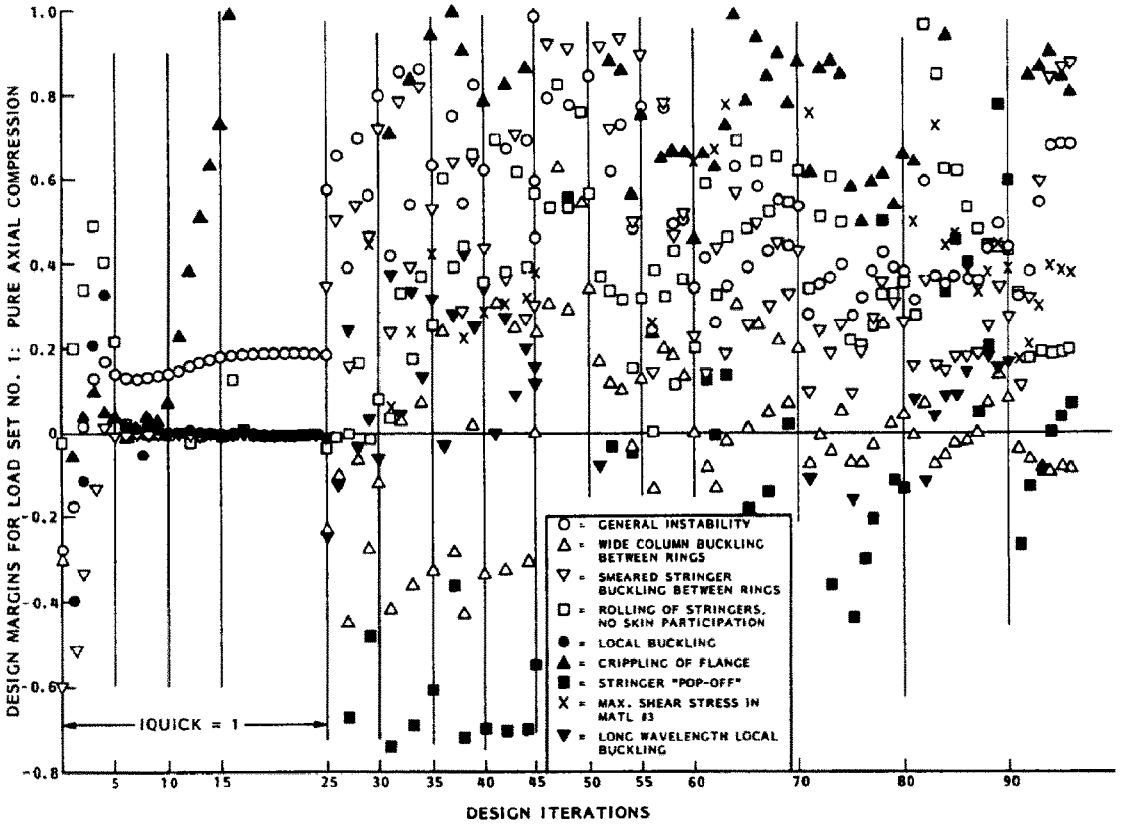

Fig. 88. Evolution of design margins corresponding to load set 1 ($N_x = -3000$ lb/in., $N_{xy} = 0$) during iterations. Local post-buckling is permitted. The most critical margins are widecolumn buckling and stringer pop-off.

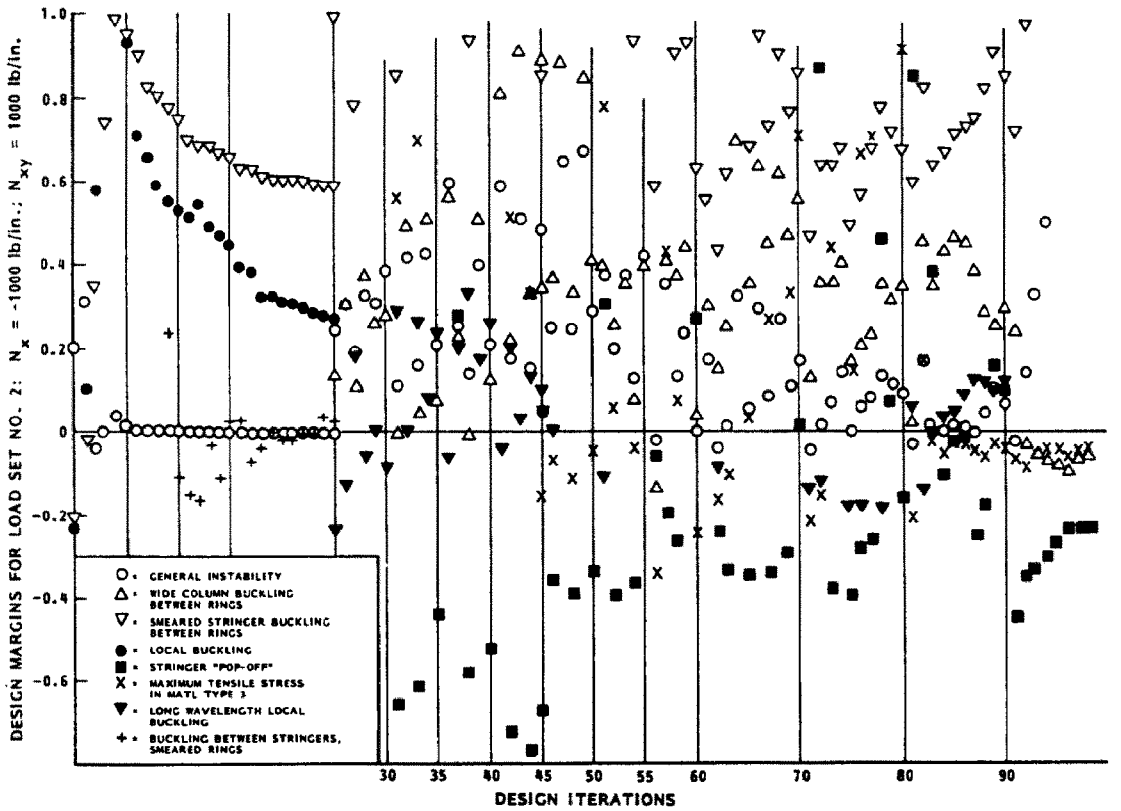

Fig. 89. Evolution of design margins corresponding to load set 2 ($N_x = -1000$ lb/in., $N_{xy} = 1000$ lb/in.) during iterations. Local post-buckling is permitted. The most critical margins are wide column buckling, stringer pop-off, and maximum tensile stress in the cloth in the peaks of the local buckles midway between stringers.

Table 9. Final design of ARIANE4, 2/3-Interstage with T-shaped stringers in which local post-buckling is permitted

```
                    SUMMARY OF INFORMATION FROM OPTIMIZATION ANALYSIS
VAR.  DEC.  ESCAPE  LINK.  LINKED   LINKING    LOWER      CURRENT     UPPER       DEFINITION
 NO.  VAR.   VAR.   VAR.     TO     CONSTANT   BOUND       VALUE      BOUND
  1    Y      N      N       0     0.00E+00  2.50E+00  4.5539E+00  5.00E+00  stiffener spacing, b
  2    Y      N      N       0     0.00E+00  3.00E-01  2.3235E+00  3.00E+00  width of stringer base, b2
  3    Y      N      N       0     0.00E+00  5.00E-01  1.1855E+00  2.00E+00  height of stringer, h
  4    Y      N      N       0     0.00E+00  2.00E-01  1.4022E+00  2.00E+00  width of outer flange of stiffener, w
  5    N      N      N       0     0.00E+00  0.00E+00  1.8000E-02  0.00E+00  thickness for layer index no.(1 )
  6    N      N      N       0     0.00E+00  0.00E+00  0.0000E+00  0.00E+00  thickness for layer index no.(2 )
  7    N      N      N       0     0.00E+00  0.00E+00  0.0000E+00  0.00E+00  thickness for layer index no.(3 )
  8    N      N      N       0     0.00E+00  0.00E+00  0.0000E+00  0.00E+00  thickness for layer index no.(4 )
  9    N      N      N       0     0.00E+00  0.00E+00  0.0000E+00  0.00E+00  thickness for layer index no.(5 )
 10    N      N      N       0     0.00E+00  0.00E+00  5.2000E-03  0.00E+00  thickness for layer index no.(6 )
 11    N      N      N       0     0.00E+00  0.00E+00  0.0000E+00  0.00E+00  thickness for layer index no.(7 )
 12    N      N      N       0     0.00E+00  0.00E+00  4.1600E-02  0.00E+00  thickness for layer index no.(8 )
 13    N      N      N       0     0.00E+00  0.00E+00  6.2000E-03  0.00E+00  thickness for layer index no.(9 )
 14    Y      Y      N       0     0.00E+00  2.08E-02  2.2954E-02  2.60E-02  thickness for layer index no.(10)
 15    N      N      N       0     0.00E+00  0.00E+00  2.6750E+01  0.00E+00  stiffener spacing, b
 16    N      N      N       0     0.00E+00  0.00E+00  1.0000E+00  0.00E+00  width of ring base, b2
 17    N      N      N       0     0.00E+00  0.00E+00  1.0000E+00  0.00E+00  height of ring, h
 18    N      N      N       0     0.00E+00  0.00E+00  0.0000E+00  0.00E+00  thickness for layer index no.(11)
 19    N      N      N       0     0.00E+00  0.00E+00  0.0000E+00  0.00E+00  thickness for layer index no.(12)
 20    N      N      N       0     0.00E+00  0.00E+00  5.2000E-03  0.00E+00  thickness for layer index no.(13)
 21    N      N      N       0     0.00E+00  0.00E+00  0.0000E+00  0.00E+00  thickness for layer index no.(14)
 22    N      N      N       0     0.00E+00  0.00E+00  1.0000E-01  0.00E+00  thickness for layer index no.(15)

   ****************************************************
 ********************* DESIGN OBJECTIVE ********************
   *************                              ************
          CURRENT VALUE OF THE OBJECTIVE FUNCTION:
  VAR. STR/ SEG. LAYER   CURRENT
  NO.  RNG  NO.   NO.     VALUE            DEFINITION
              0     0   3.381E+01   WEIGHT OF THE ENTIRE PANEL
    *************                              ************
 ********************* DESIGN OBJECTIVE ********************
   ****************************************************
```

Table 10. Margins corresponding to load set 1 applied to the final design of ARIANE4 2/3-Interstage with T-shaped stringers in which local post-buckling is permitted

```
            *********** LOAD SET NO. 1  **************
        APPLIED LOADS IN LOAD SET A ("eigenvalue" loads):
          Applied     axial       stress resultant, N1= -3.0000E+03
          Applied circumferential stress resultant, N2= -3.0000E+00
          Applied    in-plane     shear  resultant,N12=  1.5000E+01

        APPLIED LOADS IN LOAD SET B ( fixed uniform loads):
          Applied     axial       stress resultant,N10=  0.0000E+00
          Applied circumferential stress resultant,N20=  0.0000E+00
          Applied    in-plane    shear  resultant,N120=  0.0000E+00
          Applied pressure (positive for internal), P =  0.0000E+00

           CURRENT VALUES OF MARGINS CORRESPONDING TO CURRENT DESIGN
VAR.  STR/ SEG.  LAYER   CURRENT
NO.   RNG  NO.    NO.     VALUE          DEFINITION
            0      0   3.722E+00  compressive fiber: (allowable stress)/actual-1, matl type 1
            0      0   1.731E+02  in-plane shear stress margin: (allowable/actual)-1, matl 1
            0      0   9.131E+00  compressive fiber: (allowable stress)/actual-1, matl type 3
            0      0   8.679E+00  compres. transverse stress margin: (allow./actual)-1, matl 3
            0      0   2.450E+00  in-plane shear stress margin: (allowable/actual)-1, matl 3
      RNG   2      1   3.680E+02  compressive transverse stress margin: (allowable/actual) - 1
      RNG   2      1   1.896E+02  compressive fiber stress margin: (allowable/actual) - 1
      RNG   2      1   2.924E+00  in-plane shear margin: (allowable stress)/(actual stress) - 1
      RNG   2      6   4.687E+00  compressive fiber stress margin: (allowable/actual) - 1
      RNG   2      6   5.338E+02  in-plane shear margin: (allowable stress)/(actual stress) - 1
      RNG   2     15   2.097E+00  compressive transverse stress margin: (allowable/actual) - 1
      RNG   2     15   1.481E+01  tensile fiber margin: (allowable stress)/(actual stress) - 1
      RNG   2     15   2.843E+02  in-plane shear margin: (allowable stress)/(actual stress) - 1
      RNG   3      1   2.070E+01  tensile fiber margin: (allowable stress)/(actual stress) - 1
      STR   3      0   4.923E+00  crippling margin for stringer segment. 22  local halfwaves
      STR   4      0   9.753E-01  crippling margin for stringer segment. 22  local halfwaves
            0      0   1.869E-02  (Wide column panel buck. factor)/(factor of safety) - 1
            0      0   2.668E-01  buck.margin simp-support smear string;M=1  ; N=9  ; slope= 0.00
            0      0   4.484E-01  buck.margin simp-support general buck;M=2  ; N=2  ; slope= 0.00
            0      0   2.641E-01  buck.margin rolling with smear string;M=1  ; N=9  ; slope= 0.00
            0      0   1.020E+00  buck.margin rolling only of stringers;M=4  ; N=0  ; slope= 0.00
```

Table 11. Margins corresponding to load set 2 applied to the final design of ARIANE4 2/3-Interstage with T-shaped stringers in which local post-buckling is permitted

```
           ********** LOAD SET NO. 2 **************
       APPLIED LOADS IN LOAD SET A ("eigenvalue" loads):
         Applied     axial        stress resultant, N1= -1.0000E+03
         Applied circumferential  stress resultant, N2= -1.4142E+00
         Applied    in-plane      shear  resultant,N12=  1.0000E+03

       APPLIED LOADS IN LOAD SET B ( fixed uniform loads):
         Applied     axial        stress resultant,N10=  0.0000E+00
         Applied circumferential  stress resultant,N20=  0.0000E+00
         Applied    in-plane    shear  resultant,N120=  0.0000E+00
         Applied pressure (positive for internal), P =  0.0000E+00

         CURRENT VALUES OF MARGINS CORRESPONDING TO CURRENT DESIGN
VAR. STR/ SEG. LAYER   CURRENT
NO.  RNG  NO.   NO.     VALUE          DEFINITION
           0     0   6.533E+00  compressive fiber: (allowable stress)/actual-1, matl type 1
           0     0   1.611E+00  in-plane shear stress margin: (allowable/actual)-1, matl 1
           0     0   2.661E+00  tensile fiber: (allowable stress)/(actual stress)-1, matl 3
           0     0   2.527E+01  compressive fiber: (allowable stress)/actual-1, matl type 3
           0     0   2.687E+00  compres. transverse stress margin: (allow./actual)-1, matl 3
           0     0   1.499E+01  in-plane shear stress margin: (allowable/actual)-1, matl 3
      RNG  2     1   7.448E+00  tensile transverse stress margin: (allowable/actual) - 1
      RNG  2     1   1.445E+01  compressive fiber stress margin: (allowable/actual) - 1
      RNG  2     1   1.249E+01  in-plane shear margin: (allowable stress)/(actual stress) - 1
      RNG  2     6   1.719E+01  compressive fiber stress margin: (allowable/actual) - 1
      RNG  2     6   7.022E+00  in-plane shear margin: (allowable stress)/(actual stress) - 1
      RNG  2    15   7.023E+00  compressive transverse stress margin: (allowable/actual) - 1
      RNG  2    15   8.027E+01  compressive fiber stress margin: (allowable/actual) - 1
      RNG  2    15   3.280E+00  in-plane shear margin: (allowable stress)/(actual stress) - 1
      RNG  3     1   6.501E+01  tensile fiber margin: (allowable stress)/(actual stress) - 1
      STR  3     0   1.677E+01  crippling margin for stringer segment. 22  local halfwaves
      STR  4     0   4.926E+00  crippling margin for stringer segment. 22  local halfwaves
           0     0   3.931E-01  (Wide column panel buck. factor)/(factor of safety) - 1
           0     0   7.214E-01  buck.margin simp-support shear string;M=1  ; N=12 ; slope= 0.05
           0     0   1.849E-01  buck.margin simp-support general buck;M=1  ; N=2  ; slope= 0.27
           0     0   7.267E-01  buck.margin rolling with shear string;M=1  ; N=12 ; slope= 0.05
           0     0   5.059E+00  buck.margin rolling only!of stringers;M=4  ; N=0  ; slope= 0.00
```

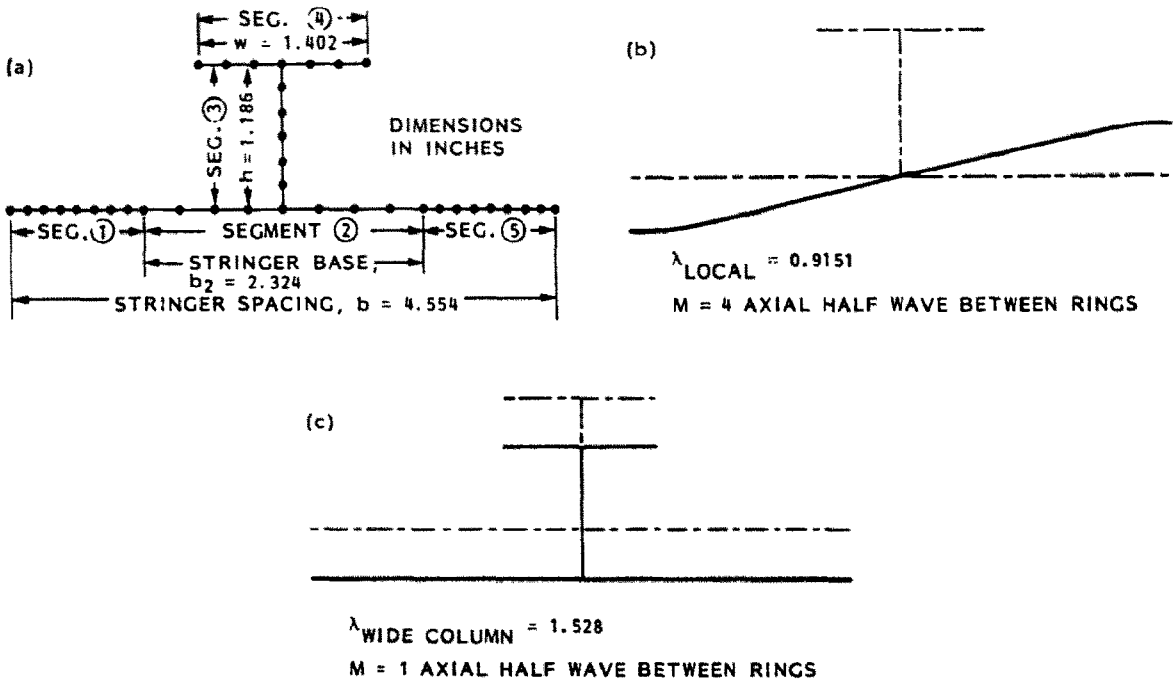

Fig. 90. Selected optimum design for the case in which local post-buckling is permitted, showing (a) discretized panel module model, and (b, c) buckling modes and load factors corresponding to load set 1; (b) local buckling mode and load factor, and (c) wide column buckling mode and load factor. The mode shapes vary as $\sin(M\pi x/L)$ along the axis of the panel, where L is the ring spacing.

that the panel is in its early post-locally-buckled state. However, in this case the Koiter post-buckling analysis yields an eigenvalue for local buckling that is slightly greater than unity, and therefore no post-buckling calculations are performed by PANDA2; the panel is assumed to remain in its unbuckled state. The eigenvalue for local buckling obtained from the Koiter analysis is different from that obtained from the BOSOR4 analysis because the two theories are different.

Figure 91 shows the results of using the PANEL processor followed by a BOSOR4 run. This represents step 8 in Table 4. The use of BOSOR4 to treat prismatic structures such as stiffened panels is described in [30, Ch. 7]. The multi-segment BOSOR4 model is depicted in Fig. 91(a) and the two lowest buckling load factors are given in Figs 91(b) and (c). The buckling modal displacements vary sinusoidally in the x-direction (normal to the plane of the page), with a half-wavelength equal to the ring spacing of 26.75 in. The buckling mode shown in Fig. 91(b) is simply another form of skin buckling because the intersections of the stringer webs with the panel skin move only slightly. It is the load factor and mode shape in Fig. 91(c) that should be compared to the wide-column buckling load factor $\lambda_{WIDECOLUMN} = 1.528$ given in Fig. 90(c).

21.7 *Results with IQUICK = 0, post-local buckling NOT permitted (step 7.3)*

Figures 92–96 and Tables 12, 13 and 14 give results that are analogous to those already given in Sec. 21.6, but with post-local-buckling not permitted. The panel weight again approaches 33 lb, but the stringers are closer together in this case than they were in the case for which local postbuckling is permitted. From Fig. 93 it is seen that the critical buckling mode for load set 1 is wide column buckling, and from Fig. 94 it is seen that the critical buckling mode for load set 2 is local buckling. After several iterations and repeated use of CHANGE and DECIDE the results become better behaved, settling down to a stable pattern as iterations proceed. This is because there is no sensitive behavior associated with the early postbuckling regime, as was the case for the optimization described in Sec. 21.6.

Figure 95 shows the optimized panel module (a), the local buckling mode and load factor $\lambda_{LOCAL}(b)$, and another buckling mode and load factor (c) corresponding to load set 1. Notice in Fig. 95(c) that the load factor $\lambda_{WIDECOL.} = 1.482$ does not correspond to a wide column buckling mode, which would resemble the mode shown in Fig. 90(c), but rather a long-wavelength side-sway of the stringer. However, the load factor λ associated with this side-sway mode is retained as a constraint for wide column buckling because it represents

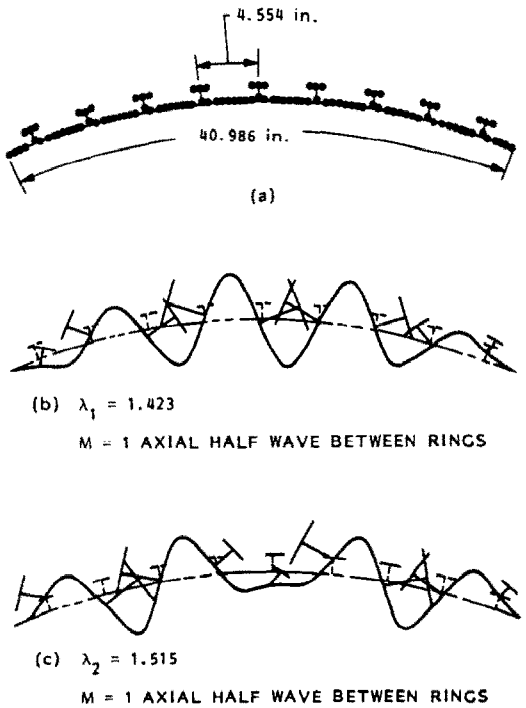

Fig. 91. (a) Multi-segment, branched BOSOR4 model of the optimized panel generated by the PANEL processor (local buckling is permitted), and (b, c) buckling modes corresponding to load set 1. (b) Lowest buckling mode represents a kind of local buckling because the stringer web lines of attachment to the panel skin do not move very much. (c) Second buckling mode represents a form of general instability. The load factor, $\lambda_2 = 1.515$, should be compared with the wide column buckling load factor, $\lambda_{WIDE\ COLUMN} = 1.528$, given in the previous figure. In (b) and (c) the mode shapes vary as $\sin(M\pi x/L)$ along the axis of the panel, where L is the ring spacing.

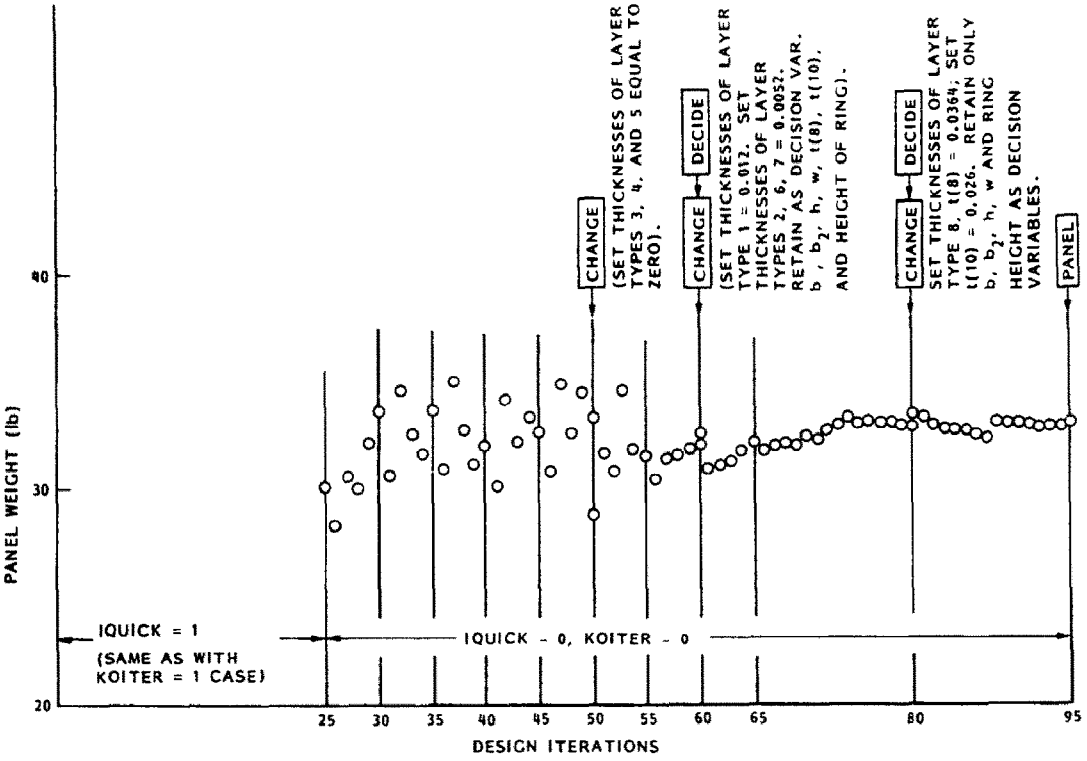

Fig. 92. Evolution of the panel weight during design iterations. Local post-buckling is not permitted (KOITER = 0).

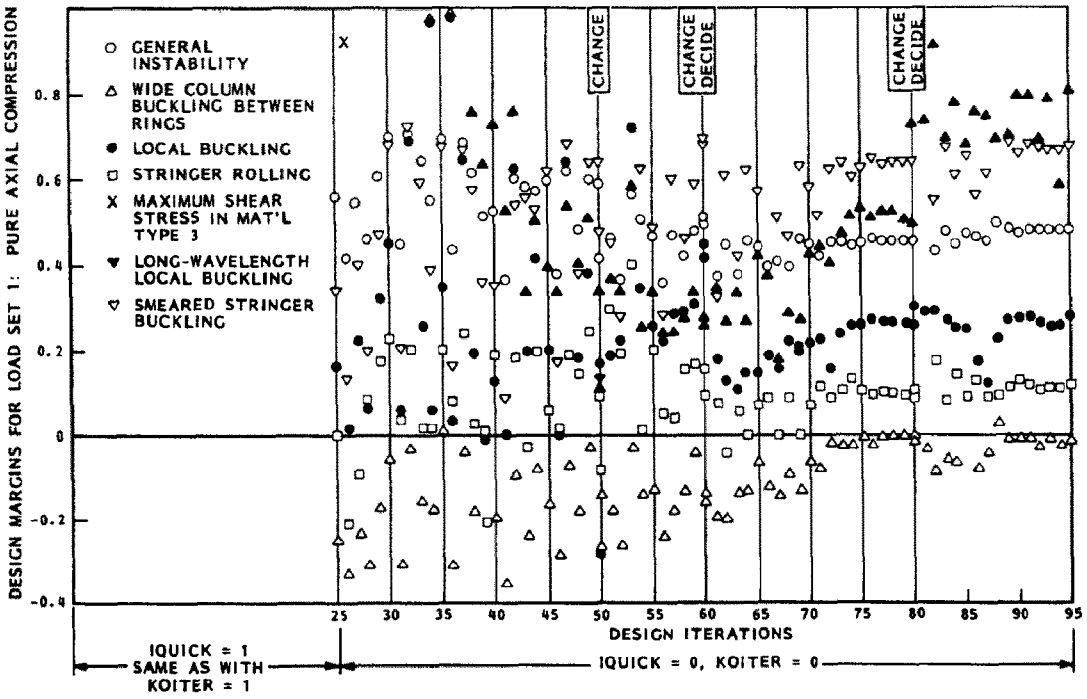

Fig. 93. Evolution of design margins corresponding to load set 1 ($N_x = -3000$ lb/in., $N_{xy} = 0$) during iterations. Local post-buckling is not permitted. The most critical margin is wide column buckling.

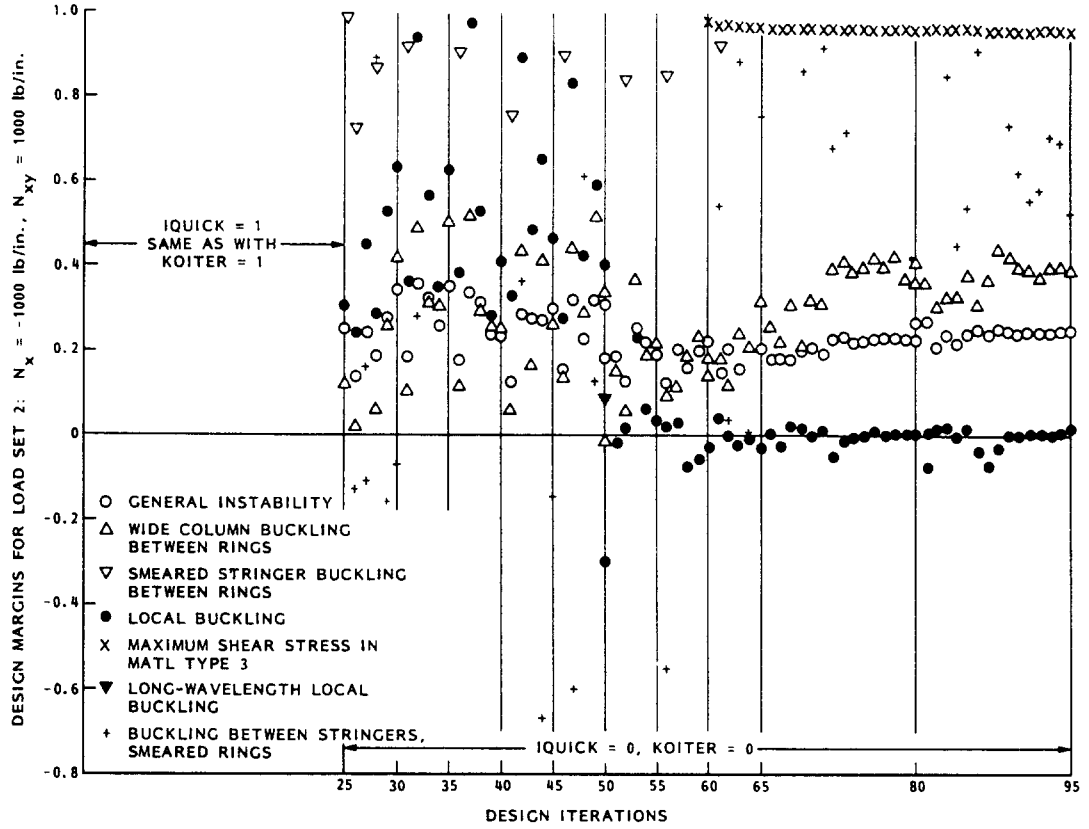

Fig. 94. Evolution of design margins corresponding to load set 2 ($N_x = -1000$ lb/in., $N_{xy} = 1000$ lb/in.) during iterations. Local post-buckling is **not** permitted. The most critical margin is local buckling.

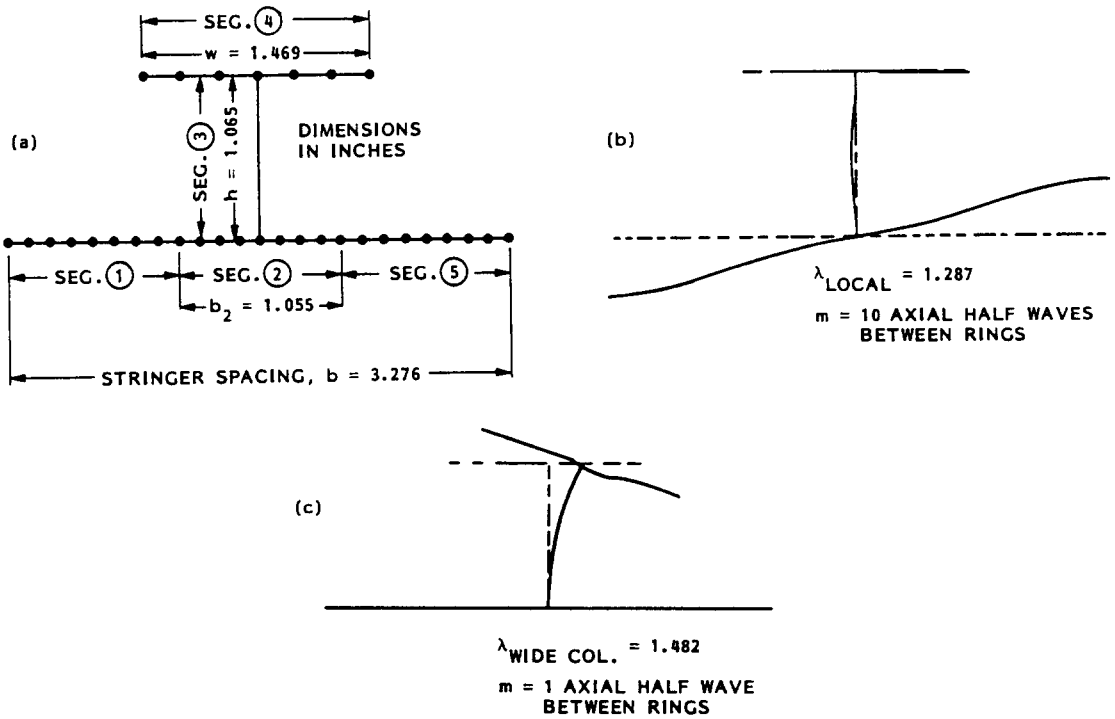

Fig. 95. Final optimum design for the case in which local post-buckling is **not** permitted, showing (a) discretized panel module model, and (b, c) buckling modes and load factors corresponding to load set 1; (b) local buckling mode and load factor, and (c) stringer side-sway buckling mode and load factor. The mode shapes vary as $\sin(m\pi x/L)$ along the axis of the panel, where L is the ring spacing.

a lower bound to the wide column buckling load. We know it is a lower bound because the eigenvalue extraction routine used in PANDA2 (same as the routine used in BOSOR4) calculates eigenvalues in increasing order. Therefore, we know what λ corresponding to a mode similar to that depicted in Fig. 90(c) is higher than 1.482.

Figure 96 shows the multisegment model generated by the processor PANEL and the three lowest eigenmodes and load factors from the BOSOR4 analysis of this model. All of the modes correspond to side-sway of one or more of the stringers. The wide-column eigenvalue must be greater than 1.309, which is the highest mode calculated in the BOSOR4 run, for which only the three lowest eigenvalues were requested by the user.

Tables 12, 13 and 14 list the final design, weight and design margins corresponding to load set 1 and load set 2.

21.8 *Conclusions from the results given in Secs* 21.6 *and* 21.7

Apparently in this case designing the panel to permit local buckling between the stringers does not lead to any reduction in weight. However, it does permit panels with stringers farther apart than is the case in which local buckling is not permitted. Another point should also be made. Since the same factors of safety were used to generate the results in both Secs 21.6 and 21.7, it might be argued that the panels operating in their locally post-buckled states are more reliable than are those in which local buckling is not permitted. This is because the former will be less sensitive in initial imperfections than the latter. In the former case the reduction in panel skin stiffness due to local buckling is accounted for when general instability load factors are computed. In the latter case there is no such reduction in skin stiffness. However, actual panels have local imperfections that reduce the effective stiffness of the skin much as if it were buckled. Since PANDA2 does not include the effect of initial imperfections, it may overestimate general instability load factors in cases for which the skin is not in its post-buckled state. (See [34] for recent inclusion in PANDA2 of the capability to handle initial imperfections.)

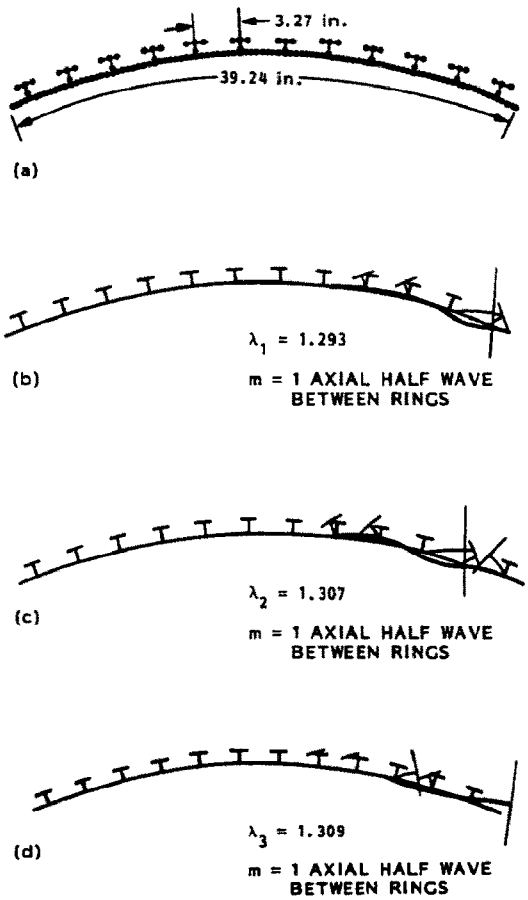

Fig. 96. (a) Multi-segment, branched BOSOR4 model of the optimized panel generated by the PANEL processor (local buckling not permitted, and (b, c, d) buckling modes corresponding to load set 1). All three buckling modes represent side-sway of the T-shaped stringers, and not wide column buckling. The mode shapes vary as $\sin(m\pi x/L)$ along the axis of the panel, where L is the ring spacing.

Table 12. Final design of ARIANE4, 2/3-Interstage with T-shaped stringers in which local post-buckling is not permitted

```
                    SUMMARY OF INFORMATION FROM OPTIMIZATION ANALYSIS
VAR.  DEC.  ESCAPE  LINK.  LINKED   LINKING    LOWER       CURRENT      UPPER       DEFINITION
 NO.  VAR.   VAR.   VAR.     TO     CONSTANT   BOUND        VALUE       BOUND
  1    Y      N      N       0     0.00E+00  2.50E+00  3.2761E+00  2.00E+01  stiffener spacing, b
  2    Y      N      N       0     0.00E+00  5.00E-01  1.0547E+00  3.00E+00  width of stringer base, b2
  3    Y      N      N       0     0.00E+00  1.00E-01  1.0654E+00  2.00E+00  height of stringer, h
  4    Y      N      N       0     0.00E+00  1.00E-01  1.4693E+00  3.00E+00  width of outer flange of stiffener, w
  5    N      N      N       0     0.00E+00  0.00E+00  1.2000E-02  0.00E+00  thickness for layer index no.(1 )
  6    N      N      N       0     0.00E+00  0.00E+00  5.2000E-03  0.00E+00  thickness for layer index no.(2 )
  7    N      N      N       0     0.00E+00  0.00E+00  0.0000E+00  0.00E+00  thickness for layer index no.(3 )
  8    N      N      N       0     0.00E+00  0.00E+00  0.0000E+00  0.00E+00  thickness for layer index no.(4 )
  9    N      N      N       0     0.00E+00  0.00E+00  0.0000E+00  0.00E+00  thickness for layer index no.(5 )
 10    N      N      N       0     0.00E+00  0.00E+00  5.2000E-03  0.00E+00  thickness for layer index no.(6 )
 11    N      N      N       0     0.00E+00  0.00E+00  5.2000E-03  0.00E+00  thickness for layer index no.(7 )
 12    N      N      N       0     0.00E+00  0.00E+00  3.6400E-02  0.00E+00  thickness for layer index no.(8 )
 13    N      N      N       0     0.00E+00  0.00E+00  5.2000E-03  0.00E+00  thickness for layer index no.(9 )
 14    N      N      N       0     0.00E+00  0.00E+00  2.6000E-02  0.00E+00  thickness for layer index no.(10)
 15    N      N      N       0     0.00E+00  0.00E+00  2.6750E+01  0.00E+00  stiffener spacing, b
 16    N      N      N       0     0.00E+00  0.00E+00  1.0000E+00  0.00E+00  width of ring base, b2
 17    Y      N      N       0     0.00E+00  1.00E+00  1.0000E+00  2.00E+00  height of ring, h
 18    N      N      N       0     0.00E+00  0.00E+00  5.2000E-03  0.00E+00  thickness for layer index no.(11)
 19    N      N      N       0     0.00E+00  0.00E+00  0.0000E+00  0.00E+00  thickness for layer index no.(12)
 20    N      N      N       0     0.00E+00  0.00E+00  5.2000E-03  0.00E+00  thickness for layer index no.(13)
 21    N      N      N       0     0.00E+00  0.00E+00  5.2000E-03  0.00E+00  thickness for layer index no.(14)
 22    N      N      N       0     0.00E+00  0.00E+00  1.0000E-01  0.00E+00  thickness for layer index no.(15)

      ****************************************************
    ********************* DESIGN OBJECTIVE ********************
      *************                              ************
         CURRENT VALUE OF THE OBJECTIVE FUNCTION:
       VAR. STR/ SEG. LAYER   CURRENT
       NO.  RNG  NO.   NO.     VALUE            DEFINITION
                  0     0   3.305E+01   WEIGHT OF THE ENTIRE PANEL
       *************                              ************
    ********************* DESIGN OBJECTIVE ********************
      ****************************************************
```

Another conclusion that might be drawn, especially from the results in Figs 88 and 89 which show that the most critical behavioral constraint is stringer pop-off, is that if the design could be revised in some way as to increase dramatically the allowable peel force in the web (the present value is 100 lb/in.), then significant reduction in weight might be attained by permitting local buckling to occur. The results given in the next section qualify this hypothesis.

21.9 *Optimum designs with increased allowable web peel force*

In the analyses reported in Secs 21.6 and 21.7 the allowable web peel force (see Figs 5–7) was set at 100 lb/in., a value close to what has been observed in tests of graphite-epoxy cloth bonded to graphite-epoxy tape. This

Table 13. Margins corresponding to load set 1 applied to the final design of ARIANE4 2/3-Interstage with T-shaped stringers in which local post-buckling is not permitted

```
            ********** LOAD SET NO. 1  **************
        APPLIED LOADS IN LOAD SET A ("eigenvalue" loads):
          Applied     axial       stress resultant, N1= -3.0000E+03
          Applied circumferential stress resultant, N2= -3.0000E+00
          Applied    in-plane     shear  resultant,N12=  1.5000E+01

        APPLIED LOADS IN LOAD SET B ( fixed uniform loads):
          Applied     axial       stress resultant,N10=  0.0000E+00
          Applied circumferential stress resultant,N20=  0.0000E+00
          Applied    in-plane    shear  resultant,N120=  0.0000E+00
          Applied pressure (positive for internal), P =  0.0000E+00

          CURRENT VALUES OF MARGINS CORRESPONDING TO CURRENT DESIGN
VAR.  STR/ SEG.  LAYER   CURRENT
NO.   RNG  NO.    NO.     VALUE            DEFINITION
            0     0   2.868E-01  Local  buckling from discrete model-1.,M=10 axial waves
          STR     3     0   2.187E+00  crippling margin for stringer segment. 25  local halfwaves
          STR     4     0   8.047E-01  crippling margin for stringer segment. 25  local halfwaves
            0     0  -4.323E-03  (Wide column panel buck. factor)/(factor of safety) - 1
            0     0   6.800E-01  buck.margin simp-support smear string;M=1  ; N=4  ; slope= 0.00
            0     0   1.999E+00  buck.margin simp-support smear rings; M=124; N=1  ; slope= 0.00
            0     0   4.832E-01  buck.margin simp-support general buck;M=2  ; N=2  ; slope= 0.00
            0     0   6.779E-01  buck.margin rolling with smear string;M=1  ; N=4  ; slope= 0.00
            0     0   1.266E+01  buck.margin rolling with smear rings; M=21 ; N=1  ; slope= 0.00
            0     0   1.212E-01  buck.margin rolling only of stringers;M=3  ; N=0  ; slope= 0.00
```

Table 14. Margins corresponding to load set 2 applied to the final design of ARIANE4 2/3-Interstage with T-shaped stringers in which local post-buckling is not permitted

```
          ********** LOAD SET NO. 2 **************
      APPLIED LOADS IN LOAD SET A ("eigenvalue" loads):
        Applied     axial       stress resultant, N1= -1.0000E+03
        Applied circumferential stress resultant, N2= -1.4142E+00
        Applied    in-plane     shear  resultant,N12=  1.0000E+03

      APPLIED LOADS IN LOAD SET B ( fixed uniform loads):
        Applied     axial       stress resultant,N10=  0.0000E+00
        Applied circumferential stress resultant,N20=  0.0000E+00
        Applied    in-plane    shear  resultant,N120=  0.0000E+00
        Applied pressure (positive for internal), P =  0.0000E+00

           ***************** NOTE   NOTE    NOTE  *************
                      WIDE COLUMN BUCKLING LOAD FACTOR
            CORRESPONDS TO SIDESWAY (ROLLING) OF THE STRINGER BY ITSELF.
            ************************************************************

               CURRENT VALUES OF MARGINS CORRESPONDING TO CURRENT DESIGN
VAR.  STR/  SEG.  LAYER   CURRENT
NO.   RNG   NO.    NO.     VALUE          DEFINITION
            0      0    1.042E-02  Local  buckling from discrete model-1.,M=10 axial waves
      STR   3      0    8.562E+00  crippling margin for stringer segment. 25  local halfwaves
      STR   4      0    4.414E+00  crippling margin for stringer segment. 25  local halfwaves
      STR   1      2    9.833E-01  in-plane shear margin: (allowable stress)/(actual stress) - 1
            0      0    3.898E-01  (Wide column panel buck. factor)/(factor of safety) - 1
            0      0    1.359E+00  buck.margin simp-support smear string;M=1   ; N=10 ; slope= 0.07
            0      0    3.935E+00  buck.margin simp-support smear rings; M=124; N=1  ; slope= 0.07
            0      0    2.441E-01  buck.margin simp-support general buck;M=1   ; N=2  ; slope= 0.27
            0      0    1.362E+00  buck.margin rolling with smear string;M=1   ; N=10 ; slope= 0.07
            0      0    5.269E-01  buck.margin rolling with smear rings; M=21  ; N=1  ; slope= 0.57
            0      0    2.364E+00  buck.margin rolling only of stringers;M=3   ; N=0  ; slope= 0.00
```

value can be greatly increased if a metal I-shaped insert can be included as a core element in the stringer, as shown in Fig. 97. The loads from web to faying flange and from web to outstanding flange can then be carried through generous fillets machined at the junctions between web and flanges of the insert.

The analyses reported in Secs 21.6 and 21.7 were repeated for the configuration shown in Fig. 97. The maximum allowable web peel force was increased to 1000 lb/in. Two new decision variables were introduced: the thickness of the flanges of the aluminum insert (faying flange thickness equal to outstanding flange thickness) and the thickness of the web of the aluminum insert.

The minimum weight designs are listed in Table 15. A weight reduction of about 10% is obtained when local buckling is allowed compared to the minimum weight for the same design concept when local buckling is not permitted. Figure 98(a) shows the optimized design for the case in which local buckling is permitted, and Fig. 98(b) gives the local buckling mode and load factor λ_{LOCAL} corresponding to load set 1. Since the local buckling load factor, λ_{LOCAL}, equals 0.339, the axial compression supported by the optimum design, $N_x = 3000$ lb/in., is about three times the local buckling load. Therefore the panel is loaded rather far into the post-local-buckling regime. Note, however, that the weight saved is not significant when compared with the minimum weight designs obtained without the aluminum insert. These designs weigh about 33 lb. Also, the concept with the aluminum insert would doubtless be significantly more expensive than the all-composite concepts.

It is concluded from these results and from the results presented in Secs 21.6 and 21.7 that without additional convincing proof that the optimum designs with local buckling permitted are more reliable than those in which local buckling is not permitted, we cannot affirm that there is much to be gained in this particular case by designing to allow local buckling.

21:10 *Optimum designs with hat-shaped stringers*

Lighter designs should be possible for panels with stringers that enclose area, since the torsional stiffness of the stringer is thereby greatly increased without much increase in weight. Table 16 lists results for optimum designs with local buckling permitted and with local buckling prohibited. There is very little reduction in weight afforded by a design that permits local buckling. For this design the panel fails under load set 1 at only 10% above the local buckling load and under load set 2 at about 31% above the local buckling load. Designs with stringers further apart are feasible and fail at a load that may be many times the local buckling load, but these designs are heavier than those listed in Table 16.

Figure 99 depicts the discretized model and the local and wide column buckling modes and load factors corresponding to load set 1 for the panel designed not to buckle locally. For the same panel Fig. 100 shows

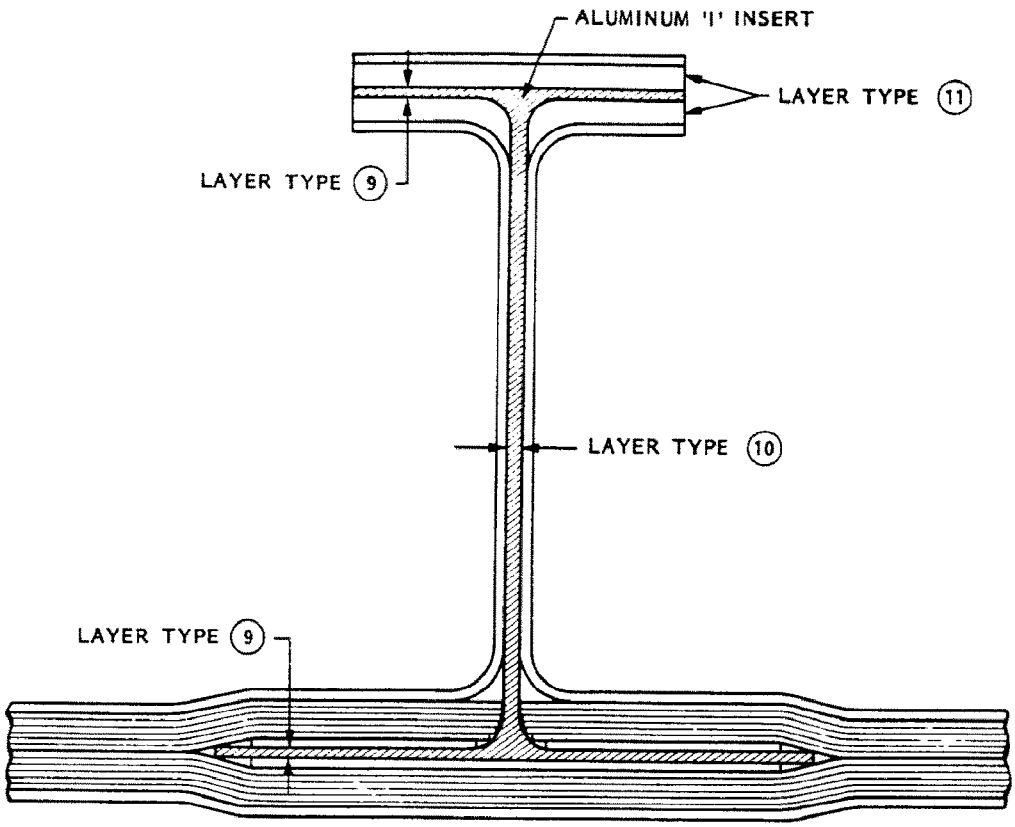

Fig. 97. Graphite-epoxy cloth and tape T-shaped stringer with aluminum insert. The purpose of the aluminum insert is to greatly increase the maximum allowable web peel force, which was only 100 lb/in. in the previous design and is 1000 lb/in. in this design. It was initially conjectured that such a concept will lead to greater weight reduction for panels designed to operate in the locally post-buckled regime. Results, however, show that although optimized designs of the panel can operate in the far-locally-post-buckled regime, these designs are not significantly lighter than those obtained without the aluminum insert.

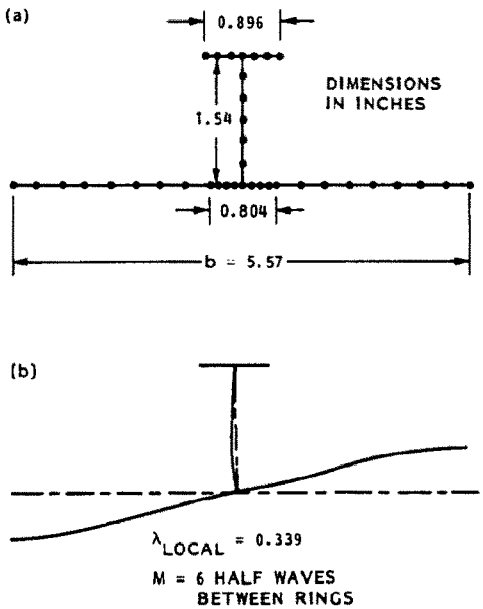

Fig. 98. Final optimum design for the case in which local post-buckling is permitted, showing (a) discretized panel module model, and (b) local buckling mode and load factor corresponding to load set 1. The mode shape varies as $\sin(M\pi x/L)$ along the axis of the panel, where L is the ring spacing. Since the load factor for local buckling is λ_{LOCAL} equals 0.339, the optimum panel is designed to operate at an axial load close to three times the local buckling load.

Table 15. Optimum designs of ARIANE4 2/3-Interstage with aluminum I-shaped insert inside stringers

		LOCAL BUCKLING: PERMITTED	NOT PERMITTED
FINAL DIMENSIONS (inches)...			
Stringer spacing,	b =	5.57	4.04
Stringer base width,	b2 =	0.804	0.832
Stringer height,	h =	1.54	1.21
Stringer flange width,	w =	0.896	0.671
Thicknesses:			
layer type 1, 45 deg. cloth	t(1) =	0.018	0.006
layer type 2, 90 deg. tape	t(2) =	0.0052	0.0052
layer type 3, 45 deg. tape	t(3) =	0.0000	0.0052
layer type 4, 0 deg. tape	t(4) =	0.0000	0.0000
layer type 5,-45 deg. tape	t(5) =	0.0000	0.0052
layer type 6, 0 deg. tape	t(6) =	0.0052	0.0000
layer type 7, 90 deg. tape	t(7) =	0.0052	0.0104
layer type 8, 0 deg. tape in base	t(8) =	0.0260	0.0468
layer type 9, AL in base & flange	t(9) =	0.0200	0.0200
layer type 10, AL in web	t(10) =	0.0201	0.0275
layer type 11,0 deg. tape in flange	t(11) =	0.0260	0.0468
PANEL WEIGHT (lbs)....		31.9	34.9
DESIGN MARGINS.....			
LOAD SET 1 (Nx = -3000 lb/in, Nxy = 0)....			
Local buckling		-----	0.501
Wide column buckling between rings		-0.0207	0.0000
Rolling of stringers without skin motion		0.0000	0.0000
General instability		0.257	0.657
Buckling between rings, smeared stringers		0.669	0.853
Crippling of stringer web		0.863	0.682
Crippling of stringer flange		0.521	2.391
Stringer popoff		0.257	-----
In-plane shear stress, GR/EP cloth, Segment 3 (web), Node 1, layer 1		-0.003	-----
Compression in aluminum insert		0.099	-----
Compression in aluminum insert, Segment 2 (stringer base)		-----	0.540
Compression in aluminum insert, Segment 4 (flange)		-----	0.594
LOAD SET 2 (Nx = -1000 lb/in, Nxy = 1000 lb/in)....			
Local buckling		-----	0.0000
Wide column buckling between rings		0.100	0.463
General instability		0.134	0.353
Stringer popoff		0.418	-----
Tension along fibers, GR/EP cloth, Seg. 5 (panel skin), node 9, layer 1		-0.0038	-----
In-plane shear stress, GR/EP cloth, Seg. 1 (panel skin), node 9, layer 1		0.621	-----
In-plane shear stress, aluminum insert, Seg. 2 (stringer base), node 1		0.912	-----

the discretized model and several inter-ring buckling modes predicted with use of PANEL and BOSOR4. The load factors for these inter-ring modes are close and agree reasonably well with the load factor calculated from the PANDA-type closed form analysis for a panel simply supported at the ring stations with stringers smeared out.

22. SUMMARY, CONCLUSIONS, PITFALLS AND LIMITATIONS AND SUGGESTIONS FOR FURTHER WORK

22.1 *Summary and conclusions*

The purpose, scope and operation of the PANDA2 system of programs has been explained through a sample case run with use of a tutorial option. Several examples are given with results compared with those

Table 16. Optimum designs of ARIANE4 2/3-Interstage with hat-shaped stringers

		LOCAL BUCKLING: PERMITTED	NOT PERMITTED
FINAL DIMENSIONS (inches)...			
Stringer spacing,	b =	5.07	4.20
Stringer base width,	b2 =	2.50	2.50
Stringer height,	h =	1.42	1.34
Stringer outer flange width,	w =	1.20	1.20
Stringer hat base width,	w2 =	1.50	1.50
Thicknesses:			
layer type 1, 45 deg. cloth	t(1) =	0.012	0.012
layer type 2, 90 deg. tape	t(2) =	0.0000	0.0052
layer type 3, 45 deg. tape	t(3) =	0.0052	0.0000
layer type 4, 0 deg. tape	t(4) =	0.0000	0.0000
layer type 5,-45 deg. tape	t(5) =	0.0052	0.0000
layer type 6, 0 deg. tape	t(6) =	0.0000	0.0052
layer type 7, 90 deg. tape	t(7) =	0.0052	0.0052
layer type 8, 0 deg. tape in base	t(8) =	0.0052	0.0104
layer type 9, 90 in base & flange	t(9) =	0.0052	0.0052
layer type 11,0 deg. tape in flange	t(11) =	0.0416	0.0208
PANEL WEIGHT (lbs)....		27.9	28.7
DESIGN MARGINS.....			
LOAD SET 1 (Nx = -3000 lb/in, Nxy = 0)....			
Local buckling		-----	0.0000
Wide column buckling between rings		-0.0400	0.0116
General instability		0.558	0.292
Buckling between rings, smeared stringers		1.22	0.694
Crippling of stringer webs		0.0697	0.410
Crippling of stringer flange		1.38	0.940
Crippling under hat		1.47	1.23
Stringer popoff		3.11	-----
In-plane shear stress, GR/EP cloth, Segment 1 (skin), Node 9, Layer 1		0.256	1.32
Compression along fibers, Seg. 1, Layer 6		-----	1.43
In-plane shear stress, tape, Segment 1 (skin), Node 9, Layer 3		0.951	-----
Compression along fibers, tape, Segment 2 (base), Node 1, Layer 8		1.06	-----
LOAD SET 2 (Nx = -1000 lb/in, Nxy = 1000 lb/in)....			
Local buckling		-----	0.108
Wide column buckling between rings		0.654	0.919
General instability		0.176	0.138
Stringer popoff		0.898	-----
Tension along fibers, GR/EP cloth, Seg. 1 (skin), Node 1, Layer 14		0.0202	-----
In-plane shear stress, GR/EP cloth, Seg. 2 (base), Node 7, Layer 1		0.621	-----
In-plane shear stress, tape, Seg. 1, Layer 2		-----	0.983

in the literature and those obtained by other computer programs such as EAL and STAGS. It is concluded that the agreement between predictions from PANDA2 and those from general purpose programs justifies the use of PANDA2 for preliminary design. An interstage for the ARIANE4 booster is designed both allowing and prohibiting local buckling. Various design concepts are tried, and it is concluded that in this case little is gained by allowing local buckling during service.

PANDA2 is similar to other sizing codes for stiffened panels, such as PASCO [10], developed at NASA Langley Research Center by Anderson and Stroud, and POSTOP [22–24], developed at Lockheed–Georgia by Dickson, Biggers and Wang. However, PANDA2 will in certain branches of its operation handle rings as well as stringers, will allow normal pressure as one of the loads, and is constructed with rather extensive

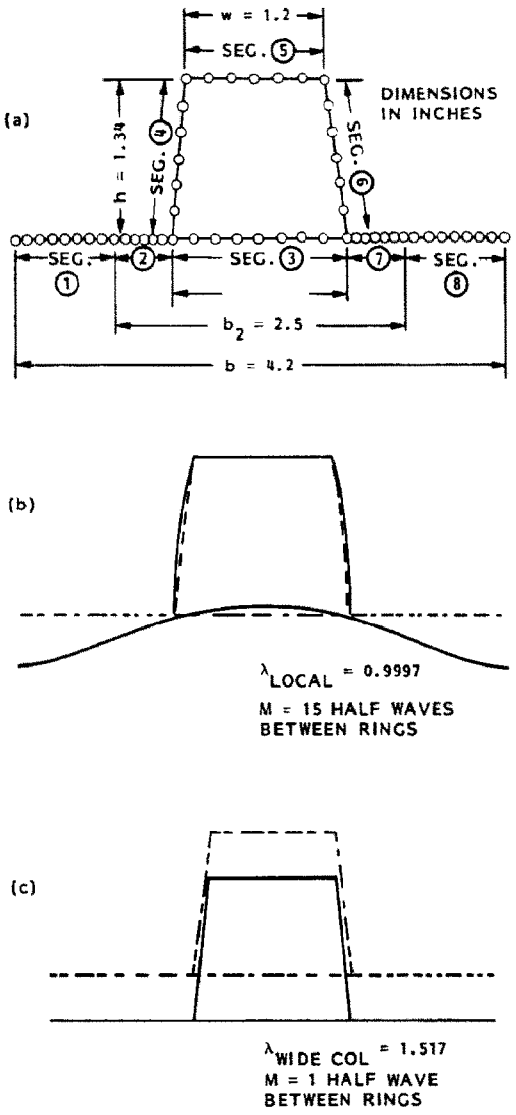

Fig. 99. Final optimum design for the hat-stiffened panel for the case in which local post-buckling is not permitted, showing: (a) discretized panel module model, and (b, c) buckling modes and load factors corresponding to Load Set 1; (b) local buckling mode and load factor; and (c) wide column buckling mode and load factor. The mode shapes vary as $\sin(M\pi x/L)$ along the axis of the panel, where L is the ring spacing.

interactive aids for users. The post-local-buckling analysis used in PANDA2 is based upon a modified form of Koiter's theory [4] which probably yields more accurate strains than those obtained by POSTOP because the local buckling mode is derived from a discretized model of the panel module cross section, rather than from an assumed shape function with only two or three coefficients. The pop-off constraint used in PANDA2 is different from that used in POSTOP. From the very limited experience of the few tests on the hat-stiffened panels (Fig. 31), this pop-off constraint, which requires results of standard peel tests, seems to work.

22.2 *Pitfalls and limitations*

PANDA2 is aimed at very difficult, complex, nonlinear structural problems, and because the goal is to obtain reasonable preliminary (and even, perhaps, final) designs in a short time, there are many assumptions and approximations used in the theories on which it is based. Therefore, any designs produced by PANDA2 should be thoroughly evaluated by application of rigorous nonlinear finite element models and tests. There is much that is unknown about the behavior of composite materials, and the user should realize that the failure criteria that he or she enter as input data affect the final outcome.

The following is a list of pitfalls the user should be aware of. They are not listed in order of importance, but rather in the order that the writer happened to think of them.

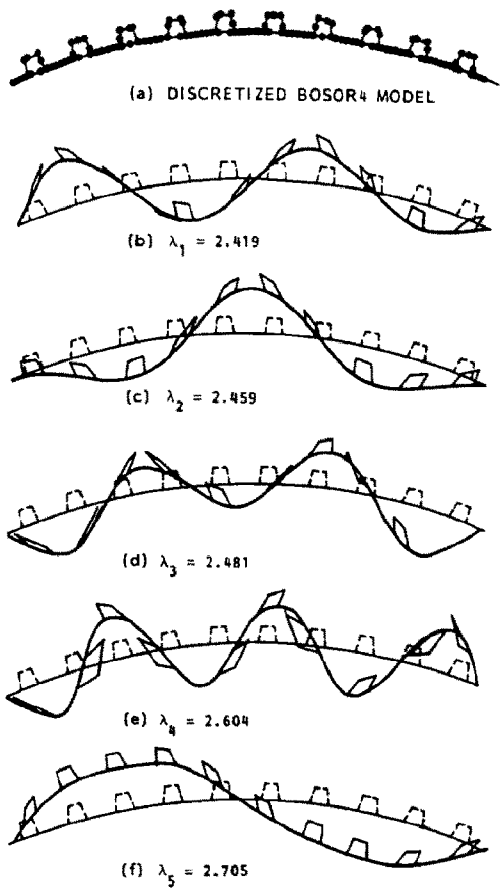

Fig. 100. (a) Multi-segment, branched BOSOR4 model of the optimized panel generated by the PANEL processor (local buckling **not** permitted), and (b, c, d, e, f) buckling modes corresponding to load set 1. All five buckling modes represent panel buckling between rings in which stringers and panel skin participate. The load factors are close to that predicted from the PANDA-type model for buckling between rings with smeared stringers. The mode shapes vary as $\sin(\pi x/L)$ along the axis of the panel, where L is the ring spacing.

1. PANDA2 is intended to be used for the analysis of uniform panels, in the sense that the panel contains regular arrays of stringers and or rings. It is not meant for use in cases in which there is only one stringer, for example.

2. In PANDA2 rings are sort of 'second-class citizens'. For example, the local postbuckling analysis is conducted only for a single panel module that represents one stringer with the panel skin and stringer base between adjacent stringers. No analogous treatment is included for local post-buckling of panels with rings only, for example. Also, local buckling load factors for panels stiffened by rings only are not calculated by means of any models in which the ring cross sections are discretized, as is the case for stringers.

3. The effect of imperfections is included [34]. Therefore, the well-known phenomenon of modal interaction, in which local imperfections in the skin between stringers have the effect of reducing the effective axial stiffness of the skin and therefore of reducing the overall buckling load, can be predicted with PANDA2.

4. The material behavior is linear. There is no plasticity.

5. In the post-buckling analysis the axial wavelength of the local buckles is assumed to be constant. There is no theory in PANDA2 allowing secondary bifurcations, that is bifurcations from the locally post-buckled state. Secondary bifurcations are frequently observed in tests.

6. Only simple failure criteria are used in PANDA2. An attempt is made to account for the fact that cracking due to tension normal to the fibers does not necessarily lead to failure of the structure but does lead to decrease in stiffness and decrease in the allowable compression along the fiber, but these portions of PANDA2 should be regarded, if not with paranoia, at least with a certain healthy scepticism.

7. Boundary conditions are rather inflexible in PANDA2. The edges normal to the screen (generators of cylindrical panel) are always assumed to be simply supported. The other two edges (curved edges in a cylindrical panel) can be either simply supported or clamped, but clamping is simulated by analyzing a simply supported panel the length of which is $L/(3.85)^{1/2}$, where L is the actual length of the panel.

8. It is possible that PANDA2 will lead to designs that are feasible in the sense that all design margins are positive, but that are unreasonable because of other considerations not formally introduced by the user, either through oversight or because of limitations in PANDA2. The user should always monitor carefully the design process to make sure that he or she has introduced sufficient lower and upper bounds, and has accounted for practical items such as possibility of fabrication, cost, clearance of parts, etc.

9. There is no guarantee that PANDA2 will find a minimum weight design in the global sense. From Figs 84–89 we see several feasible designs, many of which correspond to local minima in the surface of weight as a function of decision variables. Before the user decides to accept a design, he or she must use the CHANGE processor, alter one or more of the decision variables, and perform more design iterations. When in doubt always perform more design iterations! They are cheap compared to building and testing something and then finding out later that much better possibilities exist. Varying the stiffener spacing is perhaps the best way to search for other minimum weight designs.

10. In designing panels that are allowed to buckle locally in service, it may frequently happen that optimum designs correspond to the early post-buckling regime. This is because maximum stresses and stringer pop-off forces increase steeply in design space in the early post-buckling regime and therefore are likely to encounter maximum allowable values in this regime. Design iterations may not converge in this regime due to the discontinuity in behavior of the panel just before local buckling and just after local buckling. The user will find that it helps to allow more iterations in each iteration set in cases such as this.

11. The post-local-buckling analysis performed with PANDA2 is based on the assumption that the local buckling deformations are antisymmetric with respect to the stringer line of attachment to the panel skin. This assumption is not as good for curved panels as it is for flat panels.

12. The user should not be fooled by spurious convergence of the design due to a restricted 'window' of permitted excursion of decision variables, a property of PANDA2 described in Sec. 21.4. When in doubt perform another (and yet another!) set of design iterations.

13. Composite material is made in certain ply thicknesses. The user must ensure that his final design consists of integral numbers of ply thicknesses for every layup angle.

14. In the final stages of a design process most or all thickness variables may have been eliminated as decision variables. In such cases there may not be enough escape variables to avoid CONMIN's inability to generate moves in design space if more constraints are violated that there are decision variables remaining in the problem. In such cases the user may have to do some 'optimization by hand', that is, he or she may have to 'jiggle' one or more of the decision variables in a sequence of fixed design runs. This kind of problem only seems to arise when the design is very close to being feasible. Therefore, it can be handled in an alternative way simply by allowing slightly increased factors of safety.

22.3 *Suggestions for further work*

Perhaps the weakest part of the PANDA2 post-local-buckling analysis is the assumption that the number of axial halfwaves at bifurcation remains constant as the load increases beyond the bifurcation load. Koiter proved that for infinitely long, axially compressed flat plates the post-buckling axial wavelength becomes shorter as the load increases beyond the bifurcation load. In tests on finite panels the axial wavelength stays approximately constant for rather large load ranges, but then the buckle pattern may change abruptly into another similar pattern but with more axial waves. There is probably some complicated transition pattern or series of patterns that governs this secondary bifurcation or series of closely related bifurcations. Whether and at what axial load the secondary bifurcation or bifurcations occur seems to depend on small, perhaps unavoidable inperfections in uniformity of load and panel properties. Whatever actually occurs, it would be a good idea to allow the axial length of the local buckling pattern to be variable in the post-buckling analysis in PANDA2.

It would be beneficial to include local imperfections in the panel skin in the PANDA2 analysis. The imperfection could be in the form of the critical local bifurcation buckling mode of the perfect panel. This additional capability would be especially useful in cases for which the optimum design yields local and general buckling loads that are close. In such cases, van der Neut [25], Thompson *et al.* [26], Tvergaard [27], Byskov and Hutchinson [28], Koiter [29], and others referenced in [30] have shown that the interaction between local and general buckling causes significant reduction of the load-carrying capability below that of the perfect panel. Inclusion of initial local imperfections would also serve to smooth the transition from pre-buckling to post-buckling regimes, which might eliminate much of the jumpiness of behavior during design iterations for panels, the optimum designs of which correspond to the early post-buckling regime. (See [34]!)

The post-buckling analysis in PANDA2 is based on the treatment of a single panel module, which is assumed to be flat. The post-buckling pattern is a two-term series expansion of the local bifurcation buckling mode:

$$w(x, y) = f(\phi + a\phi^3) \sin [(\pi/L)(x - my)], \tag{22.1}$$

in which ϕ is the bifurcation buckling mode. If ϕ is antisymmetric about the stiffener line of attachment, as

it is in Figs 20(a), 22(a) and 46(c), for example, then $w(x, y)$ will always be antisymmetrical. However, if the panel is curved $w(x, y)$ observed in tests will not be antisymmetrical: outward buckles will differ from inward buckles. To predict this behavior, terms with even powers of ϕ would be required in the series exapansion for $w(x, y)$.

It would be beneficial to expand the PANDA2 capability to include nonlinear material behavior.

Inclusion of a discretization of the entire panel width inside the optimization loop, at least as a user-chosen option, would be a good idea. This would eliminate much of the difficulty associated with use of the wide column buckling load as an indicator of general instability. Of course optimization runs would take much more computer time. However, the user could choose this more elaborate model only after a reasonably good optimum design had already been obtained with use of the wide column model described in this paper.

Acknowledgements—Much of this work was sponsored by the 1983–1986 Lockheed Independent Development Program. The author is indeed grateful for the continuing support of Mr Bill Sable, Manager of Structural Analysis and Test in Lockheed Missiles and Space Company's Satellite Systems Division. The author also appreciates the support and encouragement he has received over the years from Dr Narendra Khot of the Air Force Wright Aeronautical Laboratory.

Many of the author's colleagues at Lockheed were of great help in certain aspects of this work. In particular, several people were involved in the fabrication and testing of the hat-stiffened, graphite-epoxy curved panels which are discussed in connection with Figs 31–45: Don Flaggs supplied the author with failure criteria from his extensive data bank on properties of composite materials. Don also was responsible for seeing that the hat-stiffened panels were fabricated according to specification. Pat McCormick fabricated the complex panels. Alan Holmes designed the test rig shown in Fig. 34, and was responsible for seeing that the panels were accurately trimmed, potted and installed in the test machine, that the computerized data retrieval system worked properly, and that the tests were conducted according to specification. Rick Gardner conducted the tests and prepared post-test specimens for inspection.

Charles Rankin and Frank Brogan set up the STAGS computer models and made the runs that led to the STAGS results shown in Figs 47–64. Harold Cabiness, Hugh McManus and Dick Walz helped to 'shake down' PANDA2 by playing around with it and informing the author of bugs and of some user unfriendliness which, at their suggestion, was eliminated. Harold Cabiness made several suggestions for improvement of the PANDA2 documentation. Jörgen Skogh offered many helpful comments with regard to the presentation of the data in Figs 46–77 and 78–100.

During the initial stages of the research the author had many fruitful discussions with John Dickson of Lockheed–Georgia about Koiter's post-buckling theory. John supplied the author with copies of Koiter's original 1946 report as well as copies of reports on POSTOP, a computer program that is similar to PANDA2. Norm Knight of NASA Langley Research Center supplied the author with data on the case discussed in connection with Figs 22–24.

Shelley Black helped to put the typescript in its final form, and Louise Roche, Margaret Collins and Mary Ellen Hasbrouck saw to it that the figures were artfully drawn.

REFERENCES

1. D. Bushnell, PANDA—Interactive program for minimum weight design of stiffened cylindrical panels and shells. *Comput. Struct.* **16**, 167–185 (1983). Also, see *Structural Analysis Systems*, Vol. 1 (Edited by A. Niku-Lari), pp. 171–201. Pergamon Press, Oxford (1986).
2. D. Bushnell, BOSOR4: Program for stress, buckling and vibration of complex shells of revolution. In *Structural Mechanics Software Series—Vol. 1*, (Edited by N. Perrone and W. Pilkey), pp. 11–131. University Press of Virginia (1977). See also *Comput. Struct.* **4**, 399–435 (1974); *AIAA Jnl* **9**, 2004–2013 (1971); and *Structural Analysis Systems*, Vol. 2 (Edited by A. Niku-Lari), pp. 25–54. Pergamon Press, Oxford (1986).
3. G. N. Vanderplaats, CONMIN—a FORTRAN program for constrained function minimization. NASA TM X 62-282, version updated in March 1975, Ames Research Center, Moffett Field, CA (Aug. 1973) See also G. N. Vanderplaats and F. Moses, Structural optimization by methods of feasible directions. *Comput. Struct.* **3**, 739–755 (1973).
4. W. T. Koiter, Het Schuifplooiveld by Grote Overshrijdingen van de Knikspanning. National Luchtvaart, Laboratorium, Report X295, November 1946 (in Dutch).
5. J. H. Starnes, Jr, N. F. Knight, Jr and M. Rouse, Postbuckling behavior of selected flat stiffened graphite-epoxy panels loaded in compression. AIAA Paper 82-0777, presented at AIAA 23rd Structures, Structural Dynamics and Materials Conference, New Orleans, May 1982. See also *AIAA Jnl* **23**, 1236–1246 (1985).
6. A. W. Leissa, Buckling of laminated composite plates and shell panels. AFWAL-TR-85-3069, Air Force Wright Aeronautical Laboratories, Wright-Patterson AFB, Ohio 45433, June 1985.
7. C. C. Chamis, Buckling of anisotropic composite plates. *Proc. ASCE, Jnl Struct. Div.* **95**, 2119–2139 (1969). Also see C. C. Chamis, Buckling of Anisotropic Plates, Closure and Errata. *Proc. ASCE, Jnl Struct. Div.* **97**, 960–962 (1971).
8. D. Bushnell, Panel optimization with integrated software (POIS), PANDA—Interactive program for preliminary minimum weight design. AFWAL-TR-81-3073, Vol. 1, Air Force Wright Aeronautical Laboratories, Wright-Patterson AFB, Ohio 45433, July 1981.
9. M. S. Anderson and W. J. Stroud, General panel sizing computer code and its application to composite structural panels. *AIAA Jnl* **17**, 892–897 (1979).
10. W. J. Stroud and M. S. Anderson PASCO: Structural panel analysis and sizing code, capability and analytical foundations. NASA TM-80181 (1981).
11. S. A. Ambartsumyan, *Theory of Anisotropic Plates*. Technomic, Stamford, CT (1970).
12. J. M. Whitney, The effect of transverse shear deformation on the bending of laminated plates. *J. Comp. Mat.* **3**, 534–547 (1969).
13. J. Vinson and A. P. Smith Jr, The effect of transverse shear deformation on the elastic stability of plates of composite materials. AFOSR TR-75-1628, March 1975.
14. E. J. Brunelle and G. A. Oyibo, Generic buckling curves for specially orthotropic rectangular plates. *AIAA Jnl*, Aug. 1983.

15. W. J. Stroud, W. H. Greene and M. S. Anderson, Buckling loads of stiffened panels subjected to combined longitudinal compression and shear: Results obtained with PASCO, EAL and STAGS computer programs. NASA TP 2215, NASA Langley Research Center, January 1984.
16. W. D. Whetstone, EISI-EAL, Engineering Analysis Language. Proceedings of the Second Conference on Computing in Civil Engineering, ASCE, pp. 276–285 (1980).
17. B. O. Almroth and F. A. Brogan, The STAGS Computer Code. NASA CR-2950, NASA Langley Research Center (1978).
18. D. Bushnell, A. M. C. Holmes, D. Flaggs and P. McCormick, Fabrication and test of optimized large, stiffened graphite-epoxy curved panels in axial compression. In *Buckling of Structures—Theory and Experiment* (Edited by I. Elishakott, J. Arbocz, C. D. Babcock and A. Libai). Symposium in honor of the 65th birthday of Professor Josef Singer.
19. C. C. Rankin, P. Stehlin and F. A. Brogan, Enhancements to the STAGS computer code. Lockheed Missiles and Space Co., Inc., Palo Alto, CA, LMSC-D060755, November 1985.
20. G. A. Thurston, F. A. Brogan and P. Stehlin, Postbuckling analysis using a general purpose code. AIAA Paper No. 85-0719-CP, AIAA 26th Structures, Structural Dynamics, and Materials Conference, Orlando, Florida, 15–17 April 1985.
21. R. L. Boitnott, E. R. Johnson and J. H. Starnes, Jr, A nonlinear analysis of infinitely long graphite-epoxy cylindrical panels loaded with internal pressure. AIAA 26th Structures, Structural Dynamics and Materials Conference, Orlando, Florida, 15–17 April 1985.
22. J. N. Dickson, R. T. Cole and J. T. S. Wang, Design of stiffened composite panels in the post-buckling range. In *Fibrous Composites in Structural Design* (Edited by E. M. Lenoe, D. W. Oplinger and J. J. Burke), pp. 313–327. Plenum Press, New York (1980).
23. J. N. Dickson, S. B. Biggers and J. T. S. Wang, Preliminary design procedure for composite panels with open-section stiffeners loaded in the post-buckling range. In *Advances in Composite Materials* (Edited by A. R. Bunsell *et al.*), pp. 812–825. Pergamon Press, Oxford (1980).
24. J. N. Dickson and S. B. Biggers, POSTOP: Postbuckled open-stiffened optimum panels, theory and capability. NASA Langley Research Center, NASA Contractor Report from NASA Contract NAS1-15949, May 1982.
25. A. van der Neut, The interaction of local buckling and column failure of thin-walled comporession members. *Proceedings of the Twelfth International Congress of Applied Mechanics* (Edited by M. Hetenyi and W. G. Vincenti), pp. 389–399. Springer, Berlin (1969).
26. J. M. T. Thompson, J. D. Tulk and A. C. Walker, An experimental study of imperfection-sensitivity in the interactive buckling of stiffened plates. In *Buckling of Structures* (Edited by B. Budiansky), pp. 149–159. Springer, Berlin (1976).
27. V. Tvergaard, Influence of post-buckling behavior on optimum design of stiffened panels. *Int. J. Solids Struct.* **9**, 1519–1534 (1973).
28. E. Byskov and J. W. Hutchinson, Mode interaction in axially stiffened cylindrical shells. *AIAA Jnl* **15**, 941–948 (1977).
29. W. T. Koiter and M. Pignataro, An alternative approach to the interaction between local and overall buckling in stiffened panels. In *Buckling of Structures* (Edited by B. Budiansky), pp. 133–148. Springer, Berlin (1976).
30. D. Bushnell *Computerized Buckling Analysis of Shells*. Nijhoff, The Netherlands (1985).
31. C. Blaas and J. F. M. Wiggenraad, Development and test verification of the ARIANE 4 interstage 2/3 in CFRP. Proceedings of the AIAA/ASME 27th Structures, Structural Dynamics and Materials Conference, Part 1, pp. 307–313, May 1986.
32. Timoshenko and Goodier, *Theory of Elastic Stability*, second edition, pp. 132–135. McGraw–Hill, New York (1961).
33. D. Bushnell, Local and general buckling of axially compressed, semi-sandwich, corrugated, ring-stiffened cylinders. *J. Spacecraft Rockets* **9**, 357–363 (1972).
34. D. Bushnell, Nonlinear equilibrium of imperfect, locally deformed, stringer-stiffened panels under combined in-plane loads. *Comput. Struct.* (submitted).

NOTES ADDED IN PROOF

Recent modifications have been made to PANDA2—see [34] and the Appendix for a list of PANDA2 enhancements introduced since this paper was written.

APPENDIX—RECENT ENHANCEMENTS TO PANDA2

1. Inclusion of initial local imperfection

The theory sketched in Sec. 13 for equilibrium of locally postbuckled stiffened panels is valid only for perfect panels. The capability of PANDA2 has been extended to handle nonlinear behavior of a panel with an imperfection in the form of the local buckling mode. If an axially stiffened panel has a finite imperfection in the form of the local buckling mode, there are no longer any distinct 'pre-buckling' and 'post-buckling' phases of behavior. Rather, the panel deforms in a continuous manner as the external loads are increased. Full details of the theory with numerical results appear in [34].

Two computational advantages result from the inclusion of local imperfections:

1. The behavior of stiffened panels that have been optimized is often sensitive to imperfections. If imperfections are neglected in the theory, the program user must provide a significant factor of safety to compensate for random geometric imperfections that are always present in practical structures. It is difficult to choose an appropriate factor of safety. Introduction of an imperfection in the form of the local buckling mode of the perfect structure partially eliminates this difficulty. While it may still be necessary to introduce a factor of safety larger than unity, the factor can be much closer to unity and can be thought of as a factor to compensate for uncertainties in load, material properties, and failure criteria rather than as a factor to compensate for uncertainty in geometry. Uncertainties in load, material properties, and failure criteria generally do not affect the behavior with increasing severity, as does uncertainty in geometry, as the structure approaches its optimum configuration. Therefore it is particularly advantageous to include the effect of uncertainty in geometry in the structural analysis rather than compensate for it by use of a large, rather arbitrary, factor of safety.

2. Because of discontinuous behavior that occurs at the local buckling load of a perfect panel, design iterations often lead to designs and margins that jump around. For example, this behavior occurred during optimization of the ARIANE interstage, and is evident in Figs 88 and 89. Introduction of a local imperfection smooths the behavior, as displayed in Fig. 1 of [34]. Therefore, gradients of behavior of imperfect panels with respect to design perturbations are generally smooth. They do not ordinarily lead to erratic swings in design or in design margins as the optimum state is sought.

2. Changes in the derivation of C(i, j) *for smeared stiffeners*

The integrated constitutive law for smeared stiffeners is derived in Sec. 8. Since the paper was written the derivation has been modified as follows:

1. Equations (8.7) through (8.10) have been replaced by:

$$N_x(1) = N_x(3) \quad N_y(1) = N_y(2)$$
$$M_x(1) = M_x(3) \quad M_y(1) = M_y(2), \tag{A1}$$

in which the numbers in parentheses refer to the regions (Parts) indicated in Fig. 14. Part (4) no longer enters the calculations. Also, the index (i) in eqns (8.21)–(8.24) no longer appears: The strains and changes in curvature in the stiffener webs and flanges are assumed to be equal to the averages over the entire panel. These modifications lead to more consistent results for panels with both stringer bases and ring bases.

3. In-plane shear in stiffener webs due to response to normal pressure

When a stiffened panel is loaded by uniform normal pressure considerable in-plane shear develops in the stiffener webs. These webs can buckle because of this shear. The web shear buckling failure mode is now included in PANDA2.

4. Buckling knockdown factors now include the effect of anisotropic C(i, j)

In Sec. 11 a shortcut method is described for including the effect of in-plane shear loads on general, panel, and local instability predictions obtained with use of BOSOR4-type of discretized models, which do not admit the effect of in-plane shear loads directly. The knockdown factors are obtained with PANDA-type analyses and are defined in Sec. 11 by

$$\text{KNOCKDOWN} = \text{EIGENCRIT(with shear)/EIGENCRIT(no shear)}. \tag{11.1}$$

PANDA2 has since been modified to include the effect of anisotropic $C(i,j)$ in the computation of these knockdown factors. They are now calculated from the ratio

$$\text{KNOCKDOWN} = \frac{\text{EIGENCRIT(with shear and fully populated } C(i,j))}{\text{EIGENCRIT(no shear and BOSOR4-type } C(i,j))}. \tag{A2}$$

The 'BOSOR4-type $C(i,j)$' are the constitutive law with $C(1,3)$, $C(1,6)$, $C(2,3)$, $C(2,6)$, $C(3,4)$, $C(3,5)$, $C(4,6)$, $C(5,6)$ and symmetric (j,i) terms set equal to zero. Hence, there may be knockdown factors less than unity even if there is no in-plane shear loading. Knockdown factors are never permitted to be greater than unity, so that 'beneficial' anisotropic effects, if any, are not included in the buckling estimates obtained from BOSOR4-type discretized panel module models. However, the effects of anisotropy are usually deleterious, not beneficial.

5. Two-segment crippling of stiffeners

In Sec. 15 is described the analysis of crippling of stiffener parts. Two kinds of stiffener parts are identified there, 'internal' segments and 'end' segments. In the paragraph on crippling of 'end' segments, that is, stiffener segments with one free edge, the following statement is made: 'Crippling loads are computed assuming that the stiffener end cross section does not deform and the number of axial half-waves is the same as that for the interior segment to which the end segment is attached'. In the modified PANDA2 program the number of axial half-waves is no longer thus restricted. Instead, a search over the number of axial half-waves is conducted to find the lowest crippling load factor. In many cases it turns out that the search over the number of axial half-waves is not necessary, but there are cases, such as that shown in Fig. 13 of [34], for which the new method yields a much lower crippling load than the old.

6. More extensive search for maximum stringer pop-off force

Previously stringer pop-off forces were only computed corresponding to the line of intersection between the stringer web and the panel skin. In the modified PANDA2 program stringer pop-off forces are also computed at the line of intersection between the stringer web and the outstanding flange, if any, for tee-shaped stringers and J-shaped stringers. An example in which this modification is critical is shown in Fig. 13 of [34].

7. Different factors of safety for general and panel instability

General instability refers to a buckling mode in which both stringers and rings are displaced. Panel instability refers to a mode or buckling between adjacent rings for which stringers are displaced. Originally, the same factor of safety, FSGEN, was used for both of these modes. In the recently modified PANDA2 code, there are two factors of safety, FSGEN for general instability and FSPAN for panel instability. The user can assign different values to these two factors. The benefit derived from this increased freedom is particularly advantageous when the wide column model is used for prediction of panel (inter-ring) instability, as is usually the case. In this situation, the user will probably want to use a smaller factor of safety FSPAN for panel instability than FSGEN for general instability because the wide column model is almost always more conservative than is the closed form PANDA-type model, which is used for prediction of general instability when both stringers and rings are present.